

Biomechanical design and evaluation of a Self-Powered Ankle Exoskeleton

By

Soheil Bajelan

BMechEng, MBiomechEng

Submitted in fulfilment of the requirements for the
degree of
Doctor of Philosophy

Principal supervisor: Professor Rezaul Begg

Associate supervisor: Dr Tony Sparrow

Institute for Health and Sport

Victoria University

April 2020

ABSTRACT

Walking is critical to many everyday activities, but it can be impaired by conditions including ageing, neurological disorders and muscular pathologies. One of the most serious consequences of gait impairments is the inability to maintain the adaptive lower limb mechanics typical of the characteristic, unimpaired swing foot trajectory. A principal requirement for walking safely is maintaining clearance between the forefoot and ground at critical events in the walking cycle. Foot-ground clearance, represented by the vertical component of the sagittal swing phase trajectory is, therefore, associated with tripping probability. High risk foot trajectory control can be mitigated by providing an external assistive force to lift the foot and a variety of ankle assistive devices have been designed to assist those with walking impairments.

Both passive (unpowered) and active (actuator powered) Ankle Foot Orthoses (AFOs) have been evaluated. Passive devices are low-cost, light and mechanically uncomplicated but tend to restrict ankle motion and reduce plantarflexion at push-off. Active devices have the advantage of regulating the actuator's timing and intensity. It enables them to overcome ankle restriction during stance but are disadvantaged in being more costly, bulky and mechanically complex.

An alternative approach to low cost, lightweight exoskeletons is progress toward a "minimal device". Passive exoskeletons are preferred due to their simplicity, durability, customizability, affordability, compactness, lightness and ease of use; but two challenges limit their practicality. The first is how to produce assistive forces without an actuator and external power source and the second is controlling the timing and magnitude of assistive force without sensors and control units. A further important requirement in designing such devices is detailed information concerning the swing kinematics and kinetics of ankle-controlled walking. A substantial literature has documented stance phase biomechanics, but the swing phase literature is limited and has rarely been employed in the design and evaluation of AFOs.

To address the above device design and biomechanical challenges three aims were; *(i)* investigate the effects on kinematic and kinetic gait variables of foot trajectory modulation, using either the ankle joint only or walking without ankle joint motion, *(ii)* design, construct and test an ankle exoskeleton which would be able to

modulate swing foot trajectory using heel strike energy harvesting and a mechanical controller and (iii) evaluate the constructed exoskeleton's effects on lower limb swing phase kinematics. Accordingly, three studies were designed to realise the construction and evaluation of the ankle-assisting device described in this project. The first was an experiment to predict kinematic and kinetic effects on gait mechanics of intentional ankle-controlled walking. Using a real-time biofeedback, swing foot trajectory was displayed on a monitor and a range of predefined target foot-ground clearances were projected. Participants were then asked to walk on a force-sensing treadmill while matching the pre-defined clearances in two experimental conditions; (i) using either the ankle joint only or (ii) achieving the target foot-ground clearance with no ankle joint modulation.

Intentionally ankle-controlled walking reduced the hazardous Minimum Foot Clearance (MFC) event by increasing foot-ground clearance and, in some cases, eliminating MFC. Ankle-controlled walking also decreased swing phase time to MFC and foot maximum horizontal velocity, with no effects on gait symmetry. Kinetic analyses using AnyBody, showed no significant increase in ankle moment required to lift the foot using a highly dorsiflexed ankle, but greater tibialis anterior muscle force was required. Moreover, increasing the foot-ground clearance by using the ankle joint only showed less mechanical energy than knee or hip action.

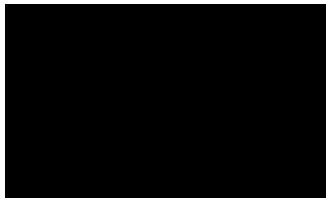
Design and construction of the Self-Powered Ankle Exoskeleton (SPAЕ) was then performed using the kinematic and kinetic variables derived from the first study by adapting a systematic engineering design procedure (second study). The design was then evaluated with a preliminary single-subject test, showing that when walking the SPAЕ could successfully harvest adequate energy during heel strike and actively dorsiflex the ankle during swing, with minimal gait disturbance. A second experiment (third study) evaluated the final SPAЕ design. SPAЕ-assistance increased the vertical component of the swing foot trajectory, incrementing MFC and tending to wash-out the hazardous MFC event, as reflected in the $Mx1$ -MFC height ratio. SPAЕ-controlled walking did not restrict ankle, knee and hip joint motion and showed no effect on the unassisted limb kinematics. The project demonstrated, therefore, that a biomechanically designed SPAЕ could provide functional active ankle assistance during swing, without an external energy source or electronic control system.

DECLARATION

“I, Soheil Bajelan, declare that the PhD thesis entitled ‘Biomechanical design and evaluation of a Self-Powered Ankle Exoskeleton’ is no more than 100,000 words in length including quotes and exclusive of tables, figures, appendices, bibliography, references and footnotes. This thesis contains no material that has been submitted previously, in whole or in part, for the award of any other academic degree or diploma. Except where otherwise indicated, this thesis is my own work”.

I have conducted my research in alignment with the Australian Code for the Responsible Conduct of Research and Victoria University’s Higher Degree by Research Policy and Procedures. All research procedures reported in the thesis were approved by the Victoria University Human Research Ethics Committee (Ref. number: 25227).

Signature:



Date: 29 April 2020

DEDICATION

I dedicate this thesis to God Almighty my creator, my strong pillar and Abbas, my source of inspiration to develop a device to assist disabled people. I also dedicate it to three beloved people who have meant and continue to mean so much to me. First, to my father whose love for me knew no bounds and, who taught me the value of hard work. He helped me with all things great and small. Second, to my mother who raised me, loved me, and always picked me up on time and encouraged me to go on every adventure, especially this one. She has been with me every step of the way, through good times and bad. And thirds, to my sister who helps me find my smile and lets me know that she will catch me if I fall.

ACKNOWLEDGEMENTS

At the very outset, I express my profound sense of reverence and sincere gratitude to my principal supervisor, Professor Rezaul Begg, for competent and inspiring guidance, ceaseless patience, valuable suggestions and constant encouragement throughout my PhD journey. His positive outlook in my research inspired me and gave me confidence to start and finish this project.

I also take the opportunity to express my deepest sense of regards and gratefulness to my associate supervisor, Dr Tony Sparrow for his sage advice, insightful criticisms, and patient encouragement aided the writing of this thesis.

Cordial thanks to Mr Michael Kusel and heartfelt regards to Robert Stokes (I will miss you) for their contributions to design and construction of my ankle exoskeleton.

My thanks to my friends, Dr Alessandro Garofolini and Dr James Peacock, whose friendship, hospitality and wisdom have supported, enlightened, and entertained me over the PhD years.

I remain grateful to all VU biomechanics team, especially Dr Simon Taylor and Dr Hanatsu Nagano. Last but not least, deepest thanks go to all my friends and people who took part in making this thesis real.

TABLE OF CONTENTS

ABSTRACT	I
DECLARATION	III
DEDICATION	IV
ACKNOWLEDGEMENTS	V
LIST OF FIGURES	X
LIST OF TABLES	XVI
1 INTRODUCTION	1
1.1 Overview.....	1
1.2 Research gaps	3
1.3 Research question, aims and hypotheses	4
1.4 Thesis organization	6
2 LITERATURE REVIEW	8
2.1 Overview.....	8
2.1.1 The global impact of gait impairments and falls	10
2.2 Ankle assistive device effects on gait biomechanics	10
2.2.1 Passive AFOs	11
2.2.2 Active AFOs	16
2.3 Alternative energy sources.....	24
2.3.1 Energy exchange during gait	24
2.3.2 Muscle work harvesting.....	24
2.3.3 Heel strike energy harvesting	25
2.4 Swing phase kinematics.....	27
2.4.1 Swing events associated with tripping risk.....	27
2.4.2 MFC and maximum velocity timing.....	28
2.4.3 Non-MFC gait cycles.....	29
2.4.4 Mx1 and MFC/Mx1	29
2.4.5 Swing phase foot trajectory control	30
2.4.6 Laterality-asymmetry	31
2.5 Swing phase kinetics.....	31
2.5.1 Mechanical energy	32
2.5.2 Joint kinetics	33

2.5.3	Tibialis Anterior (TA) kinetics	35
2.5.4	Musculoskeletal modelling	36
2.5.5	Model validation	38
3	KINEMATICS OF SWING PHASE ANKLE-CONTROLLED WALKING	40
3.1	Introduction.....	40
3.2	Methods	41
3.2.1	Participants.....	41
3.2.2	Apparatus	41
3.2.3	Experimental procedure	42
3.2.4	Data analysis	44
3.3	Results.....	47
3.3.1	Joint angles	47
3.3.2	Foot trajectory	48
3.3.3	MFC and maximum horizontal velocity	51
3.3.4	Swing asymmetry	53
3.4	Discussion of results	54
3.4.1	Joint coordination	54
3.4.2	Non-MFC cycles and the MFC/Mx1 ratio.....	55
3.4.3	MFC and horizontal velocity timing.....	57
3.4.4	Joint control effects on gait asymmetry	58
3.5	Summary of results	58
4	KINETICS OF SWING ANKLE-CONTROLLED WALKING	59
4.1	Introduction.....	59
4.2	Methods	59
4.2.1	Musculoskeletal modelling and simulation	59
4.2.2	Data analysis	62
4.3	Results.....	64
4.3.1	Foot trajectory	64
4.3.2	Joints angles and moments	65
4.3.3	Joint impulse and work	68
4.3.4	Total work and mechanical energy	74
4.3.5	Tibialis anterior muscle	74
4.4	Discussion of results	77

4.4.1	Model validation	77
4.4.2	Swing phase joint mechanics	78
4.4.3	Joint impulse and work	78
4.4.4	Total energy	80
4.4.5	Swing TA muscle mechanics.....	81
4.5	Summary of results	82
5	DESIGN AND CONSTRUCTION OF THE SPAE.....	85
5.1	Introduction.....	85
5.2	Design procedure	85
5.2.1	General planning and task clarification: setting design requirements ...	86
5.2.2	Conceptual design: specification of principal solutions	87
5.2.3	Detail design: specification of construction.....	91
5.3	Design evaluation	96
5.3.1	Methods	96
5.3.2	Results and discussion	97
5.4	Summary of results	101
6	SWING ANKLE-CONTROLLED WALKING USING THE SPAE	102
6.1	Introduction.....	102
6.2	Methods	102
6.2.1	Participants, apparatus and procedure	102
6.2.2	Data analysis	103
6.3	Results.....	104
6.3.1	Foot trajectory control	104
6.3.2	Joint angles	105
6.3.3	MFC and maximum horizontal velocity timing	108
6.3.4	Swing asymmetry	109
6.4	Discussion of results	111
6.4.1	MFC and the MFC/Mx1 ratio.....	111
6.4.2	Swing joint coordination.....	112
6.4.3	MFC and maximum horizontal velocity timing	114
6.4.4	Swing asymmetry	114
6.5	Summary of results	115

7 CONCLUSION	116
7.1 Overview.....	116
7.2 SPAE performance and future developments.....	119
7.2.1 Active swing phase ankle assistance	121
7.2.2 Foot trajectory control and MFC assistance	122
7.2.3 Swing asymmetry	123
7.3 Hardware design	124
7.4 Future directions	125
REFERENCES.....	128
APPENDIX A PUBLICATIONS, PRESENTATIONS AND PATENT APPLICATION	145
APPENDIX B CONSENT FORM.....	154
APPENDIX C QUESTIONNAIRE.....	155

LIST OF FIGURES

Figure 2.1 Swing sagittal foot trajectory.	9
Figure 2.2 Ankle angles during stance using data from normal walking recorded as part of this study.	12
Figure 2.3 Passive AFOs. Adapted from a) (Yamamoto et al., 1999), b) (Yokoyama et al., 2005), c) (Hirai et al., 2006) d) (Chin et al., 2009) and e) (Deberg et al., 2014).	15
Figure 2.4 Pneumatic active AFOs. Adapted from a) (Ferris et al., 2006), b) (Sawicki & Ferris, 2009), c) (Park et al., 2014) and d) (Boes, 2016).	19
Figure 2.5 Electromechanics active AFOs. Adapted from a) (Blaya & Herr, 2004) and b) (Yeung et al., 2017).	20
Figure 2.6 a) a passive exoskeleton to harvest ankle negative work, adapted from (Collins et al., 2015) b) a passive AFO powered using heel strike energy harvesting, adapted from (Takaiwa & Noritsugu, 2008).	26
Figure 3.1 Experimental setup and apparatus. In addition to the Vicon default marker set, four marker clusters were attached to the thigh and shank of both legs with the wrist and hand markers excluded (see text).	42
Figure 3.2 Experiment procedure flowchart. Normal walking MTC was used to define three target foot elevations displayed as horizontal lines on a monitor mounted in front of the treadmill. Participants were requested to adopt the target MTC in Normal walking and using the Ankle and No-ankle toe-elevation strategies....	44
Figure 3.3 The imaginary foot marker was defined based on the centroid point (orange triangle) of the triangle made by toe and metatarsophalangeal joint one and five markers. The foot virtual marker (green triangle) was defined by vertically projecting the centroid to the outsole.	45
Figure 3.4 Lower limb joint angles across three walking conditions (Normal, Ankle and No-ankle strategies) and target MFC heights (a positive angle was assigned for dorsiflexion/flexion and negative for plantarflexion/extension).	48
Figure 3.5 Left column: Foot trajectory during the swing phase of the gait cycle using Normal, Ankle and No-ankle strategies. Cyan, blue, orange and red lines represent Normal MFC, MFC+1.5 cm, MFC+3 cm and MFC+4.5 cm, respectively. Right column: the average MFC/Mx1 ratio calculated for each condition. Paired t-tests were used to compare each condition with control	

Normal walking. Significant differences were shown by * and associated p-values. The MFC/Mx1 ratio in A+45 condition exceeded one and showed with an arrow.	49
Figure 3.6 Typical swing foot trajectory when; a) MFC is clearly seen and b) MFC is not seen but there is either a stationary point of inflection or c) a non-stationary point of inflection.....	50
Figure 3.7 Timing of MFC (left column) and maximum foot horizontal velocity (right column) are shown for all three strategies and target MFC heights. Paired t-tests were used to compare each condition with normal walking. Significant differences shown by * with associated p-value.....	51
Figure 3.8 The coincidence of MFC and maximum horizontal velocity timing for all three strategies and normal walking. The goodness of fit is shown for each target MFC height condition with R square. Pooled slopes are also shown depicting general coincidence within each strategy.	52
Figure 3.9 Foot trajectory of the contralateral limb during the swing phase of the gait cycle using Normal, Ankle and No-ankle strategies. Cyan, blue, orange and red lines represent Normal MFC, MFC+1.5 cm, MFC+3 cm and MFC+4.5 cm, respectively.	53
Figure 3.10 The coincidence of MFC and maximum horizontal velocity timing for all three strategies and normal walking for the contralateral limb. The goodness of fit is shown for each condition with R square. Pooled slopes are also shown depicting general coincidence within each strategy.	54
Figure 4.1 Subjects were asked to walk on a dual belt tandem force-sensing treadmill when prepared with thirty-one retro-reflective markers, four marker clusters on anatomical landmarks and EMG electrodes on the Tibialis Anterior and Soleus. Real time sagittal trajectory of the toe marker was shown on a display monitor mounted on the wall in front of the subject. Subjects were requested to match their dominant limb MFC with the displayed target line. The musculoskeletal model associated with each condition is shown in the left image. The experimental markers are illustrated by blue points which matched the virtual markers (red points) using inverse kinematics simulation.....	60
Figure 4.2 Sub-phase regions of the swing cycle. a) classification based on swing cycle percentage; Initial swing, Mid-swing and Terminal swing. b) the swing cycle	

divided into three sub-phases based on Mx1, MFC and Mx2 events; 1) Impulsive sub-phase (Toe-off to Mx1), 2) Maintaining sub-phase (Mx1 to MFC) and 3) Releasing sub-phase (MFC to Mx2).....	63
Figure 4.3 The mean of foot vertical displacement during swing. Data were temporally normalized to swing cycle for Normal walking, Ankle strategy and No-ankle strategy.....	65
Figure 4.4 Ankle joint moments and angles during swing for Normal walking, Ankle strategy and No-ankle strategy. The positive values are joint flexion and negative represent extension. SPM analysis of variance (ANOVA) results depict significant ($\alpha < 0.017$) timing periods (grey). The critical thresholds (F values) are shown with a red dashed line and supra-threshold cluster probability value are depicted close to the line. The same conventions are used in Figures 4.5 and 4.6 below.....	66
Figure 4.5 Knee joint moments and angles over swing for Normal walking, Ankle strategy and No-ankle strategy.	67
Figure 4.6 Hip joint flexion-extension moments and angles over swing for Normal walking, Ankle strategy and No-ankle strategy.....	68
Figure 4.7 Flexion and extension angular impulse and work for each joint during Impulsive sub-phase. * significant difference ($p < 0.05$) between Normal Walking and either Ankle strategy or No-ankle strategy, α significant difference ($p < 0.05$) between Ankle strategy and No-ankle strategy. In some bar graphs the axes are broken for scaling.	70
Figure 4.8 Flexion and extension angular impulse and the work for each joint during Maintaining sub-phase. * significant difference ($p < 0.05$) between Normal Walking and either Ankle strategy or No-ankle strategy, α significant difference ($p < 0.05$) between Ankle strategy and No-ankle strategy. In some bar graphs the axes are broken for scaling.	71
Figure 4.9 Flexion and extension angular impulse and the work for each joint during Releasing sub-phase. * significant difference ($p < 0.05$) between Normal Walking and either Ankle strategy or No-ankle strategy, α significant difference ($p < 0.05$) between Ankle strategy and No-ankle strategy. In some bar graphs the axes are broken for scaling.	72

Figure 4.10 Total body energy. a) the sum of swing limb's joints (ankle, knee and hip) generated or absorbed work from toe-off to Mx2 event. b) the total body mechanical energy from toe-off to Mx2 event.	74
Figure 4.11 Time histories of average TA swing phase muscle force and power for Normal Walking and the Ankle strategy. The paired samples t-test statistic SPM {t} results indicate timing periods showing significant ($p<0.05$) differences (grey shaded areas). The critical thresholds (t values) are shown with a red dashed line.	75
Figure 4.12 The tibialis anterior muscle impulse and work (generated and absorbed) during each sub-phase and total swing. The * symbol indicates the statistically significant difference revealed by paired t-test ($p<0.05$).	76
Figure 4.13 Tibialis anterior and soleus swing force during Normal Walking and the Ankle strategy compared with EMG signals normalized to maximum activation.	77
Figure 5.1 The chronological order of design methodology used in this study (from Pahl & Beitz, 2013).	86
Figure 5.2 Simple mechanism to harvest heel strike energy using a compressive spring.	89
Figure 5.3 One concept developed for a harvest-store-release-reset sequence in each step.	89
Figure 5.4 Final concept of the heel strike energy harvesting mechanism. The heel strike detector (green) makes the first contact and releases the lever mechanism (light blue) to harvest heel strike energy.	90
Figure 5.5 Final concept of the energy release mechanism. The toe-off detector clutch detects the maximum predefined ankle plantarflexion angle and unlocks the orange pulley to release the stored energy.	91
Figure 5.6 a) the final detail-design and b) the constructed prototype using the aluminium material Couple of ball bearings, pulleys and clamps assembled to construct the energy release unit. The toe-off and heel-strike detectors were machined from bronze. See text for further details. Simple mechanical model.	92
Figure 5.7 Ankle moment time-histories for the Ankle and No-ankle strategies, retrieved from Chapter 4.	93

Figure 5.8 Horizontal distance between the ankle centre and the actuator cord (L=12 cm) and the actuator cord angle to the vertical ($\theta=32$ degrees).....	94
Figure 5.9 The SPAE's mechanical performance. a) actuator cord force vs. main spring deflection. b) ankle angle vs. main spring deflection. c) assistive moment provided by the SPAE vs. ankle angle.....	95
Figure 5.10 a) main spring length change during the gait cycle and b) step-to-step variability in stance phase ankle power when walking with the SPAE.....	98
Figure 5.11 The successive functions of the SPAE during the gait cycle.	98
Figure 5.12 Foot trajectory over the gait cycle when walking with and without the SPAE.....	99
Figure 5.13 Effects of walking with and without the SPAE on a) foot-ground reaction forces (GRF) and b) COP anterior-posterior path.	100
Figure 5.14 Position of the COP during walking for right foot (with the device) and left (without the device).....	100
Figure 5.15 Construction design features of the SPAE; a) heel strike energy harvester with no addition to the outsole, b) unrestricted ankle plantarflexion/dorsiflexion and c) unrestricted inversion/eversion.	101
Figure 6.1 Experimental Setup. The Vicon default lower body marker set with four additional marker clusters attached to the thigh and shank of both legs. Upper body markers were discarded.	103
Figure 6.2 Effects of wearing the SPAE on; a) Sagittal foot trajectory, b) MFC height and c) MFC/Mx1 ratio. Blue and red represent Normal and Device walking, respectively. (*) represents the statistically significant differences shown by paired t-tests.....	104
Figure 6.3 The swing normalized a) ankle, b) knee and c) hip joint angles walking with and without the device (a positive angle was assigned for dorsiflexion/flexion and negative for plantarflexion/extension). In the right column, the SPM analysis of paired t-test depicts time periods for which the functions were significantly different for each joint. The critical thresholds (t values) are shown using the red broken line and supra-threshold cluster probability values are depicted close to the line. The grey shaded area represents the interval during which a significant difference was evident ($p<0.05$).	105

Figure 6.4 The entire gait cycle normalized a) ankle, b) knee and c) hip joint angles for walking with and without the device (a positive angle was assigned for dorsiflexion/flexion and negative for plantarflexion/extension). Conventions as for Figure 6.3	106
Figure 6.5 Ankle angle (degrees) at highlighted swing events: maximum plantarflexion, Mx1, MFC, Mx2 and HC. Blue and red represent Normal and Device walking. (*) statistically significant differences.....	107
Figure 6.6 Ankle angular velocity (rad/s) at highlighted swing events. Conventions as for Figure 6.5.	108
Figure 6.7 Maximum foot horizontal velocity during swing for Normal and Device walking (blue and red, respectively).....	108
Figure 6.8 SPAE effects on the timing of: a) foot maximum horizontal velocity, b) MFC and c) their correlation.	109
Figure 6.9 SPAE effects on the unassisted limb a) sagittal foot trajectory and b) MFC height. Blue and red represent Normal and Device walking, respectively.....	110
Figure 6.10 Unassisted foot maximum horizontal velocity during swing for Normal and Device walking (blue and red respectively).....	110
Figure 6.11 SPAE effects on the unassisted limb's timing of: a) foot maximum horizontal velocity, b) MFC and c) their correlation.	111
Figure 7.1 Overview of the SPAE's functional and design possibilities.....	120
Figure 7.2 Typical ankle angle due to the SPAE. The SPAE remains inactive during stance causing no restriction to range of motion prior to and following swing.	121
Figure 7.3 Swing foot trajectory modulation provided by the SPAE for one subject. The green line represents walking before device activation (normal walking) and red dashed line represents foot trajectory following device activation. Maximum active assistance is seen at MFC with less effect at Mx1, increasing the MFC/Mx1 ratio.	123

LIST OF TABLES

Table 2-1 A summary of actuators used in reviewed studies described in section 2.2.	22
Table 4-1 P-values associated with Analysis of Variance (ANOVA) for joint impulses.	73
Table 4-2 P-values associated with Analysis of Variance (ANOVA) for joint powers.	73
Table 4-3 Summary of Findings - Chapter 4.	84

1 INTRODUCTION

1.1 Overview

Walking is crucial to most daily physical activities and we require 3500 to 5000 steps each day to conduct our lives effectively (Tudor-Locke & Bassett, 2004). Walking can, however, be impaired by a range of conditions including ageing, neurological disorders and muscular pathologies associated with a spinal cord injury, multiple sclerosis, muscular dystrophy or cerebral palsy (Perry & Davids, 1992). One of the most serious consequences of gait impairments is the inability to maintain adaptive swing phase foot trajectory control, essential to safe and efficient walking. Interruptions to foot swing are associated with tripping (Winter, 1992) due to reduced foot-ground clearance. Tripping is usually caused by the most distal part of the shoe making unanticipated contact with the supporting surface with sufficient force to destabilize the walker (Nagano et al., 2011). Falling as a consequence of a trip is one of the leading causes of injury and death among older adults (Blake et al., 1988). One report, indicated that in Australia about 18,000 senior citizens died from an accidental fall in 2007 (WCHA, 2016) with about 33% of people over 65 experiencing a fall at least once a year (Hill et al., 1999).

The swing foot's trajectory is characterized by biomechanical events that not only determine foot-ground clearance and tripping risk but also influence the capacity to maintain balance and avoid falling. A requirement for safe walking is, therefore, to preserve sufficient clearance between the forefoot and ground. In normal gait, after toe-off, the swing foot unveils an initial maximum vertical displacement ($Mx1$) after which, the lowest clearance point is seen: Minimum Foot Clearance (MFC) (Nagano et al., 2011). The second swing phase maximum clearance is seen at approximately 90% ($Mx2$). Of these three events the risk of tripping is considered highest at MFC when swing foot elevation is only 10 to 30mm (Begg & Sparrow, 2006). In addition, maximum foot horizontal velocity occurs close to MFC (Winter, 1992) and, as a swing phase event, MFC always seen during single-foot support, increasing the risk of balance loss in the event of ground contact (Lai et al., 2008; Mills et al., 2008).

When the foot is in contact with the ground during stance, MFC height is zero but to provide clearance after toe-off, when swing begins, the distance from the hip joint centre to the foot outsole must be shorter than from the hip to the floor (Moosabhoy & Gard, 2006). The hip, knee and ankle joints, therefore, are required to work in synchrony to lift the foot, increase MFC and avoid contact with either the ground or obstacles. In typical healthy gait mechanics, the shape of the sagittal foot trajectory is, therefore, dependent on progressive, coordinated movements of the swing and stance limbs at the pelvis, hip, knee, and ankle (Moosabhoy & Gard, 2006).

The principal focus of this report is swing phase ankle joint motion because small changes in ankle angle can considerably influence foot-ground clearance with minimum disruption to gait control (Begg & Sparrow, 2006; Moosabhoy & Gard, 2006). For individuals with reduced ground clearance due to muscle weakness or motor control impairments, adding an external assistive moment to the ankle joint may help to increase MFC (Young & Ferris, 2016) and restore the ability to maintain balance. Gait interventions using rapidly evolving assistive technologies appear, therefore, to have the potential to improve walking and reduce falls across a range of gait-impaired populations.

Various devices have been investigated to determine their effectiveness in assisting ankle motion and two principal Ankle Foot Orthosis concepts have been evaluated: passive and active (Alam et al., 2014; Shorter et al., 2011b). Passive devices incorporate springs, dampers or pneumatic components that restrict ankle plantarflexion to maintain swing phase dorsiflexion. Passive AFOs are simple, light and low-cost but their swing plantarflexion restriction, however, interfere stance phase performance, specifically at push-off. In contrast, active designs use electrical actuators and computer-driven controllers that can detect gait events and regulate actuators to complement the limb's force-production requirements. Active systems often required the user to be tethered to the power source or controller (Shorter et al., 2011b) but more recently, wearable systems with an integrated power source and control system have been developed (Kim et al., 2018a; Shorter et al., 2011a).

Lower limb medical exoskeletons are developing rapidly, comprising actuators, sensors and control elements which operate mechanical multi-linked elements attached to the torso, joints and limbs (He et al., 2017). The term 'exoskeleton' is more often employed to describe devices that enhance or augment the motor performance and

safety of able-bodied individuals (Herr, 2009) but a common strategy has been to first develop exoskeletons for able-bodied individuals and then adapt them for other users. The Eksobionics company developed a lower limb exoskeleton for gait impaired patients (Ekso) from a version initially developed for the able-bodied which could gain FDA approval (He et al., 2017). In 2016 the US FDA approved exoskeletons for medical individuals with paralyzed or weakened limbs (Regulation 21 CFR 890.3480) (FDA, 2016).

Progress in exoskeleton design is now increasingly focussed on meeting the challenges of the highly complex human-machine interactions required for everyday movements (He et al., 2017). There is a research focus on not only monitoring the operator's movements, using body-mounted sensors, but also predicting their intended actions using sensors and microprocessors combined with predictive machine learning applications (Cenciarini & Dollar, 2011). Furthermore, research into technologies such as microelectromechanical systems and high-power electronics has been well-funded in efforts to reduce bulk and weight. Despite these advances, many devices remain expensive and complicated (Mertz, 2012).

An alternative approach to developing low cost, lightweight and highly adaptive exoskeletons is progress toward a “minimal device”, a term proposed for future designs with “...fewer bells and whistles” (Mertz, 2012). Passive exoskeletons that do not require a motor-powered actuator have the advantages of simplicity, durability, customizability, affordability, compactness, lightness and ease of use (Collins et al., 2015; Mertz, 2012) but two challenges limit their practicality. The first is how to actively assist joint motion without an external power source and control force timing and magnitude without complex sensors or control units. A further scientific challenge is in the application of gait biomechanics to assistive device design, construction and evaluation, a problem well-recognized by engineers and biomedical scientists (Cenciarini & Dollar, 2011; Herr, 2009; Young & Ferris, 2016).

1.2 Research gaps

The primary objective this PhD project was to develop a passive ankle exoskeleton, cheaper, lighter and easier to use, which can perform similar to an actively powered ankle assistive device. There are, however, two major knowledge gaps in the literature concerning passive ankle assistive devices; (i) lack of a power

source to actively provide assistive torque after push-off and (ii) the inability to control device performance to modulate the swing foot's trajectory without electro-mechanical control systems and gait event detectors. Providing assisted ankle dorsiflexion during swing without plantarflexion restriction during push-off is impossible without providing an active assistive moment following toe-off. Active devices can provide such assistive torques and also control their application using sensors and controllable actuators, while passive devices cannot. This research project was designed to close these gaps by developing a passive ankle assistive device which could harvest biomechanical energy at heel contact to provide an adequate energy source to simulate ankle motion usually produced using motor-powered actuation. Further knowledge gaps in the development of ankle assistive devices are: (i) effects of ankle-controlled walking on swing foot kinematics and (ii) the kinetics of ankle-controlled walking i.e. ankle moment/work.

1.3 Research question, aims and hypotheses

The terms orthosis and exoskeleton are often used interchangeably but, as Herr, (2009) explained, 'orthosis' is typically used for technologies with application to pathological movement conditions, while the term 'exoskeleton' is more often employed to describe devices that enhance or augment the motor performance and safety of able-bodied individuals. The focus of this thesis was to demonstrate that walking safety could be improved by changing swing limb mechanics, specifically foot-ground clearance. The device described in this project is, therefore, a Self-Powered Ankle Exoskeleton (SPAЕ).

The research question addressed in this Thesis was whether a passive ankle assistive device, i.e., a Self-Powered Ankle Exoskeleton (SPAЕ), could effectively modulate foot-ground clearance by providing active swing phase ankle assistance. In answering this question three aims were addressed to overcome the principal limitations of existing passive ankle assistive devices and fill the research gaps concerning biomechanical effects of ankle assistive devices on swing phase biomechanics.

Aim 1 was to better understand swing phase biomechanics to inform the device design process due to limitations in the swing phase biomechanics literature. To address this, an experiment was undertaken to investigate ankle, knee and hip joint

control strategies, with the results reported in Chapter 3 (kinematics) and Chapter 4 (kinetics). Aim 2 addressed two major limitations of existing passive ankle assistive devices by designing and constructing a novel passive Ankle Exoskeleton (SPAE), that could recover mechanical energy and control its application, as described in Chapter 5. Aim 3 was to undertake a comprehensive biomechanical investigation of the developed SPAE to answer the research question (Chapter 6). The final chapter is the Thesis conclusions, with respect to both the biomechanical and technical research findings and recommendations for further developments in ankle exoskeleton design. A synopsis of aims and associated hypotheses is provided below.

Aim 1: Conduct an experiment (Experiment 1) to investigate and predict the effects on kinematic and kinetic gait variables of intentional foot trajectory modulation using either the ankle joint only or walking without ankle joint motion.

Gait kinematics hypotheses:

- i. Intentionally ankle-controlled walking will increase the MFC height/Mx1 ratio and increase the frequency of non-MFC gait cycles.
- ii. Intentionally ankle-controlled walking will reduce the gait-cycle normalized time to MFC and maximum foot horizontal velocity.
- iii. MFC and horizontal velocity of contralateral-foot will not be different from the intentionally controlled-foot.

Gait kinetics hypotheses:

- i. Less mechanical energy will be required to increase foot-ground clearance using ankle-only control.
- ii. Ankle moment and tibialis anterior forces will increase to increment foot-ground clearance using ankle-only control.
- iii. Hip joint moments and mechanical energy will increase when not using an ankle-only control strategy.

Aim 2: Design, construct and test a Self-Powered Ankle Exoskeleton (SPAE) to modulate swing foot trajectory using heel strike energy harvesting and a mechanical controller.

Aim 3: Conduct an experiment (Experiment 2) to evaluate the constructed SPAE's effects on lower limb swing phase kinematics by comparison with non-SPAE walking.

Relative to non-SPAЕ walking the following SPAЕ effects on walking kinematics were hypothesized:

- i. Greater MFC height, MFC/Mx1 ratio and ankle angle at MFC.
- ii. Decreased time to MFC and foot maximum horizontal velocity.
- iii. No effect on either swing or stance phase joint angles.
- iv. No effects on contralateral-limb kinematic variables.

1.4 Thesis organization

Chapter 2 (Literature Review): Elucidates the effects of swing foot trajectory on tripping and falls risk in older adults and other populations. The working principles of ankle foot orthoses, their technical improvements, challenges, and future requirements are described. A detailed account of swing phase biomechanics is outlined with a specific focus on the kinematic and kinetic variables incorporated into present device design and evaluation.

Chapters 3 (Kinematics of swing phase ankle-controlled walking): A first experiment was undertaken to determine precisely the biomechanics of swing phase foot control. The contribution of the hip, knee and ankle joints was examined, including muscle activation patterns of the Tibialis Anterior and Soleus. Using a real-time display of foot displacement as biofeedback, a range of predetermined increased foot-ground clearances were presented in different experimental conditions. Participants walked on a treadmill maintaining their toe trajectory to accommodate the target clearances. Kinematic analysis demonstrated how the hip, knee, and ankle joints responded to incremental changes in the targeted swing foot clearance. In addition, effects on the trajectory of the contralateral foot were determined (i.e. gait asymmetry). Results supported the hypothesis that ankle joint control is an effective strategy for increasing foot-ground clearance, confirming the proposed research and development of an ankle foot orthosis.

Chapter 4 (Kinetics of swing ankle-controlled walking): This chapter presents musculoskeletal modelling of the kinematic and kinetic data from the experimental conditions described in Chapter 3. A model was developed for each subject and condition separately using AnyBody modelling (3×8=24 models). The time-history of joint motion was computed using inverse kinematics and then inverse dynamics used

to simulate the 24 models. The ankle, knee and hip joint moments, work and impulse in addition to tibialis anterior force, work and impulse were computed.

Chapter 5 (Design and construction of the SPAE): A systematic engineering design procedure was employed to ensure timely and efficient development of the Self-Powered Ankle Exoskeleton (SPAЕ). It proceeded with planning and clarification of the research question followed by an engineering feasibility assessment. After confirming the feasibility of the principal solutions, the device was designed conceptually, followed by detailed design and construction. The device addressed two limitations of passive devices. First, providing assistive torque without either an actuator or external power source by using a novel mechanism to 'harvest' heel strike impact energy. Second, it controlled the timing and magnitude of energy release using only heel strike and toe-off mechanical detectors. A pilot study was conducted to test the initial SPAE design's success in overcoming the two principal limitations outlined above.

Chapter 6 (Swing ankle-controlled walking using the SPAE): A second gait biomechanics experiment was undertaken to confirm the performance of the SPAE based on the kinematic variables investigated for intentionally ankle-controlled walking described in Chapter 3. Nine participants walked on a treadmill with and without the SPAE. Kinematic analyses showed that the SPAE effectively modulated swing foot trajectory via ankle angle augmentation without restricting the hip and knee joints.

Chapter 7 (Conclusion): Results reported in Chapter 6 confirmed that the SPAE could harvest and utilize heel strike energy to improve swing foot trajectory without restricting normal gait. This chapter discusses the SPAE's advantages but also highlights the remaining challenges to further developments.

2 LITERATURE REVIEW

2.1 Overview

The fundamental biomechanics of human walking consists of cyclical motions of the lower limbs coordinated with movements of the head, arms and trunk; that move the body safely and efficiently through the everyday environment. Such movements are characterized as “gaits”, with the walking gait cycle defined as the interval between successive foot-ground contacts of the same foot. The walking gait cycle has two primary phases, stance and swing; during stance the foot is in contact with the ground and in the swing phase it moves forward off the ground (Whittle, 2014). For healthy adults walking normally, the stance phase occupies approximately 62% of the gait cycle and the swing phase 38% (Rose & Gamble, 1994).

During the stance phase, lower limb control could be considered less complex because the foot is confined to the ground. During swing, however, the entire limb travels forward with a modulated trajectory designed to avoid contact with obstacles or the walking surface, while also maximizing progression, mostly forward, sometimes sideways and occasionally backwards. The typical foot trajectory in the sagittal plane for normal walking is shown in Fig. 2.1. The Central Nervous System (CNS) optimizes the swing leg’s constituent joint motions to achieve this trajectory (Judge et al., 2003) but any external disturbance or motor control abnormality may lead to non-optimal swing foot trajectory control.

Adaptive gait is critical to most everyday physical activities but can be impaired by a range of conditions, including ageing, neurological disorders and muscular pathologies. One of the most serious consequences of gait impairments is falling due to tripping. The direct causes of falls are tripping, slipping and fainting (Smeesters et al., 2001) but tripping accounts for over 50% of all falls (Blake et al., 1988). Unsuccessful foot-ground clearance increases the risk of tripping, particularly at the event at which the most distal part of the shoe makes unanticipated contact with either the supporting surface or objects on it with enough force to destabilize the walker (Nagano et al., 2011). Successful swing foot control depends, therefore, on maintaining sufficient vertical displacement to avoid obstacle contact.

Increasing MFC height or decreasing MFC height variability can reduce tripping risk (Begg et al., 2007) and approaches to this problem have been proposed by augmenting swing phase ankle dorsiflexion. The ankle is the most effective joint in modulating foot-ground clearance because small dorsiflexion movements considerably increase foot elevation with little effort (Moosabhoy & Gard, 2006). Development of an assistive technology to control the ankle joint to maintain safe ground clearance could help in preventing tripping-related falls. If implemented widely, this proposed fall prevention technology could greatly improve the quality of life for individuals with gait-related impairments and contribute to the estimated \$32 million per annum in medical cost savings to Australia for every 1% reduction in falls (Gillespie et al., 2012).

In this chapter, gait biomechanics effects of passive and active ankle assistive devices are reviewed to recognize their achievements and limitations as a guide to our ankle exoskeleton development and future studies. Additionally, the swing phase biomechanics literature is reviewed and, importantly, the limitations to knowledge identified concerning swing kinematics and kinetics.

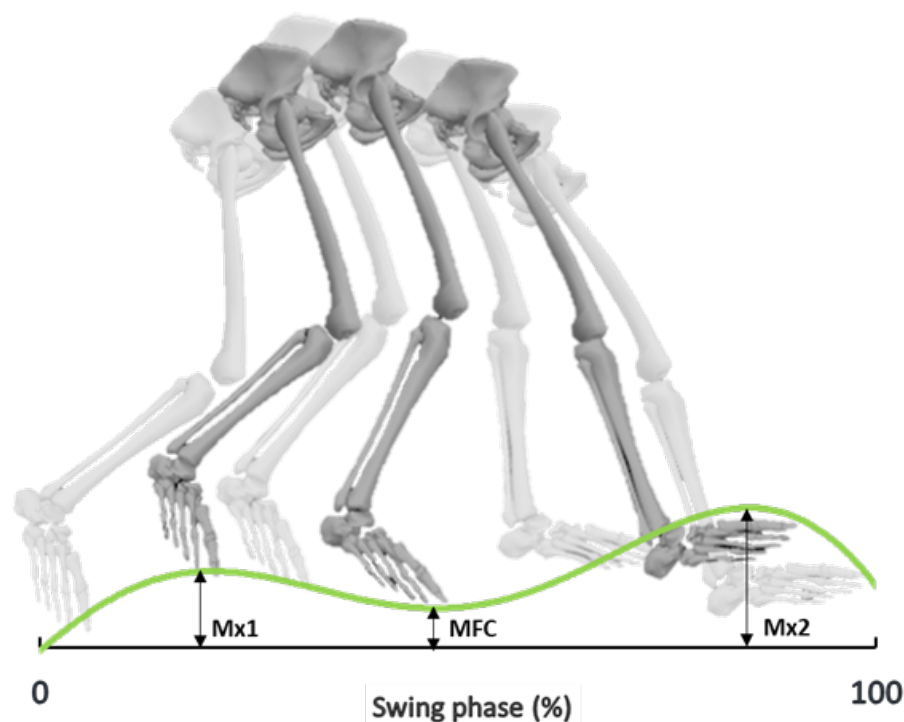


Figure 2.1 Swing sagittal foot trajectory.

2.1.1 The global impact of gait impairments and falls

Life expectancy worldwide is increasing (WHO, 2015) and the National Institutes of Health (NIH, 2007) has estimated that by 2050, 16% of the world's population (1.5 billion) will be over 65 years. The Australian Institute of Health and Welfare (AIHW) predicted that our over 65 population will increase from approximately 15% now to 23% by 2050 (Cripps & Carman, 2001). These added years can be considered positive if we remain in good health (NIH, 2007) but they can be lived less well due to physical and cognitive impairments (WHO, 2015). With ageing there is increased risk of falling due to muscle weakness and sensory-motor deficits (Iosa et al., 2016). The Australian and New Zealand falls prevention society (ANZ, 2019) identified falls as a major community health issue because approximately 30% of people over 65 years of age experience at least one fall per year. Considerable mortality and morbidity have been reported due to falls and in Australia falls mortality rates have increased by 68%, from 3,158 deaths in 2003-2004 to 5,306 in 2007, with 83% of the cases occurring in those aged 70 years and above (Gillespie et al., 2012). Moreover, the leading cause of hospitalized injury in Australia is now unintentional falls (38% of cases), followed by road accidents (13% of cases) (Tovell et al., 2012).

In addition to ageing-related declines in gait control, falls are also commonly associated with gait impairments due to neurological and muscular disorders such as stroke, polio, multiple sclerosis, spinal cord injuries, and cerebral palsy (Perry & Burnfield, 1992). Neuromuscular disorders affecting the ankle can significantly reduce foot-ground clearance (Begg et al., 2007) and gait function affected by stroke is often associated with muscle weakness and sensorimotor impairments (Danielsson et al., 2010; Jørgensen et al., 1995). With global demographic ageing stroke-related gait impairments are increasing and in Japan 20% of people experience a stroke in the second half of life (Turin et al., 2010). These trends emphasize the growing need for strategies to maintain safe walking and prevent falls.

2.2 Ankle assistive device effects on gait biomechanics

An Ankle Foot Orthosis (AFO) is a common intervention for correcting ankle-related gait impairments (Wening et al., 2013) and there is an extensive literature describing passive, semi-active and active ankle foot orthoses and exoskeletons (Adiputra et al., 2019; Alam et al., 2014; Chen et al., 2018; Lehmann, 1999; Shorter

et al., 2011b). The focus of this review, however, is the gait biomechanics-related strengths and limitations of ankle assistive devices, with the aim of informing the design considerations for our device.

2.2.1 Passive AFOs

During stance, the ankle controls both dorsiflexion and plantarflexion (Fig. 2.2) with ankle plantarflexion during the initial and terminal stance phases, sometimes called heel rocker and foot rocker, respectively (Perry & Burnfield, 1992; Webster & Murphy, 2019). Ankle plantarflexors generate propulsion (McGowan et al., 2008) and plantarflexion restriction, therefore, reduces walking performance and dynamic balance (Nadeau et al., 1999; Vistamehr et al., 2014). Furthermore, well-controlled heel strike requires dorsiflexion but, at the same time, the ankle must retain the freedom to enable relaxed foot landing during the transition to a well-balanced single support phase.

The ankle is unrestricted during swing and the primary solution to foot drop and foot slap complications has been to prevent plantarflexion by fixing the ankle angle at approximately 90 degrees. A range of AFOs has, therefore, been designed to prevent swing phase plantarflexion (Fatone & Hansen, 2007; Kesikburun et al., 2017; Singam et al., 2015; Tyson & Kent, 2013; Tyson et al., 2013). One fundamental limitation of the fixed-ankle intervention, however, is that with about 60% of the gait cycle in stance (Butler et al., 2006) a more effective AFO would focus on remedial action in both the swing and stance phases, i.e. throughout the walking cycle.

The essential problem is that in providing swing phase dorsiflexion to ensure foot-ground clearance, an AFO may also restrict ankle plantarflexion, disturbing stance biomechanics (Alam et al., 2014) and reducing torque (Burdett et al., 1988). Bregman et al., (2012) showed that ankle range of motion decreased by 12% when walking with an AFO, with the effect more notable during pre-swing. AFOs designed to assist other phases of the gait cycle also restrict ankle foot dynamics, leading to gait instability and reduced mechanical efficiency (Chin et al., 2009). Olivier et al., (2015) studied the impact of ankle locking on gait kinematics using Ski boots which enabled dorsi-flexion but restricted plantarflexion. Hip flexion was significantly larger at heel strike, compensating the restricted ankle to enable a more natural heel strike and alleviating foot slapping. A similar function is achieved by Posterior Leaf Spring ankle

foot orthoses (PAFOs) (Ramsey, 2011). Nair et al., (2010) examined the impeding or facilitating effects of a PAFO on the transitions from stance-to-swing and swing-to-stance. Their results showed significant restriction in ankle and hip range of motion during both stance-to-swing and swing-to-stance movements and concluded that even a minimally restrictive AFO influences the kinematics and kinetics of gait, specifically during gait transition phases.

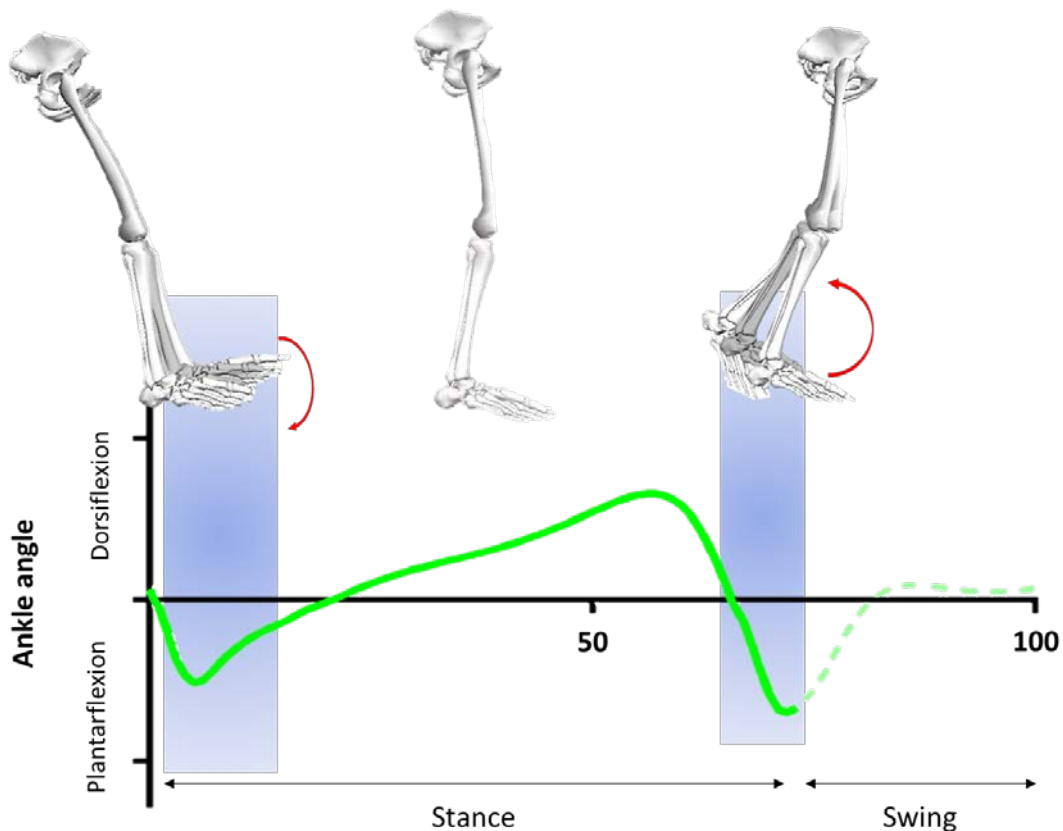


Figure 2.2 Ankle angles during stance using data from normal walking recorded as part of this study.

2.2.1.1 Articulated and Spring Activated AFOs

Second generation AFOs incorporated an articulated joint to overcome the range of motion restrictions of fixed appliances. Articulated AFOs are designed to either free up or restrict the joint when required, either passively using mechanical components such as mass-spring systems, hydraulic dampers or pneumatic devices, or actively with advanced magneto-rheological fluids (Adiputra et al., 2019). Various spring-based innovations derived from Palmer's (2002) work modelled the ankle foot complex as a linear torsional spring in which energy is absorbed by plantar flexors and

tendons. Palmer's mass-spring principles were also employed by Yamamoto et al., (1999) in their articulated Dorsiflexion Assist Controlled by Spring (DACS) device. A spring was attached posterior to resist ankle plantarflexion, it was lightweight (300 g) and provided 2 N.m to 17 N.m resistive moment depending on spring stiffness (Fig. 2.3.a). In one study, when the DACS was compared with a solid AFO it showed about 5 degrees less ankle plantarflexion at toe-off (Yamamoto et al., 1999). More recently a spring-loaded AFO developed by Amerinatanzi et al., (2017) using a super elastic NiTi spring, was compared with a simple stainless-steel spring AFO and showed around 4 degrees of reduction ankle plantarflexion at toe-off.

2.2.1.2 Oil Dampers

Springs resist change in displacement by returning to their initial position. Dampers return to their initial velocity and have been employed as a mechanical motion restrictor to control the ankle resistance associated with articulated AFOs. The earliest example is an AFO developed by Yamamoto et al., (2005) which provided speed-sensitive resistive torque for shock absorption using an oil damper. The proposed advantage was that it could resist plantarflexion and dorsiflexion independently (Yamamoto et al., 2005). A validation study supported increased swing phase dorsiflexion, but the toe-off plantarflexion angles remained essentially zero (Yokoyama et al., 2005), confirming the difficulty of supplementing dorsiflexion without plantarflexion restriction during terminal stance (Fig. 2.3.b).

More recently mechanisms have been developed using magneto-rheological dampers, controlled by kinematic or kinetic sensors as gait event detectors (Chen et al., 2017). These devices effectively control joint fixation and release-timing but use passive restriction rather than active assistance. Kikuchi et al., (2010) developed a semi-passive AFO using a magnetorheological fluid brake (i-AFO) as an angular velocity controller to limit ankle angle during swing. Test results showed a positive contribution of the i-AFO to ankle angular velocity but the effects on ankle angle and foot-ground clearance were not reported (Kikuchi et al., 2011; Kikuchi et al., 2013). The i-AFO effectively restricted ankle movement prior to push-off but could not provide an active force to maintain dorsiflexion following toe-off, a function essential to maintaining swing phase foot-ground clearance.

2.2.1.3 Pneumatics

Pneumatic elements have been introduced into articulated AFOs to adjust stiffness and reduce ankle restriction (Chin et al., 2009; Hirai et al., 2006), replacing mechanical springs and dampers. Kawamura et al., (2002), for example, introduced a mechanical joint in which the stiffness of the elastic element was adjusted by controlling air pressure. These devices have free and constrained modes triggered by pneumatic gait event detectors mounted on the shoe sole. An AFO designed by Hirai et al., (2006) utilized the Kawamura et al., (2002) pneumatically-controlled hinge joint (Fig. 2.3.c). An air buffer detected heel-off and triggered the hinge joint; experimental data indicated increased swing toe trajectory using the device, but no data were provided to show effects on stance phase mechanics or joint angles. This AFO, therefore, fixed the ankle before toe-off to maintain adequate dorsiflexion but adversely affected foot rocker motion at initial stance due to limited ankle joint release after heel strike, approaching foot-flat.

To improve manoeuvrability of the Hirai et al., (2006) device, Chin et al., (2009) developed a passive orthosis with an ankle locking mechanism triggered by a pneumatic pump embedded in the sole (Fig. 2.3.d). A heel-mounted pressure release valve disengaged the ankle at heel strike. When tested, toe-off ankle plantarflexion was highly limited by the locking mechanism, essentially immobile when walking with the device compared to 20 degrees plantarflexion in unconstrained walking (Chin et al., 2009). There were, however, some gait function improvements, with no ankle restriction at initial stance and the knee and hip joint angles not significantly affected. A further recognized disadvantage was the impractical outsole harvesting elements and, as a consequence, in-shoe design developments were proposed (Chin et al., 2009).

2.2.1.4 Shape memory alloy

An articulated passive AFO was developed by Deberg et al., (2014) using shape-memory alloy wires that recover their initial shape when deformed by temperature and stress (Fig. 2.3.e). As with earlier designs, this innovation stored energy at toe-off, during maximum plantarflexion, by stretching the SMA wires and then releasing them during swing to assist ankle dorsiflexion. To evaluate this device the gait cycle ankle angles were measured with and without the AFO and using a conventional hinged AFO. Results showed increased dorsiflexion throughout swing

but decreased plantarflexion at toe-off, i.e., it successfully increased dorsiflexion in swing but still impaired push-off.



Figure 2.3 Passive AFOs. Adapted from a) (Yamamoto et al., 1999), b) (Yokoyama et al., 2005), c) (Hirai et al., 2006) d) (Chin et al., 2009) and e) (Deberg et al., 2014).

2.2.1.5 Summary of passive devices and their limitations

Traditional AFOs have advantages in being mechanically simple, low-cost and incorporated into the shoe but a common problem is that they restrict plantarflexion during stance. One consequence of using a fixed passive AFOs is that flexor muscles atrophy because of the stance phase ankle motion restriction (Lehmann et al., 1986). As discussed, innovations in articulated AFOs have focused on overcoming stance phase restriction but all previous articulated AFOs have only applied resistive moments to the ankle without providing any assistive rotational force. In summary, all devices have focused on ankle restriction and even if the ankle has been left relatively free during initial stance and mid-stance, they have all constrained plantarflexion during terminal stance, reducing the valuable push-off forces.

As shown in Fig. 2.2, normal push-off begins with between zero degrees ankle joint angle to -10 degrees of plantarflexion. An imperative of passive AFO design should, therefore, be the capacity to lock the ankle joint at a prescribed dorsiflexion angle prior to initiating push-off. The solution to this problem in designing the AFO described below, was a mechanism that would dorsiflex the ankle only *following* toe-off, leaving stance phase plantarflexion unconstrained.

2.2.2 Active AFOs

To provide active assistive joint moments after toe-off, computer-driven electric or pneumatic actuators have been developed. Ideally, there must be no delay between toe-off detection and actuation to allow maximum plantarflexion at toe-off and then activate quickly to gain adequate dorsiflexion prior to MFC. Actively-driven AFOs are developing the capacity to improve swing phase mechanics by providing relatively precise joint control (Blaya & Herr, 2004; Boehler et al., 2008; Ferris et al., 2005). Active devices are, however, mechanically complicated, costly and bulky and sometimes tethered to an external power source or control computer (Alam et al., 2014; Shorter et al., 2011b). Technical progress has, therefore, focused on mobile power sources and electronics to enable increased mobility (Boes, 2016; Li, 2013).

2.2.2.1 Pneumatic artificial muscles

Pneumatic actuators were pioneered by Daniel Ferris at the University of Michigan who built a device to simulate the calf muscle, with successive improvements made to control algorithms, actuators and power sources (Fig. 2.4.a) (Ferris et al., 2005; Gordon et al., 2006; Takahashi et al., 2015). To assist dorsiflexion, Kao & Ferris, (2009) developed a pneumatic AFO to simulate the tibialis anterior, using EMG signals to control activation timing via a tethered computer. As discussed earlier, any mechanism to help ankle dorsiflexion must have minimum delay and in the Kao & Ferris, (2009) application EMG signals were used to detected TA activation, minimising the time required to completely shorten the artificial muscle. Experiments over two consecutive days, showed that the device increased ankle angle up to 9 degrees by mid-swing and heel strike was completed without significant negative effects on knee and hip joint movements. Significantly decreased ankle plantarflexion at push off was, however, seen on the first testing day but by the second day function improved, with less decrease in plantar flexion.

The performance of EMG-driven AFOs depends on the quality of signals recorded using surface electrodes and the algorithms developed to interpret them (Micera et al., 1998). Any limitations in these functions may, therefore, restrict their application in individuals with neurological impairments. In response to this problem Sawicki & Ferris, (2009) developed a knee-ankle-foot orthosis (KAFO) using two control algorithms; proportional myoelectric control (PM) and proportional myoelectric control with flexor inhibition (PMFI) (Fig. 2.4.b). Experimental results from the PM algorithm showed increased swing phase ankle dorsiflexion, specifically in the second half of swing but reduced maximum ankle plantarflexion angle at push-off. The second algorithm (PMFI), however, showed almost no change in maximum plantarflexion angle but less dorsiflexion.

In 2014, a Carnegie Mellon - Harvard - MIT collaboration developed a further bio-inspired ankle robotic device employing a linear time-invariant controller (Fig. 2.4.c) (Park et al., 2014). The concept was again to use lower leg muscles to provide natural inversion, eversion, dorsiflexion and plantarflexion without ankle joint restriction. Four pneumatic-powered artificial muscles were placed around the shank (one rear and three front) in addition to various embedded sensors. The success of this device was its ability to actively assist ankle movement (14 degrees of dorsiflexion and 13 degrees of plantarflexion) without ankle range of motion restriction (Park et al., 2014). This device could overcome limitations of passive devices but, as with other active systems, was bulky, complicated, and tethered to an external air pump to power the artificial muscles. There were, furthermore, no published biomechanical data to show the effects on swing foot trajectory. In summary, EMG-driven pneumatic ankle orthoses have advanced the AFO industry but are complex, externally tethered and require user-device adaptation.

2.2.2.2 Pneumatic rotary actuator with portable air pump

In 2011 the Biomedical Engineering Laboratory at the University of Illinois at Urbana-Champaign developed the first Portable Powered AFO (PPAFO) using a pneumatic rotary actuator powered by a portable air pump attached to the waist (Fig. 2.4.d). Shorter et al., (2011a) showed that the PPAFO increased ankle angle during swing from -10 degrees (plantarflexion) to +8 (dorsiflexion) degrees. At push-off,

however, the plantarflexion angle was about +10 degrees (10 degrees dorsiflexion) which demonstrated that the device significantly impeded natural push off. In 2013, the Illinois group improved the PPAFO's control system (Li, 2013) and the most recent evaluation of the PPAFO revealed increased ankle dorsiflexion during swing but less plantarflexion at toe-off compared to either normal walking or walking with the device de-activated (Boes, 2016). The authors could not, however, identify precisely why the device failed to show the plantarflexion peak seen in the data from the control conditions.

The energy source and control unit mass of the PPAFO was approximately 3 Kg with a full CO₂ fuel tank, regulators and control box, which may restrict functionality. Boes, (2016) concluded that using portable compressed gas tanks to power an active AFO depends on the user's physical capacities, making it difficult to generalize the range of application. Their conclusion was that factors such as size, weight and cost constrain the amount of fuel that can be carried and the challenge of maintaining a lasting power supply remains unresolved, despite improvements using N₂ rather than CO₂ as a fuel (Boes, 2016). While portable active pneumatic devices and artificial muscle actuator are becoming lighter and more compact, such as that developed at Arizona State University, they remain relatively heavy, bulky and power supply limited (Thalman et al., 2019).

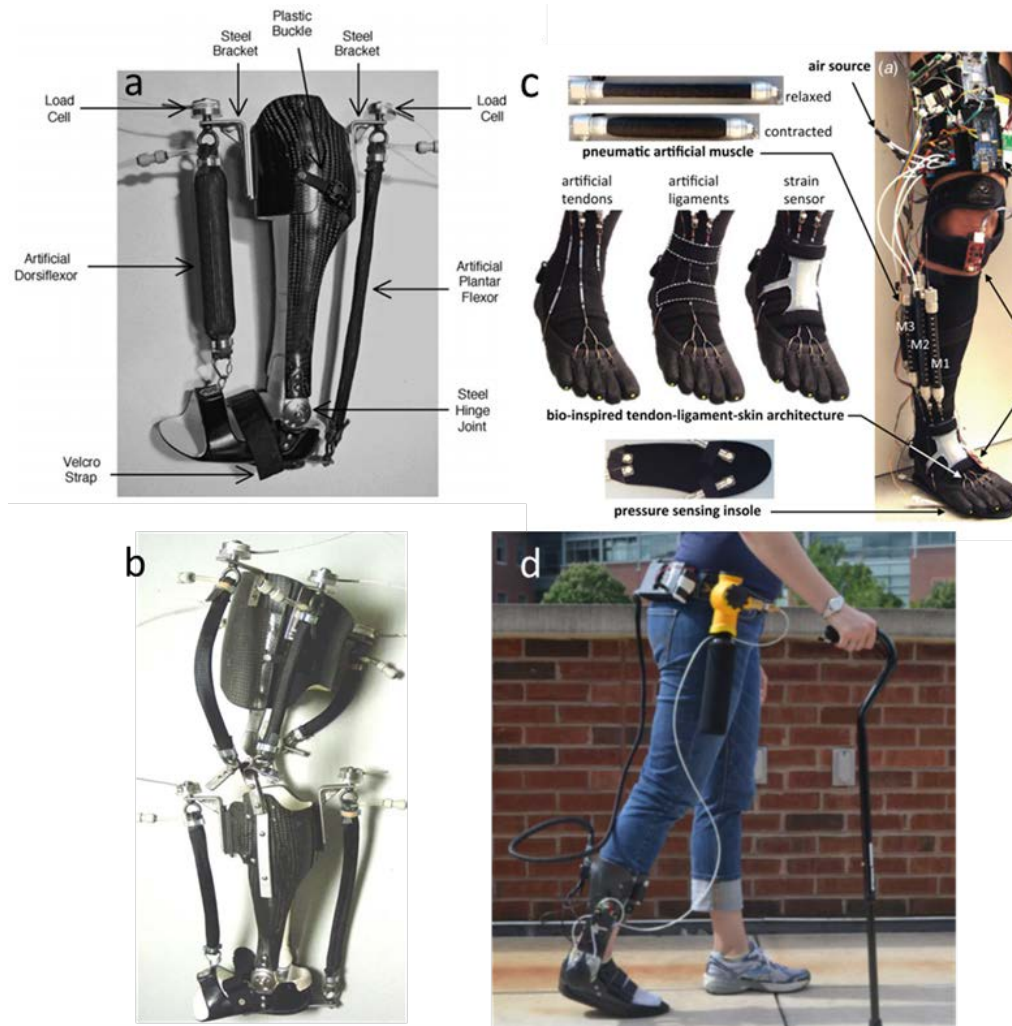


Figure 2.4 Pneumatic active AFOs. Adapted from a) (Ferris et al., 2006), b) (Sawicki & Ferris, 2009), c) (Park et al., 2014) and d) (Boes, 2016).

2.2.2.3 Electromechanical actuators

Investigation of electromechanical actuators began in 2004 at Massachusetts Institute of Technology led by Hugh Herr; with an AFO using a Serial Elastic Actuator (SEA) located posterior to the shank, controlled by an external computer (Fig. 2.5.a) (Blaya & Herr, 2004). An adaptive control algorithm to regulate joint impedance controlled the actuator to provide active assistance during initial stance and the entire swing phase. Results showed that slap foot decreased, and ankle angle increased during swing but there were no data to show the effects on other phases of the gait cycle, specifically push-off. Electromechanical actuators are, however, continuing to improve and now able to provide push-off assistance sufficient to decrease the energy cost of walking (Mooney et al., 2014).

In 2006 a group at Yonsei University, Korea also used a SEA to develop an AFO with a control system based on four force sensors, mounted under the first and second metatarsals, heel and big toe (Hwang et al., 2006). Test results confirmed that the device provided ankle movements similar to normal walking and they concluded that their active AFO would be clinically beneficial. As with the other applications discussed earlier, this SEA-based AFO was tethered to an external power source and control computer with a bulky and heavy actuator.

Following on from the U of I work, an electromechanical portable AFO was introduced by the Chinese University of Hong Kong but with the pneumatic actuator replaced by an electric motor and a control box attached to the waist (Fig. 2.5.b) (Yeung et al., 2017). The control system employed force and motion sensors to detect gait events and run the servomotor actuator. Test results indicated increased ankle angle at mid-swing, from -10 degrees (plantarflexion) to +3 degrees (dorsiflexion). Plantarflexion angle at toe-off, however, also decreased with adverse effects on push-off which were recognized as requiring improvement. The control system also required subject-specific adaptation training. In general, this work represents progress in portable powered AFO developments but still has some of the inherent limitations of active AFOs, such as control system unreliability, weight, cost and complexity.



Figure 2.5 Electromechanics active AFOs. Adapted from a) (Blaya & Herr, 2004) and b) (Yeung et al., 2017).

2.2.2.4 Summary of ankle assistive devices and their limitations

Table 1 summarizes several studies and the actuators employed. The essential problem identified by this review is that all passive AFOs designed to preserve dorsiflexion during swing also, inevitably, restrict the ankle during stance; reducing push-off forces and generally interrupting the natural stance-phase biomechanics. As discussed above, preserving dorsiflexion after toe-off, without disturbing stance phase dynamics, has only been achieved by adding external torque using pneumatic or electromechanical actuators. Despite successful results these devices remain limited for everyday applications due to weight, cost, technical complexity, power demands and other features that we reviewed (Dollar & Herr, 2008; Krebs et al., 2006; Shorter et al., 2011b). Active AFOs using sensors and control algorithms may also be hazardous due to misdetection of gait events. Shorter, (2011) indicated that their device's sensory system did not detect gait events reliably. Their control strategy also tended to perturb ankle joint kinematics. Active devices, furthermore, often have customized control and actuation timing systems, with some AFO projects focused on control systems specific to either treadmill or overground walking with additional modifications to accommodate walking-speed dependent gait event detection (Islam & Hsiao-Weckslar, 2016; Li, 2013; Malcolm et al., 2013).

Table 2-1 A summary of actuators used in reviewed studies described in section 2.2.

	Passive					Active			
	Fixed	Articulated				Tethered		Untethered	
		Spring	Oil damper	MR fluid	Pneumatic	Shape memory alloy	Pneumatic	Electro-mechanics	Pneumatic
(Fatone & Hansen, 2007)	*								
(Tyson et al., 2013)	*								
(Tyson & Kent, 2013)	*								
(Kesikburun et al., 2017)	*								
(Yamamoto et al., 1999)		*							
(Amerinatanzi et al., 2017)		*							
(Yamamoto et al., 2005)			*						
(Yokoyama et al., 2005)			*						
(Kikuchi et al., 2010)			*						
(Kikuchi et al., 2011)			*						
(Kikuchi et al., 2013)			*						
(Hirai et al., 2006)				*					
(Takaiwa & Noritsugu, 2008)				*					
(Chin et al., 2009)				*					
(Deberg et al., 2014)					*				
(Ferris et al., 2005)						*			
(Gordon et al., 2006)						*			

(Takahashi et al., 2015)	*	
(Kao & Ferris, 2009)	*	
(Sawicki & Ferris, 2009)	*	
(Park et al., 2014)	*	
(Blaya & Herr, 2004)		*
(Mooney et al., 2014)		*
(Hwang et al., 2006)		*
(Shorter et al., 2011a)		*
(Li, 2013)		*
(Boes, 2016)		*
(Petrucci, 2016)		*
(Yeung et al., 2017)		*

2.3 Alternative energy sources

2.3.1 Energy exchange during gait

Harvesting energy generated by human movement appears to be a worthwhile research direction to find an energy supply to power otherwise entirely passive AFOs. Human musculoskeletal, physiological and neural systems have evolved to minimize the mechanical and metabolic energy costs of locomotion (Biewener et al., 2004; Forssberg, 1985; Lovejoy, 2005). Strategies such as counterbalancing arm motion and optimizing step length relative to walking speed are such adaptations (Zarrugh et al., 1974). Human muscle efficiency in converting metabolic energy to mechanical work has been estimated to be 5% to 30% while the remainder dissipates as heat (Winter, 2009). Gait is characterized by a cyclic exchange of energy (Hallemans et al., 2004) such that, in principle, no power input is needed during level walking at constant speed (Collins et al., 2015). Soft tissues restore some of this energy due to elastic features but most dissipates as heat due to muscle activation (Zelik & Kuo, 2010). Cavagna et al., (2000) quantified gait dissipated energy and estimated that almost one-third of mechanical energy is lost. At initial foot-ground contact, kinetic energy rises but the ankle muscle-tendon system and soft tissues of the heel then begin to dissipate this energy to reduce speed (Ren et al., 2008). Later the ankle stabilizes during single limb support and eccentric contractions store kinetic energy in the elastic features of tendons and muscles.

2.3.2 Muscle work harvesting

There have been attempts to harvest dissipated biomechanical energy and use it in a range of technical innovations requiring continuous mobile power (Bogue, 2015). There are, however, challenges in retrieving maximum energy while minimally disturbing natural movements that would mitigate the effort (Houng et al., 2014; Riemer & Shapiro, 2011; Zhou et al., 2018).

In biomechanical energy harvesting both positive and negative work due to joint movements can be targeted (Winter, 2009). Harvesting the negative work often required as a brake in various actions appears to be more promising than re-directing positive work. Winter calculated positive and negative work at the ankle, knee and hip during gait (Winter, 1991). Most important is that, for the ankle joint, two phases of

negative work were identified; -0.0074 ± 0.0072 Joules/Kg during heel rocker and at the following ankle rocker -0.111 ± 0.042 Joules/Kg. These values were, however, associated with considerable variability, which is a problem because a consistent, i.e., step-to-step, energy input is required to reliably power an AFO. This step-to-step variability appears to be due to eccentric contributions associated with each muscle's strength and the inherent kinematic variability of the gait cycle. Moreover, co-contraction of agonist and antagonist muscles is complex and variable, making it difficult to distinguish muscle groups that generate energy from those that absorb energy (Riemer & Shapiro, 2011). Additionally, the metabolic cost of mechanical power generation may increase when using a harvester because a muscle operating across multiple joints may contribute to both negative and positive work at a same time and restricting it may transfer load to other muscles. Harvesting negative work absorbed by elastic tissues that is usually returned to the system later, may further disturb gait mechanics (Alexander, 1987).

Collins et al., (2015) introduced the concept of using a mechanical clutch to harvest ankle negative work and reapply it to assist plantarflexion (Fig. 2.6.a). Following on from this work others modified the Collins system (Dežman et al., 2017; Dežman et al., 2016; Wang et al., 2019) with the aim of decreasing the energy cost of walking by using a clutch that was triggered to lock a spring after loading and harvest ankle dorsiflexion energy mid-stance. The clutch, afterwards, released the stored energy before toe-off to assist push-off. While negative work harvesting using this device hindered mid-stance mechanics, they confirmed a balance between recovered negative work and metabolic energy cost due to spring stiffness. Optimal stiffness decreased the metabolic energy cost of walking by about 7% whereas stiffer or more compliant springs increased metabolic energy expenditure (Collins et al., 2015).

2.3.3 Heel strike energy harvesting

In addition to negative work recovery, energy is available when the swing limb first contacts the ground but most heel strike energy converts to heat in the foot tissues and shoe sole (Shorten, 1993). To investigate energy loss due to the mechanics of heel strike, Donelan et al., (2002) modelled the heel-ground collision as a perfectly plastic phenomenon while (Shorten, 1993) considered it an elastic impact, which can recoil following foot-strike. Zelik et al., (2015) estimated 13J total energy dissipation at heel

strike while Baines et al., (2018) estimated only 3.8J, comprising 15-20% of the total metabolic cost of walking lost during heel strike. This discrepancy may be due to the different calculation methods.

Heel impact energy also dissipates due to the cushioning features of footwear, such as construction material stiffness (Nigg et al., 1987; Ros et al., 2010). The harvestable energy, therefore, depends on the mechanism used as the harvester. Riemer & Shapiro, (2011) estimated harvestable heel strike energy at 2 J/step for a person of 80 kg body mass by using 4 cm spring displacement under the foot. Different spring characteristics may enable greater energy harvesting but may limit device design due to increased bulk. As well as reducing manoeuvrability, heel-ground clearance during swing may be decreased due to the additional volume of a heel strike harvester, an important consideration in minimizing tripping-related foot-ground contacts (Mariani et al., 2012; Riemer & Shapiro, 2011; Rome et al., 2005). The only AFO developed to harvest heel strike energy and apply it to actively assist swing dorsiflexion was introduced by Takaiwa & Noritsugu, (2008) using a pneumatic actuator to support dorsiflexion. The device provided 2 N.m active assistive moment but, as can be appreciated from Fig. 2.6.b, is very bulky, which could prove hazardous due to collision of the air pump with obstacles or the ground surface. In summary, heel impact energy can be used as an alternative source of energy to enable a passive ankle assistive device but the limitation of adding bulk to the outsole remains.

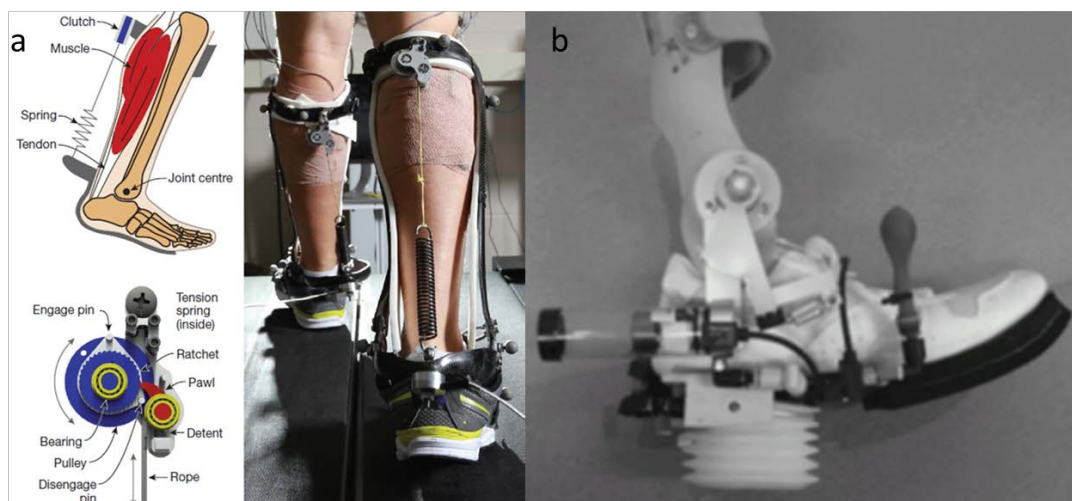


Figure 2.6 a) a passive exoskeleton to harvest ankle negative work, adapted from (Collins et al., 2015) b) a passive AFO powered using heel strike energy harvesting, adapted from (Takaiwa & Noritsugu, 2008).

2.4 Swing phase kinematics

The performance of an assistive device relies on the quality of human-machine interaction and one approach to solving the human factors problems has been to apply principles and findings from gait biomechanics to inform design and evaluation (Cenciarini & Dollar, 2011; Herr, 2009). Young & Ferris, (2016) encouraged industry-based engineers to collaborate with movement scientists at all stages of development, to more productively move towards commercialization. Some researchers have employed stance phase biomechanics to develop their lower limb prostheses (Herr, 2009; Malcolm et al., 2015) but swing phase biomechanics, specifically the minimum foot clearance event, has not previously featured in the design and evaluation of AFOs. The musculoskeletal characteristics of walking are also important to ensure that the individuals' *assisted* gait is well adapted to the specific demands of everyday walking (Young & Ferris, 2016). In this section, therefore, the swing phase kinematics and kinetics considered in our device design process are addressed.

2.4.1 Swing events associated with tripping risk

The swing cycle initiates when the foot leaves the ground at toe-off and terminates at the following foot-ground contact, usually the heel (Winter, 1991). The swing phase can be divided into sub-phases based on a range of criteria but the sagittal foot trajectory is most often used to define swing events and sub-phases (Perry & Burnfield, 1992; Whittle, 2014). In normal walking (Fig. 2.1) maximum vertical displacement of the foot is seen at two swing phase events 'Mx1' and 'Mx2' (Begg et al., 2007) and between them is Minimum Toe Clearance (MTC) or Minimum Foot Clearance (MFC) (Begg et al., 2007; Loverro et al., 2013; Schulz, 2017; Schulz et al., 2013). The term 'MTC' is usually used to describe the trajectory of a point above the big toe while 'MFC' commonly refers to a point beneath the shoe at the lowest part of the forefoot (Loverro et al., 2013). These terms are often used interchangeably but Loverro et al., (2013) compared MTC and MFC systematically for different walking conditions. They concluded that MFC is preferable for studies investigating the risk of foot-ground collision affected by gait conditions and in the present study MFC was, therefore, used as the general term to describe the swing phase minimum foot-ground clearance event.

Tripping risk is considered highest at minimum foot clearance (MFC) (Schulz, 2017), the mid-swing phase event at which vertical displacement of the swing foot from the walking surface is minimal (MFC ~10-40mm) (Fig. 2.1) (Dadashi et al., 2014; Mills et al., 2008). MFC is, therefore, fundamental to tripping prevention (Begg et al., 2007). In addition to height, Begg et al., (2007) indicated that MFC variability also influences tripping probability, reflecting the capacity to adapt swing phase foot kinematics from step-to-step to accommodate the natural variation in ground surface elevation.

2.4.2 MFC and maximum velocity timing

The risk of tripping is maximum at MFC due to decreased foot-ground clearance but balance recovery is dependent on the timing of the MFC event (Nagano, 2014). Balance during walking has often been defined as secure when the body Centre of Mass (CoM) remains within the Base of Support (BoS) formed by the transverse position of the feet (Hof et al., 2005; Lee & Chou, 2006). During double support, the BoS is defined by step length and step width i.e., the area described by both feet, but during single support the BoS is limited to one foot, the stance foot (Granata & Lockhart, 2008). Balance loss during swing can, therefore, be characterized when the CoM locates away from the stance foot (Hof et al., 2005) and balance loss due to tripping is anterior because the CoM continues to move forward when the arrested foot stops (Smeesters et al., 2001). If an MFC-associated trip occurs earlier, more posterior to the stance limb, the stance leg muscles have more time to activate, facilitating balance recovery. Earlier MFC-related tripping also provides more space and time for the swing limb to adopt a landing strategy that will help to preserve balance (Nagano, 2014). Winter, (2009) reported MFC timing at approximately 50% of swing but 45% to 60% has been reported, primarily due to different foot landmarks, such as using either the bottom of the foot or the toe, as discussed earlier (Begg et al., 2007; Mariani et al., 2012). No previous studies have examined MFC timing due to swing phase foot-trajectory modifications using an AFO.

Horizontal foot velocity is maximum close to MFC (Winter, 1992) and, therefore, either foot-ground contact or collision with an obstacle provides maximum negative acceleration and proportionately high reactive forces, contributing further to gait destabilization (Smeesters et al., 2001). Some investigators have suggested that

peak swing phase horizontal velocity is coincident with MFC (Begg et al., 2007; Mills & Barrett, 2001; Winter, 1992) but, to our knowledge, there are no confirmatory data. There is, however, research indicating that the relative timing of maximum horizontal velocity and MFC is affected by walking speed (De Asha & Buckley, 2015).

2.4.3 Non-MFC gait cycles

Schulz, (2011) reported that for young healthy individuals MFC can be clearly identified in 98% of normal walking gait cycles. Similarly Santhiranayagam et al., (2015) showed that 2.9% of young people's gait cycles also did not clearly show an MFC event, which they called *non*-MFC gait cycles. The characteristic foot trajectory of two maxima and one minimum is, therefore, not always apparent (Schulz, 2011) and as a consequence, MFC is not as frequent in older adults or in individuals with atypical gait patterns. Santhiranayagam et al., (2017) found 18.7% non-MFC gait cycles in a healthy older group and concluded lower limb trajectories that eliminate the MFC event, may be adaptive in reducing the probability of foot-ground contact. It can, therefore, be inferred that eliminating or 'washing out' MFC from the foot trajectory, may make walking safer. Schulz, (2011) also showed that well-defined MFC cycles decreased to 80% due to adapting foot trajectory to accommodate an irregular walking surface. Later he proposed that tripping risk is better quantified if the entire swing phase trajectory is considered rather than only the MFC event (Schulz, 2017).

The studies cited above have recognized non-MFC gait cycles but there has been no detailed examination of what causes MFC to be attenuated. A research focus of this project was the contribution of swing limb constituent joints to eliminating MFC, as a precursor to developing an ankle assisting device that would improve walking safety.

2.4.4 Mx1 and MFC/Mx1

In addition to MFC, the swing events Mx1 and Mx2 are also important when considering ankle joint effects on foot trajectory control. Mx1 usually occurs at close to 50% of swing duration and Mx2 at about 90% (Nagano et al., 2011) (Fig. 2.1). Nagano et al., (2011) showed a high correlation between Mx1 and MFC height, suggesting some dependency. The amplitude and timing of Mx1 reflect the

requirement to maintain adequate clearance during the transition from stance to swing. From toe-off to Mx1, foot-ground clearance is minimal but if obstacle contact occurs here, as mentioned earlier, balance can be better maintained because the CoM is more comfortably positioned posterior to the BoS. After Mx1, when foot-ground clearance increases to maximum, the swing foot comes closer to the stance foot and clearance decreases up to MFC. This foot-ground clearance reduction has been investigated to examine tripping risk and Nagano et al., (2011) reported a higher correlation between Mx1 and MFC for older people than for young adults but there have been no subsequent reports of the relationship between Mx1 and MFC. Further study of the Mx1 and MFC correlation may, therefore, contribute to better understanding the impulsive reaction required to terminate stance using an assistive device.

2.4.5 Swing phase foot trajectory control

The leg can be biomechanically modelled as linked segments, the thigh, shank and foot, controlled by the hip, knee and ankle joints. Since the hip joint is fixed to the pelvis, each joint's flexion effectively shortens the entire limb length and can increase MFC height (Moosabhoy & Gard, 2006). The clearance between foot and ground is, therefore, primarily determined by hip, knee and ankle flexion (Moosabhoy & Gard, 2006). Of the three principal joints, however, the ankle is considered most effective in changing swing foot trajectory, including MFC, and minimally disturbs gait mechanics. Moosabhoy & Gard, (2006) showed that knee flexion and hip flexion have more sensitivity in controlling foot clearance at initial swing and terminal swing. Closer to MFC, however, minimal ankle dorsiflexion can considerably increase ground clearance. The hypothesized ankle priority in MFC control, however, requires the further investigation of swing phase kinetics and kinematics undertaken later in this report.

Swing phase control can be characterized as strategies that shape the swing leg's constituent joints to adapt foot trajectory to variations in walking surface height (Maki & McIlroy, 1997; Matsuda et al., 2016). Pre-swing, the motor control system may plan the swing limb's coordination architecture to guide the foot from toe-off to heel strike (Goldberg et al., 2003). The pre-planned swing control strategy may be affected by neuromuscular conditions, such as stroke, trauma, and ageing (Martin et al., 2015; Sulzer et al., 2010). Stroke survivors employ specific strategies to

compensate their ankle weakness, such as hip hiking (Stanhope et al., 2014) or circumduction to lift the leg (Kerrigan et al., 2000). An ankle assistive device may provide sufficient foot-ground clearance to preclude such compensation strategies.

2.4.6 Laterality-asymmetry

The walking gait can be viewed as dependent on a biomechanical collaboration between the two feet but Sadeghi et al., (2000) have shown that walking is not naturally symmetrical. They also suggested why asymmetry is seen, even in young healthy people and one major cause appears to be limb dominance (Sadeghi, 2003). Asymmetry is more accentuated in older adults and those with gait pathology (Perry et al., 2007; Skelton et al., 2002), with older adults using their dominant limb mainly for progression while the non-dominant limb appears to have a stabilizing role (Sadeghi et al., 2000). Swing phase asymmetry is associated with tripping risk (Lewek et al., 2014) because, as illustrated by Nagano et al., (2011), older adults' MFC height is greater in their non-dominant limb. It has been suggested, however, that this response may be adaptive because recovery from a trip is more difficult for the non-dominant limb (Perry et al., 2007; Pijnappels et al., 2008). It is, therefore, very important to investigate the biomechanical effects of an AFO on the contralateral limb.

2.5 Swing phase kinetics

Gait biomechanics has been studied using two principal methods; analysis of constituent movements (kinematics) and analyses of the associated internal forces/moments (kinetics). Thus, as strongly recommended by Young & Ferris, (2016), when including biomechanics into assistive device design, swing kinetics must also be considered. From a kinetics point of view, the swing phase can be modelled as two linked segments (thigh and shank) connected to a fixed joint, the hip. There are two ways this system can move forward and upward (Lewis & Ferris, 2008). First, by providing an impulsive push-off prior to swing and second, following push-off, by applying a flexion moment to constituent joints. Impulsive push-off provides the energy to lift the foot off the ground but during swing the hip, knee and ankle joints modulate the foot's trajectory. Investigation of the intersegmental energy flow during swing is, therefore, critical to understanding the contribution of swing leg segments to initiating and maintaining the swing phase kinematics. In developing an assistive

device these finding will be beneficial in determining each principal lower limb joint's contribution to swing phase control.

The application of biomechanics to designing both ankle foot orthoses and prosthetics has been shown by previous researchers (Herr, 2009; Malcolm et al., 2015). For more advanced robotic ankle assistive devices artificial muscles have been employed to power devices such as a Knee-Ankle-Foot Orthosis (KAFO) (Sawicki & Ferris, 2009), Robotic Gait Trainer (RGT) (Bharadwaj & Sugar, 2006) and a “bio-inspired active soft orthotic device” (Park et al., 2014). Artificial muscle developments are, therefore, evolving to ensure that the assisted motion will reliably simulate that produced by living-muscle activity (Dzahir & Yamamoto, 2014). Prediction of the joint and muscle mechanical reactions to different conditions is, therefore, necessary to improve such devices. One essential requirement of these devices is to control the timing and magnitude of assistive forces/moments, such that the individuals' assisted gait is well adapted to the specific demands of everyday walking. In summary, determining the timing and magnitude of moment, impulse, work and energy flows in joints and muscles underlying different movements are useful in developing any assistive/rehabilitation device (Zelik et al., 2015).

2.5.1 Mechanical energy

Swing phase kinetics were not usually a focus of earlier gait biomechanics studies, with interest primarily in the metabolic cost of walking due to muscle forces generated during stance; because metabolic energy expenditure during swing is relatively low (Gottschall & Kram, 2003; Griffin et al., 2003). More recently, however, it has been argued that the energy consumed during swing is not negligible. Umberger, (2010), Doke et al., (2005) and Marsh et al., (2004) concluded that swing phase muscle activity consumes between one-quarter to one-third of the total gait energy. Umberger, (2010) used a modelling approach to determine that around 10% to 33% of total gait energy is consumed during swing. Most important for assistive device designers is that the metabolic energy cost of walking is increased markedly by attaching a mass to the foot, rather than the hip (Browning et al., 2007).

A number of studies have investigated the contribution of lower body joints to energy consumption during swing. Umberger, (2010) revealed that hip and ankle flexors dominate in the first half of the swing phase, while hip and knee extensor

muscles consume most energy during the second half. The energetic contribution of the ankle joint during swing has, however, only previously been documented for pre-swing push-off. Kuo, (2002) showed that using the hip joint alone to lift the foot for adequate swing phase motion consumes four times more energy than push-off alone. It appears, therefore, that energy consumption associated with the ankle joint during swing has not been considered, possibly due to the assumption that ankle energy is inconsequential relative to the knee and hip.

As described earlier, the ankle has been nominated as most effective in modulating the foot's swing trajectory, but this proposition has not been tested in terms of energy consumption. It can be assumed that the ankle is the most mechanically energy-efficient joint to lift the foot within a small range because the foot's mass is lower than the shank or thigh. Analyses of the swing phase mechanical energy exchange (Winter, 2009) were, therefore, employed in this study to re-evaluate this assumption.

2.5.2 Joint kinetics

For developing an ankle assistive device, the moments, impulses, power and work associated with the ankle during swing are required. Computing these variables for the other principal joints, knee and hip, is also important because if ankle motion is either modulated intentionally or actively changed using an assistive device, those joints may also adapt to the new ankle joint constraints. Siegel et al., (1996) showed that knee joint mechanical work increased with ankle restriction and Tzu-wei et al., (2015) also found that peak hip power decreased when the ankle was restricted.

Ankle dorsiflexion moments can be investigated either statically or when walking. Studies of static ankle moment have revealed ankle dorsiflexion moment increasing exponentially with greater ankle angle but there is a complex relationship between ankle moment and joint angle. Riener & Edrich, (1999) and Silder et al., (2007) demonstrated that moment-angle functions range from 5 N.m to 15 N.m depending on knee joint angle. To help us in the design of an ankle assistive device ankle moments should, therefore, be measured during active walking, rather than statically.

Ankle dorsiflexion moment during normal walking is usually presented for the entire gait cycle, with the general conclusion that the swing phase moment is

essentially zero, relative to the critical plantarflexion moment prior to toe-off (Silder et al., 2007). It has also been indicated that ankle moments and power change during swing, but the magnitude is difficult to determine because in graphical comparisons with considerable plantarflexion, the scaling shows values close to zero. To overcome this problem ankle moments and power during swing were retrieved from three sources (Richards, 2018; Robertson et al., 2013; Whittle, 2014). A peak dorsiflexion moment of between 0.02 and 0.03 N.m/Kg is observed just after toe-off and dorsiflexion power also has a maximum negative peak at about the same time, approximately -0.08 W/Kg. Power then increases to a maximum positive (0.04 W/Kg) mid-swing, reducing to zero by the end of swing.

Measurements of ankle moments prior to developing an active AFO have sometimes been undertaken. Takaiwa & Noritsugu, (2008) experimentally determined 2 N.m to be the required ankle moment to achieve 20 degrees ankle dorsiflexion, i.e. from -15 degrees plantar flexion to +5 degrees dorsiflexion. The University of Illinois design team, however, used Perry & Burnfield, (1992) data for calibrating their powered AFO to generate a constant 3 N.m ankle torque throughout swing (Boes, 2016; Li, 2013; Petrucci, 2016; Shorter, 2011). At Michigan University Kao & Ferris, (2009) used inverse dynamics in Visual 3D software to estimate ankle dorsiflexion moments and power in normal walking at 1.25 m/s. They found a maximum ankle moment after toe-off of 0.016 N.m/Kg which decreased gradually until end of swing; with ankle power in the range -0.08 W/Kg to 0.05 W/Kg. In designing the KAFO, a later version of the Michigan group's device, Sawicki & Ferris, (2009) computed peak ankle moment (0.04 N.m/Kg), peak negative power (-0.018 W/Kg) and positive power (0.027 W/Kg), again using Visual 3D.

A clear picture of joint moment and power time-histories is particularly helpful when developing an assistive device requiring gait-energy recovery. Thelen et al., (1996) concluded that the ability to reduce balance-recovery response time following tripping relies more on joint power generation than joint moments. Joint angular impulse is the time-integral of moment and the angular impulse acting on a joint is directly related to change in angular momentum. If, therefore, the same moment is applied in shorter time, impulse increases, changing the critical joint rotation velocity. Impulse information is, therefore, helpful in determining the impulsive assistance required immediately after toe-off to quickly provide safe foot-ground clearance.

In addition to impulse, joint power can be used to show the work associated with elevating the foot (Voloshina & Ferris, 2018). The swing limb's absolute work, the sum of all positive and negative work of the swing limb's joints, can be used to determine the energy expenditure of a foot lifting strategy. Investigation of the biomechanical work generated or absorbed during specific limb movement is important in understanding specific joint contributions, muscle function and energy cost (Zelik et al., 2015).

2.5.3 Tibialis Anterior (TA) kinetics

The principal muscle in ankle joint dorsiflexion is the Tibialis Anterior (TA) (Palastanga & Soames, 2011). Knowing the TA force and response time between toe-off and MFC is instructive because an impulsive force is required in a very short time to effect the transition from plantarflexion after toe-off to dorsiflexion (Rosenberg & Steele, 2017; van den Bogert et al., 2002). The short activation time also constrains TA power generation from toe-off to MFC (Neptune et al., 2008). By calculating power, the work done by each muscle can be determined, giving more insight into the energy flows between joints and limbs (Neptune et al., 2000). Muscle force and power are also valuable in showing agonist/antagonist balance (Richards, 2018).

TA force synchronization with ankle moment is invaluable in optimizing the timing and magnitude of an ankle assistive device and there have been developments in artificial muscles designed to assist ankle plantarflexion and dorsiflexion. One essential requirement of such devices is to control the timing and magnitude of assistive moments, such that the individuals' assisted gait is well adapted to the specific demands of everyday walking. The field of artificial muscle development is, therefore, evolving to ensure that artificial muscles reliably simulate living-muscle activity (Dzahir & Yamamoto, 2014) such as the Knee-Ankle-Foot Orthosis (KAFO) (Sawicki & Ferris, 2009), Robotic Gait Trainer (RGT) (Bharadwaj & Sugar, 2006) and a "bio-inspired active soft orthotic device" (Park et al., 2014).

TA activity during swing has widely investigated by recording EMG signals (Trinler, 2016). Lee & Hogan, (2014) demonstrated that TA activation mirrors the ankle moment, with a peak after toe-off and activation decreasing up to the end of swing. Kao & Ferris, (2009) used the TA activation envelope in designing their artificial muscle powered device and demonstrated that the force-time history of their

artificial muscle simulated the natural TA muscle activation pattern. They did not, however, calculate TA kinetics to illustrate the associated force, impulse, power and work.

In addition to TA activation, force production across the gait cycle has been computed. Błażkiewicz, (2013) showed a maximum TA force of 2 N/Kg, after toe-off, with a systematic review of twelve studies indicating results from 1 to 4 N/Kg (Trinler et al., 2018). In addition to TA force, Bogey et al., (2010) computed TA power, with an initial negative peak of almost -2 Watts and a subsequent positive maximum of 12 Watts. These data were, however, time-normalized to the gait cycle and could not be used to calculate impulse and work and there are no previous reports of TA kinetics as a function of ankle dorsiflexion angle. In the present study TA force and power were determined, from which impulse and work were calculated.

2.5.4 Musculoskeletal modelling

Recently, it has been shown that computational models of the foot-ankle complex can be useful in designing orthoses and prostheses (Oosterwaal et al., 2011). Herr & Grabowski, (2012) and Malcolm et al., (2015) employed stance phase biomechanics to develop their lower limb prosthesis but foot-ankle swing phase biomechanics requires further investigation to guide the design of an assistive device serving a primary function during swing.

To calculate kinetic variables, musculoskeletal modelling has been developed, based on a mechanical system in which bones, joints, and muscles are represented as rigid links with connecting joints and actuators (Zajac, 2003). The approach employed to calculate dynamic variables incorporated into such systems is inverse dynamics analysis, by which the time-histories of constituent forces and moments are estimated (Damsgaard et al., 2006; Dumas et al., 2007; Winter, 2009). The classic inverse dynamics analysis for gait uses ground reaction forces combined with limb segment metrics and positions to calculate joint moments, beginning with the ankle joint and then calculating the knee and hip parameters (Buchanan et al., 2005). This technique, however, cannot provide muscle forces and joint reaction forces, for which a more complex musculoskeletal model is required (Damsgaard et al., 2006). Musculoskeletal models incorporate the geometric and mechanical properties of bones, joints, ligaments and tendons and, in addition, take into account muscle attachment

characteristics that affect moment arms (Damsgaard et al., 2006). The essential challenge in musculoskeletal modelling, however, is that the system is mechanically indeterminate, because many muscles may produce the same mechanical effects. This challenge is has been referred to as the ‘redundancy problem’ of muscle recruitment (Damsgaard et al., 2006) but over the last two decades optimization techniques have been developed to address it (Crowinshield, 1978; Prilutsky & Zatsiorsky, 2002; Rasmussen et al., 2001).

The two most frequently cited musculoskeletal modelling applications in human gait biomechanics are AnyBody (Damsgaard et al., 2006) and OpenSim (Delp et al., 2007). The AnyBody Modelling System (AMS) was established at Aalborg University and introduced in 2002 by Rasmussen et al., (2002) and OpenSim was initially released in 2007 at Stanford University (Delp et al., 2007). They have similar approaches, involving the following principal steps: (i) scaling to produce a subject-specific anthropometric skeletal model, (ii) modelling joint motion using inverse kinematics to determine joint angle time-histories, (iii) inverse dynamics and optimization to compute joint moments and muscle forces, (iv) joint reaction force computations using muscle forces. OpenSim uses static scaling (Trinler et al., 2018) while AnyBody uses dynamic scaling, in which segment length and width are computed actively, i.e., during movement (Damsgaard et al., 2006). Both packages use least squared minimization incorporated into inverse kinematics to activate the model and static optimization for muscle force estimation following inverse dynamics.

While there may be no broad consensus on the benchmarks by which to compare the two modelling systems, Trinler et al., (2019) estimated muscle forces during normal walking using both packages. Their results showed small differences in estimated joint moments and muscle forces and argued that the data were not sufficient to recommend one application rather than another. Similarly, Kim et al., (2018b) evaluated the two applications and were also unable to determine a preference. One commentator, however, has argued the advantages of AnyBody in modelling the human masticatory system (Cadovaa, 2013). Langholz et al., (2016) also favoured AnyBody arguing that it is more versatile and well-suited to modelling human-environment interactions, advantageous in gait biomechanics.

The author's previous experience confirmed the versatility of AnyBody in a human-environment interaction project involving a sit-to-stand task (Bajelan & Azghani, 2011, 2014) and subsequently constructing a sit-to-stand assistive device (Bajelan et al., 2010). The author has, furthermore, recently used AnyBody to effectively model fall recovery in a tether-release experiment (Bajelan et al., 2017a). The capability of AnyBody was also confirmed in modelling swing phase kinetics in a wide step walking task (Bajelan et al., 2017b) and AnyBody worked effectively with data from a pilot study of the ankle-controlled walking procedure to be used in the first experiment undertaken in this Thesis (Bajelan et al., 2019a).

Practical considerations have also influenced decision making concerning the two applications. For example, Cadovaa, (2013) argued that OpenSim is more menu-driven and easier to use, while more complicated Anyscript programming is required for producing AnyBody models. Cadovaa, (2013), however, recommended AnyBody because Anyscript incorporates a detailed and highly adaptable human body model. The c3d files output from our Laboratory's Vicon (Nexus) pre-processing package can be imported directly into AnyBody. Additionally, AnyBody has ground reaction force prediction feature, which assist modelling when GRF measurements are either unavailable or of poorer quality (Fluit et al., 2014; Jung et al., 2014). It is important to emphasize, however, that GRF prediction feature was not used in the present experiments. An advantage of OpenSim is that it is public domain, with support from a considerable user group, while an AnyBody license is priced at approximately 7000 euros for a faculty researcher.

2.5.5 Model validation

Musculoskeletal modelling is a valuable tool for investigating internal forces non-invasively but, as discussed above, due to the software's assumptions, reservations have been expressed with respect to the clinical application of musculoskeletal modelling results (Lund et al., 2012). Model validation has, therefore, been attempted but, again, there has been no widely accepted criterion (Griffin, 2001). Nigg & Herzog, (2007) proposed three methods, (i) direct validation: comparing simulation results with in-vivo measurements, (ii) indirect validation: comparing estimated muscle forces with EMG measurements and (iii) trend validation: examination of the trend in changing a variable rather than absolute magnitude. The

second method has been commonly used, i.e. using EMG data to validate muscle force estimations. Erdemir et al., (2007) found that 65% of musculoskeletal modelling validations relied on EMG. Some researchers have simply compared the onset and offset of estimated muscle force with EMG (Griffin, 2001) while others have looked at the EMG amplitude's congruence with the estimated force peaks (Martinez et al., 2018). There are also limitations associated with the quality of EMG signals due to skin preparation, electrode placement, external noise and cross-talk (De Luca, 1997; Halaki & Ginn, 2012). Despite these limitations, Lund et al., (2012) considered EMG data to be useful for rejecting or retaining a model.

3 KINEMATICS OF SWING PHASE ANKLE-CONTROLLED WALKING

3.1 Introduction

Investigating the biomechanics of the lower limbs to determine how they lift the foot to achieve safe and effective ground clearance is valuable in developing assistive technologies to compensate a range of gait defects. An essential precursor to lower limb exoskeleton design is identifying the complex interactions between the hip, knee and ankle joints. The ankle joint is particularly important because it has been recognized as most effective in increasing MFC by controlling swing foot trajectory with minimal disturbance to gait (Moosabhoy & Gard, 2006). Despite previous work showing the role of the ankle in controlling the foot's swing phase trajectory, further investigation of swing kinematics affected by intentionally ankle-controlled walking would be applicable in the design and evaluation of our ankle assistive device.

The aim of this first experiment, outlined in the aims and hypotheses (section 1.3), was to examine and predict the effects of intentional foot trajectory modulation on the swing kinematic characteristic, simulating how an ankle assistive device will influence the swing phase foot control. An experimental procedure was designed in which, in one condition, participants were required to attain an experimenter-defined target or criterion MFC using only an ankle strategy. Previous work has reported MFC characteristics in young and older subjects (Barrett et al., 2010), individuals with gait impairments, such as stroke patients (Begg et al., 2014) and people with diabetes (Suda et al., 2019). The biomechanical response of the lower extremity to achieve a range of predefined foot clearances by either using or not using the ankle joint has, however, not been studied. In this study, real-time biofeedback was employed to control foot-ground clearance by monitoring the toe marker trajectory (Begg et al., 2019).

Participants walked on a treadmill at preferred speed while maintaining their foot trajectory to accommodate predetermined foot-ground clearances, using either ankle joint control only or no-ankle control. Kinematic analysis of recorded data was performed to evaluate the role of the lower limbs in achieving these continuous, low amplitude foot elevations. The primary focus was the timing and magnitude of swing

phase events because they would be used to evaluate the developed ankle assistive device (SPA-E).

3.2 Methods

3.2.1 Participants

Ten healthy, physically active males aged 30 to 40 years (mean 34.2) were recruited from the academic community of Victoria University; their mean stature was 175 cm (SD=5.6) and body mass 78.0 kg (SD=8.9). All participants undertook informed consent procedures (Appendix B) mandated and approved by the Victoria University Human Research Ethics Committee (Ref. number: 25227) and screened using a health questionnaire to confirm no orthopaedic, respiratory or cardiac conditions that would preclude participation (Appendix C). Prospective participants with the following conditions were excluded: diabetes (Type 1 or 2), chronic heart disease, severe overweight/obese (BMI > 30), uncontrolled metabolic and/or cardiovascular disease, previous history of back or knee pain/injury, any recent significant injury that impedes the ability to perform exercise or any other contraindications that may compromise safety during exercise.

3.2.2 Apparatus

The experiments were conducted in the Victoria University Biomechanics Laboratory using the configuration shown in Fig. 3.1. Three-dimensional position-time coordinates of body segments were captured using a Vicon Bonita motion capture system (Vicon Motion Systems, Oxford Metrics Inc., Oxford, UK) with 14 high speed cameras sampling at 100 Hz. Foot-ground reaction forces were sampled at 1000 Hz using a time-synchronized AMTI (dual plate) force-sensing treadmill (AMTI, MA, USA). A 16-channel EMG system was synchronized to record Tibialis Anterior and Soleus muscle activity using a Telemetry 2400T wireless transmitter (Noraxon, Scottsdale, AZ, USA), described in Chapter 4. A video monitor was mounted on the wall in front of the subject to display real-time feedback of the participant's toe trajectory.

Following a questionnaire to obtain demographic information and anthropometric measures, thirty retro-reflective markers were attached to anatomical landmarks using Vicon standard Plug-in-Gait marker set (Plug-In Gait Marker Set,

Vicon Peak, Oxford, UK) as shown in Fig. 3.1 (Clark et al., 2016); this study focused on the lower body extremity and the head and forearm markers were, therefore, excluded. In place of TIB and THI markers a marker cluster was attached to the tibia and thigh. The right-side clusters included five reflective markers, with four markers mounted on the left-side clusters for reliable recognition during data capture and analysis (Fig. 3.1). Two additional markers were also attached to the first and fifth metatarsophalangeal joints (MT1 and MT5) to define a virtual marker under the shoe (Fig. 3.1).

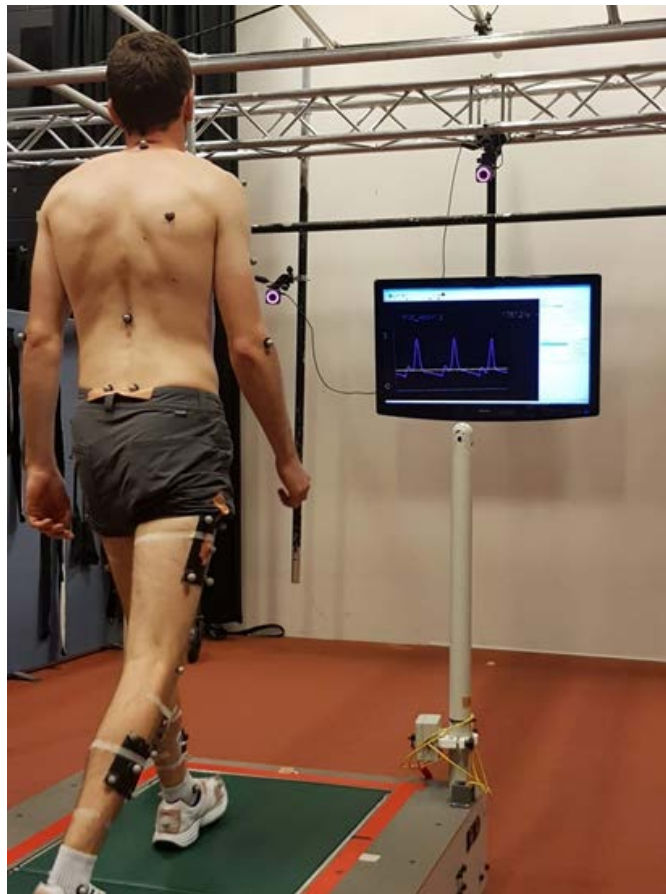


Figure 3.1 Experimental setup and apparatus. In addition to the Vicon default marker set, four marker clusters were attached to the thigh and shank of both legs with the wrist and hand markers excluded (see text).

3.2.3 Experimental procedure

To study the biomechanics of walking when lifting the foot to achieve small foot-ground clearances, three predefined target clearance heights were presented. These experimental heights were defined by adding 1.5 cm, 3 cm and 4.5 cm to each subject's MFC height during normal walking. These three conditions (Normal

MFC+1.5 cm, Normal MFC+3 cm and Normal MFC+4.5 cm) were selected because elevations exceeding 6 cm require adaptations at all the lower limb joints while lifting the foot less than 6 cm was anticipated to be achievable using ankle dorsiflexion only (Begg & Sparrow, 2000; Chen et al., 2008). Since it was hypothesized that MFC height below 6 cm could be controlled using only the ankle, three walking conditions were randomly presented; 1) a normal walking control (Normal strategy), 2) Lifting the foot using the ankle only, as provided by an assistive device (Ankle strategy) and 3) Lifting the foot by not using the ankle joint, as would be seen in individuals with foot-drop or similar conditions (No-ankle strategy). Ten experimental conditions were, therefore, created; 1) Normal walking, 2-4) Normal walking +1.5 cm, 3 cm and 4.5 cm, 5-7) Ankle strategy +1.5 cm, 3 cm and 4.5 cm and 8-10) No-ankle strategy +1.5 cm, 3 cm and 4.5 cm. To control foot elevation across the above experimental conditions a real-time feedback technique (Begg et al., 2009) was employed in which the trajectory of the dominant limb big toe marker was displayed on a digital monitor to indicate the target Minimum Toe Clearance (MTC) event.

In each experimental condition participants were asked to walk on the treadmill at preferred speed (3.32 ± 0.62 Km/h) for two minutes (Fig. 3.2). Initially, the dominant big toe marker trajectory was recorded and imported into Visual 3D (C-Motion, Rockville, MD) to compute the mean baseline MTC. As described above, using this mean the vertical height for the three target foot-ground clearances were calculated for each subject and then presented as a horizontal target line displayed on the monitor positioned in front of the treadmill (Fig. 3.2).

In the experimental conditions, the biofeedback monitoring technique developed by Begg et al., (2019) was employed by which real time sagittal trajectory of the toe marker was shown on the display. This technique, however, was modified requesting participants to intentionally match the MTC event of only their dominant limb with the displayed target ground clearance. Two minutes were recorded for each MTC height condition with participants requested to adopt one of the three elevation strategies: Normal, Ankle and No-ankle in randomized order. In the Normal condition, participants were requested to achieve the target MTC walking normally with no change to their gait pattern. For the Ankle strategy, subjects were asked to maintain target MTC by changing ankle angle only. In the No-ankle strategy condition changes

to both hip and knee joint modulations were requested with specific instructions not to use the ankle.

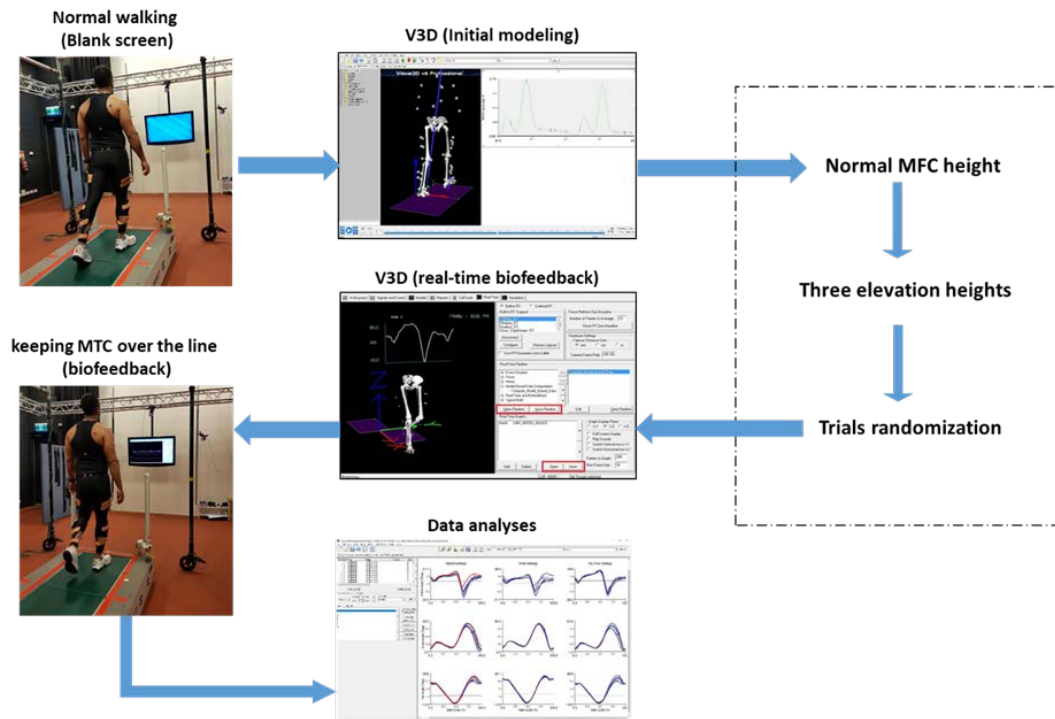


Figure 3.2 Experiment procedure flowchart. Normal walking MTC was used to define three target foot elevations displayed as horizontal lines on a monitor mounted in front of the treadmill. Participants were requested to adopt the target MTC in Normal walking and using the Ankle and No-ankle toe-elevation strategies.

3.2.4 Data analysis

3.2.4.1 Modelling

A static trial was first recorded to develop a skeletal model for each subject. Position-time data of all markers included in each subject/trial were gap-filled using Vicon Nexus software (version 2.7.0, Vicon MX, Oxford, United Kingdom) and exported as c3d files into Visual 3D (C-Motion, Rockville, MD). A whole-body model was specified for each subject using body mass and height, along with captured anatomical landmarks and marker clusters. The pelvis segment was defined using the markers located on the Anterior Superior Iliac Spine (ASIS) and Posterior Superior Iliac Spine (PSIS) for right and left sides. The femur segment was then modelled using the greater trochanter as the proximal head, pre-defined in the pelvis model, and the lateral-medial knee markers were used to define the segment's distal head. Proximal and distal extremities of the shank were also defined by the medio-lateral knee and

medio-lateral ankle markers respectively. The orientation of these segments was specified using shank and thigh marker clusters. The distal foot was created with metatarsals 1 and 5 (i.e., MT1 and MT5) and the heel, lateral ankle and medial ankle were used as proximal landmarks.

3.2.4.2 Defining the foot virtual marker

A point above the big toe was used to control toe trajectory in the experimental presentation, i.e. MTC. In subsequent analysis, however, a point beneath the shoe at the lowest part of the forefoot i.e. MFC, was defined, as discussed in the earlier review. Two additional markers were placed on the 1st and 5th metatarsal heads to form a triangle with the forefoot toe marker with the centroid defining the foot position (Fig. 3.3). A Visual3D pipeline was developed to locate the real-time centroid position two-thirds of the distance from the triangle vertex of the opposite side. The foot virtual marker was defined by adding the fixed distance between the surface of the shoe and sole (Fig. 3.3).

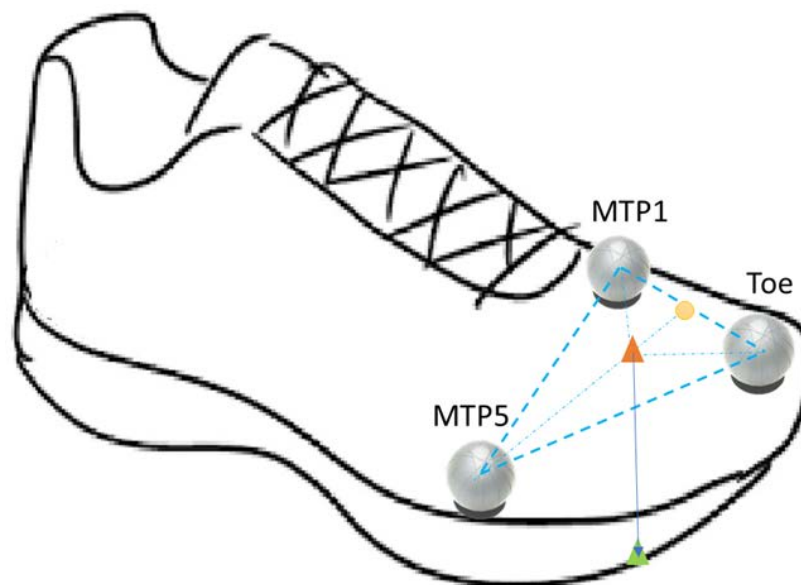


Figure 3.3 The imaginary foot marker was defined based on the centroid point (orange triangle) of the triangle made by toe and metatarsophalangeal joint one and five markers. The foot virtual marker (green triangle) was defined by vertically projecting the centroid to the outsole.

3.2.4.3 Defining swing phase events

Using Visual 3D, the raw data were smoothed using a 4th order zero-lag Butterworth filter with a cut-off frequency of 10 Hz. The swing phase was defined

using toe-off and heel strike events (Winter, 1991) employing kinematic rules based on the vertical and horizontal displacement, velocity and acceleration of foot virtual marker and heel markers (Fusco & Crétual, 2008; O'Connor et al., 2007). Toe-off was defined as when the foot virtual marker's global minimum vertical displacement was followed by zero anterior-posterior and medio-lateral velocity and heel strike coincided with minimum heel marker vertical velocity.

The global maximum vertical displacement of the foot between toe-off and heel strike was used to define Mx2 and the local maximum between toe-off and Mx2 defined Mx1; MFC could then be identified as the local minimum between Mx1 and Mx2. When a clearly defined MFC event could not be identified, a point of inflection was defined using the first and second derivative of foot vertical displacement, described later (section 3.3.2).

3.2.4.4 Joint angles

The time-history of ankle, knee and hip joint angles were normalized to swing phase duration (Winter, 1991). Joint angles were defined as follows: Knee - greater trochanter, lateral knee and lateral malleolus; ankle - metatarsophalangeals, lateral malleolus and lateral knee; pelvis - acetabulum and lateral knee for the hip. Joint angle orientations were defined as dorsiflexion/flexion (positive) and plantarflexion/extension (negative) (Wu et al., 2002).

3.2.4.5 Statistical analysis

MFC, foot maximum horizontal velocity timing and MFC/Mx1 ratios were compared for Normal walking and the MFC elevation conditions using paired t-test (SPSS, Version 22, Chicago, IL, USA). Linear regression analysis was used to investigate the coincidence of MFC and foot maximum horizontal velocity timing. R-squared values were computed to determine the interdependence of maximum horizontal velocity timing variance and MFC timing. When the MFC event was not clearly defined, inflection points were used in the analysis (section 3.3.2).

3.3 Results

3.3.1 Joint angles

Experimental conditions were recorded for ten subjects at preferred walking speed (mean=3.67m/s, SD=0.67). Adaptation of joint angles as a consequence of incremental MFC changes using either the ankle joint only or by not employing the ankle are shown in Fig. 3.4; each column displays the results for Normal, Ankle and No-ankle strategies across the experimental MFC elevations, i.e. Normal walking MFC, Normal MFC+1.5 cm, Normal MFC+3.0 cm and Normal MFC+4.5 cm.

The effects of strategy can be clearly seen in the swing phase ankle angles. Using an Ankle strategy, the ankle angle changed from negative (plantarflexion) to positive (dorsiflexion) beyond 30% of swing while remaining essentially negative in the other two strategies. The hip and knee joint adaptations were similar using Normal and No-ankle strategies, but the Ankle strategy led to different hip and knee adaptations. The knee flexion angle decreased by lifting the foot using an Ankle strategy while it increased in the No-ankle and Normal strategies. Moreover, no hip adaptation was seen when using an Ankle strategy while hip angle increased to lift the foot in the Normal and No-ankle strategies.

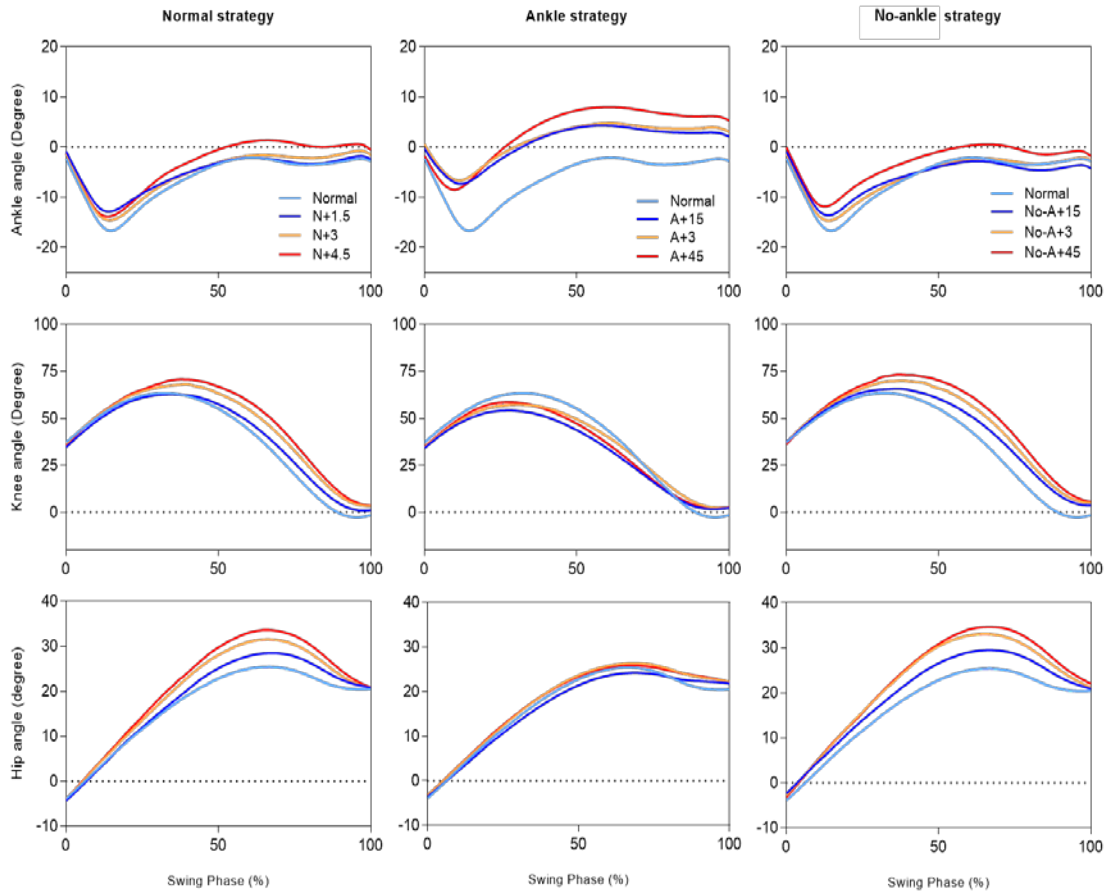


Figure 3.4 Lower limb joint angles across three walking conditions (Normal, Ankle and No-ankle strategies) and target MFC heights (a positive angle was assigned for dorsiflexion/flexion and negative for plantarflexion/extension).

3.3.2 Foot trajectory

From the data presented in Fig. 3.5, intentionally increasing MFC to cross small obstacles (<60mm) changed the normal pattern of foot trajectory events. The pattern modifications are shown with Cyan, Blue, Orange and Red lines for the experimental conditions of Normal MFC, Normal MFC+1.5 cm, Normal MFC+3.0 cm and Normal MFC+4.5 cm, respectively. Normal and No-ankle strategies showed an approximately similar pattern in which Mx1 height remained higher than MFC across all MFC height manipulations. Mx2 height, however, decreased marginally using a No-ankle strategy. By using an Ankle strategy, on the other hand, Mx1 height was little affected but Mx2 height was raised.

To further understand ankle modification effects on foot trajectory control, the MFC/Mx1 ratio was calculated (Fig. 3.5). In both the Normal and Ankle strategies, the

MFC/Mx1 ratio increased significantly above normal walking but remained less than one, with a maximum 0.72 for the N+4.5. Using the Ankle strategy, however, MFC height approximated Mx1 and, as a consequence, the usually distinctive MFC event tended to disappear above 4.5 cm elevation. When the ratio reached one, Mx1 and MFC events were absent and the MFC/Mx1 ratio was unquantifiable.

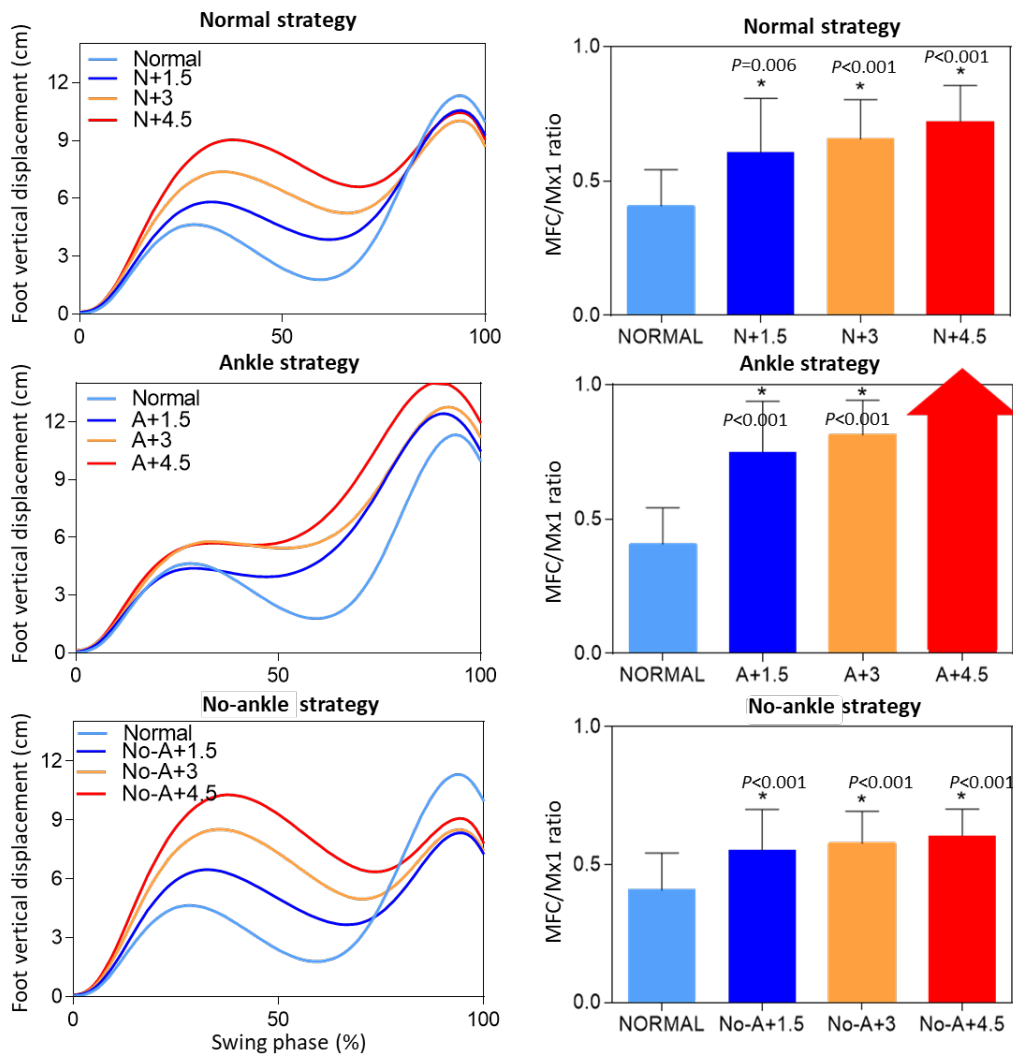


Figure 3.5 Left column: Foot trajectory during the swing phase of the gait cycle using Normal, Ankle and No-ankle strategies. Cyan, blue, orange and red lines represent Normal MFC, MFC+1.5 cm, MFC+3 cm and MFC+4.5 cm, respectively. Right column: the average MFC/Mx1 ratio calculated for each condition. Paired t-tests were used to compare each condition with control Normal walking. Significant differences were shown by * and associated p-values. The MFC/Mx1 ratio in A+4.5 condition exceeded one and showed with an arrow.

Because of ankle-controlled walking, foot trajectory shifted from having clearly defined MX1 and MFC events to trajectories in which MX1 and MFC were not

clearly seen, as shown in Fig. 3.6 (a to c). In normal walking (Fig. 3.6.a) Mx1 and MFC events are evident, the MFC/Mx1 ratio remains below one and the first derivatives of vertical displacement (dz/dt) at those points are also zero. The second derivative, however, is negative at Mx1 (concave down) and positive at MFC (concave up). When MFC height approached Mx1 (Fig. 3.6.b), these two events disappeared and became equal (MFC/Mx1=1). In this situation, Mx1 and MFC merged when the first and second derivative of vertical displacement (z) was zero at a stationary point of inflection. As shown in Fig. 3.6.c, both events are washed out and the first derivation is non-zero. But there remains a point at which the second derivative is zero, a non-stationary point of inflection; when the first derivative (the vertical lifting velocity) is minimum and the sign of second derivative changes from negative (concave down) to positive (concave up). To determine the importance of these two inflection points when MFC disappears, the timing of maximum horizontal velocity relative to those points was investigated.

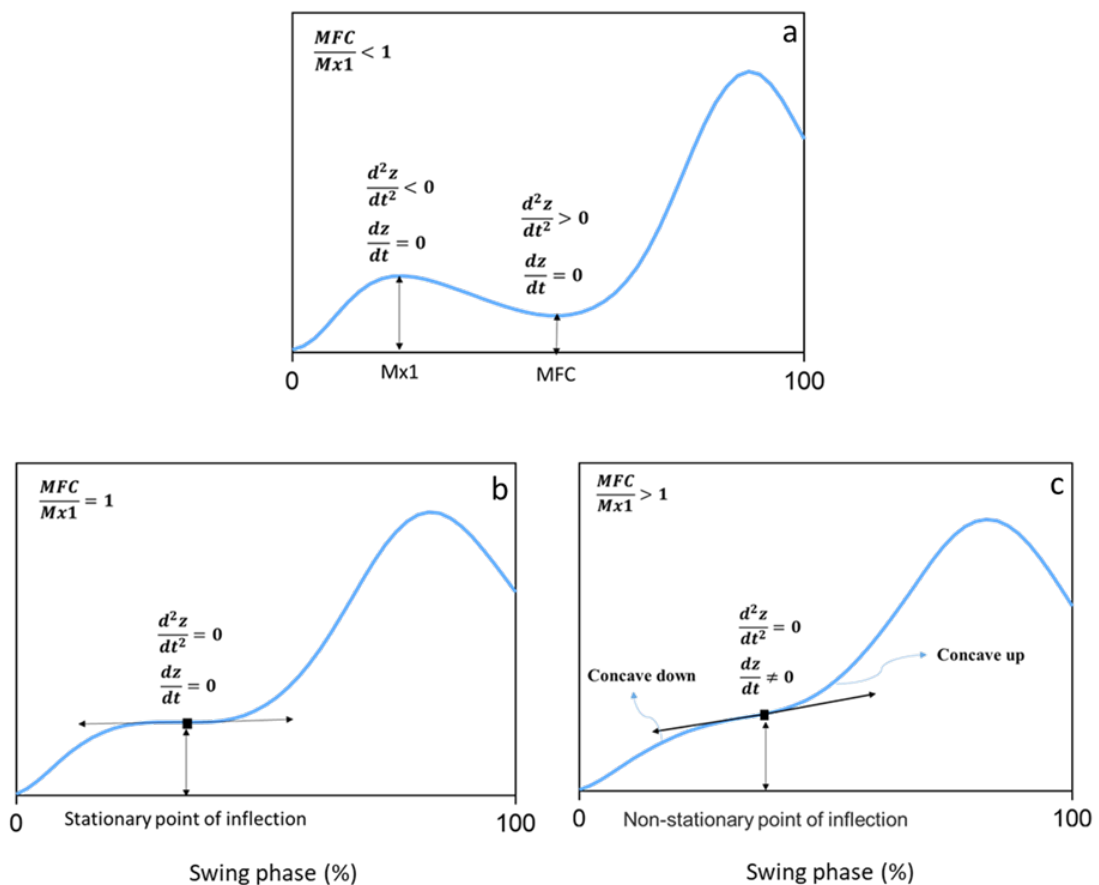


Figure 3.6 Typical swing foot trajectory when; a) MFC is clearly seen and b) MFC is not seen but there is either a stationary point of inflection or c) a non-stationary point of inflection.

3.3.3 MFC and maximum horizontal velocity

The experimentally-constrained foot lifting strategies affected MFC timing and in previous work maximum horizontal velocity of the foot has been reported to closely approximate the MFC event's timing (Winter, 1992). In the extended analysis of MFC timing undertaken here it was also of interest to investigate the horizontal velocity-MFC timing relationship in some detail (Fig. 3.7). For cycles in which MFC could not be recognized (particularly in the A+4.5 condition), the stationary and non-stationary trajectory inflection points were used.

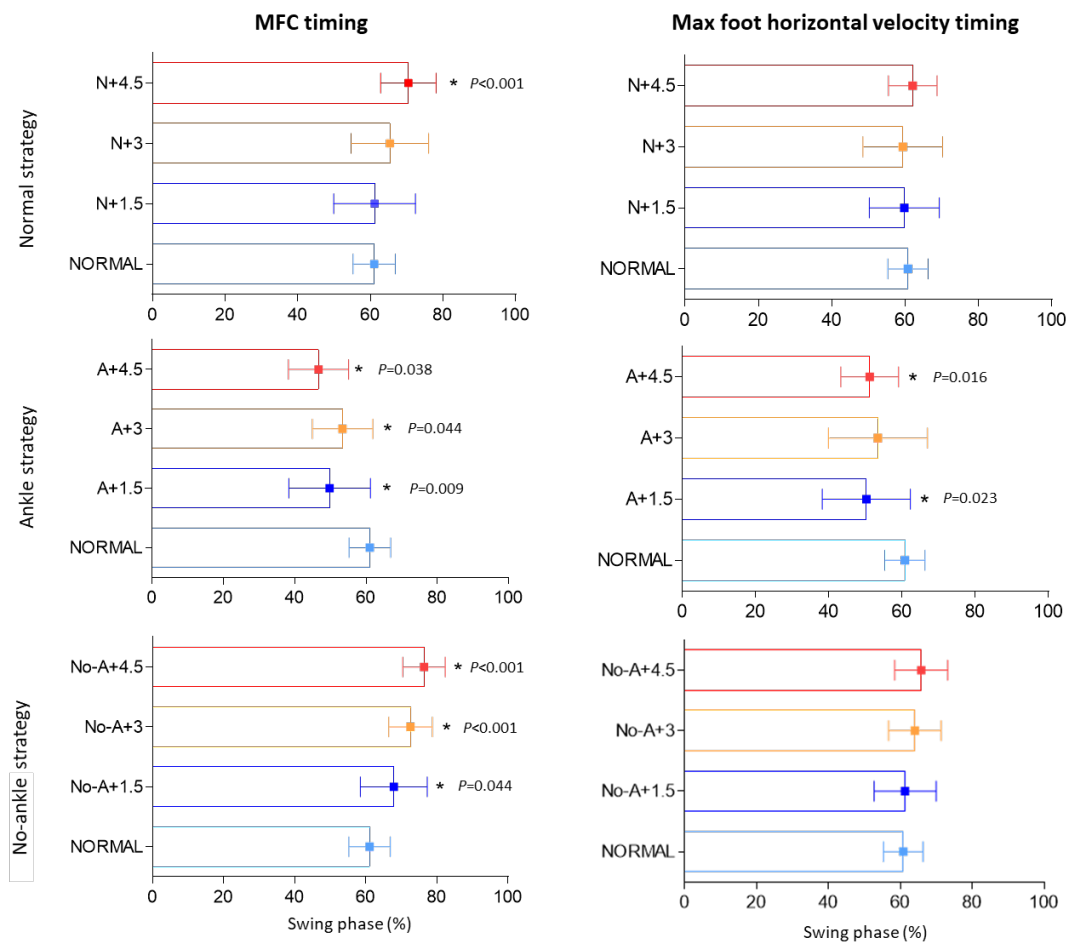


Figure 3.7 Timing of MFC (left column) and maximum foot horizontal velocity (right column) are shown for all three strategies and target MFC heights. Paired t-tests were used to compare each condition with normal walking. Significant differences shown by * with associated p-value.

As shown in Fig. 3.7, MFC timing shifted forward, i.e. later in the swing phase, for both Normal and No-ankle strategies, with this delayed-timing effect statistically significant for N+45, No-A+1.5, No-A+3.0 and No-A+4.5 conditions. Maximum

horizontal foot velocity timing also shifted forward in both the Normal and No-ankle conditions, but no statistically significant effects were observed. For the Ankle strategy, however, the opposite effect was seen, with both MFC timing and maximum foot velocity appearing earlier, as shown by statistically reliable effects across all foot-elevation conditions for MFC (A+1.5, A+3 and A+4.5) but only the A+1.5 and A+4.5 conditions for maximum horizontal foot velocity.

The coincidence of MFC and Maximum horizontal velocity for each condition was investigated using linear regression with goodness of fit shown by R square (Fig. 3.8). The regression line slopes of the timing-velocity functions across strategies were not different (P-values = 0.5078, 0.7788 and 0.972 for Normal, Ankle and No-ankle strategies, respectively). The data were then pooled and regression coefficients recalculated. The pooled data slopes were 0.7775, 0.9586 and 0.4127 for Normal, Ankle and No-ankle strategies, respectively, indicating that MFC timing and maximum foot horizontal velocity were generally coincident, with the Ankle strategy showing the strongest relationship (0.9586).

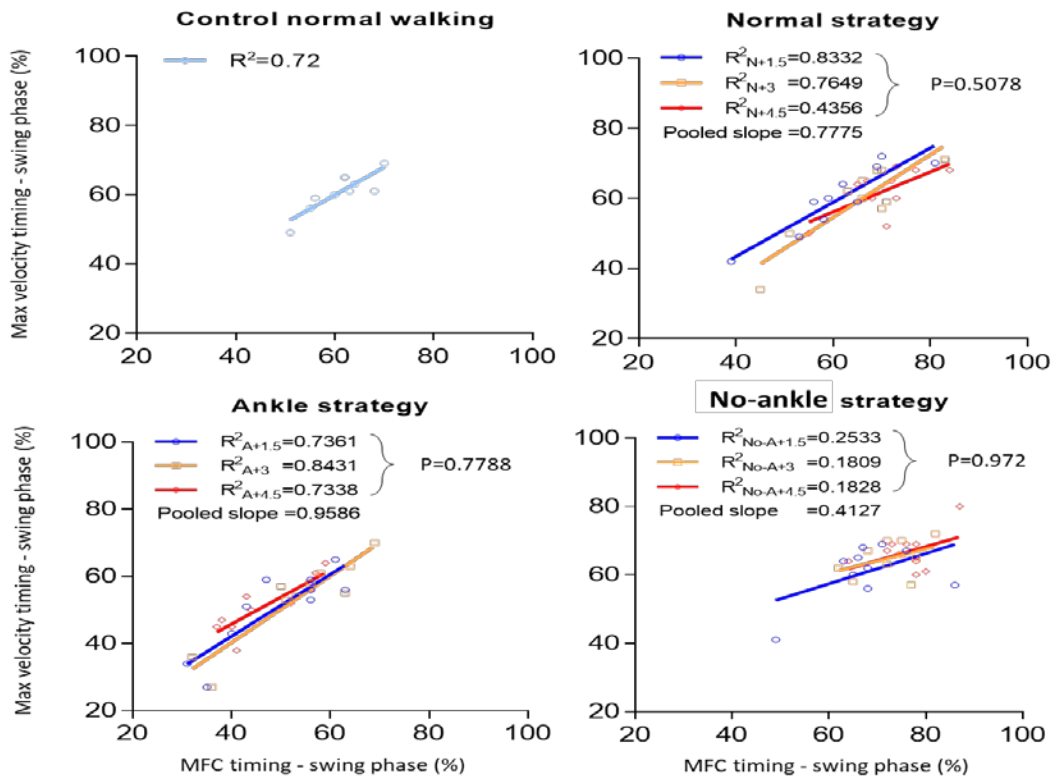


Figure 3.8 The coincidence of MFC and maximum horizontal velocity timing for all three strategies and normal walking. The goodness of fit is shown for each target MFC height condition with R square. Pooled slopes are also shown depicting general coincidence within each strategy.

3.3.4 Swing asymmetry

To determine foot lifting effects on symmetry, the non-dominant limb's sagittal foot trajectory was investigated (Fig. 3.9). Interestingly, in normal walking the non-dominant limb tended to mirror the dominant limb by also increasing MFC (1.7 cm, 2.64 cm, 3.63 cm and 3.22 cm for Normal, N+15, N+3 and N+45 conditions, respectively) but did not when using either the Ankle and or No-ankle strategies.

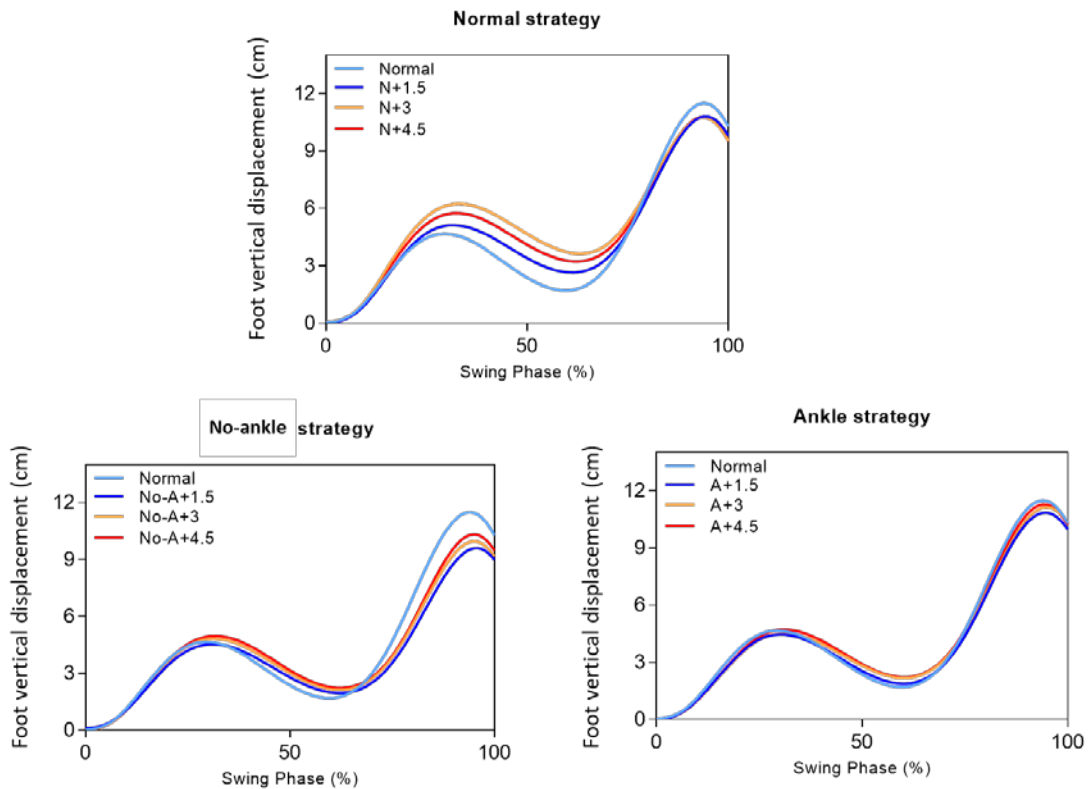


Figure 3.9 Foot trajectory of the contralateral limb during the swing phase of the gait cycle using Normal, Ankle and No-ankle strategies. Cyan, blue, orange and red lines represent Normal MFC, MFC+1.5 cm, MFC+3 cm and MFC+4.5 cm, respectively.

The coincidence of MFC timing and maximum horizontal velocity was also investigated for the non-dominant limb (Fig. 3.10). Similarly, the regression line slopes were not different across strategies with P-values = 0.9726, 0.6265 and 0.9024 for Normal, Ankle and No-ankle strategies, respectively. The pooled slopes were, therefore, calculated as 0.4743, 0.6243 and 0.4880 for Normal, Ankle and No-ankle strategies, respectively showing that MFC timing and maximum horizontal velocity were also coincident for the non-dominant limb. The strongest correlation was again found for the Ankle strategy.

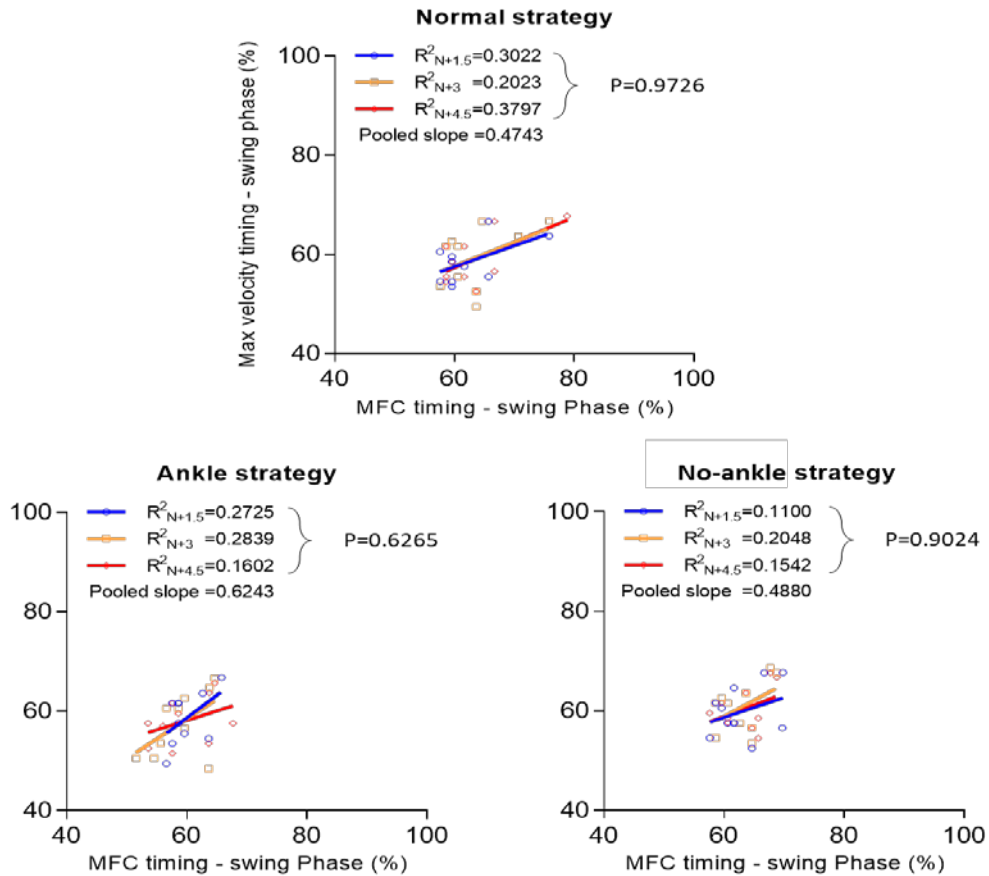


Figure 3.10 The coincidence of MFC and maximum horizontal velocity timing for all three strategies and normal walking for the contralateral limb. The goodness of fit is shown for each condition with R square. Pooled slopes are also shown depicting general coincidence within each strategy.

3.4 Discussion of results

This experiment investigated the kinematics of swing phase control due to intentionally lifting the foot using the ankle joint only, simulating the biomechanical effects of an ankle assistive device. We hypothesized that timing and displacement variables would be affected differently depending on the foot elevation strategy. The following sections summarise and evaluate these findings with an emphasis on the results essential to the ankle exoskeleton developments to be undertaken later in the project.

3.4.1 Joint coordination

Coordination of the three principal lower limb joints, essential to maintaining safe, consistent, foot trajectory control can be considered a (complex) equifinality or

“redundancy” problem; i.e., the same motor task (or action) can be achieved using a range of movements comprising many mechanical degrees of freedom (Bernstein, 1966; Osaki et al., 2007). Similarly, in the present foot-elevation task, all lower limb joints could, potentially, contribute to increasing MFC height, for example by effectively shortening the swing limb (Nagano et al., 2011). In this experiment the contributions of hip, knee and ankle joints were artificially constrained by the experimentally imposed control strategy.

Swing limb joint angles were measured to confirm the specific effects of using only the ankle to control foot elevation. The time-histories of hip, knee and ankle angles showed that the experimental procedure successfully modulated foot elevation using the different control strategies. Ankle angle was higher using an Ankle strategy and the No-ankle strategy showed less ankle involvement than the Normal strategy. Hip angles were not affected by the Ankle strategy, confirming that subjects primarily used their ankle to elevate the foot. The knee, furthermore, showed less contribution in the Ankle strategy compared to Normal and No-ankle strategies, reinforcing that subjects successfully used the ankle to control swing phase foot trajectory.

3.4.2 Non-MFC cycles and the MFC/Mx1 ratio

As shown in Fig. 3.5, in addition to MFC, the experimental strategies also influenced other features of the swing phase trajectory, specifically foot clearance at Mx1 and Mx2. Previous studies have discussed the relationship between these three events and Nagano et al., (2011) showed a significant positive correlation between Mx1 and MFC height, concluding that strengthening exercises associated with Mx1 would also positively affect the following MFC event. Our results also indicated a similar correlation between Mx1 and MFC for Normal and No-ankle strategies. In our data, however, there was no Mx1-MFC correlation for the Ankle strategy with Mx1 height remaining at 5 to 6 cm with only MFC height increasing when the angle was the primary joint activator (Fig. 3.5). In the present study, furthermore, the interdependence of Mx1 and MFC was quantified precisely by computing the ratio of MFC height to Mx1 height (MFC/Mx1). As shown in Fig. 3.5, this ratio increased significantly for all strategies but remained less than 1.0 using the Normal and No-ankle strategies and only exceeded 1.0 when using the Ankle joint predominantly. According to definition MFC is the mid-swing event at which foot-ground clearance

is a minimum and our MFC/Mx1 ratio must remain less than 1.0 for the MFC event to be seen. The importance of the MFC/Mx1 concept is, therefore, that values exceeding 1.0 indicate that MFC and Mx1 events cannot be detected.

The absence of a typical swing phase trajectory, comprising two maxima, one minimum and a clearly defined MFC event, has been discussed elsewhere (Santhiranayagam et al., 2017; Schulz, 2011, 2017). Schulz, (2011) identified MFC in 98% of young participants' swing cycles but suggested that the event may be less well identified in older adults or pathological gaits. Santhiranayagam et al., (2017) revealed about the same proportion as Schulz, (2011), i.e., 2.9% non-MFC cycles for young participants but found 8.7% non-MFC in an older group. Schulz, (2011) and Schulz, (2017) also showed that non-MFC cycles emerge to accommodate uneven walking surfaces, with well-defined MFC cycles decreasing to 80%. Their results mirror the findings reported here, such that when in their experiments the foot was unusually elevated during swing, the characteristic progressive series of events changed and MFC is "washed out", exactly as described by the MFC-Mx1 ratio model presented above.

Santhiranayagam et al., (2017) suggested that the higher frequency of non-MFC gait cycles in older adults, could be seen as an adaptive strategy to reduce the likelihood of tripping. The biomechanics of MFC elimination, with respect to lower limb joint control, had not previously been investigated but here we found that MFC is most likely to be eliminated using ankle joint control. This finding is critical to the present project in suggesting that ankle dorsiflexion is most effective in increasing foot-ground clearance *and* attenuating or eliminating the hazardous MFC event. An ankle assistive device that can increase foot-ground clearance by increasing ankle dorsiflexion should, therefore, have potential as an intervention to reduce tripping risk.

It is, however, important to note that even with MFC absent, there remain swing phase events that can be considered hazardous. It was shown earlier that two conditions were observed when MFC was beginning to dissolve. The first was when MFC/Mx1 was equal to one and vertical velocity was also zero. This event is located at either a local minimum or maximum and mathematically identical to MFC or Mx1, with zero first derivation. For this event, however, the second derivation is also zero, but that condition does not hold for Mx1 and MFC. It can, therefore, be supposed that MFC

and Mx1 events merge to produce a stationary point of inflection which can introduce a hazard similar to MFC if maximum horizontal velocity occurs at the same time.

The second event was when $MFC/Mx1 > 1$ at which the first derivative was not equal to zero, but the second derivative was zero. This can be considered an event with a non-stationary point of inflection. If it is assumed that the foot motion is essentially constant, the horizontal velocity component can approximate maximum when vertical velocity is either zero or minimum. According to this assumption it was, therefore, hypothesized that this event is hazardous because with horizontal velocity approximating maximum, forceful ground contact would be destabilizing. To investigate that hypothesis, the correlation between MFC timing and maximum horizontal velocity was considered.

3.4.3 MFC and horizontal velocity timing

In unconstrained, preferred speed, walking MFC appears at approximately 50% into the swing phase (Winter, 1991), with Mx1 at 25% and Mx2 at 90% of swing (Nagano et al., 2011). In addition to MFC, swing phase maximum horizontal velocity can also be considered a hazardous event (Smeesters et al., 2001), and it is, therefore, important to understand the effects of joint control interventions on maximum foot velocity timing. In this study, therefore, the effects of strategy modification on both MFC and maximum velocity timing were examined.

Winter, (1992) was the first to report that horizontal velocity is maximum at MFC and later work corroborated his findings (Begg et al., 2007; Mills & Barrett, 2001). There are, however, no previous accounts of the correlation between MFC and maximum velocity timing due to walking conditions affecting the ankle joint. In the findings presented here, lifting the foot using both Normal and No-ankle strategies shifted MFC and maximum velocity forward in time, i.e. later. The Ankle strategy caused them to occur earlier, which may be a safer adaptation because there would be more time to recover from any tripping-related instability (Nagano, 2014).

Linear regression analysis indicated less variability in foot elevation using the Ankle strategy. The high positive correlation between MFC and foot velocity in the A+45 condition ($R^2=0.73$) also revealed that even with MFC eliminated, there were stationary and non-stationary inflection points on the foot trajectory; with horizontal velocity approaching maximum and minimum vertical velocity. The study's findings

suggested, therefore, that ankle assisted trajectory control had the potential to reduce tripping risk by attenuating or eliminating MFC. A potentially hazardous point of inflection was, however, discovered that we considered further in determining the biomechanical effects of an ankle exoskeleton.

3.4.4 Joint control effects on gait asymmetry

Asymmetry is frequently considered to indicate gait pathology and Nasirzade et al., (2017) explained the importance of asymmetry in designing orthoses and prostheses. The term “laterality” is used to express the preferential use (limb dominance) of one limb in voluntary motor acts (Sadeghi et al., 2000). Sadeghi, (2003) showed that the dominant leg contributes more to mobility while the non-dominant limb helped in maintaining stability with the effect more pronounced in older people. The findings reported here indicated that the effects of intentionally lifting the dominant foot during normal walking are mirrored in the contralateral limb but, interestingly, was not seen using the Ankle and No-ankle strategies.

3.5 Summary of results

The ankle’s contribution to MFC height adaptation has been of interest to previous researchers (Moosabhoy & Gard, 2006; Sato, 2015). These reports were, however, re-evaluated in preparing to design a device to control swing foot trajectory via the ankle joint. Ankle-controlled walking led to earlier MFC, providing more recovery time if a trip occurred. It was also found that ankle control could attenuate or eliminate MFC by either increasing foot-ground clearance or changing swing trajectory timing. Despite these positive effects of ankle control, the risk posed by high horizontal velocity remains and this event can still be considered hazardous. This event has not been reported previously but may contribute to understanding the biomechanics of lower limb control as an adjunct to the MFC literature. When MFC is not identifiable, the maximum horizontal foot velocity inflection point can be used to reflect high-risk foot trajectory control. Finally, in normal walking, the contralateral limb was seen to mirror the dominant-limb, it was, therefore, assumed that if ankle-controlled walking provided by our exoskeleton could simulate normal gait the device would provide similarly positive effects on the unassisted foot’s trajectory.

4 KINETICS OF SWING ANKLE-CONTROLLED WALKING

4.1 Introduction

As described in the literature review, there are few previous reports of ankle kinetics and mechanical energy exchange during swing. Some studies focused on ankle mechanics during normal walking but not during walking with enhanced ankle dorsiflexion. Following the swing phase kinematics investigation in Chapter 3, kinetic analyses were, therefore, performed to examine ankle joint and associated dorsi-flexor muscle activity in response to intentional ankle-controlled walking. These analyses were particularly important in determining the kinetic demands of ankle-related foot trajectory control.

Moments, impulses, power and work of the three principal joints and the tibialis anterior were computed using AnyBody modelling of recorded data described in the previous chapter. It was hypothesized that using only the ankle to increase foot-ground clearance would require less mechanical energy. In addition, ankle moments and tibialis anterior forces were expected to increase to elevate foot-ground clearance. It was anticipated, furthermore, that hip joint moment and mechanical energy would be greater when primarily using the hip joint to lift the foot and not using an ankle-related foot trajectory control strategy.

4.2 Methods

4.2.1 Musculoskeletal modelling and simulation

Using AnyBody, swing phase musculoskeletal models were also developed for each subject for the Ankle and No-ankle strategies and Normal walking. To target the maximum kinetic contribution of lower body constituents, however, only the Ankle-strategy+45mm and No-ankle strategy+45mm conditions were modelled, providing a total of 24 models; i.e., 3 conditions, Normal walking and the Ankle and No-ankle strategies \times 8 subjects. Models for 8 of the 10 participants were derived because two subjects were excluded due to unsuitable data, as described later.

The 24 musculoskeletal models were developed using the AMS version 6.0 AnyBody Modelling System (AnyBody Technology A/S, Aalborg, Denmark) (Damsgaard et al., 2006). By employing an existing generic model 'MoCapModel' (Managed Model Repository-version 1.6.3) arms were excluded and the lower body model switched to the Twente Lower Extremity Model (TLEM) comprising foot, talus, shank, patella, thigh and hip segments (Carbone et al., 2015).

Initial scaling was performed using body height and mass, pelvis width, trunk height and length of thigh, shank and foot, followed by kinematic optimization. Using the least squared minimization algorithm developed by Andersen et al., (2010), virtual markers assigned to the model (red points in Fig. 4.1) were then fit to experimental markers to specify anthropometric parameters and the local segment coordinates for each subject (blue points in Fig. 4.1). Following optimization, inverse kinematics analysis was used to compute time-histories of joint angles, using the over-determinate kinematic solver developed by Andersen et al., (2009).

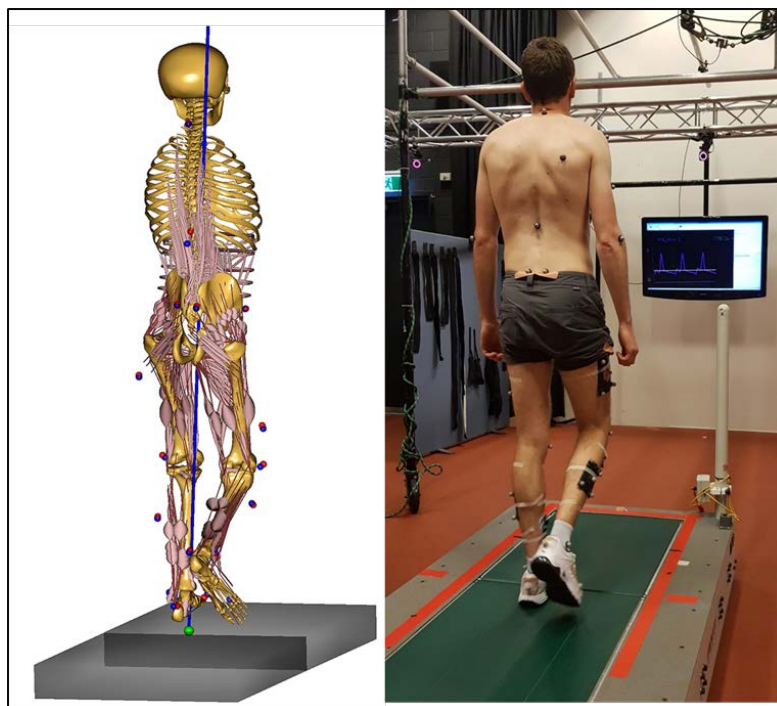


Figure 4.1 Subjects were asked to walk on a dual belt tandem force-sensing treadmill when prepared with thirty-one retro-reflective markers, four marker clusters on anatomical landmarks and EMG electrodes on the Tibialis Anterior and Soleus. Real time sagittal trajectory of the toe marker was shown on a display monitor mounted on the wall in front of the subject. Subjects were requested to match their dominant limb MFC with the displayed target line. The musculoskeletal model associated with each condition is shown in the left image. The experimental markers are illustrated by blue points which matched the virtual markers (red points) using inverse kinematics simulation.

4.2.1.1 Model adaptation for walking on a dual belt tandem (end-to-end) force-sensing treadmill

Using a motor-driven treadmill enabled recording of two minutes walking at constant speed while toe trajectory was under control using the real-time biofeedback technique (Begg et al., 2019). There are, however, challenges when investigating treadmill walking compared to overground (Alton et al., 1998; Lee & Hidler, 2008). The first is measuring Ground Reaction Forces (GRFs) continuously, such that six GRF components should be assigned to each limb with the correct timing of foot contact with each plate. In overground walking, force-event synchronization is less problematic because each foot lands on each plate separately. On a tandem treadmill, each limb contacts the anterior plate first and then travels backwards onto the posterior plate. An analysis method was, therefore, required to detect which limb (left or right) touches each plate and recognise the data from simultaneous foot contact with both plates, when travelling from the anterior to the posterior plate during mid-stance. It was also necessary to exclude data when both limbs contacted the same plate simultaneously.

By using foot horizontal velocity and vertical height thresholds embedded in the model, an algorithm was developed for each subject/condition to detect when the left or right foot made clean contact with the anterior or posterior plate. Two subjects were excluded from simulation because either heel strike or toe-off could not be clearly identified. One clean swing step of each subject/condition in the specified MFC height range was then selected to perform the following inverse dynamics simulation.

4.2.1.2 Simulation

Following GRF detection, the implemented Hill-type three-element muscle model was added to the scaled model (Zajac, 1989) to run inverse dynamics simulation. The muscle redundancy problem was solved by employing the min/max optimization criterion included in the model (Rasmussen et al., 2001) by which the maximum force of each muscle was minimized to ensure the least muscle fatigue. The min/max criterion is defined by minimizing a function of muscle force as follow:

$$G(F^{(M)}) = \max\left(\frac{f_i^{(M)}}{N_i}\right), \quad i = \{1, \dots, n^{(M)}\} \quad \text{eq. 4.1}$$

Subject to:

$$\mathbf{C}\mathbf{f}=\mathbf{r} \text{ and } f_i^{(M)} \geq 0 \quad \text{eq. 4.2}$$

Where:

G: scalar function of muscle forces

F: target muscle force

f: unknown muscle forces

M: number of muscles in the same mechanism

N: maximum muscle strength

C: matrix of coefficients depending on the current position

f: vector of unknown forces

r: matrix of external forces

4.2.2 Data analysis

4.2.2.1 Kinetic variables and swing sub-phases

In previous studies, the swing phase has been described as having three sub-phases, Initial swing, Mid swing and Terminal swing (Fig. 4.2.a) (Whittle, 2014). Unusual or pathological gaits may not, however, always be described adequately using these sub-phases (Wall et al., 1987) and investigation of time-dependent variables such as impulse or energy cost may also require dividing the swing phases into different sub-phases (Donelan et al., 2002). In this study we introduced three new sub-phases; 1) Impulsive sub-phase (Toe-off to Mx1), 2) Maintaining sub-phase (Mx1 to MFC) and 3) Releasing sub-phase (MFC to Mx2) (Fig. 4.2.b). The first sub-phase was labelled Impulsive because rapid muscle reactions are required to adapt to swing after stance phase termination. During the second Maintaining sub-phase, lower-body muscles control the limbs to maintain the foot-ground clearance provided by the previous Impulsive sub-phase. Following MFC muscle activation is designed to provide controlled foot-ground contact, by releasing the potential energy gained by lifting the foot off the ground, the Releasing sub-phase.

The experimental kinematic data computed in Chapter 3 (joint angles and angular velocities vs. time) were used with the simulated time-histories of joint moments in this Chapter to calculate; (i) angular impulse by integrating joint moment over time, (ii) power, joint moment multiplied by angular velocity and (iii) work, integral of power over time. TA impulse and work were similarly calculated using time-histories of force and power. Results of the moments and power calculations are

presented in Fig. 4.2.a using the above sub-phases, with work and impulse shown similarly in Fig. 4.2.b.

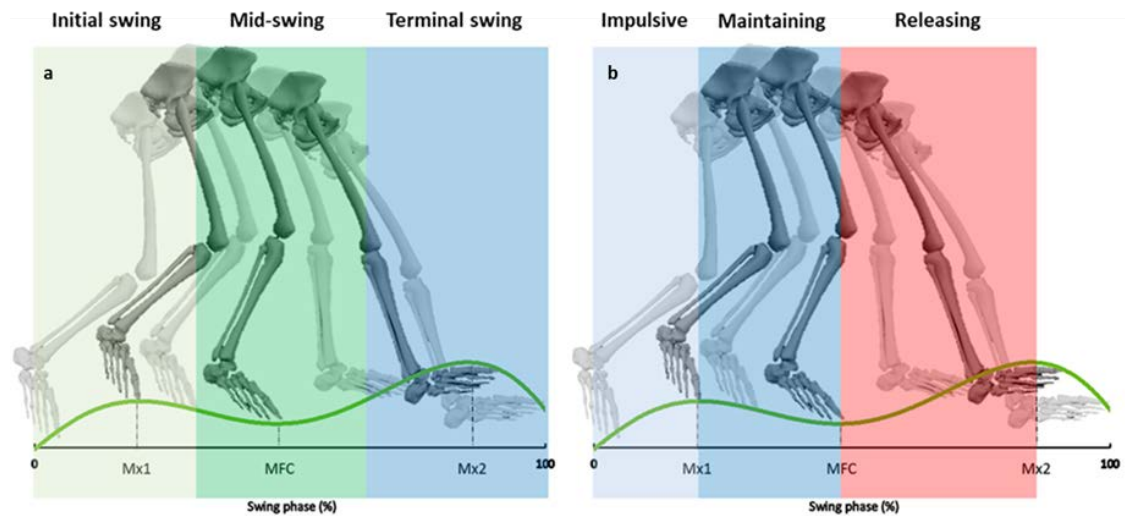


Figure 4.2 Sub-phase regions of the swing cycle. a) classification based on swing cycle percentage; Initial swing, Mid-swing and Terminal swing. b) the swing cycle divided into three sub-phases based on Mx1, MFC and Mx2 events; 1) Impulsive sub-phase (Toe-off to Mx1), 2) Maintaining sub-phase (Mx1 to MFC) and 3) Releasing sub-phase (MFC to Mx2).

4.2.2.2 Muscle Activation

Activity of the tibialis anterior and Soleus was recorded using a 16-channel EMG system sampling at 1000 Hz via a Telemetry 2400T wireless transmitter (Noraxon, Scottsdale, AZ, USA). The skin preparation, electrode placement and recording procedure corresponded to the European recommendations for Surface Electromyography for the Non-Invasive Assessment of Muscle (SENIAM) (Hermens et al., 1999). EMG signals were band-pass filtered (10-500Hz), full waved rectified, low-pass filtered (10Hz) and normalized to maximum activation. Results were then compared with simulated muscle forces to determine the effects of co-contraction during swing (Hortobágyi et al., 2009).

4.2.2.3 Statistical analysis

The mean and standard deviation of the time histories of joints moments and angles were computed. To determine the effect of strategy (Normal walking, Ankle strategy and No-ankle strategy), SPM one-way repeated measures Analysis of Variance (ANOVA) procedures were executed in Matlab (R2018b, the Mathworks Inc., Natick, MA, USA) using the open-source spm1d code (v.M0.1, www.spm1d.org)

(Penny et al., 2011). The SPM{F}, scalar output statistic was calculated and areas in which SPM{F} exceeded the critical F ratio highlighted statistically significant differences.

To investigate condition effects on joint impulse and work, a two-way (3×3) repeated measures Analysis of Variance (ANOVA) was applied (SPSS, Version 22, Chicago, IL, USA), with Conditions (Normal walking, Ankle strategy and No-ankle strategy), and Joints (ankle, knee and hip)

SPM two-tailed paired t-tests were used to compare the Normal walking and Ankle strategy group mean (n=8) TA force and power. The No-ankle strategy was *not* included in this analysis because only the ankle's contribution to dorsiflexion kinetics was of primary interest. A curve analysis was conducted and suprathreshold areas highlighted to demonstrate significant differences between the two walking conditions. Using paired t-tests, TA impulse and work means were also compared within each time-dependent sub-phase i.e., Impulsive, Maintaining and Releasing.

4.3 Results

4.3.1 Foot trajectory

In Fig. 4.3 vertical displacement of the foot during swing is presented and, as discussed in the previous chapter, these results confirmed that by using biofeedback MFC height increments of approximately 40 mm could be achieved in both Ankle and No-ankle trajectory control strategies. As a further reminder, while MFC height increased by about the same magnitude, it appeared later (~70%) using the No-ankle strategy and earlier (~30%) when employing the Ankle strategy. Mx2 timing was unaffected by strategy but Mx1 shifted forward (~35%) during No-ankle walking. These effects also caused the Maintaining sub-phase to decrease using the Ankle strategy and increase using the No-ankle strategy.

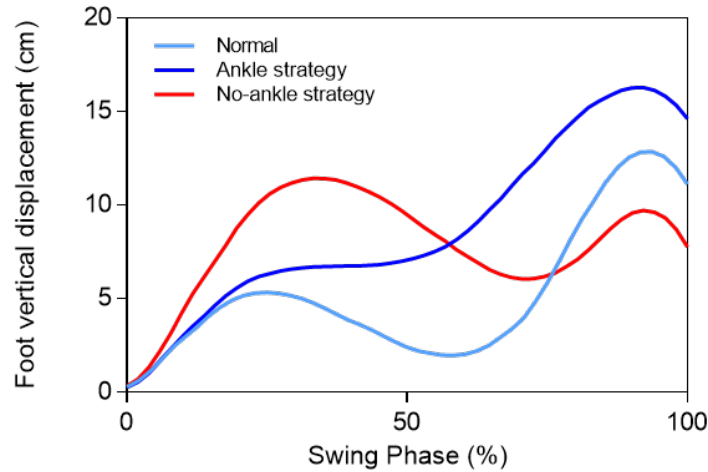


Figure 4.3 The mean of foot vertical displacement during swing. Data were temporally normalized to swing cycle for Normal walking, Ankle strategy and No-ankle strategy.

4.3.2 Joints angles and moments

4.3.2.1 Ankle

The ankle angle data in Figure 4.4.a show a significant increase in ankle dorsiflexion angle throughout the swing phase when participants used an Ankle strategy to elevate the foot. In contrast, the No-ankle strategy did not change relative to Normal walking. The ankle moments, interestingly, were not influenced by the walking strategy and were similar across the three conditions. Most important is that there was no significant difference between Normal walking and the Ankle strategy throughout the swing phase while for the No-ankle strategy, there was a significant decrease in ankle moment only between 30% and 60% of swing.

4.3.2.2 Knee

Compared to Normal walking, knee angle appeared to increase using the No-ankle strategy, with approximately 25 degrees greater flexion around mid-swing but less difference during initial swing and terminal swing (Fig. 4.5.a). The SPM analysis, however, showed significant differences only throughout the initial 50% of swing. In contrast, there was no difference in knee angle between the Ankle strategy and Normal walking. The Ankle-strategy provided a positive flexion joint moment during initial swing while Normal walking and No-ankle strategy showed a negative moment, i.e. extension (Fig. 4.5.b). SPM analysis of the No-ankle strategy confirmed greater knee

joint moment contribution to foot elevation during the initial swing compared to Normal walking and No-ankle strategy.

4.3.2.3 Hip

Hip joint angles for all three conditions were similar (Fig. 4.6.a) but when comparing the hip moments for the Ankle strategy and Normal walking, the Ankle strategy showed greater hip flexion moments during initial swing and greater extension moments during terminal swing (Fig. 4.6.b). A similar difference pattern was seen when comparing the No-ankle strategy with the Ankle strategy in initial swing but opposite in terminal swing.

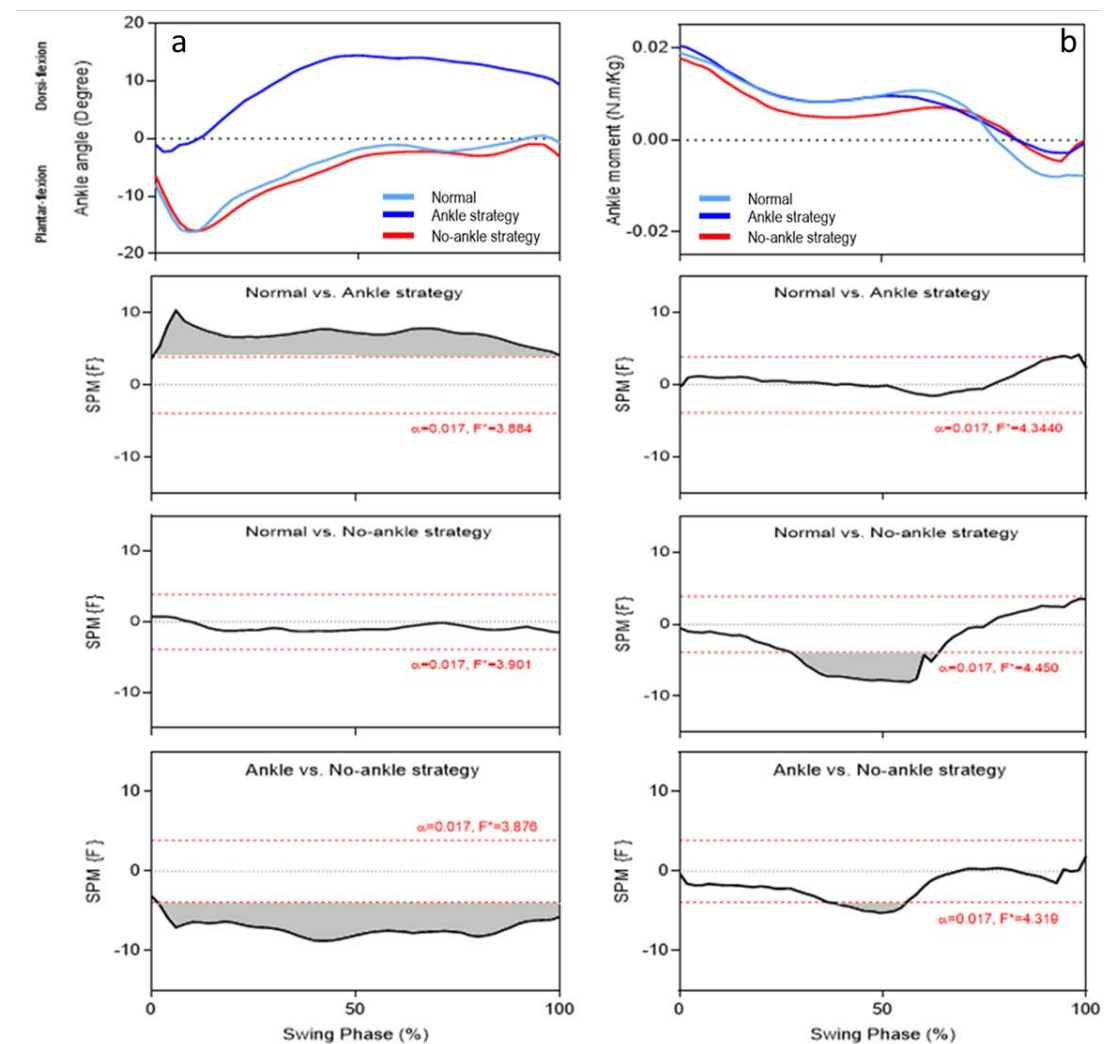


Figure 4.4 Ankle joint moments and angles during swing for Normal walking, Ankle strategy and No-ankle strategy. The positive values are joint flexion and negative represent extension. SPM analysis of variance (ANOVA) results depict significant ($\alpha < 0.017$) timing periods (grey). The critical thresholds (F values) are shown with a red dashed line and supra-threshold cluster probability value are depicted close to the line. The same dashed conventions are used in Figures 4.5 and 4.6 below.

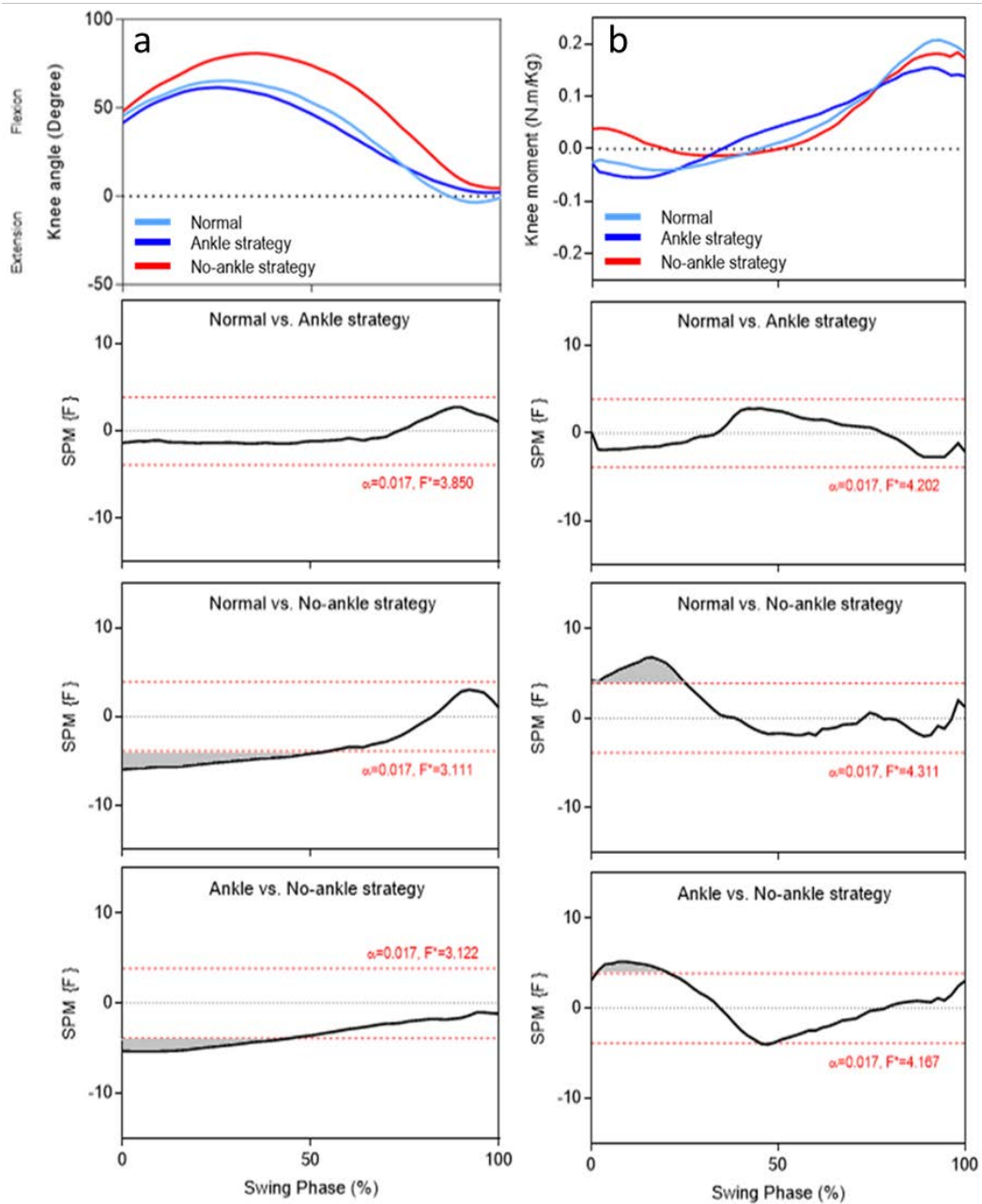


Figure 4.5 Knee joint moments and angles over swing for Normal walking, Ankle strategy and No-ankle strategy.

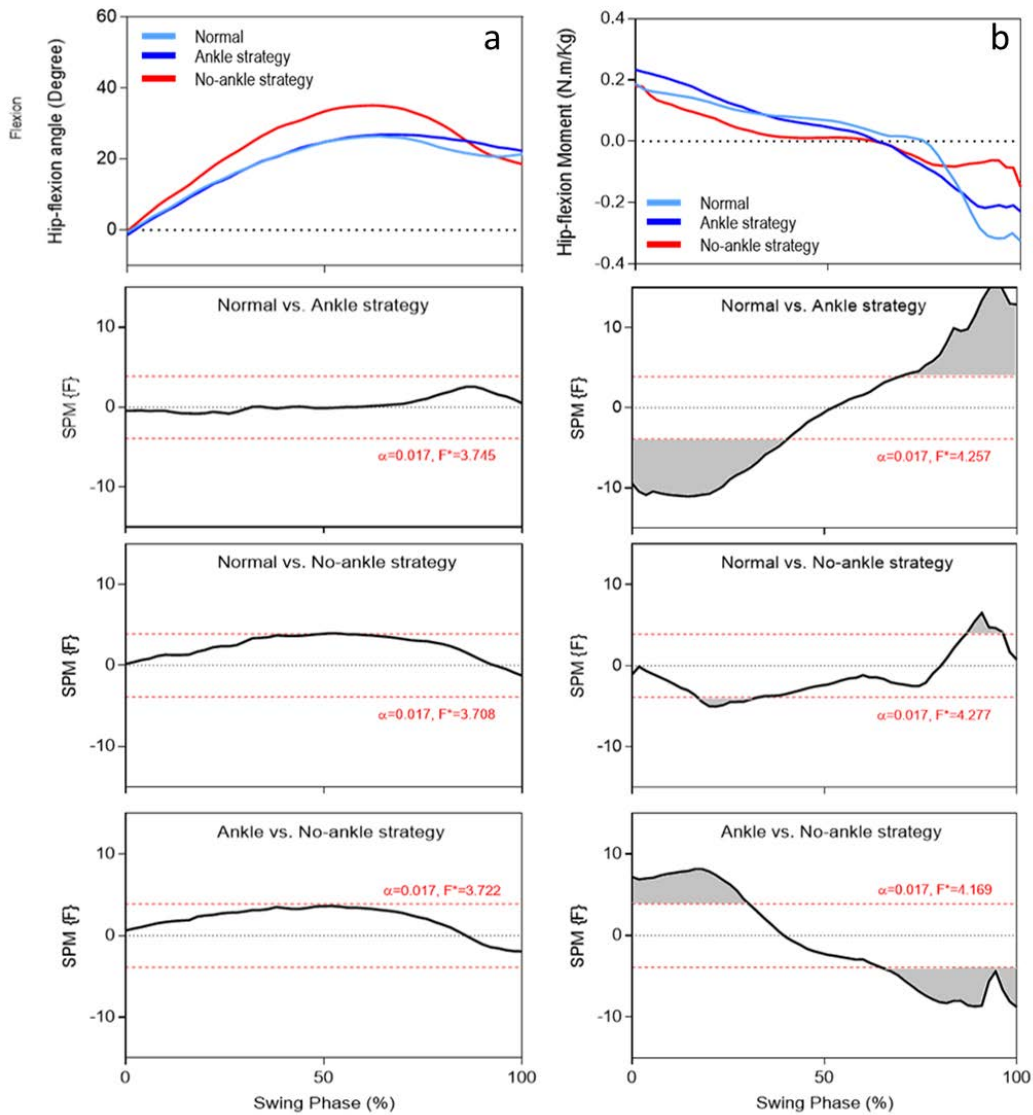


Figure 4.6 Hip joint flexion-extension moments and angles over swing for Normal walking, Ankle strategy and No-ankle strategy.

4.3.3 Joint impulse and work

Flexion/extension impulse and generation/absorption work produced by each joint are shown in Figs. 4.7, 4.8 and 4.9 for Impulsive Maintaining and Releasing sub-phases, respectively. Data were body mass normalized and multiplied by 1000 for scaling; p-values for the Analysis of Variance (ANOVA) are summarized in Tables 4.1 and 4.2.

4.3.3.1 Impulsive sub-phase (Fig. 4.7)

Impulse: Ankle joint (angular) impulse for the Ankle and No-ankle strategies was not different from Normal walking. The knee joint, however, revealed an increased flexion impulse in the No-ankle strategy (2.79×10^{-3} N.m.s/Kg) compared with both Normal walking and the Ankle strategy. The opposite pattern was seen for knee extension which was lower than the other strategies. Surprisingly, hip flexion impulse using the Ankle strategy (20.56×10^{-3} N.m.s/Kg) was significantly greater than No-ankle strategy and Normal Walking.

Work: Work generated by the Ankle strategy (3.01×10^{-3} Joules/Kg) appeared to be higher than Normal walking and the No-ankle strategy. Analysis of Variance (ANOVA) only confirmed, however, that No-ankle strategy work was significantly greater than the Ankle strategy. As with impulse, the knee joint showed a significant increase using the No-ankle strategy and although work generated by the hip was also higher using the Ankle strategy (53.19×10^{-3} Joules/Kg) the difference was not supported by the statistical analysis.

4.3.3.2 Maintaining sub-phase (Fig. 4.8)

Impulse: As shown in Fig. 4.8, statistical tests confirmed that ankle joint flexion impulses for both Ankle and No-ankle strategies were lower than Normal walking. The No-ankle strategy, however, showed higher knee flexion impulse and lower hip flexion impulse than both other strategies. The only effect on extension impulse was seen in the knee using the Ankle strategy relative to Normal walking.

Work: The work generated at the ankle joint was lower in No-ankle strategy than Ankle strategy and Normal walking. The knee joint revealed significant absorption work and zero generation using the No-ankle strategy. The hip also showed less work generation than the other two conditions.

4.3.3.3 Releasing sub-phase (Fig. 4.9)

Impulse: The Ankle strategy showed higher flexion and lower plantarflexion ankle joint impulses than for both other strategies. Knee joint impulse was not affected by strategy but the hip joint impulse in extension and flexion was the lowest of the three strategies.

Work: There was no significant difference in joint work generation or absorption across the strategies.

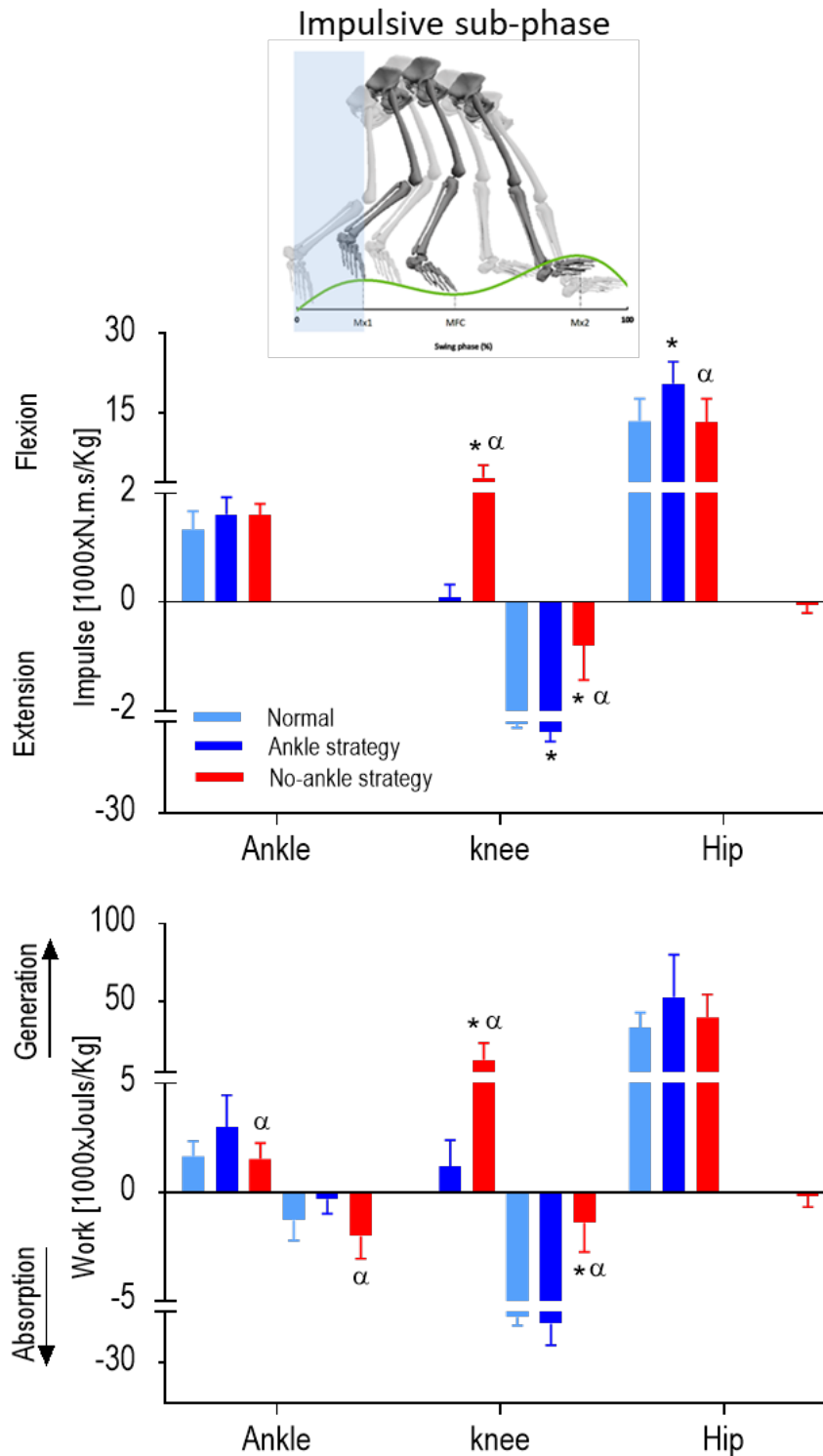


Figure 4.7 Flexion and extension angular impulse and work for each joint during Impulsive sub-phase. * significant difference ($p < 0.05$) between Normal Walking and either Ankle strategy or No-ankle strategy, α significant difference ($p < 0.05$) between Ankle strategy and No-ankle strategy. In some bar graphs the axes are broken for scaling.

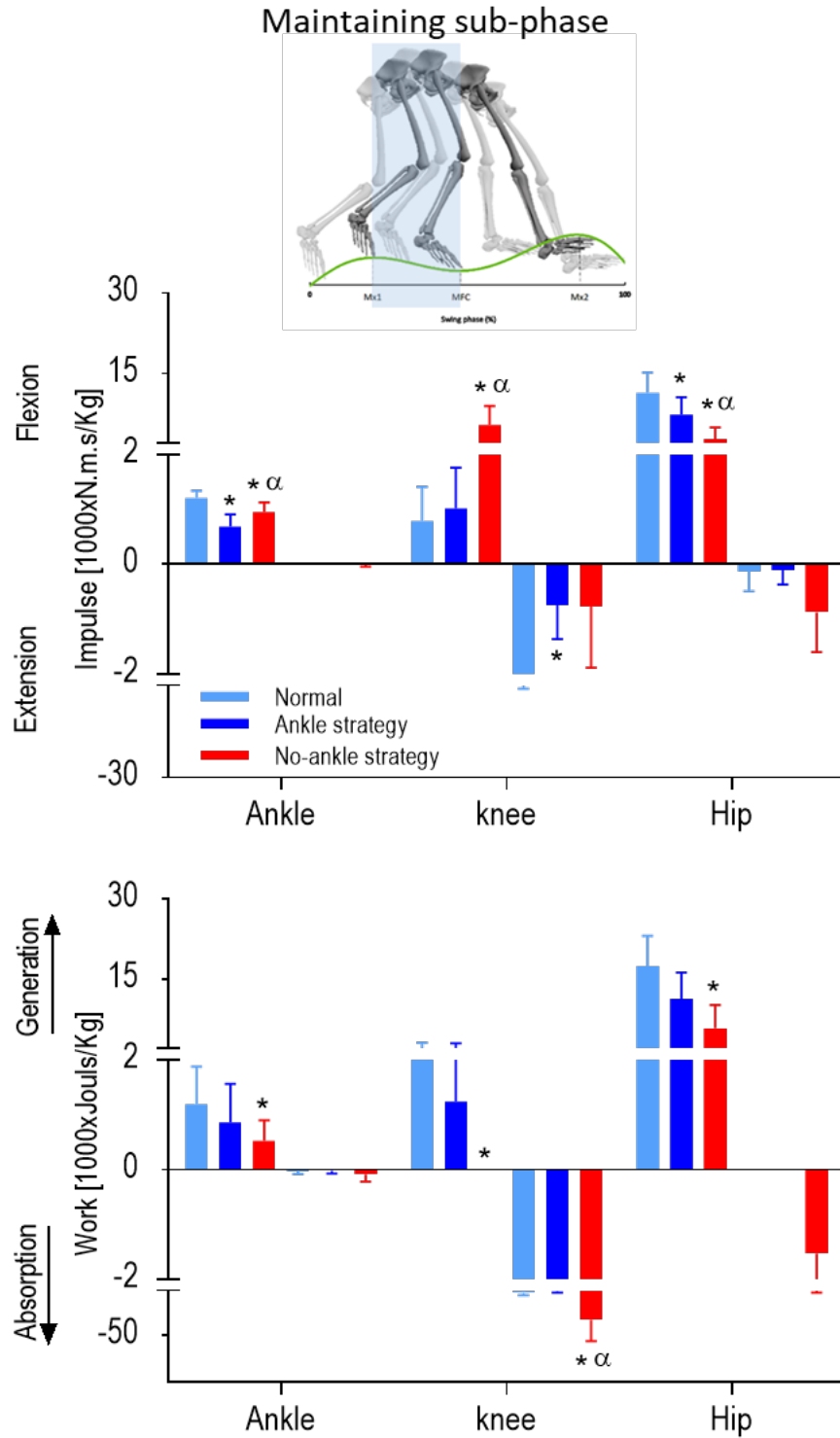


Figure 4.8 Flexion and extension angular impulse and the work for each joint during Maintaining sub-phase. * significant difference ($p < 0.05$) between Normal Walking and either Ankle strategy or No-ankle strategy, α significant difference ($p < 0.05$) between Ankle strategy and No-ankle strategy. In some bar graphs the axes are broken for scaling.

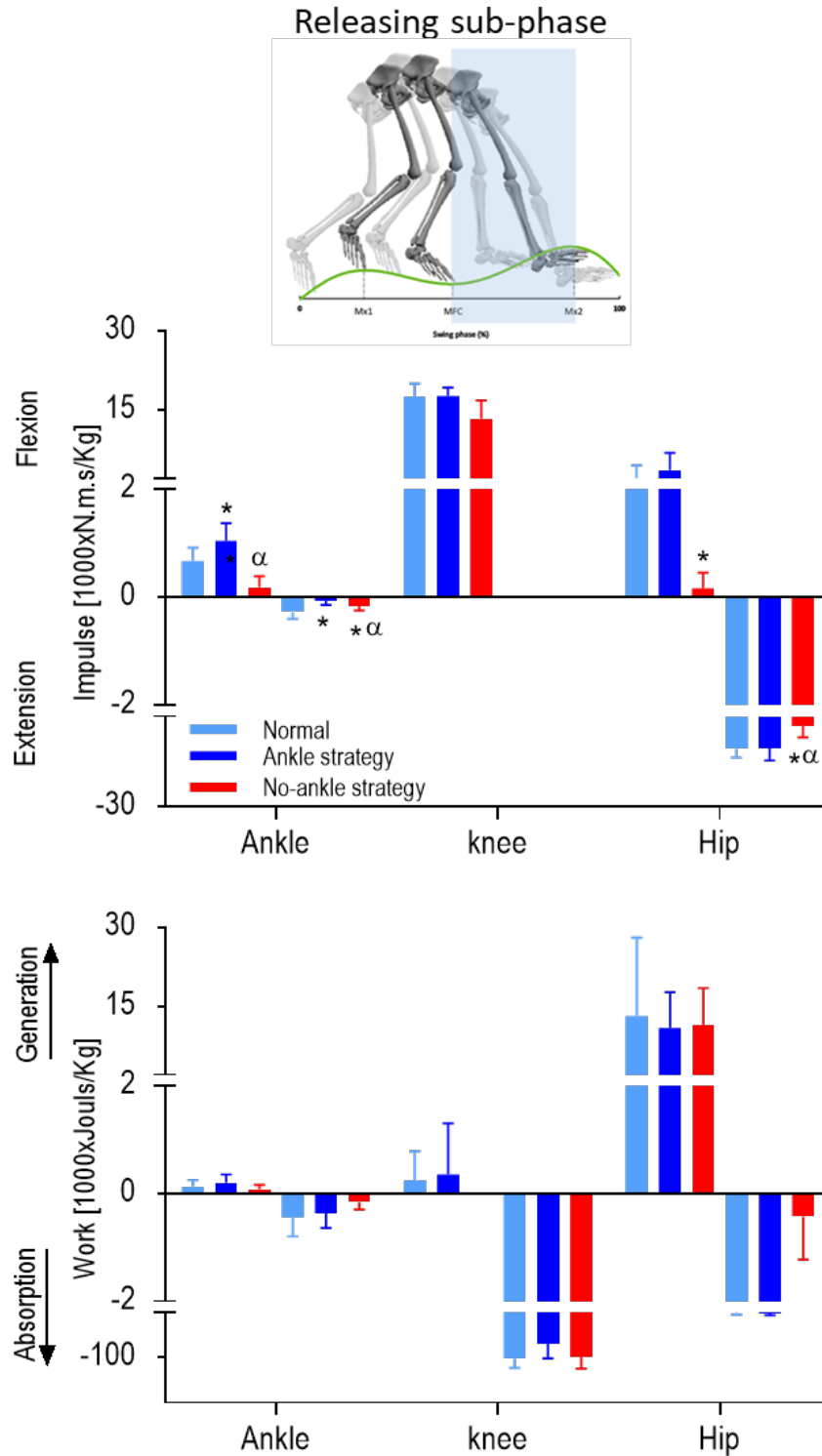


Figure 4.9 Flexion and extension angular impulse and the work for each joint during Releasing sub-phase. * significant difference ($p < 0.05$) between Normal Walking and either Ankle strategy or No-ankle strategy, α significant difference ($p < 0.05$) between Ankle strategy and No-ankle strategy. In some bar graphs the axes are broken for scaling.

Table 4-1 P-values associated with Analysis of Variance (ANOVA) for joint impulses.

	Impulsive			Maintaining			Releasing		
	Ankle vs. Normal walking	No-ankle vs. Normal walking	No-ankle vs. Ankle strategy	Ankle vs. Normal walking	No-ankle vs. Normal walking	No-ankle vs. Ankle strategy	Ankle vs. Normal walking	No-ankle vs. Normal walking	No-ankle vs. Ankle strategy
Ankle dorsiflexion	-	-	-	0.0005	0.0125	0.0484	0.0477	0.0004	< 0.0001
Ankle plantarflexion	-	-	-	-	-	-	0.0003	0.0136	0.0081
Knee flexion	-	0.0292	0.0286	-	0.0233	0.0179	-	-	-
Knee extension	0.0343	0.0014	0.0052	0.0015	-	-	-	-	-
Hip flexion	0.0212	-	0.0327	0.0084	0.0008	0.0123	-	-	-
Hip extension	-	-	-	-	-	-	-	0.0073	-

Table 4-2 P-values associated with Analysis of Variance (ANOVA) for joint powers.

	Impulsive			Maintaining			Releasing		
	Ankle vs. Normal walking	No-ankle vs. Normal walking	No-ankle vs. Ankle strategy	Ankle vs. Normal walking	No-ankle vs. Normal walking	No-ankle vs. Ankle strategy	Ankle vs. Normal walking	No-ankle vs. Normal walking	No-ankle vs. Ankle strategy
Ankle dorsiflexion	0.0587	-	0.004	-	0.0179	-	-	-	-
Ankle plantarflexion	-	-	0.0232	-	-	-	-	-	-
Knee flexion	-	0.0258	0.0398	-	0.0016	-	-	-	-
Knee extension	-	0.0033	0.0444	-	0.0229	0.018	-	-	-
Hip flexion	-	-	-	-	0.0104	-	-	-	-
Hip extension	-	-	-	-	-	-	-	-	-

4.3.4 Total work and mechanical energy

Fig. 4.10.a shows generation and absorption work summed across the three sub-phases for the swing limb ankle, knee and hip (total work). There was no difference in total work generation for the three strategies but for absorption, ANOVA results indicated higher total work in the No-ankle strategy than Normal walking ($p=0.034$). Total body mechanical energy from toe-off to Mx2 was also derived from the AnyBody simulation for each of the three strategies. As shown in Fig. 4.10.b, the Impulsive sub-phase required the least energy and the Maintaining sub-phase showed the highest energy demand but these sub-phase means were not significantly different.

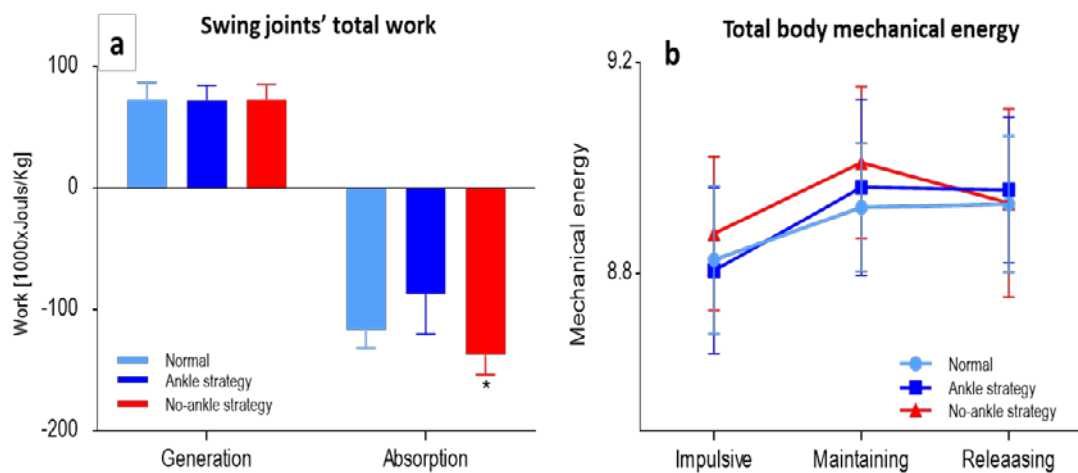


Figure 4.10 Total body energy. a) the sum of swing limb's joints (ankle, knee and hip) generated or absorbed work from toe-off to Mx2 event. b) the total body mechanical energy from toe-off to Mx2 event.

4.3.5 Tibialis anterior muscle

TA muscle force and power for Normal walking and the Ankle strategy are compared in Fig. 4.11 showing that TA force increased using the Ankle strategy throughout swing ($p<0.001$). In contrast, the TA power did not change, except at approximately 25% of swing at which greater power (0.14 Joules/Kg) was seen for the Ankle strategy ($p=0.004$).

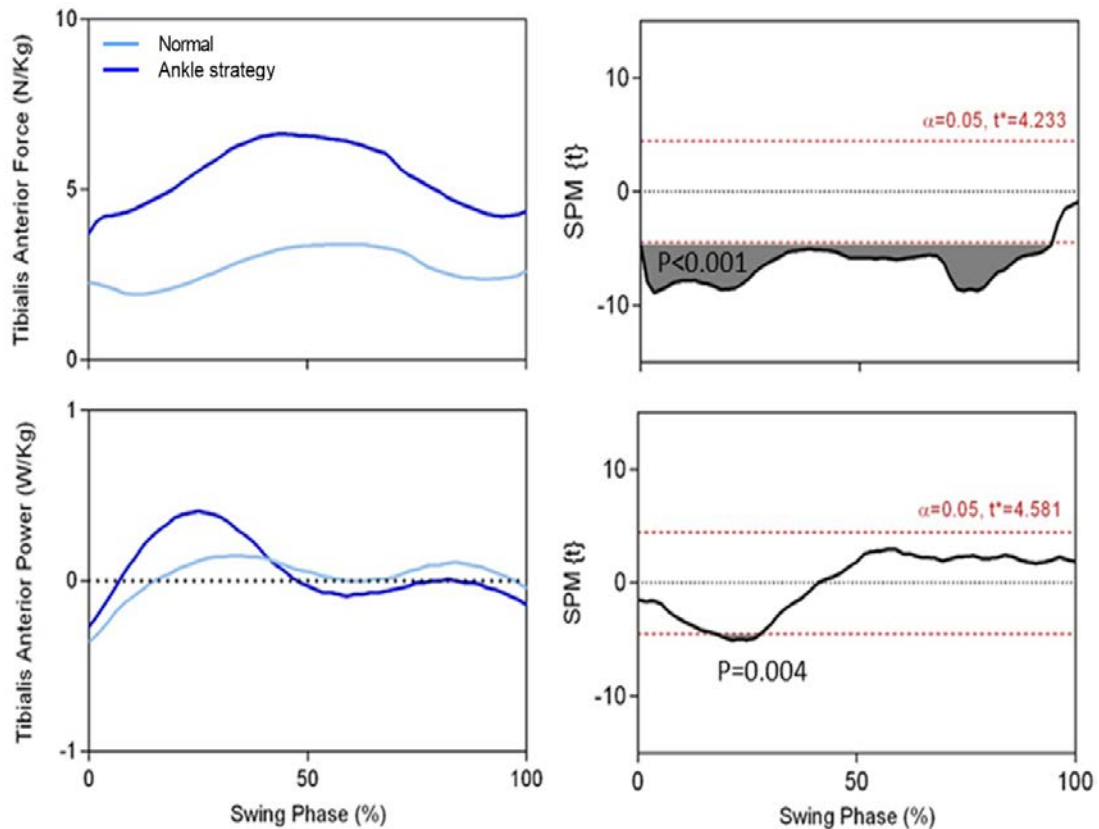


Figure 4.11 Time histories of average TA swing phase muscle force and power for Normal Walking and the Ankle strategy. The paired samples t-test statistic SPM {t} results indicate timing periods showing significant ($p < 0.05$) differences (grey shaded areas). The critical thresholds (t values) are shown with a red dashed line.

As for the joint mechanics, TA muscle impulse and work were compared for Normal walking and the Ankle strategy (Fig. 4.12.a and b). *Total* TA impulse and impulse for the Impulsive and Releasing sub-phases separately were greater using the Ankle strategy. The Ankle strategy also affected TA concentric work generation during the Impulsive sub-phase, with no influence on eccentric work absorption.

Further analysis was undertaken to determine why TA force increased significantly using the Ankle strategy, but ankle moment was unchanged. To do this the TA simulated forces and EMG signals were compared with the Soleus (Fig. 4.13). In the Ankle strategy, the measured Soleus EMG signal showed an increasing pattern similar to TA force, likewise the Soleus revealed force and EMG signal increases during swing that appear to be due to agonist-antagonist co-contraction.

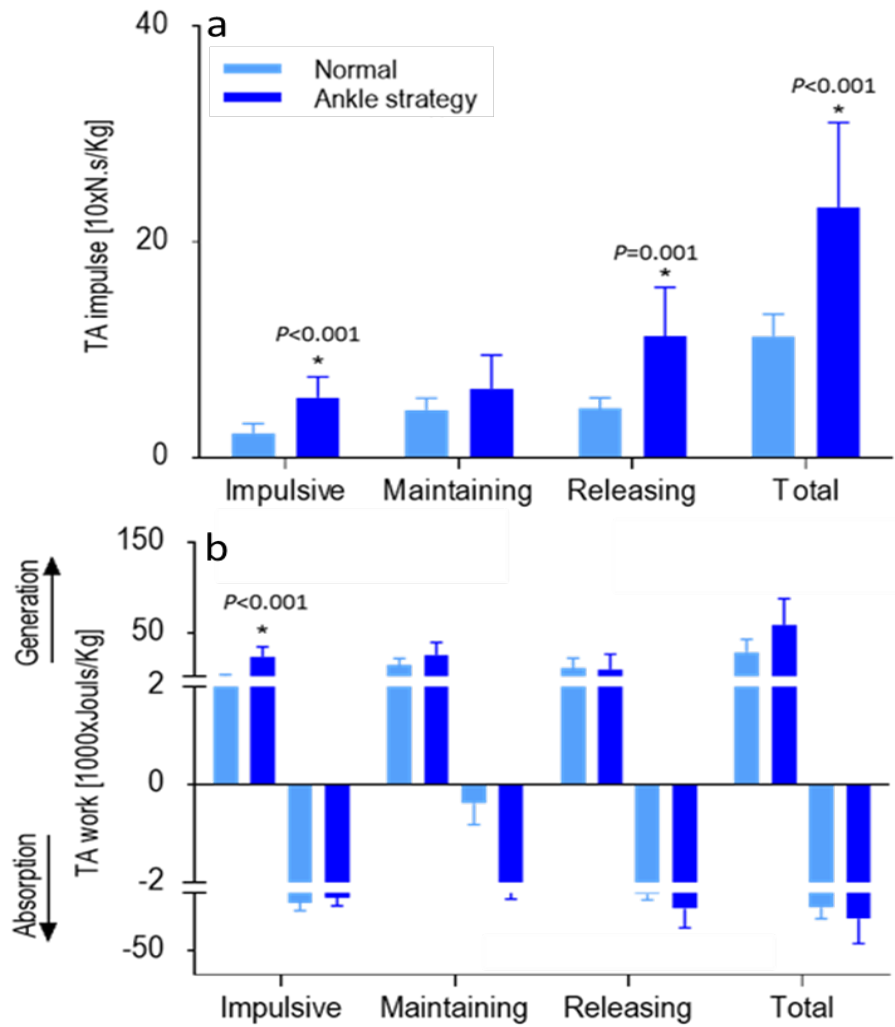


Figure 4.12 The tibialis anterior muscle impulse and work (generated and absorbed) during each sub-phase and total swing. The * symbol indicates the statistically significant difference revealed by paired t-test ($p < 0.05$).

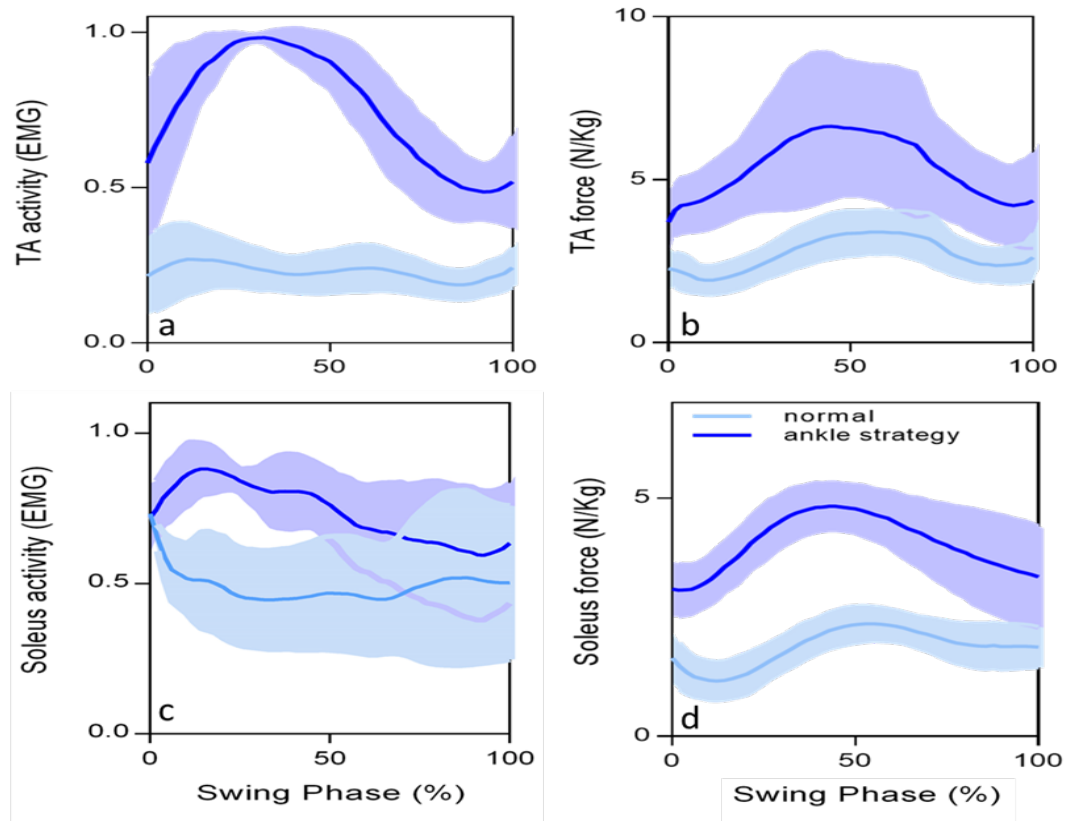


Figure 4.13 Tibialis anterior and soleus swing force during Normal Walking and the Ankle strategy compared with EMG signals normalized to maximum activation.

4.4 Discussion of results

4.4.1 Model validation

Joint moments and power for normal walking, computed using the musculoskeletal model developed to accommodate the tandem treadmill, were supported by published data (Richards, 2018; Robertson et al., 2013; Steinicke et al., 2013; Tözeren, 1999; Whittle, 2014). Our model’s muscle force computations were also confirmed in a recent systematic review of estimated muscle forces during normal walking (Trinler et al., 2018). The simulated and measured TA activation patterns were also consistent with published reports (Arnold et al., 2007; Barrett et al., 2007; Byrne et al., 2007; Di Nardo et al., 2013; Hortobágyi et al., 2009). The TA power time history during normal walking was also confirmed (Bogey et al., 2010).

4.4.2 Swing phase joint mechanics

The kinetics of swing phase ankle motion is important in ankle assistive device design. Computing the time-history of the swing ankle moments was, for example, essential because there were no suitably detailed data in the published literature. Results of this study showed no difference in ankle moment between the Ankle strategy and Normal walking, while the No-ankle strategy showed slightly decreased ankle moment during mid-swing. These findings were, therefore, contrary to our hypothesis that supplementary ankle moment would be required to increase foot-ground clearance via greater ankle dorsiflexion.

Ankle assisted foot trajectory modulation may also affect the kinetics of other joints. The swing phase usually begins with a knee extension moment (Whittle, 2014) but in our experiment, walking with a No-ankle strategy caused a positive knee flexion, significantly higher than both Normal walking and the Ankle strategy. This finding suggests that knee flexor muscles may play an important role as a compensator if ankle function is impaired. Previous studies have also indicated that if ankle power decreases due to gait impairment, the hip joint may play the primary role in compensation, reflected in exaggerated hip flexion (Mueller et al., 1994). In the present study, however, a significant increase in hip flexion and extension moments were seen using the Ankle strategy, during initial and terminal swing sub-phases. The explanation for this finding could be that when using an Ankle strategy, the radius of gyration associated with a straighter, more stiffed-leg gait, may increase during the swing phase, resulting in a greater hip moment. These findings, therefore, failed to support the hypothesis that the hip joint would compensate the absence of ankle joint movement to adjust foot-ground clearance.

4.4.3 Joint impulse and work

In addition to joint moments, the importance of joint impulses has also been shown in both normal and pathological conditions (Chang et al., 2015; Teng et al., 2015a; Teng et al., 2015b). Limb joint work has, additionally, been proposed as an important variable in investigating gait mechanical energy demands (Gordon et al., 1980; Kuo, 2002). In this study, therefore, joint work and impulse were compared between strategies within our time-dependent sub-phases (Impulsive, Maintaining and Releasing).

4.4.3.1 Impulsive sub-phase

Ankle dorsiflexion impulse was similar across strategies, consistent with the earlier observation that joint moments were also not influenced by condition. The Ankle strategy, however, required significantly more work than the others and it can be inferred that more ankle work was required to increase foot-ground clearance but in this condition, not greater moment.

Knee joint motion showed no contribution to either Normal walking or the Ankle strategy, with negligible flexion impulse and positive work. The No-ankle strategy, however, produced an active knee joint contribution by considerably increasing angular impulse and positive work but knee extension impulse and absorbed work were significantly lower in the No-ankle strategy. The knee joint appeared, therefore, to be the most important compensator when walking with a No-ankle strategy and this conclusion is supported by the hip kinetic data showing significantly less hip flexion impulse in the No-ankle strategy than the Ankle strategy. This finding provided further grounds for rejecting the hypothesis that the hip would be important in compensating No-ankle walking.

The more surprising finding, contrary to our hypothesis, was higher flexion impulse and higher average work at the hip joint using the Ankle strategy. The explanation for considerably greater knee work and impulse during No-ankle walking may be the reduction in the swing leg moment of inertia, decreasing the radius of gyration (Bento et al., 2010). Hip joint work and impulse, however, may have increased during the Ankle strategy as the radius of gyration remained close to maximum.

4.4.3.2 Maintaining sub-phase

The Maintaining sub-phase (Mx1 to MFC) varied considerably across conditions, primarily due to Mx1 timing remaining approximately unchanged while MFC moved forward in No-ankle and backward in the Ankle strategy. The Maintaining sub-phase was, therefore, shorter than normal for the Ankle strategy and longer for the No-ankle strategy. The importance of this changed sub-phase timing was that it affected the time-dependent kinetic variables, joint angular impulse and power. The No-ankle strategy showed higher ankle dorsiflexion impulse than the Ankle strategy in the Maintaining sub-phase while demanding significantly less ankle

moment during mid-swing phase due to the longer sub-phase. Knee joint motion in the No-ankle strategy, on the other hand, showed significantly higher negative work, indicating that the knee joint contributed predominantly in the No-ankle strategy by absorbing energy generated during the Maintaining sub-phase.

4.4.3.3 Releasing sub-phase

During the Releasing sub-phase, it was expected that the swing leg would no longer generate energy, and this was supported by ankle and knee absorption work greater than generation work for all strategies. In contrast, the hip showed more generation work than absorption across all strategies. Given that higher hip positive work was also shown in the Impulsive and Maintaining sub-phases, the hip appears to continue energy generation whatever the constraints on limb trajectory.

4.4.4 Total energy

Whole body mechanical energy was investigated to determine the locomotor economy of each swing phase control strategy. Since net mechanical work is equivalent to the change in mechanical energy (Gordon et al., 1980), the sum of generated or absorbed work for each joint across the three swing sub-phases can be used to reveal the total swing phase energy cost. Cavagna et al., (2000) and Ebrahimi et al., (2017) utilized whole body mechanical work to evaluate the energy cost of walking at various speeds. A more detailed analysis of walking speed effects on mechanical work was undertaken by Zelik et al., (2015) summing positive and absolute negative work of the hip, knee and ankle joints independently.

In the present study, using a similar approach, swing leg total positive and negative work were computed. These data revealed no difference in positive work for the three strategies, but negative work was lower using the Ankle strategy. Similar findings of constant total positive work, independent of constituent components, have been reported elsewhere for joint moments. Winter, (1984) found the same total ankle, knee, and hip moments across gait velocities while the individual joint moments varied as a function of walking speed; this phenomenon has been described as “equivalent work sharing” or “mechanical cost-of-transport” to characterize constant total work even with different work values for each constituent (Ebrahimi, 2018). In summary, while swing phase total positive work was equivalent across strategies, lifting the foot

primarily using the ankle can be more economical, possibly due to less eccentric muscle activation.

Total whole-body mechanical energy during gait is not only defined by the swing leg but the support limb also generates and absorbs energy. In early swing the contralateral stance limb first assists by lifting the pelvis, later in swing releasing potential energy (Whittle, 2014). In the present study, whole body mechanical energy was obtained directly from musculoskeletal modelling for the three walking strategies across swing sub-phases. Total body mechanical energy was highest during the Maintaining sub-phase and generally lowest in the Impulsive sub-phase. Since maximum foot horizontal velocity occurs mid-swing and the whole-body centre of mass is highest (Chou et al., 2003) both kinetic energy and potential energy increase at that time. When time-dependent sub-phases were examined, the Ankle strategy required less mechanical energy than the No-ankle strategy in both the Impulsive and Maintaining sub-phases. During release, however, total mechanical energy of the No-ankle strategy was less than the Ankle strategy. In summary, the results from the total energy data supported the hypothesis that a No-ankle strategy would consume more mechanical energy than an Ankle strategy.

4.4.5 Swing TA muscle mechanics

Time-histories of TA force and power are invaluable in optimizing the external timing and magnitude of any ankle-related assistive device. Previous studies investigated the TA contribution to ankle dorsiflexion statically (Bento et al., 2010; Muñoz et al., 2015; Ruiz-Muñoz et al., 2016) but no previous work had examined the kinetics of voluntary changes to ankle dorsiflexion when walking. There is not a direct relationship between EMG signals and muscle forces (Erdemir et al., 2007; Trinler et al., 2018) but we used EMG data only to compare the increasing pattern of TA activity and computed force for model validation. Modelling results from the present study showed that ankle dorsiflexion using the Ankle strategy increased TA force significantly throughout swing. This finding was supported by the EMG data, such that TA activity changed proportionately, supporting our hypothesis that increased tibialis anterior force would be required to lift the foot using high ankle joint dorsiflexion.

An important finding was that ankle moment did not change using the ankle strategy but as discussed above TA force increased. To explain the unchanged moment, the simulated Soleus plantarflexion force and EMG were examined and also shown to increase, contributing to dorsiflexion via co-contraction (Fig. 4.13). It can, therefore, be inferred that intentionally increasing swing ankle dorsiflexion requires a Soleus contribution, which may not be seen if an external assistive device performs this role (Bajelan et al., 2019a).

The time history of TA muscle power was different only around Mx1 and TA positive work was only significantly higher during the Impulsive sub-phase (Fig. 4.12). It was, therefore, concluded that an external device designed to increase ankle dorsiflexion would not be required to provide a significantly greater moment. Higher TA muscle force, specifically during the Impulsive sub-phase should, however, be considered in developing any biomimetic artificial TA muscle.

4.5 Summary of results

This chapter examined the swing phase kinetics of lifting the foot using the ankle joint only, as would be achieved by an ankle assisting device. The conclusions here focus only on the ankle joint but may also contribute to understanding the swing phase joint kinetics associated with other foot trajectory control strategies, such as provided by knee- or hip-related external assistance.

The findings did not confirm the hypothesis that a greater ankle moment would be required to lift the foot using high ankle joint dorsiflexion but there was support for increased TA force. As expected, increased foot-ground clearance required less mechanical energy using the ankle joint than employing the knee or hip. Contrary to expectation, hip joint moments and work did not increase when using only the ankle to lift the foot.

A finding invaluable to ankle assistive device design was the swing time dependency of ankle moments, because previous ankle joint research had considered either the effects of incremental dorsiflexion in static, isometric conditions or walking with no requirement to increase ankle dorsiflexion. The total body energy consumption findings re-emphasized the advantage of ankle joint modulation over the knee or hip joint. The sub-phase analysis was also informative in identifying that energy injection

at early swing was essential to increased foot-ground clearance by mid-swing, at which, in normal walking, lowest clearance is seen, and tripping risk heightened.

Our detailed examination of joint work and impulse during the swing sub-phases can be used in the development of assistive power sources and actuators. Biomimetic-inspired ankle devices using artificial muscles, such as humanoid robots (Schaal, 1999), mimicking prostheses and exoskeletons (Grimmer & Seyfarth, 2014), could also employ our findings to determine how TA mechanics contribute to modulating the swing foot sagittal trajectory. There are, however, some limitations to our findings with respect to assumptions underlying the muscle modelling and optimization methods (Lund et al., 2012). Moreover, parameters such as ankle stiffness or muscle spasm may affect ankle joint kinetics and TA muscle function, which have not been considered (Maganaris, 2000; Roy et al., 2011). In addition to strength, muscle firing rate may also need to be taken into account (Miszko et al., 2003). Further studies would also be important to confirm the role of flexor muscles in swing phase trajectory control.

In summary, it was confirmed that energy injection immediately following toe-off would be a key design feature of our device, to ensure sufficient mid-swing foot-ground clearance. The primary conclusion from the kinetics analysis was that our proposed ankle assistive device would not be required to generate significantly greater ankle moments than for normal unconstrained walking. Key findings are summarized in the following table:

Table 4-3 Summary of Findings - Chapter 4.

No.	Results	Associated Hypothesis	Findings an Interpretation
1	There was no difference in ankle moment between the Ankle strategy and Normal walking	Rejected	The proposed ankle assistive device would not be required to generate significantly greater ankle moments than for normal unconstrained walking
2	Walking with a No-ankle strategy caused a significantly higher positive knee flexion moment and impulse, than both Normal walking and the Ankle strategy.	Rejected	The knee joint appeared to be the most important compensator when walking with a No-ankle strategy.
3	No-ankle strategy consumed more total mechanical energy than Ankle strategy.	Supported	This finding re-emphasized the advantage of ankle joint modulation over the knee or hip joint.
4	Ankle strategy increased TA force significantly throughout swing which was supported by the EMG data.	Supported	Increased tibialis anterior force would be required to lift the foot using high ankle joint dorsiflexion which should be considered in developing Biomimetic-inspired ankle devices using artificial muscles.
5	The simulated Soleus plantarflexion force and EMG were shown to increase, contributing to dorsiflexion via co-contraction.	-	The primary conclusion was that ankle moment did not change using the ankle strategy, but TA force increased due to muscle co-contraction.

5 DESIGN AND CONSTRUCTION OF THE SPAE

5.1 Introduction

As discussed in literature review, the primary challenge was to develop a passive exoskeleton to provide active ankle assistance immediately after toe-off, without push-off restriction. To this end the design and construction of a Self-Powered Ankle Exoskeleton (SPAЕ) was undertaken, using heel strike energy as a power source. Combining the experimental gait analysis findings in Chapters 3 and 4 with the research direction suggested by the literature review of AFOs and exoskeletons, the next stage was developmental project planning, conceptual design and construction of the SPAЕ.

5.2 Design procedure

A systematic chronological, engineering design procedure devised by Pahl & Beitz, (2013) was employed to meet the design requirements for the SPAЕ (Fig. 5.1). Employing the kinetics and kinematics findings in Chapters 3 and 4, the first stage was general planning and task clarification, followed by conceptual design, detailed design, construction and, finally, evaluation (Chapter 6). The entire design phase demanded extensive testing and modifications to the exoskeleton, guided by lower level steps involving information collection, problem solving, modelling, computation and technical drawings using Solidworks.

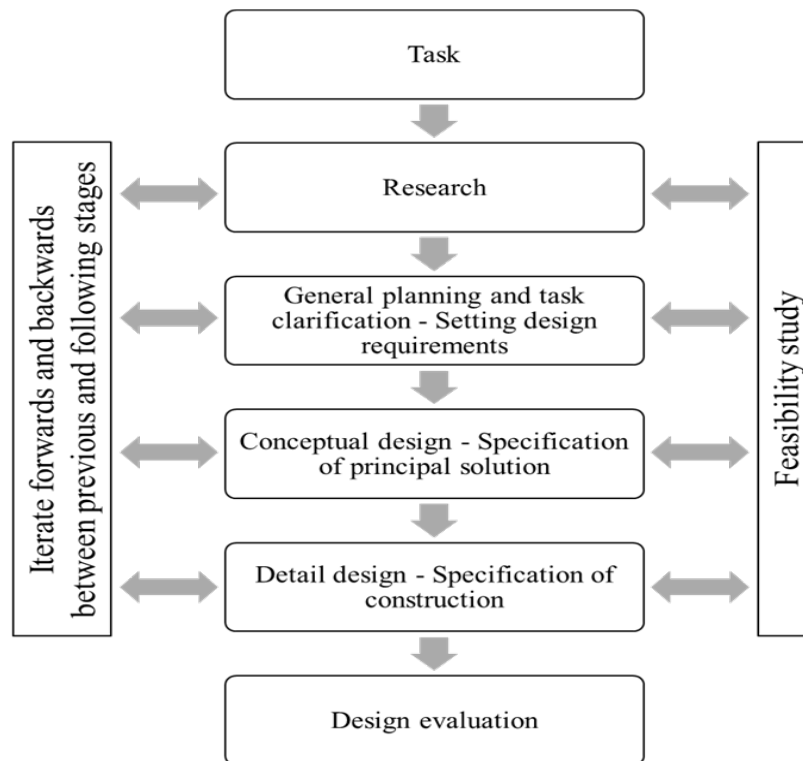


Figure 5.1 The chronological order of design methodology used in this study (from Pahl & Beitz, 2013).

5.2.1 General planning and task clarification: setting design requirements

Having confirmed that ankle control is most effective in increasing foot-ground clearance, the task was to develop an exoskeleton that could actively provide ankle-controlled walking, similar to the intentional ankle control strategy described in Chapter 3. Passive devices are often preferred due to compactness, lightness, low cost, simplicity and portability. But they have two fundamental limitations; (i) no actuators or external power sources and (ii) no gait event detection to control the timing and magnitude of assistive forces. The aim, therefore, was to develop a passive device which would simulate an active device, leading to two major design questions:

- 1) How to generate energy without an electrical power source.
- 2) How to control the timing and magnitude of assistive force application.

Further requirements were that the device should not influence the Centre of Pressure (CoP) path or restrict either sagittal or medio-lateral ankle motion. It was also important that the device should be lightweight and integrated into an ordinary shoe, with no modifications to the outsole.

5.2.2 Conceptual design: specification of principal solutions

Following task clarification, there was a conceptual design phase to determine the principal solutions to the design requirements (Pahl & Beitz, 2013). A range of problems were considered, and solutions proposed (brainstorming) with potential designs changing to meet all requirements. Ease of construction was a constraint given the project's scope and limited budget. Following this process, over two years, the prototype design described below was finalised.

5.2.2.1 Biomechanical energy harvesting principles

As discussed in section 2.3, two biomechanical energy sources have been considered for developing energy harvesting devices. The first is energy provided by negative work via joint loading (Winter, 2009) in which muscles act as a brake and dissipate energy as heat. The second source is heel impact energy, usually lost via footwear and soft tissue cushioning (Nigg et al., 1987; Shorten, 1993). When comparing negative work harvesting with heel strike harvesting, as discussed in the earlier review, heel strike energy recovery is more efficient because muscle negative work recovery requires active contributions by the muscles (Ros et al., 2010). Zelik et al., (2015) estimated heel strike energy dissipation to be approximately 13J while Baines et al., (2018) proposed a 3.8J mechanical energy loss due to force absorption at heel strike.

Discrepancies in calculated harvestable heel strike energy could be due to the nature of the device's mechanism. One method for estimating maximum harvestable energy via a mechanical device is a compressive spring attached to the shoe outsole, as shown in Fig. 5.2. Spring stiffness and compression can then be used to calculate the maximum harvestable heel strike energy. Compression will vary as a function of spring stiffness and imposed load, in our device design spring loading will be due to body mass as shown below:

$$k \times L = BM \times g$$

k: spring stiffness

L: spring length

BM: body mass

g: gravitational acceleration

Maximum stiffness is found when body mass is sufficient to completely compress the spring as;

$$k = \frac{BM \times g}{L} \quad eq.5.1$$

We can write the equation for spring energy as;

$$E = \frac{1}{2}kL^2 \quad eq.5.2$$

Taking k from equation 5.1, the maximum harvestable energy is:

$$E = \frac{1}{2} \left(\frac{BM \times g}{L} \right) L^2$$

Then,

$$E = \frac{g}{2} \times BM \times L \quad eq.5.3$$

As shown in eq. 5.3, harvestable energy depends on spring length, such that greater spring compression enables more energy storage. For example, for a maximum spring compression of 4 cm and 100 kg body mass, theoretical harvestable energy would be:

$$E = \frac{g}{2} \times 100 \times 0.04 = 20 \text{ Joules} \quad eq.5.4$$

It has, however, been estimated that only 50% to 80% of heel strike energy is recoverable, with the balance dissipated (Riemer & Shapiro, 2011). Using this criterion, the harvestable energy computation in in eq. 5.4 would reduce to 10 to 16 Joules. In Chapter 4, it was estimated that only 0.004 Joules/Kg would be required to adequately increase swing phase dorsiflexion, i.e., 0.4 Joules for 100 Kg body mass. This energy requirement appeared, therefore, to be easily harvestable from heel-ground impact using a customized spring mechanism incorporated into the heel.



Figure 5.2 Simple mechanism to harvest heel strike energy using a compressive spring.

5.2.2.2 Energy harvesting, storage and release mechanisms design

Our first design concept was a hinge joint attached to a flat base, which the user could wear like a shoe (Fig. 5.3). At heel strike, the hinged outsole would harvest energy and transfer it to an energy storage-release unit. This mechanism was designed to maintain the foot centre of pressure closer to the ankle joint to prevent an unwanted ankle moment. This design was, however, considered unsuitable because due to its bulk, when open during the swing phase it was unlikely to maintain heel-ground clearance.



Figure 5.3 One concept developed for a harvest-store-release-reset sequence in each step.

A later development minimized the above limitation by using a lever which retracted into the shoe during swing and late stance but, using a synchronized heel strike detector, sprung out when triggered at heel strike (Fig. 5.4). This detector activated immediately at heel strike, allowing the lever to harvest energy throughout the loading response. Furthermore, at foot-flat the system locked, retaining the lever inside the shoe until the following heel strike, with no encumbrance to swing.

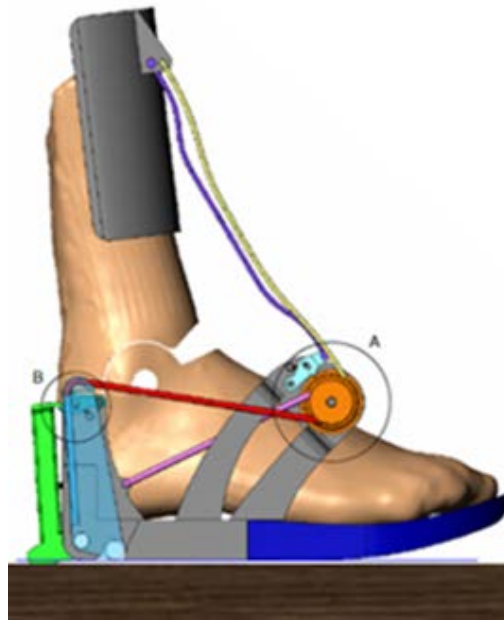


Figure 5.4 Final concept of the heel strike energy harvesting mechanism. The heel strike detector (green) makes the first contact and releases the lever mechanism (light blue) to harvest heel strike energy.

To store energy following harvesting, the concept of using two extension springs was developed. One spring stored the harvested energy and the other reset the system at heel strike (Fig. 5.5). The stored energy then required a mechanical trigger to release it following toe-off, permitting adequate ankle plantarflexion to enable unrestricted push-off. To this end, the conceptual design illustrated in Fig. 5.5 was developed. It comprised a mechanical clutch which locked and unlocked a pulley mechanism, using a cord connected to a calf brace (Fig. 5.5). When the ankle joint exceeded a predetermined plantarflexion angle, the cord unlocked the pulley which, following a short delay, rotated and lifted the foot via a second cord.

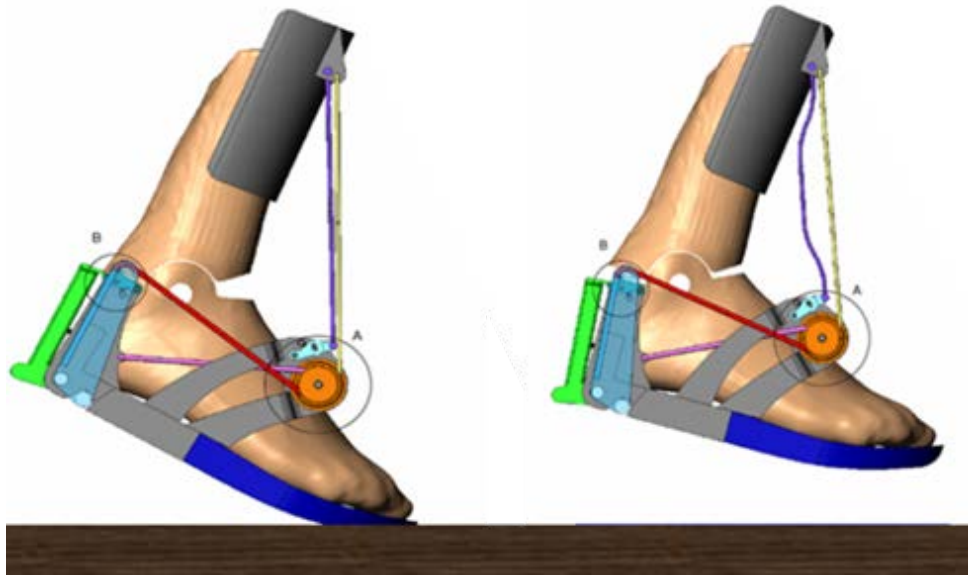


Figure 5.5 Final concept of the energy release mechanism. The toe-off detector clutch detects the maximum predefined ankle plantarflexion angle and unlocks the orange pulley to release the stored energy.

5.2.3 Detail design: specification of construction

To begin construction, a detailed design procedure was used to refine the dimensions, ranges of motion, materials, off-the-shelf and customized components. The feasibility of machining and constructing customized parts was carefully considered. This extensive detailed design phase culminated in the device depicted in Fig. 5.6.a, mounted on the right shoe. As shown in Fig. 5.6.b the SPAE consists of three mechanical units. First the energy harvesting system, that comprises a heel strike detector to activate the harvester lever at initial stance to recover energy up to foot-flat (Fig. 5.6.b). This energy is then redirected to a second storage unit constructed from two extension springs. One spring stores the harvested energy and the second resets the system prior to the following heel strike (Fig. 5.6.b). The third unit is a clutch and pulley that releases energy when the ankle angle reaches a pre-defined plantarflexion. In addition, the stabilizing calf brace incorporates a two degrees of freedom mechanical joint, such that it bends left when walking and then returns to the calf. It is attached with a velcro strap and 3D printed with Nylon 12 (PA2200), making it rigid and lightweight.

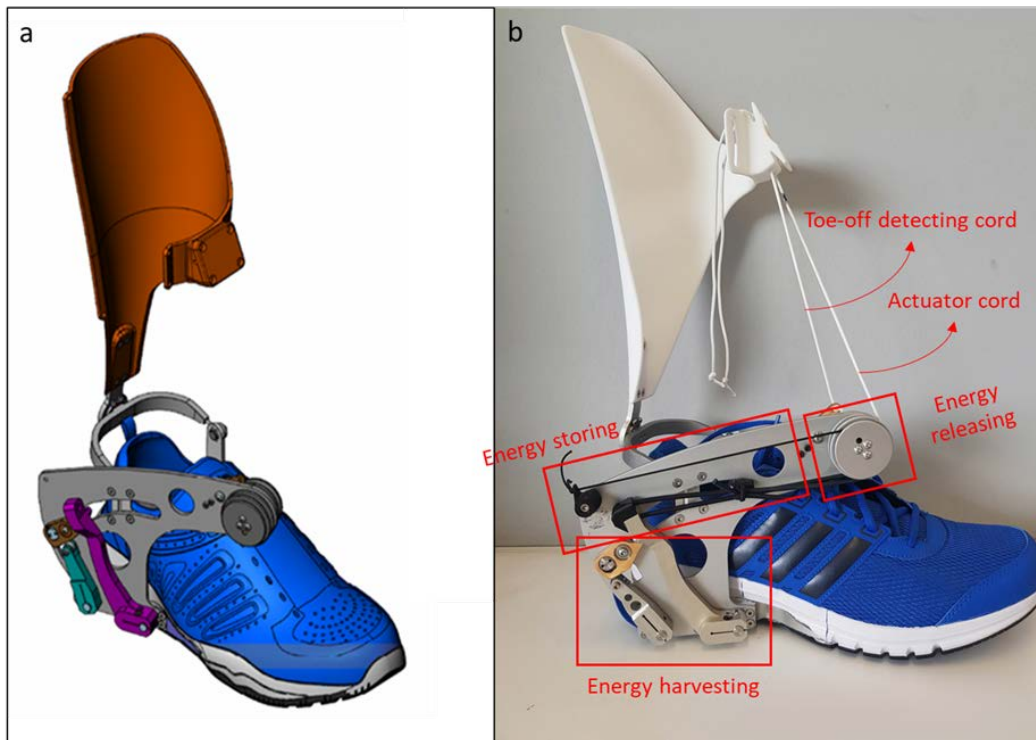


Figure 5.6 a) the final detail-design and b) the constructed prototype using the aluminium material Couple of ball bearings, pulleys and clamps assembled to construct the energy release unit. The toe-off and heel-strike detectors were machined from bronze. See text for further details. Simple mechanical model.

The spring specifications were calculated based on swing phase ankle joint moments for Ankle and No-ankle strategies (Chapter 4). To recap, as shown in Fig. 5.7, there was no significant difference in ankle moments between Ankle and No-ankle strategies. A single ankle moment was, therefore, used to calculate the spring characteristics required to provide ankle dorsiflexion. Maximum ankle moment (0.02 N.m/Kg) occurred immediately after toe-off and decreased gradually up to the end of swing (Fig. 5.7). Furthermore, positive work for the ankle strategy was approximately 0.003 Joules/Kg, 0.00086 Joules/Kg and 0.00021 Joules/Kg for Impulsive, Maintaining and Releasing sub-phases respectively, and 0.004 Joules/Kg for the entire swing phase (Chapter 4).

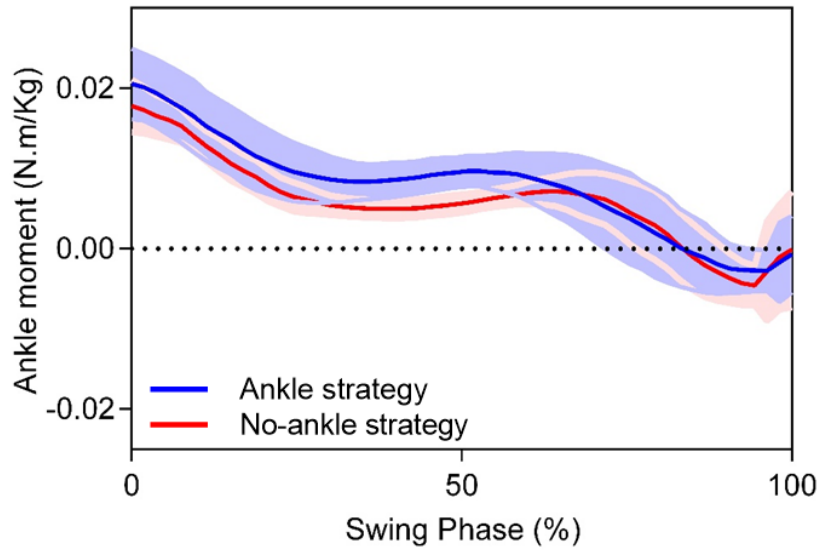


Figure 5.7 Ankle moment time-histories for the Ankle and No-ankle strategies, retrieved from Chapter 4.

The progressively decreasing ankle moments shown in Fig. 5.7, could be simulated using a mechanical spring because, similarly, spring force decreases linearly from its maximum to zero, following either extension or compression (Alexander, 1990). Two extension springs were mounted in parallel to harvest energy and reset the device at each step (Fig. 5.6.b). The results of the mechanical modelling to determine the required harvesting spring's characteristics are presented below. It was unnecessary to model the reset spring because it could be easily adjusted by trial and error.

The assistive moment provided by the SPAE can be calculated as;

$$M_{Assistive} = F_{A-Cord} \times (L \times \cos \theta) \quad \text{eq. 5.4}$$

A-Cord=actuator cord.

L=horizontal distance between ankle centre and actuator cord.

θ =angle of actuator cord with vertical line.

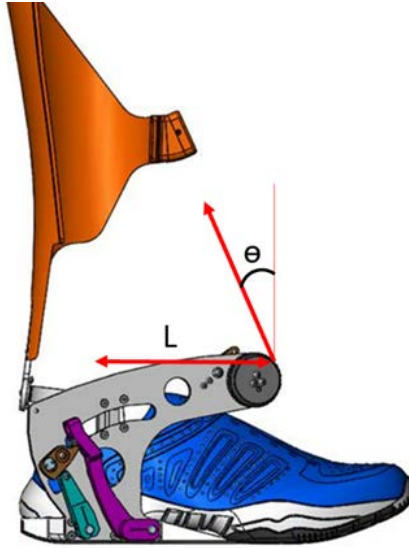


Figure 5.8 Horizontal distance between the ankle centre and the actuator cord ($L=12$ cm) and the actuator cord angle to the vertical ($\theta=32$ degrees).

From Fig. 5.7, the maximum ankle moment required for a 100 kg subject is 2 N.m., given $L=0.12$ (m) and $\theta=32^\circ$ (Fig. 5.8), with a maximum 16.6 N required from the actuator cord. The energy storage unit comprises a main spring and reset spring, working in synchrony. As described above, the main spring stores the harvested energy and the reset spring prepares the device for the next heel strike. We chose a spring that could reset the system sufficiently quickly to allow the harvesting mechanism to activate immediately after heel strike, as follows:

- ✓ *The range of reset spring displacement:* $5 \text{ (mm)} < \Delta x < 90 \text{ (mm)}$
- ✓ *Reset spring stiffness:* $K = 0.05 \left(\frac{\text{N}}{\text{mm}} \right)$, $F_i \text{ (initial tension)} = 4 \text{ (N)}$

$$\text{Thus, } 4 \text{ (N)} < F_{\text{(Reset-spring)}} < 6 \text{ (N)}$$

We can, therefore, write:

$$F_{\text{(Main-spring)}} - F_{\text{(Reset-spring)}} = F_{\text{(A-Cord)}} \quad \text{eq. 5.5}$$

Consider a maximum reset spring force of 6 N, with actuator cord force calculated as 22.6 N, the required spring stiffness is:

$$F_{\text{(Main-spring)}} = K \times \Delta x \quad \text{eq. 5.6}$$

For spring extension of $\Delta x = 40 \text{ mm}$, a spring with at least 0.56 N/mm stiffness, therefore, is required. Two springs were, therefore, employed to evaluate device design with following specification:

Main spring:

- Diameter of Material: $d=1.2$ (mm)
- Coil mean Diameter: $D=11$ (mm)
- Free Length: $L=470$ (mm)
- Spring Stiffness: $K=0.75$ (N/mm)
- Initial Tension: $F_i=9$ (N)

Reset spring:

- Diameter of Material: $d=0.64$ (mm)
- Coil mean Diameter: $D=8.7$ (mm)
- Free Length: $L=470$ (mm)
- Spring Stiffness: $K=0.05$ (N/mm)
- Initial Tension: $F_i=4$ (N)

The main and reset springs work opposite but in synchrony and the actuator cord force due to main spring deflection, i.e., shortening after extension, was required to be calculated (Fig. 5.9.a). Furthermore, the relation between main spring deflection and ankle angle was measured based on the SPAE components' geometry (Fig. 5.9.b). Considering all computations, Fig. 5.9.c shows the assistive moment provided by the SPAE as a function of ankle angle.

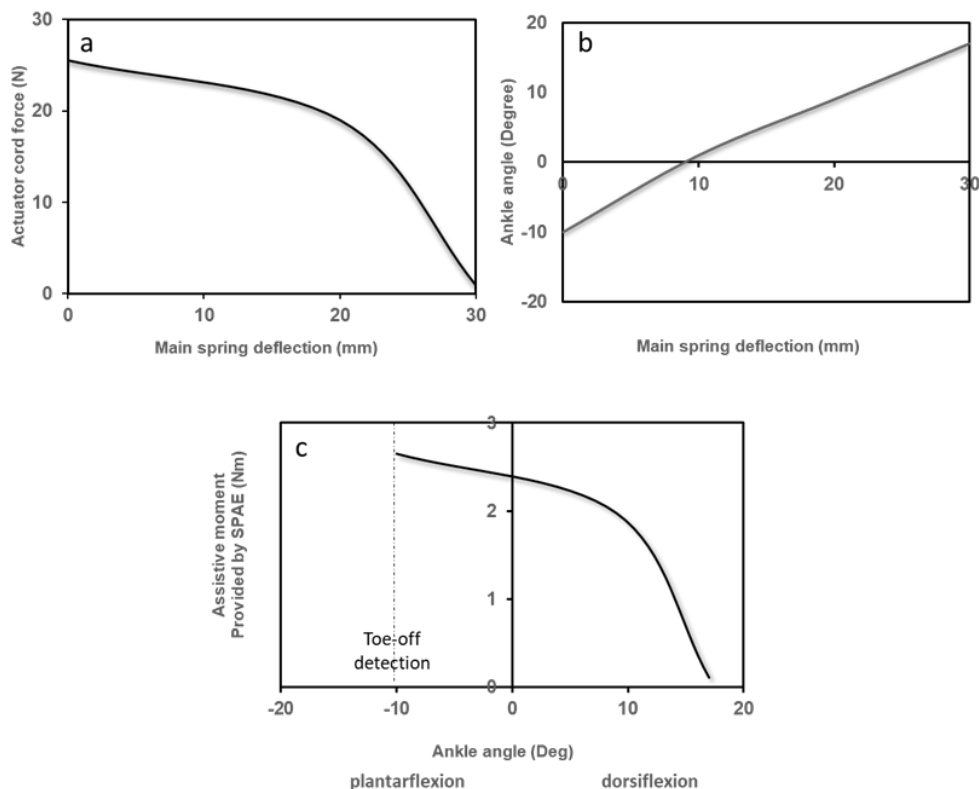


Figure 5.9 The SPAE's mechanical performance. a) actuator cord force vs. main spring deflection. b) ankle angle vs. main spring deflection. c) assistive moment provided by the SPAE vs. ankle angle.

5.3 Design evaluation

5.3.1 Methods

To evaluate the initial device design, biomechanical data were obtained at the Victoria University Biomechanics Laboratory using one healthy, physically active male aged 36 years (1.80 m stature and 84.0 kg body mass). Following a brief description of the task he walked on the treadmill at preferred speed with the SPAE on his right foot and in a second condition without the SPAE. The toe-off trigger was set at 10 degrees plantarflexion. Two minutes data were recorded for each condition.

The same apparatus employed in Chapter 3 was used to collect the biomechanical data. Twelve reflective markers were attached to anatomical landmarks of the ankle, knee and pelvis of both limbs. Two marker clusters of TIB and THI were attached to the tibia and thigh of each leg. Four markers were also attached to the shoes on the Heel, Toe, MT1 and MT5 landmarks. In this test, however, on the right side, an additional marker was attached to each end of the main spring to record the extent and timing of spring deflection.

5.3.1.1 Data analysis:

The same analyses as described in Chapter 3 were performed to build a skeletal model using Visual 3D. Gait events were also defined with the pipelines developed in Chapter 3. The time-histories of ankle sagittal power (W/kg) for both conditions were computed using the Visual 3D inverse dynamics procedure. The ground reaction force and centre of pressure anterior-posterior path were also computed for both feet and time normalized over the gait cycle.

The time-history of the harvesting spring's length, showing spring extension, was computed based on the temporal position of the two markers at the ends of the spring. Following filtering, the time-history of distance between two markers in 3D space was computed with generalization of the distance formula as below:

$$d(t) = \sqrt{(x_2(t) - x_1(t))^2 + (y_2(t) - y_1(t))^2 + (z_2(t) - z_1(t))^2} \quad eq.5.7$$

Posterior marker position: (x₁, y₁, z₁)

Anterior marker position: (x₂, y₂, z₂)

5.3.2 Results and discussion

5.3.2.1 Heel strike energy harvesting system

It was hypothesized that the heel strike energy harvesting system would recover the same amount of energy on each step, independent of the ankle muscles' contribution. This hypothesis was investigated for the SPAE by measuring each step's harvested energy and ankle joint power.

As shown in Fig. 5.10.a, the time-history of main spring length was computed and normalized within the gait cycle. At approximately 5% of the gait cycle, i.e. after heel contact, the heel strike detector released the lever mechanism allowing the spring to extend, with maximum extension achieved in the final 15% prior to contralateral toe-off, at which time the entire body mass is supported by the SPAE-assisted foot. As shown in Fig. 5.10.a, the harvesting spring's free length was about 6 cm, which extended to approximately 11 cm on each step. It was confirmed, therefore, that the same energy was harvested each step and can be calculated as follows:

$$E = \frac{1}{2}k\Delta x^2, \Delta x \approx 5 \text{ cm}, k = 750 \text{ N/m} \quad \text{eq.5.8}$$

$$E = 0.93 \text{ Joules}$$

The average of each step time was 0.4 second. Therefore, the energy producing power was:

$$\text{Power} = \frac{\Delta E}{\Delta t} = 2.34 \text{ Watts} \quad \text{eq.5.9}$$

The 0.93 Joules calculated above is less than the 3.8 Joules of dissipated heel strike energy reported by Baines et al., (2018). This suggests that, despite the 0.93 Joules recovered, there was still considerable energy dissipation. The recovered 0.93 Joules did, however, provide adequate ankle dorsiflexion because 0.004 Joules/Kg (0.4 Joules for a 100 Kg subject) was shown to be required for the Ankle strategy swing phase, as reported in Chapter 4. More energy could, however, be harvested using a stronger spring but the effect on walking mechanics would need to be determined.

As discussed earlier, two biomechanical energy sources can be harvested at the ankle, muscle negative work and heel strike energy. Stance phase muscle negative work, commonly reported, shows considerable step-to-step variability (Riemer & Shapiro, 2011), also shown in the test data here when walking with the SPAE (Fig.

5.10.b). The constant spring deflection in Fig. 5.10.a, however, corresponds to *constant energy* recovery using the SPAE, independent of ankle muscle contribution.

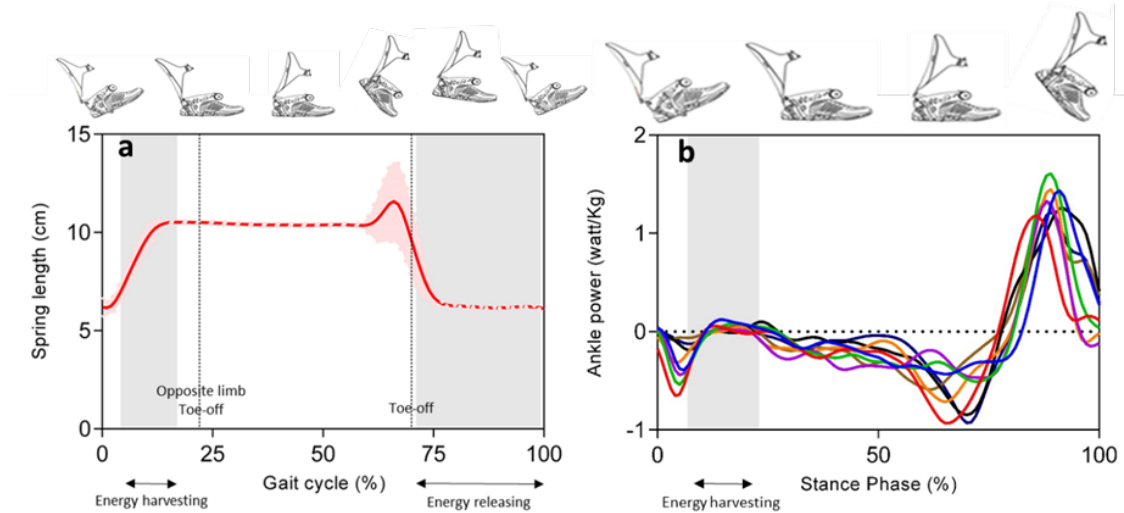


Figure 5.10 a) main spring length change during the gait cycle and b) step-to-step variability in stance phase ankle power when walking with the SPAE.

5.3.2.2 Mechanical energy flow controller

The successive functions of the SPAE during the gait cycle are shown in Fig. 5.11. Following ground contact detection by the heel strike detector, the device simultaneously disengages the actuator cord and harvesting mechanism, allowing unconstrained loading and energy harvesting. The device then remains disengaged until toe-off, at which time at a predefined ankle angle, the trigger cord releases the mechanism to lift the foot.

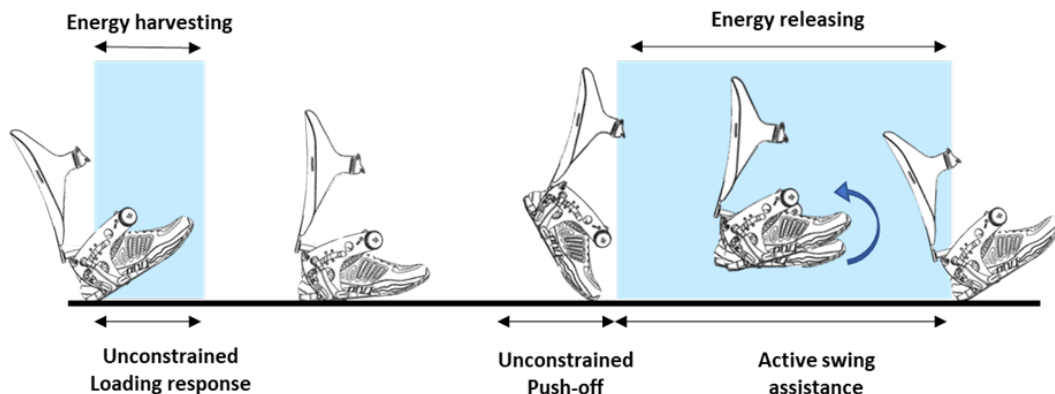


Figure 5.11 The successive functions of the SPAE during the gait cycle.

The primary design requirement was active contribution during swing to dorsiflex the ankle, with minimal range of motion restriction during stance, specifically at push-off (Chapter 3). When walking with the SPAE, there was no change in the foot virtual marker trajectory during mid-stance, showing that this requirement was met (Fig. 5.12). Increased foot-ground clearance was seen throughout swing but foot elevation during initial stance was due to the ankle dorsiflexion provided by the SPAE at heel strike.

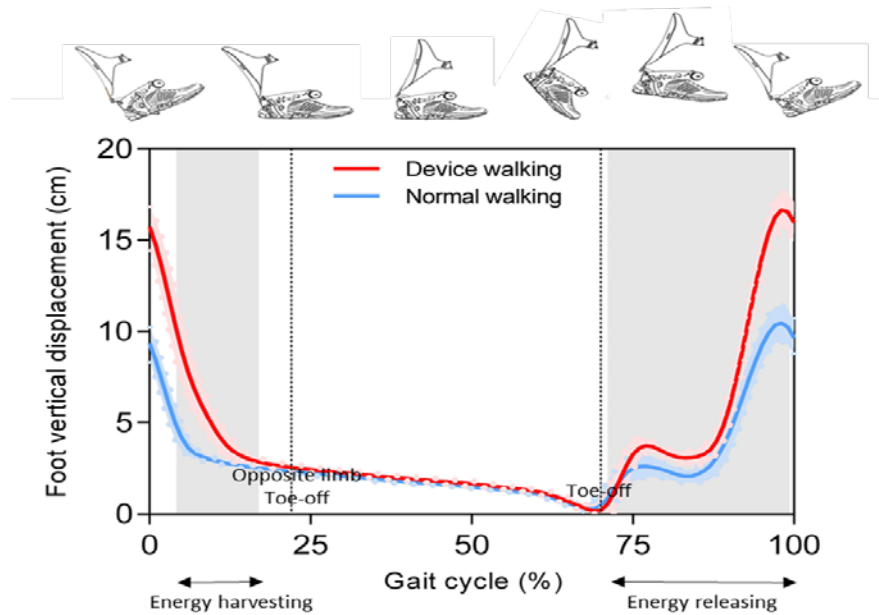


Figure 5.12 Foot trajectory over the gait cycle when walking with and without the SPAE.

5.3.2.3 SPAE effects ground reaction forces and centre of pressure

For normal walking, the vertical force-time curve comprises early and terminal stance peaks and minimum force at mid-stance (Whittle, 2014). Fig. 5.13.a shows that the stance phase vertical ground reaction forces when walking with the device were lower during the energy harvesting period, suggesting that the SPAE spring absorbed impact energy. This finding is consistent with Ros et al., (2010) who found that footwear with softer cushioning material reduces peak vertical force at heel strike. The atypical mid-stance force increase during walking with the device was due to the ball bearing of the harvesting lever mechanism striking the posterior force plate due to the treadmill belt's action.

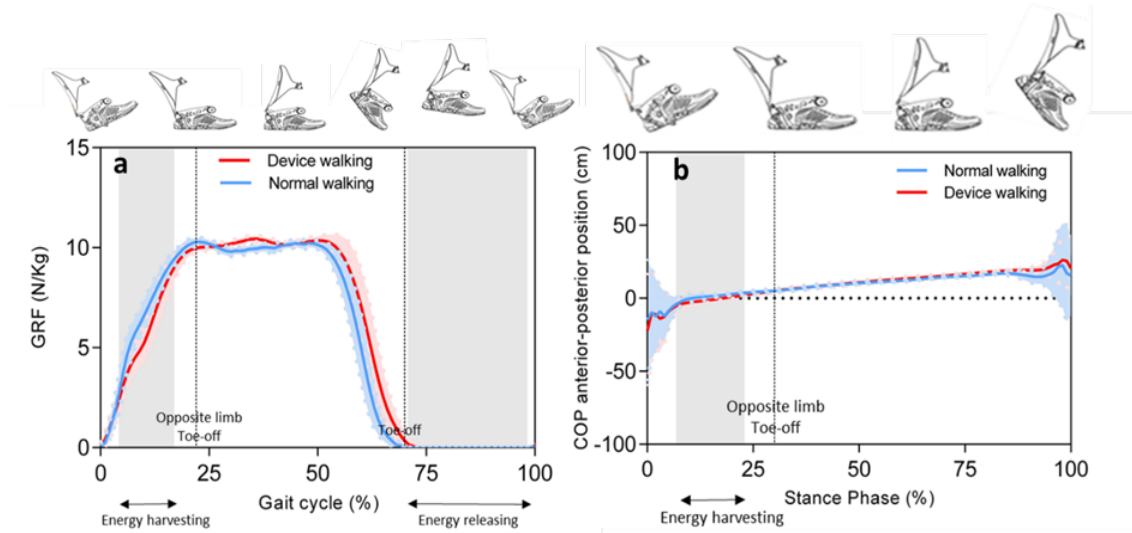


Figure 5.13 Effects of walking with and without the SPAE on a) foot-ground reaction forces (GRF) and b) COP anterior-posterior path.

Our design placed the harvesting lever mechanism as close as possible to the ankle joint centre to prevent anterior Centre of Pressure (COP) movement. Fig. 5.13.b shows that the SPAE did not influence stance phase anterior-posterior COP path. The unchanged COP location is further illustrated in Fig. 5.14, which compares the left foot without the device with the SPAE right foot. Taken together, the GRF and COP analyses showed that the SPAE could harvest heel strike energy with minimal adverse effects.

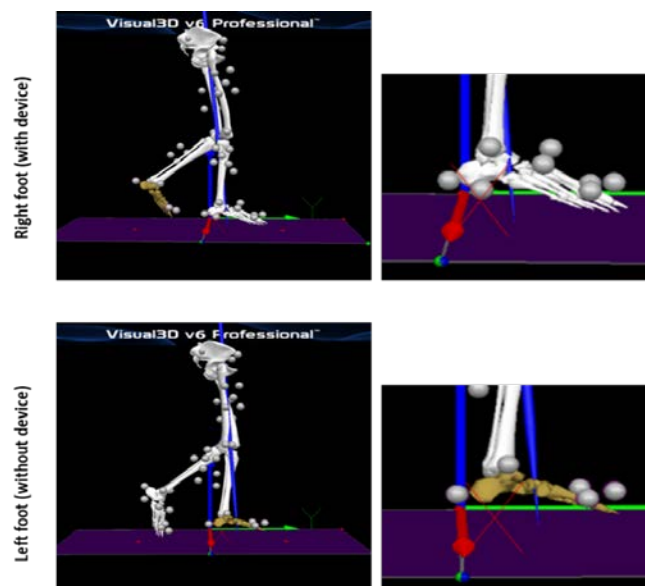


Figure 5.14 Position of the COP during walking for right foot (with the device) and left foot (without the device).

5.3.2.4 Construction design features

The components, including the harvesting mechanism, were fully integrated into a running shoe with no addition to the outsole (Fig. 5.15.a). A further design feature was a two degrees of freedom mechanical joint which allowed unrestricted ankle plantarflexion/dorsiflexion and inversion/eversion (Figs. 5.15.b and 5.15.c).

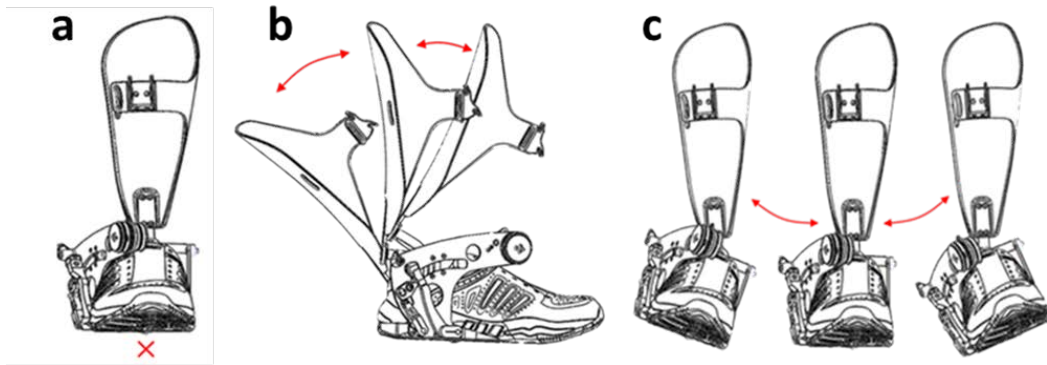


Figure 5.15 Construction design features of the SPAE; a) heel strike energy harvester with no addition to the outsole, b) unrestricted ankle plantarflexion/dorsiflexion and c) unrestricted inversion/eversion.

5.4 Summary of results

In this Chapter, the device design was described using an engineering design approach involving problem definition, brainstorming, a feasibility study, conceptual design, detailed design and construction (Pahl & Beitz, 2013). The design process also included swing kinematics and kinetics findings from our experiment described in Chapters 3 and 4.

It will be an important step forward for clinical rehabilitation if a passive ankle assistive device with its inherent advantages can provide active assistance without gait restriction. An ideal AFO should provide required dorsiflexion/plantarflexion assistance without limiting ankle range of motion. This preliminary study showed that the trialled SPAE could harvest adequate energy during stance to actively dorsiflex the ankle with minimal gait disturbance. Other design features were also met which are summarized in General Conclusion Chapter (section 7.2, Fig. 7.1). The following chapter reports a considerably more detailed investigation of the final SPAE design using the findings from a comprehensive laboratory experiment.

6 SWING ANKLE-CONTROLLED WALKING USING THE SPAE

6.1 Introduction

This chapter describes the evaluation of the self-powered ankle exoskeleton, designed to provide active swing phase assistance without an external energy source or electronic control unit. Chapter 5 confirmed success in using synchronized energy harvesting and release in addition to mechanical gait event detectors. The current chapter, however, seeks to further confirm the performance of the SPAE using the kinematic variables investigated for intentional ankle-controlled walking in Chapter 3.

It was hypothesized that kinematic analysis of walking with the SPAE would replicate the intentional gait modifications observed in Chapter 3 when using an ankle control strategy. Aim of this study was, therefore, to evaluate performance of SPAE, compared with unassisted normal walking, by addressing following hypotheses.

The primary hypotheses were walking with the SPAE would demonstrate; (i) greater MFC height, ankle dorsiflexion and MFC/Mx1 ratio and (ii) decreased MFC and foot maximum horizontal velocity timing. The secondary hypotheses were the SPAE would not affect; (i) joint angles (ankle, knee and hip) during the stance and swing phases and (ii) MFC magnitude and timing of the unassisted contralateral limb.

6.2 Methods

6.2.1 Participants, apparatus and procedure

Nine healthy physically active males aged 30 to 40 years (mean 35.4 years) with stature of 176 cm (SD=5.2) and body mass of 77.6 kg (SD=9.3) were recruited. The informed consent procedures were as described in Chapter 3 for the preliminary gait biomechanics study. As in the first experiment the Vicon Bonita motion capture system and the AMTI tandem treadmill were used for data sampling. The lower body marker set was the same as Chapter 3 while upper body markers were discarded (Fig. 6.1). Two additional markers were attached to the energy harvesting lever and energy releasing pulley of the device, as described in Chapter 5, to track the device's function in each step.

Subjects initially walked on the treadmill at self-selected speed (mean 2.88 ± 0.35 Km/h) for two minutes wearing the same design of running shoe as used to mount the device (Fig. 6.1). Following a brief introduction to describe the task, participants then walked for two minutes with the SPAE on their right foot at their previously determined preferred speed with the toe-off trigger was set at 10 degrees of plantarflexion, as trialed in Chapter 5.



Figure 6.1 Experimental Setup. The Vicon default lower body marker set with four additional marker clusters attached to the thigh and shank of both legs. Upper body markers were discarded.

6.2.2 Data analysis

The Vicon Nexus software was used for raw data interpolation and exporting c3d files to Visual 3D for skeletal modelling, using the same procedures as in Chapter 3. Calculations of joints angles, foot trajectory and event detection were also identical to Chapter 3. Paired t-tests were used to compare the timing and magnitude of MFC and maximum horizontal velocity for walking with and without the device. P values greater than .05 were considered statistically significant. For comparing time-dependent functions, such as joint angles, SPM two-tailed paired t-tests were used, as described in Chapter 4, and significantly different time periods quantified. Linear regression analysis was again used to examine the coincidence of MFC and foot

maximum horizontal velocity. Paired t-tests were also used to compare ankle angle, ankle angular velocity, MFC height, MFC/Mx1 ratio and maximum horizontal velocity at specific events (Mx1, MFC and Mx2) between Normal and Device walking.

6.3 Results

6.3.1 Foot trajectory control

The first analyses examined the impact of the SPAE on swing foot trajectory. The temporally normalized vertical foot displacement is shown in Fig. 6.2.a in which Normal walking is graphed in blue and walking with device shown in red. Using the SPAE the foot was lifted throughout swing, with an additional 1 cm elevation at MFC, and an additional 3 cm by Mx2. Comparing the average MFC height for all participants without time normalization (Fig. 6.2.b) revealed that the SPAE increased MFC from 2.27 cm to 3.35 cm ($p=0.0017$). The MFC/Mx1 ratio increased using the SPAE from 0.56 to 0.73 ($p=0.0038$) and revealed the MFC washing-out phenomenon seen in the Ankle strategy condition described in Chapter 3.

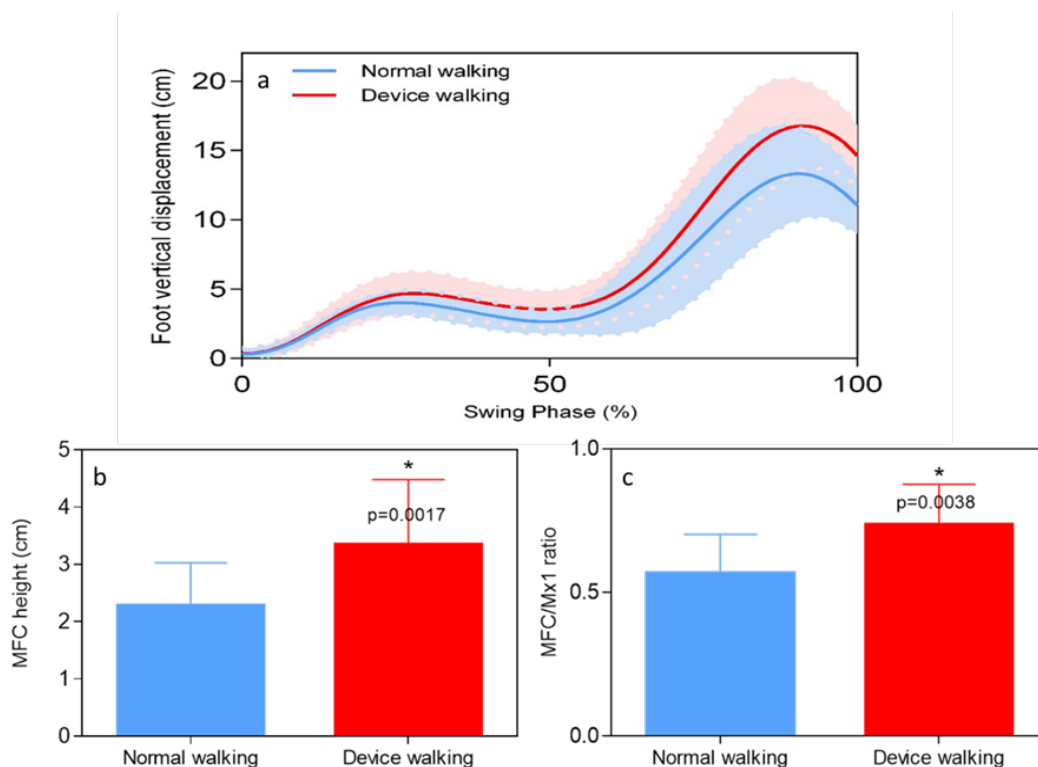


Figure 6.2 Effects of wearing the SPAE on; a) Sagittal foot trajectory, b) MFC height and c) MFC/Mx1 ratio. Blue and red represent Normal and Device walking, respectively. (*) represents the statistically significant differences shown by paired t-tests.

6.3.2 Joint angles

The mean and standard deviation of temporally normalized time-histories of ankle, knee and hip joints for the entire stride cycle are presented in left columns of Figs. 6.3 and 6.4. The right column shows the intervals during which the SMP analysis found the functions to be significantly different. The contribution of the SPAE to modulating the ankle angle is clearly seen in the second half of swing, with a significant increase in ankle dorsiflexion ($p < 0.001$) (Fig 6.3.a). Swing phase knee and hip joint functions were unaffected by the SPAE (Figs. 6.3.b and 6.3.c).

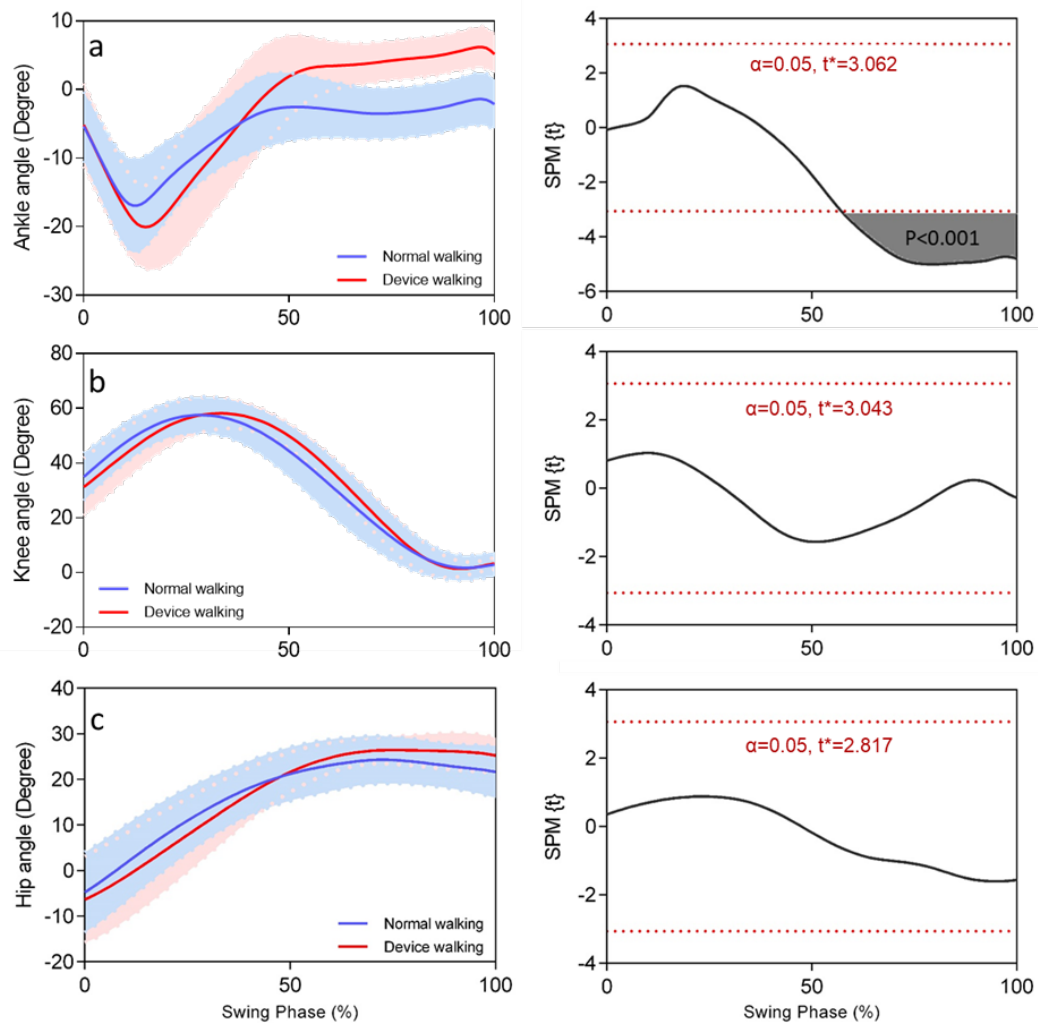


Figure 6.3 The swing normalized a) ankle, b) knee and c) hip joint angles walking with and without the device (a positive angle was assigned for dorsiflexion/flexion and negative for plantarflexion/extension). In the right column, the SPM analysis of paired t-test depicts time periods for which the functions were significantly different for each joint. The critical thresholds (t values) are shown using the red broken line and supra-threshold cluster probability values are depicted close to the line. The grey shaded area represents the interval during which a significant difference was evident ($p < 0.05$).

During entire gait, ankle angle increased for a short time following initial contact ($p=0.047$) and again at terminal swing ($p=0.01$) (Fig. 6.4.a). As for swing, the knee and hip angles, were not modified by the device (Figs. 6.4.b and 6.4.c). Taken together, the results of the temporally normalized joint angles suggested, therefore, a significant increase in ankle angle during terminal swing and heel strike, with no effects on the knee walking and hip joints.

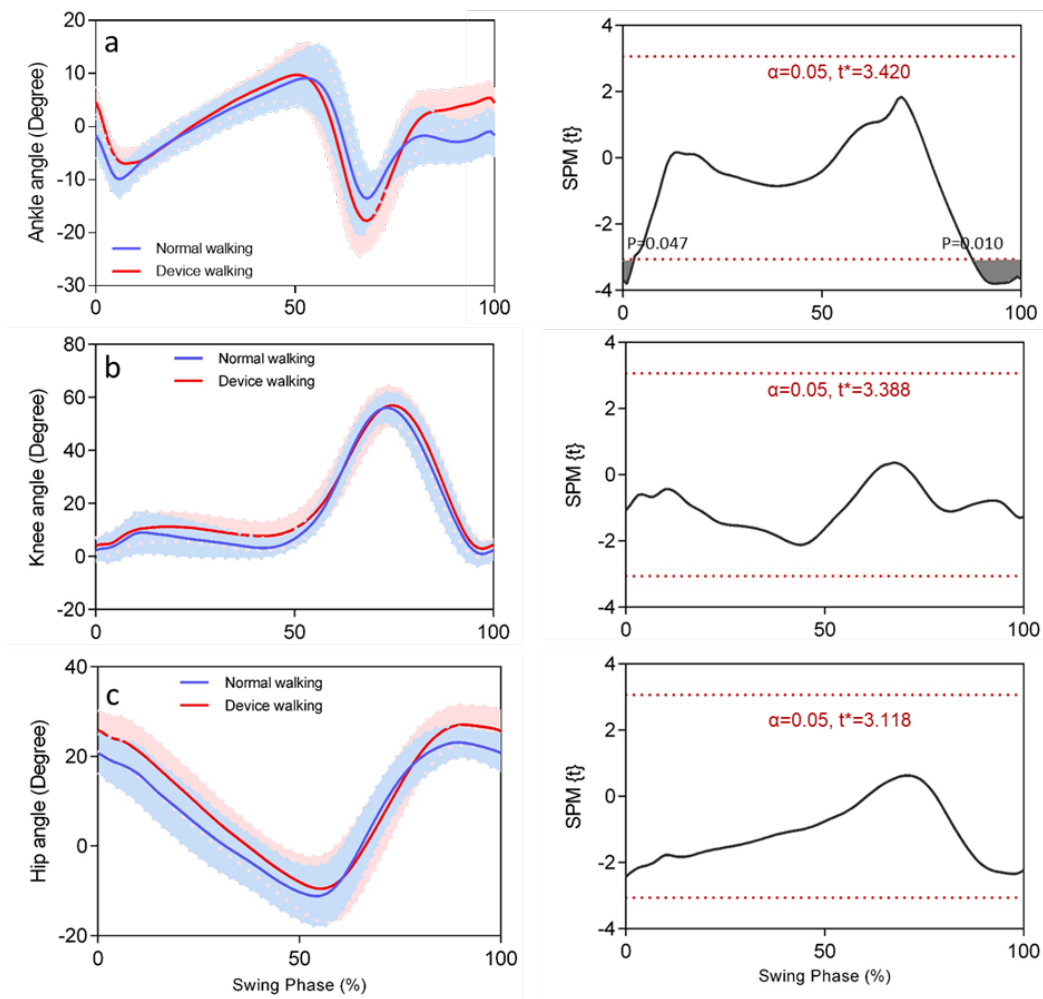


Figure 6.4 The entire gait cycle normalized a) ankle, b) knee and c) hip joint angles for walking with and without the device (a positive angle was assigned for dorsiflexion/flexion and negative for plantarflexion/extension). Conventions as for Figure 6.3

To provide further insight into the device's effects on foot trajectory control the mean and standard deviation of ankle angle and ankle angular velocity at specific gait events were also derived (Figs. 6.5 and 6.6, respectively). As illustrated in Fig. 6.5, at maximum ankle plantar flexion there was no difference in ankle angle for walking with and without the SPAE. Angular velocity was also approximately zero, suggesting

normal push-off forces for both conditions (Fig. 6.6). At Mx1, there was still no significant difference due to the device, but ankle angle decreased while its angular velocity increased. It appeared that the device began to function between maximum plantar flexion and Mx1, but not significantly. At the critical MFC event, however, both ankle angle and ankle angular velocity increased ($p=0.001$ and $p=0.016$, respectively). The ankle angle increment was from -2.9 to 1.48 degrees and ankle angular velocity from 0.13 to 0.90 rad/s. The increased ankle angle continued up to Mx2 ($p=0.0009$) while by that time angular velocity was unchanged. Additionally, ankle angle was still greater at Heel Contact (HC) ($p=0.003$) but angular velocity became negative, confirming that the device's heel strike detector released the device at the appropriate time, allowing foot-ground contact similar to normal walking.

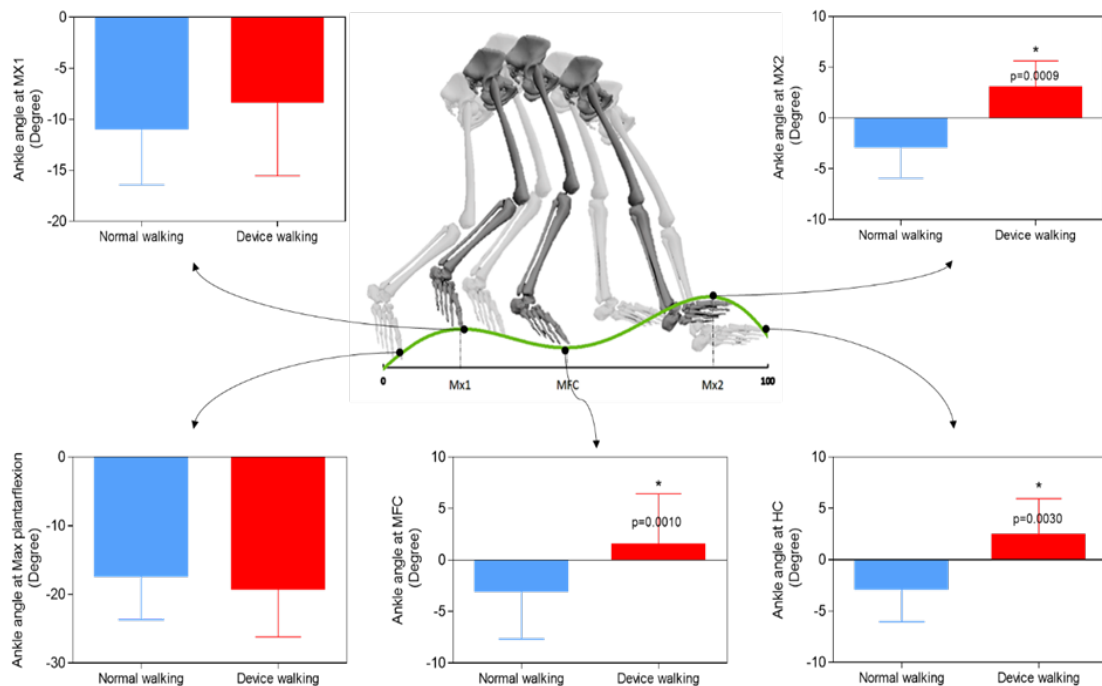


Figure 6.5 Ankle angle (degrees) at highlighted swing events: maximum plantarflexion, Mx1, MFC, Mx2 and HC. Blue and red represent Normal and Device walking. (*) statistically significant differences.

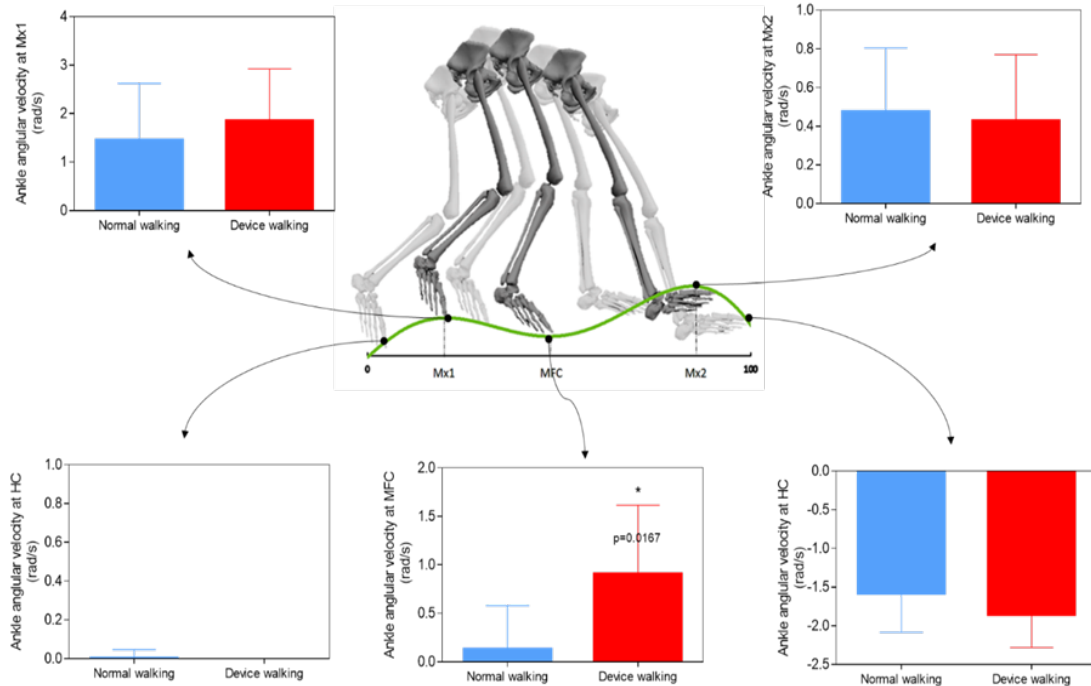


Figure 6.6 Ankle angular velocity (rad/s) at highlighted swing events. Conventions as for Figure 6.5.

6.3.3 MFC and maximum horizontal velocity timing

In addition to MFC height, maximum horizontal velocity of the foot relative to MFC was of interest. The same approach as in Chapter 3 was, therefore, taken to compute these variables and determine any interdependency. As shown in Fig. 6.7, maximum horizontal foot velocity was not affected by the device.

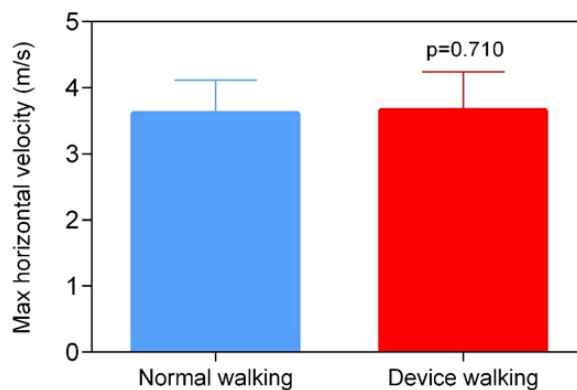


Figure 6.7 Maximum foot horizontal velocity during swing for Normal and Device walking (blue and red, respectively).

MFC timing within the swing phase and maximum horizontal velocity timing also did not change (Fig. 6.8.a and b). The coincidence of these two events, furthermore, was shown using R square from the correlation analysis, as a determinant of goodness of fit (Fig. 6.8.c). Results showed that walking with the SPAE provided lower R square indicating less coincidence between MFC and maximum horizontal velocity.

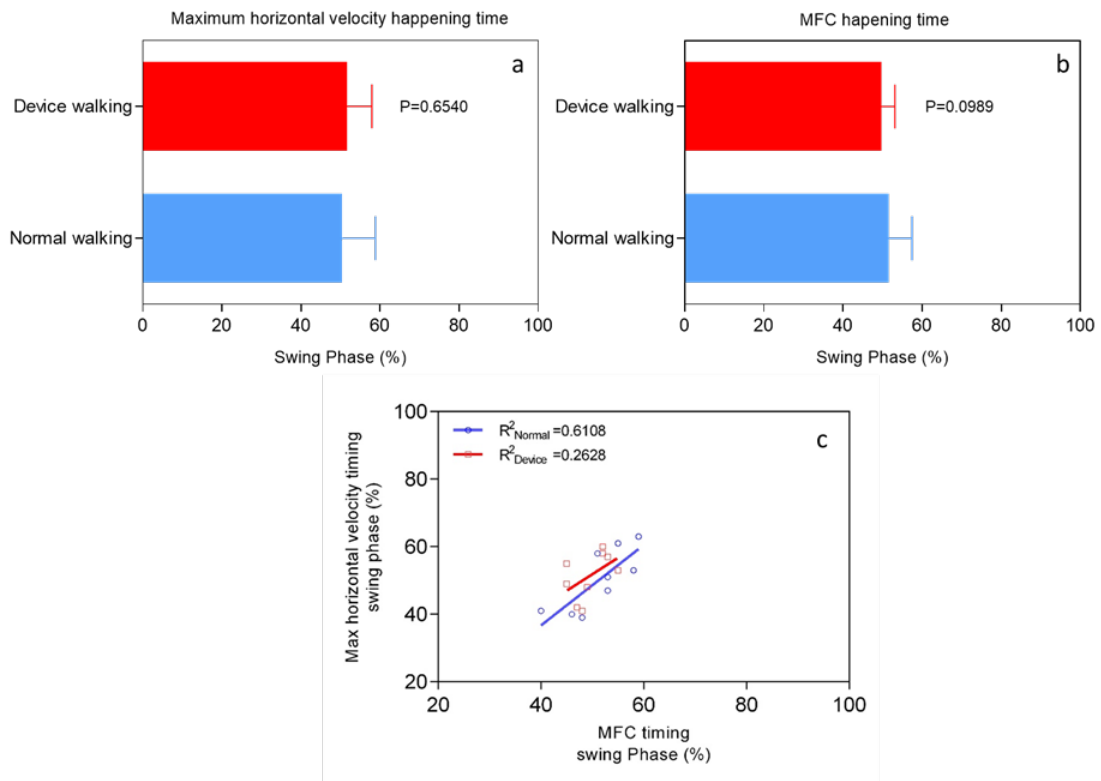


Figure 6.8 SPAE effects on the timing of: a) foot maximum horizontal velocity, b) MFC and c) their correlation.

6.3.4 Swing asymmetry

To investigate gait asymmetry effects due to the device, foot sagittal trajectory variables were computed for the unassisted limb in the same way as for the SPAE limb. From the data in Fig. 6.9.a, it is apparent that the time-normalized swing phase foot trajectory of the unassisted limb did not change and, consequently, MFC height was also unaffected (Fig. 6.9.b).

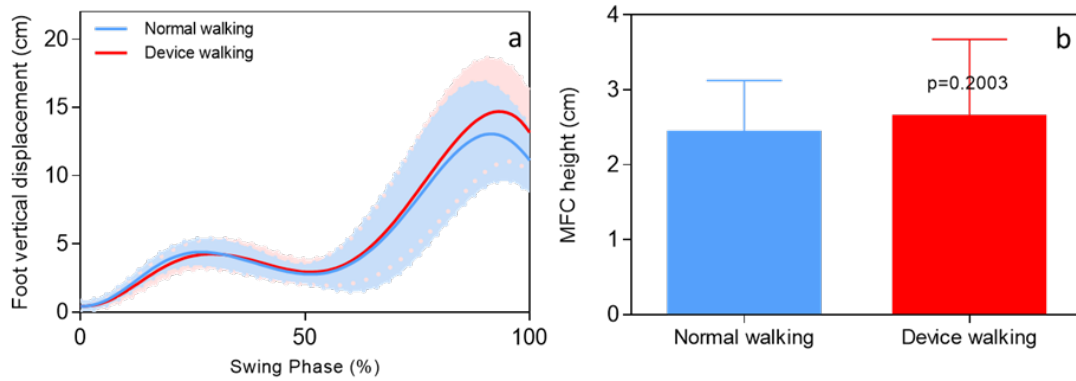


Figure 6.9 SPAE effects on the unassisted limb a) sagittal foot trajectory and b) MFC height. Blue and red represent Normal and Device walking, respectively.

As for the assisted limb, in addition to MFC timing, foot maximum horizontal velocity and timing time were also derived for the unassisted limb. As shown in Fig. 6.10, there was no difference of maximum horizontal velocity between the two conditions, i.e. no asymmetry.

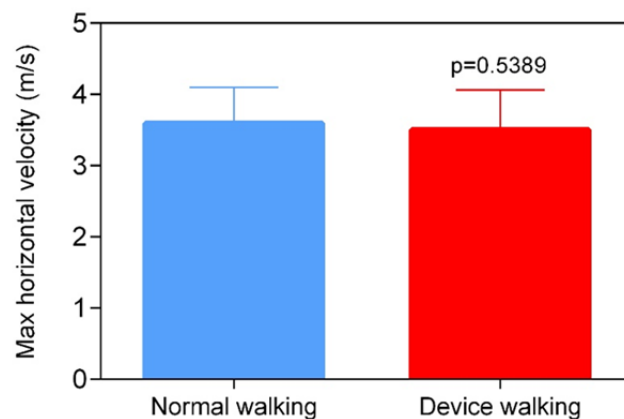


Figure 6.10 Unassisted foot maximum horizontal velocity during swing for Normal and Device walking (blue and red respectively).

The timing of MFC and maximum horizontal velocity also showed no difference (Figs. 6.11.a and 6.11.b). The coincidence of these two events (Fig. 6.11.c), therefore, was highly correlated for both conditions, with $R^2=0.756$ and $R^2=0.509$ for Normal walking and Device walking respectively.

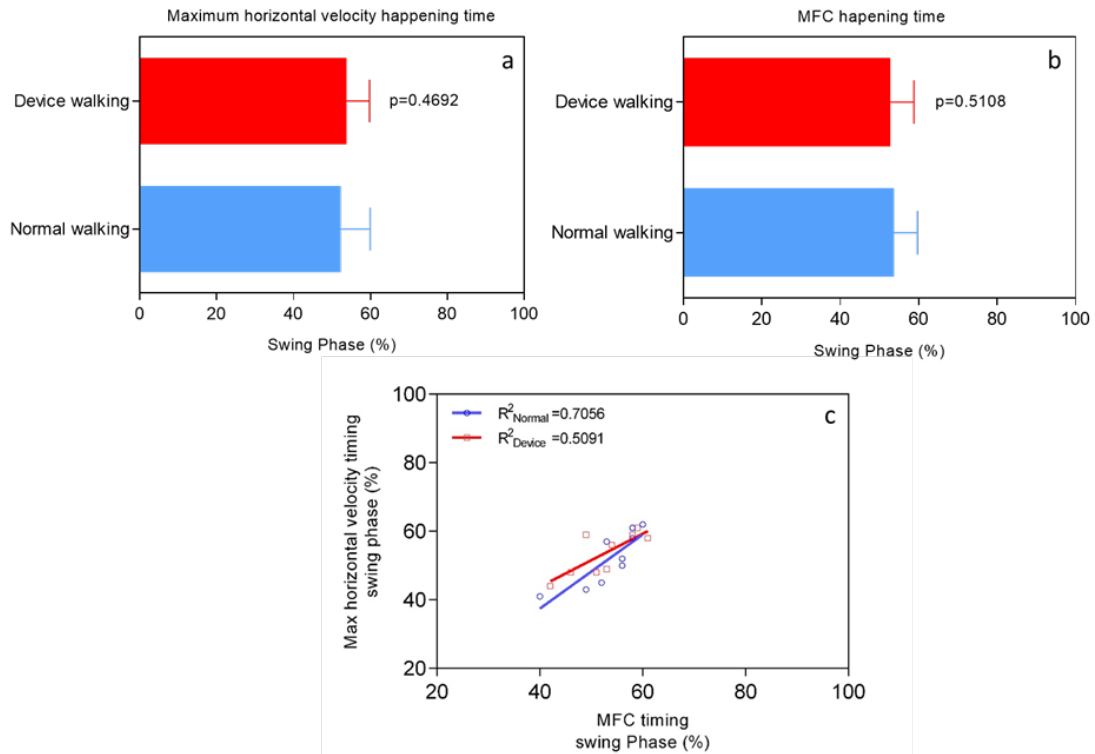


Figure 6.11 SPAE effects on the unassisted limb's timing of: a) foot maximum horizontal velocity, b) MFC and c) their correlation.

6.4 Discussion of results

Performance of the SPAE was quantified for healthy active subjects using the same experimental approach and gait variables as in Chapter 3. A similar marker configuration was used to compare foot trajectories, joints angles, foot horizontal velocities and asymmetry of walking with and without the device. Most previous studies presented only the sagittal ankle angles and moments to demonstrate the contribution of their device to foot drop assistance during swing (Alam et al., 2014; Boes, 2016; Chin et al., 2009; Petrucci, 2016; Shorter et al., 2011a; Shorter et al., 2011b; Yamamoto et al., 1999). No previous work had demonstrated the effects of an AFO or ankle exoskeleton on foot trajectory and related parameters, such as the MFC event.

6.4.1 MFC and the MFC/Mx1 ratio

Maintaining sufficient swing phase foot-ground clearance, especially at MFC, has been considered essential to understanding tripping risk and the mechanics of stability recovery (Begg & Sparrow, 2000; Berg et al., 1997; Blake et al., 1988; Prince

et al., 1997). The perceptual-motor system has an extraordinary capacity to continuously adapt swing phase foot trajectory to accommodate surface elevation variations due to the terrain. Schulz, (2011) showed that MFC height also increases as we walk faster, without any conscious or pre-planned biomechanical adaptation. This autonomous foot trajectory control process is, however, impaired by ageing and neuromuscular disorders. It was, therefore, hypothesised that a system providing autonomous active assistance could compensate perceptual-motor impairments affecting gait control. As an aside, it has been made clear that when surface height reaches some critical amplitude, foot trajectory adaptation appears to switch from an automatic or autonomous process, to pre-planned obstacle crossing strategies, now well documented in the gait biomechanics literature. As far as is known, there has been no systematic investigation of this obstacle-height dependent transition, i.e. the shift from more autonomous foot-ground clearance to slower, controlled, pre-planned, obstacle crossing.

The results supported the hypothesis that walking with the SPAE would demonstrate the same kinematics seen in the intentionally ankle-controlled walking task, described in Chapter 3. It is also reasonable to conjecture that, if the SPAE was implemented to remediate ankle-related gait disorders, foot trajectory control would be improved. We saw enhanced swing phase control as revealed in increased MFC height (Fig. 6.2.a and 6.2.b) and a corresponding increase in the MFC/Mx1 ratio (Fig. 6.2.c). It can be reasonably inferred, therefore, that an SPAE could improve walking safety by lifting the foot and, in some cases, eliminating the problematic MFC event.

6.4.2 Swing joint coordination

As discussed, a drawback of conventional AFOs is restricted ankle motion during stance and even minimally restrictive AFOs may inhibit essential kinematic and kinetic characteristics of the stance-swing and swing-stance transitions (Nair et al., 2010). Ankle restriction also affects range of motion at the knee and hip and exaggerated ankle plantarflexion resistance during stance leads to excessive knee flexion (Lehmann, 1993). Nair et al., (2010) also highlighted ankle restriction effects on hip extension, such that limiting ankle motion also reduces ankle power generation at push-off that may be compensated by additional hip joint activity (Wutzke et al., 2012).

The primary aim of our SPAE was to provide active ankle assistance without restricting stance and, in particular, the late-stance propulsion-generating toe-off phase. Operationally the SPAE was hypothesised to increase ankle dorsiflexion during swing with no effects on either ankle motion during stance or knee and hip joint angles. Results showed that the SPAE only changed the ankle joint angle in the second half of swing and initial stance, with no effects on the knee and hip angles (Figs. 6.3 and 6.4). The statistically reliable increase in ankle angle close to MFC, with no effects on knee and hip joint angles, provided further evidence of the device's successful contribution to swing-phase ankle modulation.

By looking closely at swing phase ankle angle and angular velocity the functional assistance provided by the SPAE (Figs. 6.5 and 6.6) was revealed further. The device facilitated the late-stance plantarflexion necessary for push-off, as in unassisted walking. As discussed earlier, no previous passive ankle assistive device has had the capability to do this. Additionally, ankle angle increased at MFC but was unaffected at Mx1, a response that again confirmed the effectiveness of the SPAE.

As the foot approaches terminal swing, following MFC, the knee and hip joints work together to position the foot on the ground and stabilize the body (Nagano et al., 2011; Winter, 1991). The ankle may not participate in this activity but defines the shape of the ground approach to ensure a well-controlled heel strike for effective shock absorption. If ankle dorsiflexion decreases excessively prior to heel strike, foot-slap walking is seen. Results of this study showed that ankle angles at Mx2 and HC were higher than for normal walking (Fig. 6.5), confirming a contribution to preventing foot-slap and allowing well-controlled foot-ground contact.

Ankle angular velocity results (Fig. 6.6) showed that the SPAE did not disengage the ankle prior to maximum ankle plantarflexion, ensuring normal push-off; operationally, angular velocity remaining essentially zero for both unconstrained walking and SPAE walking. Following push-off, from toe-off to Mx1, ankle angular velocity began to increase more rapidly with assistance from the SPAE. Subsequently, following Mx1, when angular velocity decreased close to zero for normal walking, the device continued to assist by increasing ankle angle at MFC. At heel strike, on the other hand, ankle angular velocity changed from positive to negative, indicating braking prior to landing. The magnitude of negative angular velocity at landing when

walking with the device was not different from normal walking, showing that the heel strike detector worked well, releasing the ankle with the optimal timing.

6.4.3 MFC and maximum horizontal velocity timing

MFC and maximum horizontal velocity timing may also affect the risk of foot-ground contact and, therefore, must be considered in any evaluation of an ankle assistive device (Begg et al., 2007; Nagano, 2014). Intentionally ankle-controlled walking, described in Chapter 3, showed a higher correlation between MFC and peak foot horizontal velocity timing than observed using the SPAE (Fig. 6.8). Further research is necessary to explain this less highly correlated MFC - maximum horizontal velocity timing.

SPAE walking was also associated with slightly earlier average MFC (not statistically significant, $p=0.098$), which is adaptive because there would be more recovery time in the event of destabilizing ground contact (Lugade et al., 2011; Nagano, 2014). Maximum foot horizontal velocity did not change using the SPAE, which showed that the device did not interfere with push-off and the knee and hip joint contribution, all of which influence the swing phase trajectory profile (Fig. 6.7).

6.4.4 Swing asymmetry

Asymmetry has been used to identify elements of gait pathology (Griffin et al., 1995) and the effects of changing gait parameters, such as step width (Nagano et al., 2011). The stronger dominant limb tends to contribute more to propulsion (Sadeghi et al., 2000) while the non-dominant limb maintains foot-ground clearance. These asymmetry effects may be adaptive in preventing tripping and assisting balance recovery, which is more difficult for the non-dominant limb (Pijnappels et al., 2008). Additionally, Nasirzade et al., (2017) indicated that if the knee, hip or ankle joints are restricted on one side, there may be a trajectory compensation by the contralateral-foot. They, therefore, insisted that measures of gait asymmetry are important in developing orthoses and prostheses.

In this project, the unassisted limb's response was used as a further measure of gait restriction due to the SPAE. Results showed that walking with the SPAE did not change average MFC height in the unassisted limb but slightly perturbed MFC height variability (Fig. 6.9.b). Moreover, SPAE effects on the unassisted limb's MFC timing

and foot maximum horizontal velocity were negligible, with no statistically significant differences between limbs (Figs. 6.10 and 6.11). Overall, the asymmetry analyses showed that the SPAE did not impair the contralateral limb.

6.5 Summary of results

In Chapter 3, it was shown ankle-controlled walking optimized sagittal foot trajectory. It was, therefore, hypothesized that walking with assistance from the SPAE would demonstrate the same effects on lower limb biomechanics as seen for intentional ankle-control. Functional performance of the device was, therefore, evaluated using two principal criteria: (i) active and functional assistance to swing phase ankle dorsiflexion and (ii) no restriction on ankle, knee or hip joint motion during both swing and stance. The results confirmed that the SPAE provided functional, active assistance to the foot during the swing phase. The SPAE also increased MFC, allowed maximum ankle plantarflexion after toe-off and unrestricted movement following heel strike. Additionally, there were no negative effects on knee and hip angles when walking with the SPAE. Some asymmetry was seen in the unassisted limb's MFC variability but no other SPAE asymmetry effects were observed. In conclusion, the results of this experiment confirmed that the SPAE could harvest and utilize heel strike energy with minimal restriction to normal gait function.

7 CONCLUSION

7.1 Overview

Walking is critical to most everyday physical activities but can be impaired by a range of conditions, including ageing, neurological disorders and muscular pathologies (Bronstein & Brandt, 2004). One of the most serious consequences of gait impairments is falling due to tripping (Pavol et al., 1999). Decreased foot-ground clearance during the gait cycle swing phase leads to increased risk of tripping but this may be avoided by providing an assistive force to lift the foot (Begg et al., 2007).

All ankle assistance devices, from conventional fixed AFOs to complex robotic applications, have been developed to generally improve swing foot trajectory by either restricting or assisting ankle joint dorsiflexion. Conventional AFOs can maintain the ankle dorsi-flexed but restrict ankle motion during stance, with negative consequences for other phases of the gait cycle. One solution is to keep the ankle free during stance and provide active assistance after toe-off.

Advances in ankle assistive devices have, therefore, mainly focussed on active ankle assistance via an external moment controlled by complex systems comprising advanced power sources, sensors and microprocessors (Dollar & Herr, 2008; Herr, 2009, Shorter et al., 2011b). These devices, however, remain prohibitively costly and complicated for everyday use. According to Mertz, (2012), the Berkeley Robotics and Human Engineering Laboratory director and *Ekso Bionics* founder, Professor Kazerooni proposed; "...the biggest problem is that the existing exoskeleton systems are extremely expensive, and people with mobility disorders can't afford them". The need for a minimal device that is smaller, with less hardware and fewer "bells and whistles" has also been recognised (Mertz, 2012). The development of devices with some of the functionality of advanced robotic systems, but technically minimal and lower cost, would increase accessibility for the considerable number of people worldwide with correctable lower limb disorders.

The question addressed in this project was, therefore, whether we could develop a compact passive ankle exoskeleton to actively augment ankle joint motion without stance phase restriction. The primary aim of ankle augmentation was to positively

affect the swing foot trajectory to achieve safer ground clearance. To address the research question we incorporated gait biomechanics considerations (Young & Ferris, 2016) into the design and evaluation programme and three aims with associated hypotheses were addressed. As summarised below, the first aim was to determine the kinematics and kinetics of swing foot-controlled walking and then, in aims 2 and 3, apply these findings to device design and evaluation.

Aim 1: Determine the biomechanical effects of intentional ankle-controlled walking. Prior to device design, an experiment was carried out to better understand the biomechanical effects of changing ankle joint angles. Participants intentionally controlled ankle motion when walking, to simulate the proposed device's effects on lower limb mechanics. A range of predetermined foot-ground clearances were presented as boundary lines on a video monitor using real-time biofeedback. Participants were asked to walk on a treadmill while accommodating the defined clearances by maintaining their foot trajectory within predefined boundaries when either intentionally using the ankle only (Ankle strategy) or not using it (No-ankle strategy). As described in Chapter 3, kinematic analysis of the recorded position-time data was performed using Visual 3D software and associated statistical analyses. Further analyses using AnyBody modelling, described in Chapter 4, were performed using musculoskeletal modelling to uncover subject-specific time-histories of joint and muscle moments, forces, impulses, powers and work.

Results confirmed that ankle joint control was effective for optimizing foot swing phase trajectory; such that ankle-controlled walking increased foot-ground clearance and reduced the frequency of hazardous MFC events, a response not seen in the No-ankle strategy. The MFC height/Mx1 ratio also increased using ankle-controlled walking, approaching MFC elimination (Bajelan et al., 2019b). Furthermore, ankle-controlled walking decreased the times to MFC and maximum horizontal velocity. Gait symmetry was also shown to not be affected by ankle-controlled walking.

As described in Chapter 4, ankle-controlled walking required less mechanical energy to modulate swing foot trajectory than using the knee and hip joints. Furthermore, musculoskeletal analyses of intentionally increasing ankle dorsiflexion during swing did not support the hypothesis that ankle moment must be significantly

increased to accommodate exaggerated dorsiflexion. It was, however, found that a greater contribution from the tibialis anterior was required of the ankle strategy. To explain the unchanged ankle moment, the simulated Soleus plantarflexion force and EMG activation were examined and shown to also increase, contributing to dorsiflexion via co-contraction.

The hip joint did not compensate for the experimentally restrained ankle joint motion, rather greater knee moment, impulse and work were brought into play. The experiment found, therefore, that it was not possible to intentionally increase ankle dorsiflexion during swing without a contribution from either the hip or knee.

The first experiment confirmed that intentionally ankle-controlled walking provided additive positive effects on swing foot trajectory. It was, therefore, hypothesized that ankle-assisting device could be designed with the same positive effects. Moreover, from Chapter 4, the time-history of swing ankle moment was computed and shown that in comparison with normal walking, significantly greater external moment is not required. Higher TA muscle force should, however, be considered in developing any biomimetic artificial TA muscle (Bajelan et al., 2019a).

Aim 2: Design, construct and evaluate a Self-Powered Ankle Exoskeleton (SPAЕ). By computing the required kinematic and kinetic variables, a systematic engineering design procedure was employed to develop a Self-Powered Ankle Exoskeleton (SPAЕ). After confirming the feasibility of the principal solutions, the device was designed conceptually, followed by detailed design and construction, described in Chapter 5.

The initial SPAЕ design's success was evaluated with a feasibility assessment of energy recovery from heel strike, which was found to be sufficient to increase swing phase ankle dorsiflexion, specifically at MFC. Results from the preliminary study also confirmed that the proposed SPAЕ should be able to harvest constant heel strike energy (2.34 Watts) from step to step, independent of ankle power. The vertical ground reaction force decreased during spring loading due to energy absorption by the SPAЕ and there was no change of the position of foot centre of pressure.

Aim 3: Evaluation of SPAЕ effects on swing kinematics. The biomechanical response to walking with the SPAЕ was investigated using essentially the same apparatus and procedures as in Experiment One. The principal proposition that the

vertical component of the swing foot trajectory would be increased using the SPAE was confirmed by the experimental results showing significantly increased ankle dorsiflexion and foot elevation at MFC and increased MFC/Mx1 ratio.

The hypothesis that Device walking would not restrict knee and hip joint motion was also supported by showing that the ankle, knee and hip angle time-histories were not different for walking with and without the SPAE. Analyses of gait asymmetry also showed no effects on any contralateral-limb kinematics.

7.2 SPAE performance and future developments

This dissertation addressed the design dilemma posed by conventional AFOs and more recent ankle robotic exoskeletons. The former are restrictive and do not provide assistive joint moments, while the latter have limitations due to cost, weight and complexity (Alam et al., 2014; Cenciarini & Dollar, 2011; Herr, 2009; Mertz, 2012; Young & Ferris, 2016). The research question to guide this research project was whether an unpowered ankle assistive device (the SPAE) could be designed and constructed to effectively modulate foot-ground clearance. The design, construction and evaluation of the self-powered ankle exoskeleton (SPAE) described here confirmed the project's successful outcome. In this section, the SPAE's features are summarized, as shown in Fig. 7.1, with limitations and future research directions outlined.

Active ankle assistance

- SPAE keeps ankle free during stance but contributes actively during swing
- SPAE users may keep thinking the concept of 'normal' gait

Swing foot trajectory improvement

- Increasing minimum foot-ground clearance
- Keeps adequate Ankle dorsiflexion at heel strike
- Tent to wash out the MFC (MFC/Mx1 raising)
- No change to knee and hip joints movement
- Minimum asymmetry effects
- Minimum effects on maximum horizontal velocity

Innovative Biomechanically-safe heel strike energy harvesting system

- Nothing added to outsole (normal heel clearance)
- No change in foot center of pressure
- No requirement of ankle joint contribution

Passive mechanical gait events detectors

- Mechanical Heel strike detector to provide unrestricted loading response
- Mechanical Toe-off detector to provide active assistance after toe off

Passive Mechanical controller

- Control timing of assistive force
- Control magnitude of assistive force

In-shoe integrated design

- Device integrated with shoe
- No brace inside the shoe

No gait range of motion restriction

- Allow maximum plantarflexion at toe-off
- Allow free rocker-ankle after heel strike

Minimum added moment of inertia

- Designed to keep device's center of mass closer to center of ankle joint

Two degrees of freedom joint

- Allow Flexion/Extension movement
- Allow Inversion/Eversion movement



Figure 7.1 Overview of the SPAE's functional and design possibilities.

7.2.1 Active swing phase ankle assistance

As described in the literature review, an ideal ankle assistive device should provide dorsiflexion assistance similar to healthy walking. The timing and magnitude of assistive forces, for example, are required to simulate healthy dorsi-flexor muscle control, with no limiting constraints on ankle ROM. Immediately following heel strike ankle plantarflexion increases rapidly to maintain stability before contralateral toe-off (Webster & Murphy, 2019). Available AFOs often limit plantarflexion, leading to reduced stability (Perry & Burnfield, 1992; van der Wilk et al., 2015). Plantarflexion restriction at mid-stance using AFOs also increases knee extension (Perry & Burnfield, 1992). At terminal stance adequate ROM is necessary to allow ankle plantar-flexor muscles to generate sufficient power to propel the limb forward, a feature not incorporated into previous AFOs (Fig. 7.2). This push-off limitation leads AFO users to compensate with increased swing phase contributions by the knee and hip, imposing a higher energy cost (Wutzke et al., 2012).

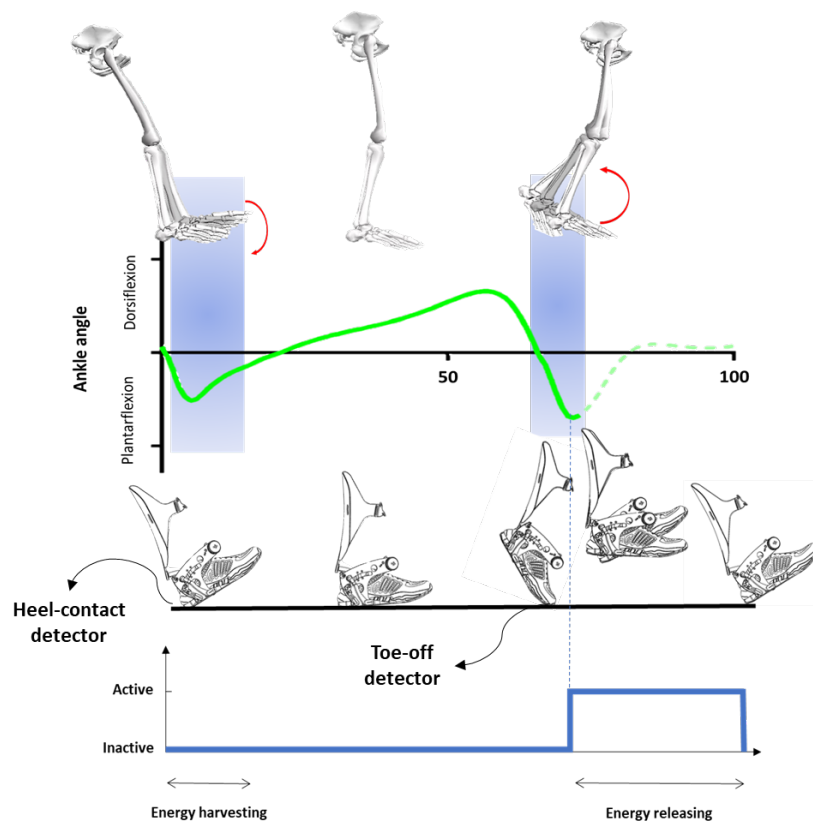


Figure 7.2 Typical ankle angle due to the SPAE. The SPAE remains inactive during stance causing no restriction to range of motion prior to and following swing.

Two mechanical gait event detectors incorporated into the SPAE allowed unrestricted ankle movement during loading and push-off (Fig. 7.2). At the beginning of loading, following ground contact, the heel strike detector released the clutch, allowing unrestricted foot landing. The mechanical toe-off detector, sensitive to ankle angle, released stored energy just following maximum plantarflexion, allowing normal push-off and enabling greater foot-ground clearance (Adamczyk & Kuo, 2014; Lehmann, 1993). In contrast, when ankle function is restricted it is often compensated by strategies such as hip circumduction or hiking (Kerrigan et al., 1998). No effects on knee and hip joint angles were found with the SPAE, confirming that the ankle was unrestricted with no requirement for compensation in other joints.

Activation of the SPAE's toe-off detector, however, required adequate ankle plantarflexion. Our device worked smoothly at preferred speed and may operate effectively at higher walking speeds. Reduced ankle plantarflexion is seen at toe-off when walking slowly and the SPAE may, therefore, also need to be tested at slow walking speeds. Furthermore, in the elderly or individuals with gait disorders, there may not be adequate ankle plantar flexion to activate the device. In future, a plantarflexion-activated toe-off detector may need modification to accommodate slower walking and impaired ankle plantarflexion.

7.2.2 Foot trajectory control and MFC assistance

To provide active assistance without push-off restriction, an impulsive moment is required to transition the ankle quickly from plantarflexion to dorsiflexion following toe-off. When using the SPAE, following release of the spring-stored energy by the toe-off detector, there is a delay as the spring-pulley mechanism engages the assistive cord to lift the foot. From toe-off to Mx1 there is a brief period in which the actuator remains almost disengaged. After Mx1 the stored energy is completely released, achieving the primary objective; maximum increase in ankle angle at MFC without restriction (Fig. 7.3). Reduced assistance at Mx1 and more at MFC, furthermore, increases foot elevation at Mx1 less than at MFC, increasing the MFC/Mx1 ratio, washing-out MFC (Fig. 7.3).

Activation of the assistive cord would be ideal if it operated similar to the TA when working in parallel. In future work, the real-time activation-time synchrony of

the SPAE's assistive cord could, therefore, be validated using EMG data from the TA muscle.

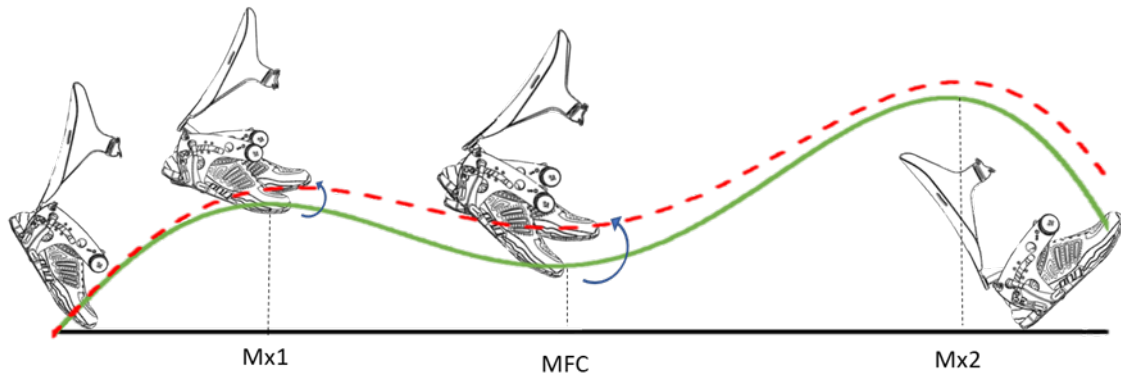


Figure 7.3 Swing foot trajectory modulation provided by the SPAE for one subject. The green line represents walking before device activation (normal walking) and red dashed line represents foot trajectory following device activation. Maximum active assistance is seen at MFC with less effect at Mx1, increasing the MFC/Mx1 ratio.

In addition to MFC elevation, we found that the SPAE slightly (but not significantly) decreased time to MFC (Chapter 6). Foot-ground clearance immediately following toe-off is lower than at MFC but tripping very early in swing tends to be less hazardous because the swing foot is more posterior to the stance limb, keeping the centre of mass within the base of support (Nagano, 2014). In contrast, tripping at MFC places the centre of mass either closer to, or even outside, the base of support (Nagano, 2014). Earlier MFC timing would provide additional time to regain stability after tripping; an SPAE may, therefore, improve the prospects of balance recovery due to earlier MFC timing. Further studies are, however, required to address this hypothesis.

7.2.3 Swing asymmetry

In addition to the assisted foot, the same analyses of MFC height and timing were performed for the contralateral limb (Chapter 6). This analysis was important because swing asymmetry is usually seen in older adults (Chen et al., 2005) in which the stronger dominant limb contributes more to propulsion than the non-dominant limb (Sadeghi et al., 2000). The non-dominant limb must, however, maintain clearance to avoid tripping, since balance recovery following a trip is more difficult for the non-dominant limb (Perry et al., 2007). The asymmetrical MFC elevation of non-dominant limb has also been observed when gait is disturbed by physical or behavioural

abnormalities (Graci et al., 2009). Walking with the SPAE, however, showed no change in the contralateral (unassisted) foot MFC height and timing but slightly increased MFC height variability. This study, therefore, provided a preliminary evaluation of SPAE effects on gait asymmetry but more comprehensive work is required.

7.3 Hardware design

Harvesting the biomechanical energy exchanged during gait can be used to activate an assistive device, without an external power source (Riemer & Shapiro, 2011). Walking accounts for a considerable proportion of daily metabolic energy expenditure, estimated at one-quarter of the daytime energy expended by an office worker (Passmore & Durnin, 1955). Everyday walking involves approximately ten thousand steps per day (Tudor-Locke et al., 2010) but a considerable proportion of the energy expended in walking dissipates due to negative mechanical work (Kuo et al., 2005), soft tissue deformation (Riddick & Kuo, 2016) and footwear cushioning (Ros et al., 2010).

Collins et al., (2015) investigated calf muscle negative work harvesting using a self-powered, self-controlled exoskeleton. This approach is dependent on step-to-step muscle activation which creates variability in the energy recovered each step cycle. They showed, therefore, that only an optimal spring stiffness could decrease energy cost while the harder or softer springs could not. Heel impact energy is dissipated directly to the environment and this harvesting technique has the advantage of being independent of active muscle contribution (Riemer & Shapiro, 2011). In the present project, it was hypothesized that enough energy could be harvested at heel strike to provide dorsiflexion assistance following toe-off. Findings from the SPAE design and evaluation (Chapters 5 and 6) combined with the kinetic analyses of the first experiment (Chapter 4), confirmed that harvested heel strike energy is adequate to effectively increase foot-ground clearance, specifically at MFC.

While heel strike energy harvesting has potential as an unlimited mobile power source, there may be adverse effects. To maintain heel-ground and foot-ground clearance a device using this method must not encumber the shoe outsole (Mariani et al., 2012). In the SPAE described in this project the heel strike harvesting mechanism did not add unacceptable volume or mass to the outsole. Additionally, the entire

mechanism was connected to a calf brace using a two degrees of freedom mechanical joint, allowing unrestricted plantarflexion-dorsiflexion and inversion-eversion. A further requirement is that heel strike harvesting mechanisms should not influence the COP, creating unanticipated additional ankle moments. The harvesting lever of our SPAE was attached close to the ankle joint centre to minimize this effect and the results in Chapter 5 confirmed no difference in COP when walking with and without the SPAE.

Despite the joint assistance provided by a mechanical device, adding mass distally to the swing limb proportionately increases the energy cost of walking (Browning et al., 2007). Bipedal locomotion is optimized by the harmonic coordination of engaged joints and muscles and changes to this balance may increase metabolic cost (Biewener & Patek, 2018; Ferris, 2019). The metabolic energy expenditure of walking using our SPAE was not measured but requires future investigation to guide further design improvements. The future of the SPAE will depend on weight reduction and a more compact design. Our device used aluminium for the major structure and steel and bronze for the shafts and clutches, giving a mass of 1.4 Kg, not including the shoe. Mass could be decreased by modifying the design and using lighter materials, such as carbon fibre and compressed plastic, targeting a proposed mass of 0.4 Kg for a commercial AFO (Smith et al., 1982). In future designs harvested heel strike energy could be directed toward plantarflexion assistance during push-off, as a further measure to decrease metabolic energy cost.

7.4 Future directions

This Thesis has shown that a biomechanically designed SPAE can provide functional active ankle assistance during swing, without an external energy source or electronic control system. The results were promising but there were limitations, and improvements have been suggested. Gait mechanics improve with practice but in this study, subjects were only tested while wearing the device for the first time, with no previous experience. SPAE adaptations due to more extended training should, therefore, be investigated and the biomechanical differences between overground and treadmill walking taken into account (Parvataneni et al., 2009). Moreover, because heel strike is necessary for stabilizing bipedal locomotion (Goswami et al., 1998;

Hürmüzlü & Moskowitz, 1987), further consideration of balance-related spatial-temporal variables would also be instructive.

Principal device design features were investigated by testing one subject and the kinetics of SPAE walking, such as the position of center of pressure and ankle power, were also determined. An extended sample was recruited to confirm proof of concept, with respect to heel strike energy harvesting and the capacity to use this energy to increase minimum foot clearance (MFC), which was successfully demonstrated. In future, however, larger and more targeted populations will be recruited for further kinetics investigation and design modifications.

Current exoskeleton technology faces challenges in the commercial market for medical devices, requiring further consideration of their neurological and biomechanical effects and improvements in control systems and fuel-efficiency. The effects of an exoskeleton must, therefore, initially be investigated in able-bodied subjects before exploring their clinical use. The “*Eksø*” is an exoskeleton which recently received FDA approval for the commercial market but required years of research and development (Mertz, 2012). The SPAE concepts developed here may have potential for clinical application but require further development prior to trials with gait impaired individuals. The research presented in this dissertation, however, provides proof-of-concept for active ankle assistance using heel strike energy harvesting.

The SPAE’s proof-of-concept was confirmed by evaluating walking with and without the SPAE in treadmill walking, essential for comparing the device’s performance with data from the intentionally augmented ankle dorsiflexion using biofeedback, reported in Chapter 3. Overground walking, specifically over irregular and natural surfaces would, however, be important in further evaluating the SPAE prior to implementation in everyday settings. Overground walking tests are, therefore, one of our group’s objectives in future development of the SPAE.

Using passive AFOs in the longer term may result in muscle atrophy because the user becomes dependent on the device (Appell, 1990; Geboers et al., 2000; Lehmann et al., 1986). Ankle movement restriction provided by passive AFOs may, moreover, cause dysfunctional neural adaptations associated with reduced muscle activity (Bruehlmeier et al., 1998; Geboers et al., 2002). Passive AFOs, therefore, may

increase the physical therapy required to improve muscle participation (Park et al., 2014). Active orthoses and exoskeletons, on the other hand, not only grant assistance but may also prevent the development of gait irregularities (Park et al., 2014). The efficacy of active devices to re-educate the neuro-motor control system has been shown by Krebs et al., (2006) and Blaya & Herr, (2004).

Neural damage due to events such as stroke may not be permanent because the central nervous system has some capacity to recover (Xu et al., 2014). The preferred treatment for ankle joint impairments may, therefore, combine rehabilitation training with practice using an assistive device (Shorter et al., 2011a). Our SPAE, has the potential to provide that active assistance and serve as a rehabilitation intervention. These concepts are encouraging for further investigation, but much work remains before the design concepts underpinning our SPAE can be focussed on clinical applications. Future research questions would be aimed toward improving toe-off and heel contact detectors across a range of speeds, decreasing mass and bulk and investigating the device's performance in overground walking, including the adaptation to irregular surfaces.

REFERENCES

- Adamczyk, P. G., & Kuo, A. D. (2014). Mechanisms of gait asymmetry due to push-off deficiency in unilateral amputees. *IEEE Transactions on Neural Systems and Rehabilitation Engineering*, 23(5), 776-785.
- Adiputra, D., Nazmi, N., Bahiuddin, I., Ubaidillah, U., Imaduddin, F., Rahman, A., . . . Zamzuri, H. (2019). A review on the control of the mechanical properties of ankle foot orthosis for gait assistance. *Actuators*, 8(1), 10.
- Alam, M., Choudhury, I. A., & Mamat, A. B. (2014). Mechanism and design analysis of articulated ankle foot orthoses for drop-foot. *The Scientific World Journal*, 2014.
- Alexander, R. (1987). The spring in your step. *New Scientist*, 30, 42-44.
- Alexander, R. (1990). Three uses for springs in legged locomotion. *International Journal of Robotics Research*, 9(2), 53-61.
- Alton, F., Baldey, L., Caplan, S., & Morrissey, M. (1998). A kinematic comparison of overground and treadmill walking. *Clinical Biomechanics*, 13(6), 434-440.
- Amerinatanzi, A., Zamanian, H., Shayesteh Moghaddam, N., Jahadakbar, A., & Elahinia, M. (2017). Application of the superelastic NiTi spring in ankle foot orthosis (AFO) to create normal ankle joint behavior. *Bioengineering*, 4(4), 95.
- Andersen, M. S., Damsgaard, M., MacWilliams, B., & Rasmussen, J. (2010). A computationally efficient optimisation-based method for parameter identification of kinematically determinate and over-determinate biomechanical systems. *Computer Methods in Biomechanics and Biomedical Engineering*, 13(2), 171-183.
- Andersen, M. S., Damsgaard, M., & Rasmussen, J. (2009). Kinematic analysis of over-determinate biomechanical systems. *Computer Methods in Biomechanics and Biomedical Engineering*, 12(4), 371-384.
- ANZ. (2019). Australian and New Zealand falls prevention society. Retrieved from <http://www.anzfallsprevention.org/>
- Appell, H.-J. (1990). Muscular atrophy following immobilisation. *Sports Medicine*, 10(1), 42-58.
- Arnold, A. S., Schwartz, M. H., Thelen, D. G., & Delp, S. L. (2007). Contributions of muscles to terminal-swing knee motions vary with walking speed. *Journal of Biomechanics*, 40(16), 3660-3671.
- Baines, P. M., Schwab, A., & Van Soest, A. (2018). Experimental estimation of energy absorption during heel strike in human barefoot walking. *PloS one*, 13(6).
- Bajelan, S., & Azghani, M. R. (2011). *Musculoskeletal analysis of sit-to-stand maneuver in order to compare the various standing up strategies*. Paper presented at the 2011 18th Iranian Conference of Biomedical Engineering (ICBME).
- Bajelan, S., & Azghani, M. R. (2014). Musculoskeletal modeling and simulation of three various Sit-to-Stand strategies: An evaluation of the biomechanical effects of the chair-rise strategy modification. *Technology and Health Care*, 22(4), 627-644.
- Bajelan, S., Azghani, M. R., & Niroomand-Oscuii, H. (2010). *A novel design of sit-to-stand assistive device for elderly and infirm people*. Paper presented at the 6th World Congress of Biomechanics, Singapore Suntec Convention Centre.
- Bajelan, S., Levinger, P., Nagano, H., Downie, C., & Begg, R. (2017a). *The contribution of hip abductor muscles during two-steps balance recovery*. Paper presented at the XXVI Congress of the International Society of Biomechanics.

- Bajelan, S., Nagano, H., Sparrow, T., & Begg, R. (2017b). *Effects of wide step walking on swing phase hip muscle forces and spatio-temporal gait parameters*. Paper presented at the 39th Annual International Conference of the IEEE Engineering in Medicine and Biology Society (EMBC).
- Bajelan, S., Sparrow, T., & Begg, R. (2019a). *The mechanics of tibialis anterior muscle during swing phase ankle dorsiflexion: implications for biomimetic device design*. Paper presented at the 41st Annual International Conference of the IEEE Engineering in Medicine & Biology Society (EMBC), July 23-27, 2019, Berlin, Germany.
- Bajelan, S., Sparrow, T., & Begg, R. (2019b). *Walking more safely by increasing swing phase ankle dorsiflexion*. Paper presented at the XXVII Congress of the International Society of Biomechanics (ISB) / American Society of Biomechanics (ASB) 2019.
- Barrett, R., Besier, T. F., & Lloyd, D. G. (2007). Individual muscle contributions to the swing phase of gait: An EMG-based forward dynamics modelling approach. *Simulation Modelling Practice and Theory*, 15(9), 1146-1155.
- Barrett, R., Mills, P. M., & Begg, R. (2010). A systematic review of the effect of ageing and falls history on minimum foot clearance characteristics during level walking. *Gait & Posture*, 32(4), 429-435.
- Begg, R., Best, R., Dell'Oro, L., & Taylor, S. (2007). Minimum foot clearance during walking: strategies for the minimisation of trip-related falls. *Gait & Posture*, 25(2), 191-198.
- Begg, R., Galea, M. P., James, L., Sparrow, T., Levinger, P., Khan, F., & Said, C. M. (2019). Real-time foot clearance biofeedback to assist gait rehabilitation following stroke: a randomized controlled trial protocol. *Trials*, 20(1), 317.
- Begg, R., & Sparrow, T. (2000). Gait characteristics of young and older individuals negotiating a raised surface: implications for the prevention of falls. *The Journals of Gerontology Series A: Biological Sciences and Medical Sciences*, 55(3), M147-M154.
- Begg, R., & Sparrow, T. (2006). Ageing effects on knee and ankle joint angles at key events and phases of the gait cycle. *Journal of Medical Engineering & Technology*, 30(6), 382-389.
- Begg, R., Tirosh, O., Said, C. M., Sparrow, T., Steinberg, N., Levinger, P., & Galea, M. P. (2014). Gait training with real-time augmented toe-ground clearance information decreases tripping risk in older adults and a person with chronic stroke. *Frontiers in Human Neuroscience*, 8, 243.
- Bento, P. C. B., Pereira, G., Ugrinowitsch, C., & Rodacki, A. L. F. (2010). Peak torque and rate of torque development in elderly with and without fall history. *Clinical Biomechanics*, 25(5), 450-454.
- Berg, W. P., Alessio, H. M., Mills, E. M., & Tong, C. (1997). Circumstances and consequences of falls in independent community-dwelling older adults. *Age and Ageing*, 26(4), 261-268.
- Bernstein, N. A. (1967). The co-ordination and regulation of movements: Conclusions towards the Study of Motor Co-ordination. *Biodynamics of Locomotion*, 104-113.
- Bharadwaj, K., & Sugar, T. G. (2006). *Kinematics of a robotic gait trainer for stroke rehabilitation*. Paper presented at the Proceedings 2006 IEEE International Conference on Robotics and Automation, 2006. ICRA 2006.

- Biewener, A., Farley, C. T., Roberts, T. J., & Temaner, M. (2004). Muscle mechanical advantage of human walking and running: implications for energy cost. *Journal of applied physiology*, *97*(6), 2266-2274.
- Biewener, A., & Patek, S. (2018). *Animal locomotion*: Oxford University Press.
- Blake, A., Morgan, K., Bendall, M., Dallosso, H., Ebrahim, S., Arie, T. a., . . . Bassey, E. (1988). Falls by elderly people at home: prevalence and associated factors. *Age and Ageing*, *17*(6), 365-372.
- Blaya, J. A., & Herr, H. (2004). Adaptive control of a variable-impedance ankle-foot orthosis to assist drop-foot gait. *IEEE Transactions on Neural Systems and Rehabilitation Engineering*, *12*(1), 24-31.
- Błażkiewicz, M. (2013). Muscle force distribution during forward and backward locomotion. *Acta of Bioengineering and Biomechanics*, *15*(3), 3--9.
- Boehler, A. W., Hollander, K. W., Sugar, T. G., & Shin, D. (2008). *Design, implementation and test results of a robust control method for a powered ankle foot orthosis (AFO)*. Paper presented at the 2008 IEEE International Conference on Robotics and Automation.
- Boes, M. K. (2016). Evaluation of a pneumatic ankle-foot orthosis: portability and functionality (Doctoral dissertation, University of Illinois at Urbana-Champaign).
- Bogey, R., Gitter, A. J., & Barnes, L. (2010). Determination of ankle muscle power in normal gait using an EMG-to-force processing approach. *Journal of Electromyography and Kinesiology*, *20*(1), 46-54.
- Bogue, R. (2015). Energy harvesting: a review of recent developments. *Sensor Review*.
- Bregman, D., Harlaar, J., Meskers, C., & De Groot, V. (2012). Spring-like Ankle Foot Orthoses reduce the energy cost of walking by taking over ankle work. *Gait & Posture*, *35*(1), 148-153.
- Bronstein, A., & Brandt, T. (2004). *Clinical disorders of balance, posture and gait*: CRC Press.
- Browning, R. C., Modica, J. R., Kram, R., & Goswami, A. (2007). The effects of adding mass to the legs on the energetics and biomechanics of walking. *Medicine & Science in Sports & Exercise*, *39*(3), 515-525.
- Bruehlmeier, M., Dietz, V., Leenders, K., Roelcke, U., Missimer, J., & Curt, A. (1998). How does the human brain deal with a spinal cord injury? *European Journal of Neuroscience*, *10*(12), 3918-3922.
- Buchanan, T. S., Lloyd, D. G., Manal, K., & Besier, T. F. (2005). Estimation of muscle forces and joint moments using a forward-inverse dynamics model. *Medicine & Science in Sports & Exercise*, *37*(11), 1911-1916.
- Burdett, R. G., Borello-France, D., Blatchly, C., & Potter, C. (1988). Gait comparison of subjects with hemiplegia walking unbraced, with ankle-foot orthosis, and with Air-Stirrup® brace. *Physical Therapy*, *68*(8), 1197-1203.
- Butler, E., Druizin, M., Sullivan, E., Rose, J., & Gamble, J. G. (2006). Human walking. *Vol. third ed.. Philadelphia, MD: Lippincott, Williams and Wilkins*, 131-147.
- Byrne, C., O'keeffe, D., Donnelly, A., & Lyons, G. (2007). Effect of walking speed changes on tibialis anterior EMG during healthy gait for FES envelope design in drop foot correction. *Journal of Electromyography and Kinesiology*, *17*(5), 605-616.
- Cadovaa, M. (2013). *Use of OpenSim and AnyBody modelling software for dynamic simulation of the human masticatory system*. Paper presented at the 18th International Symposium on Computational Biomechanics in Ulm CBU.

- Carbone, V., Fluit, R., Pellikaan, P., Van Der Krogt, M., Janssen, D., Damsgaard, M., . . . Verdonchot, N. (2015). TLEM 2.0—A comprehensive musculoskeletal geometry dataset for subject-specific modeling of lower extremity. *Journal of Biomechanics*, *48*(5), 734-741.
- Cavagna, G., Willems, P., & Heglund, N. (2000). The role of gravity in human walking: pendular energy exchange, external work and optimal speed. *The Journal of Physiology*, *528*(3), 657-668.
- Cenciarini, M., & Dollar, A. M. (2011). *Biomechanical considerations in the design of lower limb exoskeletons*. Paper presented at the 2011 IEEE International Conference on Rehabilitation Robotics.
- Chang, A. H., Moisio, K. C., Chmiel, J. S., Eckstein, F., Guermazi, A., Prasad, P. V., . . . Hayes, K. (2015). External knee adduction and flexion moments during gait and medial tibiofemoral disease progression in knee osteoarthritis. *Osteoarthritis and Cartilage*, *23*(7), 1099-1106.
- Chen, B., Zhao, X., Ma, H., Qin, L., & Liao, W.-H. (2017). Design and characterization of a magneto-rheological series elastic actuator for a lower extremity exoskeleton. *Smart Materials and Structures*, *26*(10), 105008.
- Chen, B., Zi, B., Zeng, Y., Qin, L., & Liao, W.-H. (2018). Ankle-foot orthoses for rehabilitation and reducing metabolic cost of walking: Possibilities and challenges. *Mechatronics*, *53*, 241-250.
- Chen, G., Patten, C., Kothari, D. H., & Zajac, F. E. (2005). Gait differences between individuals with post-stroke hemiparesis and non-disabled controls at matched speeds. *Gait & Posture*, *22*(1), 51-56.
- Chen, H.-L., Lu, T.-W., Wang, T.-M., & Huang, S.-C. (2008). Biomechanical strategies for successful obstacle crossing with the trailing limb in older adults with medial compartment knee osteoarthritis. *Journal of Biomechanics*, *41*(4), 753-761.
- Chin, R., Hsiao-Weckler, E. T., Loth, E., Kogler, G. F., Manwaring, S. D., Tyson, S. N., . . . Gilmer, J. N. (2009). A pneumatic power harvesting ankle-foot orthosis to prevent foot-drop. *Journal of Neuroengineering and Rehabilitation*, *6*(1), 19.
- Chou, L.-S., Kaufman, K. R., Hahn, M. E., & Brey, R. H. (2003). Medio-lateral motion of the center of mass during obstacle crossing distinguishes elderly individuals with imbalance. *Gait & Posture*, *18*(3), 125-133.
- Clark, C. C., Barnes, C. M., Holton, M., Summers, H. D., & Stratton, G. (2016). A kinematic analysis of fundamental movement skills. *Sport Science Review*, *25*(3-4), 261-275.
- Collins, S. H., Wiggin, M. B., & Sawicki, G. S. (2015). Reducing the energy cost of human walking using an unpowered exoskeleton. *Nature*, *522*(7555), 212-215.
- Cripps, R. A., & Carman, J. (2001). *Falls by the elderly in Australia: Trends and data for 1998*: Australian Institute of Health and Welfare.
- Crowninshield, R. D. (1978). Use of optimization techniques to predict muscle forces.
- Dadashi, F., Mariani, B., Rochat, S., Büla, C. J., Santos-Eggimann, B., & Aminian, K. (2014). Gait and foot clearance parameters obtained using shoe-worn inertial sensors in a large-population sample of older adults. *Sensors*, *14*(1), 443-457.
- Damsgaard, M., Rasmussen, J., Christensen, S. T., Surma, E., & De Zee, M. (2006). Analysis of musculoskeletal systems in the AnyBody Modeling System. *Simulation Modelling Practice and Theory*, *14*(8), 1100-1111.
- Danielsson, A., Willén, C., & Sunnerhagen, K. S. (2010). *Comparison of energy cost of walking with and without a carbon composite ankle foot orthosis in stroke*

- subjects*. Paper presented at the 13th ISPO World Congress, 10-15 May 2010, Leipzig, Germany.
- De Asha, A. R., & Buckley, J. G. (2015). The effects of walking speed on minimum toe clearance and on the temporal relationship between minimum clearance and peak swing-foot velocity in unilateral trans-tibial amputees. *Prosthetics and Orthotics International*, 39(2), 120-125.
- De Luca, C. J. (1997). The use of surface electromyography in biomechanics. *Journal of Applied Biomechanics*, 13(2), 135-163.
- Deberg, L., Taheri Andani, M., Hosseinipour, M., & Elahinia, M. (2014). An SMA passive ankle foot orthosis: Design, modeling, and experimental evaluation. *Smart Materials Research*, 2014.
- Delp, S. L., Anderson, F. C., Arnold, A. S., Loan, P., Habib, A., John, C. T., . . . Thelen, D. G. (2007). OpenSim: open-source software to create and analyze dynamic simulations of movement. *IEEE Transactions on Biomedical Engineering*, 54(11), 1940-1950.
- Dežman, M., Babič, J., & Gams, A. (2017). *Qualitative Assessment of a Clutch-Actuated Ankle Exoskeleton*. Paper presented at the International Conference on Robotics in Alpe-Adria Danube Region.
- Dežman, M., Debevec, T., Babič, J., & Gams, A. (2016). *Effects of passive ankle exoskeleton on human energy expenditure: pilot evaluation*. Paper presented at the International Conference on Robotics in Alpe-Adria Danube Region.
- Di Nardo, F., Ghetti, G., & Fioretti, S. (2013). Assessment of the activation modalities of gastrocnemius lateralis and tibialis anterior during gait: a statistical analysis. *Journal of Electromyography and Kinesiology*, 23(6), 1428-1433.
- Doke, J., Donelan, J. M., & Kuo, A. D. (2005). Mechanics and energetics of swinging the human leg. *Journal of Experimental Biology*, 208(3), 439-445.
- Dollar, A. M., & Herr, H. (2008). Lower extremity exoskeletons and active orthoses: Challenges and state-of-the-art. *IEEE Transactions on Robotics*, 24(1), 144-158.
- Donelan, J. M., Kram, R., & Kuo, A. D. (2002). Mechanical work for step-to-step transitions is a major determinant of the metabolic cost of human walking. *Journal of Experimental Biology*, 205(23), 3717-3727.
- Dumas, R., Nicol, E., & Chèze, L. (2007). Influence of the 3D inverse dynamic method on the joint forces and moments during gait: 786-790.
- Dzahir, M. A. M., & Yamamoto, S.-i. (2014). Recent trends in lower-limb robotic rehabilitation orthosis: Control scheme and strategy for pneumatic muscle actuated gait trainers. *Robotics*, 3(2), 120-148.
- Ebrahimi, A. (2018). The development and application of a framework for exploring the energetics of gait strategy adaptations (Doctoral dissertation, University of Delaware).
- Ebrahimi, A., Goldberg, S. R., & Stanhope, S. J. (2017). Changes in relative work of the lower extremity joints and distal foot with walking speed. *Journal of Biomechanics*, 58, 212-216.
- Erdemir, A., McLean, S., Herzog, W., & van den Bogert, A. J. (2007). Model-based estimation of muscle forces exerted during movements. *Clinical Biomechanics*, 22(2), 131-154.
- Fatone, S., & Hansen, A. H. (2007). Effect of ankle-foot orthosis on roll-over shape in adults with hemiplegia. *Journal of Rehabilitation Research & Development*, 44(1), 11.

- FDA. (2016). Food and Drug Administration. 21 CFR 890.3480. Retrieved from https://www.ecfr.gov/cgi-bin/retrieveECFR?gp=1&SID=b37c513bf62af085f32e31c0a1310078&ty=HTML&h=L&mc=true&r=SECTION&n=se21.8.890_13480
- Ferris, D. (2019). Merging Humans and Machines to Assist Legged Locomotion.
- Ferris, D., Czerniecki, J. M., & Hannaford, B. (2005). An ankle-foot orthosis powered by artificial pneumatic muscles. *Journal of Applied Biomechanics*, 21(2), 189-197.
- Ferris, D., Gordon, K. E., Sawicki, G. S., & Peethambaran, A. (2006). An improved powered ankle-foot orthosis using proportional myoelectric control. *Gait & Posture*, 23(4), 425-428.
- Fluit, R., Andersen, M. S., Kolk, S., Verdonschot, N., & Koopman, H. F. (2014). Prediction of ground reaction forces and moments during various activities of daily living. *Journal of Biomechanics*, 47(10), 2321-2329.
- Forsberg, H. (1985). Ontogeny of human locomotor control I. Infant stepping, supported locomotion and transition to independent locomotion. *Experimental Brain Research*, 57(3), 480-493.
- Fusco, N., & Crétual, A. (2008). Instantaneous treadmill speed determination using subject's kinematic data. *Gait & Posture*, 28(4), 663-667.
- Geboers, J. F., Drost, M. R., Spaans, F., Kuipers, H., & Seelen, H. A. (2002). Immediate and long-term effects of ankle-foot orthosis on muscle activity during walking: a randomized study of patients with unilateral foot drop. *Archives of Physical Medicine and Rehabilitation*, 83(2), 240-245.
- Geboers, J. F., Tuijl, J. v., Seelen, H., & Drost, M. (2000). Effect of immobilization on ankle dorsiflexion strength. *Scandinavian Journal of Rehabilitation Medicine*, 32(2), 66-71.
- Gillespie, L. D., Robertson, M. C., Gillespie, W. J., Sherrington, C., Gates, S., Clemson, L. M., & Lamb, S. E. (2012). Interventions for preventing falls in older people living in the community. *Cochrane Database of Systematic Reviews*(9).
- Goldberg, S. R., Öunpuu, S., & Delp, S. L. (2003). The importance of swing-phase initial conditions in stiff-knee gait. *Journal of Biomechanics*, 36(8), 1111-1116.
- Gordon, D., Robertson, E., & Winter, D. A. (1980). Mechanical energy generation, absorption and transfer amongst segments during walking. *Journal of Biomechanics*, 13(10), 845-854.
- Gordon, K. E., Sawicki, G. S., & Ferris, D. (2006). Mechanical performance of artificial pneumatic muscles to power an ankle-foot orthosis. *Journal of Biomechanics*, 39(10), 1832-1841.
- Goswami, A., Thuilot, B., & Espiau, B. (1998). A study of the passive gait of a compass-like biped robot: Symmetry and chaos. *The International Journal of Robotics Research*, 17(12), 1282-1301.
- Gottschall, J. S., & Kram, R. (2003). Energy cost and muscular activity required for propulsion during walking. *Journal of Applied Physiology*, 94(5), 1766-1772.
- Graci, V., Elliott, D. B., & Buckley, J. G. (2009). Peripheral visual cues affect minimum-foot-clearance during overground locomotion. *Gait & Posture*, 30(3), 370-374.
- Granata, K. P., & Lockhart, T. E. (2008). Dynamic stability differences in fall-prone and healthy adults. *Journal of Electromyography and Kinesiology*, 18(2), 172-178.

- Griffin, M., Olney, S., & McBride, I. (1995). Role of symmetry in gait performance of stroke subjects with hemiplegia. *Gait & Posture*, 3(3), 132-142.
- Griffin, M. J. (2001). The validation of biodynamic models. *Clinical Biomechanics*, 16, S81-S92.
- Griffin, T. M., Roberts, T. J., & Kram, R. (2003). Metabolic cost of generating muscular force in human walking: insights from load-carrying and speed experiments. *Journal of Applied Physiology*, 95(1), 172-183.
- Grimmer, M., & Seyfarth, A. (2014). Mimicking human-like leg function in prosthetic limbs *Neuro-Robotics* (pp. 105-155): Springer.
- Halaki, M., & Ginn, K. (2012). Normalization of EMG signals: to normalize or not to normalize and what to normalize to. *Computational Intelligence in Electromyography Analysis-a Perspective on Current Applications and Future Challenges*, 175-194.
- Hallems, A., Aerts, P., Otten, B., De Deyn, P. P., & De Clercq, D. (2004). Mechanical energy in toddler gait A trade-off between economy and stability? *Journal of Experimental Biology*, 207(14), 2417-2431.
- He, Y., Eguren, D., Luu, T. P., & Contreras-Vidal, J. L. (2017). Risk management and regulations for lower limb medical exoskeletons: a review. *Medical Devices (Auckland, NZ)*, 10, 89.
- Hermens, H. J., Freriks, B., Merletti, R., Stegeman, D., Blok, J., Rau, G., . . . Hägg, G. (1999). European recommendations for surface electromyography. *Roessingh Research and Development*, 8(2), 13-54.
- Herr, H. (2009). Exoskeletons and orthoses: classification, design challenges and future directions. *Journal of Neuroengineering and Rehabilitation*, 6(1), 21.
- Herr, H., & Grabowski, A. M. (2012). Bionic ankle-foot prosthesis normalizes walking gait for persons with leg amputation. *Proceedings of the Royal Society B: Biological Sciences*, 279(1728), 457-464.
- Hill, K., Schwarz, J., Flicker, L., & Carroll, S. (1999). Falls among healthy, community-dwelling, older women: a prospective study of frequency, circumstances, consequences and prediction accuracy. *Australian and New Zealand Journal of Public Health*, 23(1), 41-48.
- Hirai, H., Ozawa, R., Goto, S., Fujigaya, H., Yamasaki, S., Hatanaka, Y., & Kawamura, S. (2006). *Development of an ankle-foot orthosis with a pneumatic passive element*. Paper presented at the ROMAN 2006-The 15th IEEE International Symposium on Robot and Human Interactive Communication.
- Hof, A., Gazendam, M., & Sinke, W. (2005). The condition for dynamic stability. *Journal of Biomechanics*, 38(1), 1-8.
- Hortobágyi, T., Solnik, S., Gruber, A., Rider, P., Steinweg, K., Helseth, J., & DeVita, P. (2009). Interaction between age and gait velocity in the amplitude and timing of antagonist muscle coactivation. *Gait & Posture*, 29(4), 558-564.
- Houng, H. O. C., Sarah, S., Parasuraman, S., Khan, A., & Elamvazuthi, I. (2014). Energy harvesting from human locomotion: gait analysis, design and state of art. *Procedia Computer Science*, 42, 327-335.
- Hürmüzlü, Y., & Moskowitz, G. D. (1987). Bipedal locomotion stabilized by impact and switching: I. two-and three-dimensional, three-element models. *Dynamics and Stability of Systems*, 2(2), 73-96.
- Hwang, S., Kim, J., Yi, J., Tae, K., Ryu, K., & Kim, Y. (2006). *Development of an active ankle foot orthosis for the prevention of foot drop and toe drag*. Paper presented at the 2006 International Conference on Biomedical and Pharmaceutical Engineering.

- Iosa, M., Bini, F., Marinozzi, F., Fusco, A., Morone, G., Koch, G., . . . Paolucci, S. (2016). Stability and harmony of gait in patients with subacute stroke. *Journal of Medical and Biological Engineering*, 36(5), 635-643.
- Islam, M., & Hsiao-Wecksler, E. T. (2016). Developing a Classification Algorithm for Plantarflexor Actuation Timing of a Powered Ankle–Foot Orthosis. *Journal of Medical Devices*, 10(3).
- Jørgensen, H. S., Nakayama, H., Raaschou, H. O., & Olsen, T. S. (1995). Recovery of walking function in stroke patients: the Copenhagen Stroke Study. *Archives of Physical Medicine and Rehabilitation*, 76(1), 27-32.
- Judge, L., Moreau, C., & Burke, J. (2003). Neural adaptations with sport-specific resistance training in highly skilled athletes. *Journal of Sports Sciences*, 21(5), 419-427.
- Jung, Y., Jung, M., Lee, K., & Koo, S. (2014). Ground reaction force estimation using an insole-type pressure mat and joint kinematics during walking. *Journal of Biomechanics*, 47(11), 2693-2699.
- Kao, P.-C., & Ferris, D. (2009). Motor adaptation during dorsiflexion-assisted walking with a powered orthosis. *Gait & Posture*, 29(2), 230-236.
- Kawamura, S., Yamamoto, T., Ishida, D., Ogata, T., Nakayama, Y., Tabata, O., & Sugiyama, S. (2002). *Development of passive elements with variable mechanical impedance for wearable robots*. Paper presented at the Proceedings 2002 IEEE International Conference on Robotics and Automation (Cat. No. 02CH37292).
- Kerrigan, D. C., Frates, E. P., Rogan, S., & Riley, P. O. (2000). Hip hiking and circumduction: quantitative definitions. *American Journal of Physical Medicine & Rehabilitation*, 79(3), 247-252.
- Kerrigan, D. C., Todd, M. K., Della Croce, U., Lipsitz, L. A., & Collins, J. J. (1998). Biomechanical gait alterations independent of speed in the healthy elderly: evidence for specific limiting impairments. *Archives of Physical Medicine and Rehabilitation*, 79(3), 317-322.
- Kesikburun, S., Yavuz, F., Güzelküçük, Ü., Yaşar, E., & Balaban, B. (2017). Effect of ankle foot orthosis on gait parameters and functional ambulation in patients with stroke. *Turkish Journal of Physical Medicine and Rehabilitation*, 63(2), 143.
- Kikuchi, T., Tanaka, T., Shoji, A., Tanida, S., & Kato, M. (2011). *Gait measurement system to develop control model of intelligently controllable ankle-foot orthosis*. Paper presented at the 2011 IEEE/SICE International Symposium on System Integration (SII).
- Kikuchi, T., Tanida, S., Otsuki, K., Yasuda, T., & Furusho, J. (2010). *Development of third-generation intelligently controllable ankle-foot orthosis with compact MR fluid brake*. Paper presented at the 2010 IEEE International Conference on Robotics and Automation.
- Kikuchi, T., Tanida, S., Yasuda, T., & Fujikawa, T. (2013). *Automatic adjustment of initial drop speed of foot for intelligently controllable ankle foot orthosis*. Paper presented at the Proceedings of the 2013 IEEE/SICE International Symposium on System Integration.
- Kim, S. J., Chang, H., Cho, H., & Kim, J. (2018a). *Design of a seamless active ankle foot orthosis empowered by a custom portable pneumatic pump*. Paper presented at the 2018 18th International Conference on Control, Automation and Systems (ICCAS).

- Kim, Y., Jung, Y., Choi, W., Lee, K., & Koo, S. (2018b). Similarities and differences between musculoskeletal simulations of OpenSim and AnyBody modeling system. *Journal of Mechanical Science and Technology*, 32(12), 6037-6044.
- Krebs, H. I., Hogan, N., Durfee, W., & Herr, H. (2006). Rehabilitation robotics, orthotics, and prosthetics. *Textbook of Neural Repair and Rehabilitation*, 2, 165-181.
- Kuo, A. D. (2002). Energetics of actively powered locomotion using the simplest walking model. *J. Biomech. Eng.*, 124(1), 113-120.
- Kuo, A. D., Donelan, J. M., & Ruina, A. (2005). Energetic consequences of walking like an inverted pendulum: step-to-step transitions. *Exercise and Sport Sciences Reviews*, 33(2), 88-97.
- Lai, D. T., Begg, R., Taylor, S., & Palaniswami, M. (2008). Detection of tripping gait patterns in the elderly using autoregressive features and support vector machines. *Journal of Biomechanics*, 41(8), 1762-1772.
- Langholz, J. B., Westman, G., & Karlsteen, M. (2016). Musculoskeletal modelling in sports-evaluation of different software tools with focus on swimming. *Procedia Eng*, 147, 281-287.
- Lee, H.-J., & Chou, L.-S. (2006). Detection of gait instability using the center of mass and center of pressure inclination angles. *Archives of Physical Medicine and Rehabilitation*, 87(4), 569-575.
- Lee, H., & Hogan, N. (2014). Time-varying ankle mechanical impedance during human locomotion. *IEEE Transactions on Neural Systems and Rehabilitation Engineering*, 23(5), 755-764.
- Lee, S. J., & Hidler, J. (2008). Biomechanics of overground vs. treadmill walking in healthy individuals. *Journal of Applied Physiology*, 104(3), 747-755.
- Lehmann, J. F. (1993). Push-off and propulsion of the body in normal and abnormal gait. Correction by ankle-foot orthoses. *Clinical Orthopaedics and Related Research*(288), 97-108.
- Lehmann, J. F. (1999). Orthotics for the wounded combatant *Textbook of Military Medicine. Part IV. Rehabilitation of the Injured Combatant* (Vol. 2, pp. 703-740): Citeseer.
- Lehmann, J. F., Condon, S., & Price, R. (1986). Gait abnormalities in peroneal nerve paralysis and their corrections by orthoses: a biomechanical study. *Archives of Physical Medicine and Rehabilitation*, 67(6), 380-386.
- Lewek, M. D., Bradley, C., Wutzke, C. J., & Zinder, S. M. (2014). The relationship between spatiotemporal gait asymmetry and balance in individuals with chronic stroke. *Journal of Applied Biomechanics*, 30(1), 31-36.
- Lewis, C. L., & Ferris, D. (2008). Walking with increased ankle pushoff decreases hip muscle moments. *Journal of Biomechanics*, 41(10), 2082-2089.
- Li, Y. (2013). On improving control and efficiency of a portable pneumatically powered ankle-foot orthosis (Doctoral dissertation, University of Illinois at Urbana-Champaign).
- Lovejoy, C. O. (2005). The natural history of human gait and posture: Part 1. Spine and pelvis. *Gait & Posture*, 21(1), 95-112.
- Loverro, K. L., Mueske, N. M., & Hamel, K. A. (2013). Location of minimum foot clearance on the shoe and with respect to the obstacle changes with locomotor task. *Journal of Biomechanics*, 46(11), 1842-1850.
- Lugade, V., Lin, V., & Chou, L.-S. (2011). Center of mass and base of support interaction during gait. *Gait & Posture*, 33(3), 406-411.

- Lund, M. E., de Zee, M., Andersen, M. S., & Rasmussen, J. (2012). On validation of multibody musculoskeletal models. *Proceedings of the Institution of Mechanical Engineers, Part H: Journal of Engineering in Medicine*, 226(2), 82-94.
- Maganaris, C. N. (2000). In vivo measurement-based estimations of the moment arm in the human tibialis anterior muscle-tendon unit. *Journal of Biomechanics*, 33(3), 375-379.
- Maki, B. E., & McIlroy, W. E. (1997). The role of limb movements in maintaining upright stance: the “change-in-support” strategy. *Physical Therapy*, 77(5), 488-507.
- Malcolm, P., Derave, W., Galle, S., & De Clercq, D. (2013). A simple exoskeleton that assists plantarflexion can reduce the metabolic cost of human walking. *PloS One*, 8(2).
- Malcolm, P., Quesada, R. E., Caputo, J. M., & Collins, S. H. (2015). The influence of push-off timing in a robotic ankle-foot prosthesis on the energetics and mechanics of walking. *Journal of Neuroengineering and Rehabilitation*, 12(1), 21.
- Mariani, B., Rochat, S., Büla, C. J., & Aminian, K. (2012). Heel and toe clearance estimation for gait analysis using wireless inertial sensors. *IEEE Transactions on Biomedical Engineering*, 59(11), 3162-3168.
- Marsh, R. L., Ellerby, D. J., Carr, J. A., Henry, H. T., & Buchanan, C. I. (2004). Partitioning the energetics of walking and running: swinging the limbs is expensive. *Science*, 303(5654), 80-83.
- Martin, K. D., Polanski, W., Schackert, G., & Sobottka, S. B. (2015). New therapeutic option for drop foot with the ActiGait peroneal nerve stimulator—a technical note. *World Neurosurgery*, 84(6), 2037-2042.
- Martinez, I. J. R., Clemente, F., Kanitz, G., Mannini, A., Sabatini, A. M., & Cipriani, C. (2018). *Grasp force estimation from HD-EMG recordings with channel selection using elastic nets: preliminary study*. Paper presented at the 2018 7th IEEE International Conference on Biomedical Robotics and Biomechatronics (Biorob).
- Matsuda, F., Mukaino, M., Ohtsuka, K., Tanikawa, H., Tsuchiyama, K., Teranishi, T., . . . Saitoh, E. (2016). Analysis of strategies used by hemiplegic stroke patients to achieve toe clearance. *Japanese Journal of Comprehensive Rehabilitation Science*, 7, 111-118.
- McGowan, C. P., Neptune, R. R., & Kram, R. (2008). Independent effects of weight and mass on plantar flexor activity during walking: implications for their contributions to body support and forward propulsion. *Journal of Applied Physiology*, 105(2), 486-494.
- Mertz, L. (2012). The next generation of exoskeletons: lighter, cheaper devices are in the works. *IEEE Pulse*, 3(4), 56-61.
- Micera, S., Sabatini, A. M., & Dario, P. (1998). An algorithm for detecting the onset of muscle contraction by EMG signal processing. *Medical Engineering & Physics*, 20(3), 211-215.
- Mills, P. M., & Barrett, R. (2001). Swing phase mechanics of healthy young and elderly men. *Human Movement Science*, 20(4-5), 427-446.
- Mills, P. M., Barrett, R., & Morrison, S. (2008). Toe clearance variability during walking in young and elderly men. *Gait & Posture*, 28(1), 101-107.
- Miszko, T. A., Cress, M. E., Slade, J. M., Covey, C. J., Agrawal, S. K., & Doerr, C. E. (2003). Effect of strength and power training on physical function in

- community-dwelling older adults. *The Journals of Gerontology Series A: Biological Sciences and Medical Sciences*, 58(2), M171-M175.
- Mooney, L. M., Rouse, E. J., & Herr, H. (2014). Autonomous exoskeleton reduces metabolic cost of human walking during load carriage. *Journal of Neuroengineering and Rehabilitation*, 11(1), 80.
- Moosabhoy, M. A., & Gard, S. A. (2006). Methodology for determining the sensitivity of swing leg toe clearance and leg length to swing leg joint angles during gait. *Gait & Posture*, 24(4), 493-501.
- Mueller, M. J., Minor, S. D., Sahrman, S. A., Schaaf, J. A., & Strube, M. J. (1994). Differences in the gait characteristics of patients with diabetes and peripheral neuropathy compared with age-matched controls. *Physical Therapy*, 74(4), 299-308.
- Muñoz, M. R., González-Sánchez, M., & Cuesta-Vargas, A. I. (2015). Tibialis anterior analysis from functional and architectural perspective during isometric foot dorsiflexion: a cross-sectional study of repeated measures. *Journal of Foot and Ankle Research*, 8(1), 74.
- Nadeau, S., Gravel, D., Arseneault, A. B., & Bourbonnais, D. (1999). Plantarflexor weakness as a limiting factor of gait speed in stroke subjects and the compensating role of hip flexors. *Clinical Biomechanics*, 14(2), 125-135.
- Nagano, H. (2014). *Understanding Gait Control Dynamics: Ageing Effects on Falling Risks*. Victoria University.
- Nagano, H., Begg, R., Sparrow, T., & Taylor, S. (2011). Ageing and limb dominance effects on foot-ground clearance during treadmill and overground walking. *Clinical Biomechanics*, 26(9), 962-968.
- Nair, P. M., Rooney, K. L., Kautz, S. A., & Behrman, A. L. (2010). Stepping with an ankle foot orthosis re-examined: a mechanical perspective for clinical decision making. *Clinical Biomechanics*, 25(6), 618-622.
- Nasirzade, A., Sadeghi, H., Mokhtarinia, H. R., & Rahimi, A. (2017). A review of selected factors affecting gait symmetry. *Physical Treatments-Specific Physical Therapy Journal*, 7(1), 3-12.
- Neptune, R. R., Kautz, S. A., & Zajac, F. (2000). Muscle contributions to specific biomechanical functions do not change in forward versus backward pedaling. *Journal of Biomechanics*, 33(2), 155-164.
- Neptune, R. R., Sasaki, K., & Kautz, S. A. (2008). The effect of walking speed on muscle function and mechanical energetics. *Gait & Posture*, 28(1), 135-143.
- Nigg, B. M., Bahlsen, H., Luethi, S., & Stokes, S. (1987). The influence of running velocity and midsole hardness on external impact forces in heel-toe running. *Journal of Biomechanics*, 20(10), 951-959.
- Nigg, B. M., & Herzog, W. (2007). *Biomechanics of the musculo-skeletal system*: John Wiley & Sons.
- NIH. (2007). Why Population Aging Matters. Retrieved from <https://www.nia.nih.gov/sites/default/files/2017-06/WPAM.pdf>
- O'Connor, C. M., Thorpe, S. K., O'Malley, M. J., & Vaughan, C. L. (2007). Automatic detection of gait events using kinematic data. *Gait & Posture*, 25(3), 469-474.
- Olivier, J., Ortlieb, A., Bertusi, P., Vouga, T., Bouri, M., & Bleuler, H. (2015). *Impact of ankle locking on gait implications for the design of hip and knee exoskeletons*. Paper presented at the 2015 IEEE International Conference on Rehabilitation Robotics (ICORR).
- Oosterwaal, M., Telfer, S., Tørholm, S., Carbes, S., van Rhijn, L. W., Macduff, R., . . . Woodburn, J. (2011). Generation of subject-specific, dynamic, multisegment

- ankle and foot models to improve orthotic design: a feasibility study. *BMC Musculoskeletal Disorders*, 12(1), 256.
- Osaki, Y., Kunin, M., Cohen, B., & Raphan, T. (2007). Three-dimensional kinematics and dynamics of the foot during walking: a model of central control mechanisms. *Experimental Brain Research*, 176(3), 476-496.
- Pahl, G., & Beitz, W. (2013). *Engineering design: a systematic approach*: Springer Science & Business Media.
- Palastanga, N., & Soames, R. (2011). *Anatomy and human movement, structure and function with PAGEBURST access, 6: anatomy and human movement*: Elsevier Health Sciences.
- Palmer, M. L. (2002). Sagittal plane characterization of normal human ankle function across a range of walking gait speeds (Doctoral dissertation, Massachusetts Institute of Technology).
- Park, Y.-L., Chen, B.-r., Pérez-Arancibia, N. O., Young, D., Stirling, L., Wood, R. J., . . . Nagpal, R. (2014). Design and control of a bio-inspired soft wearable robotic device for ankle-foot rehabilitation. *Bioinspiration & Biomimetics*, 9(1), 016007.
- Parvataneni, K., Ploeg, L., Olney, S. J., & Brouwer, B. (2009). Kinematic, kinetic and metabolic parameters of treadmill versus overground walking in healthy older adults. *Clinical Biomechanics*, 24(1), 95-100.
- Passmore, R., & Durnin, J. V. (1955). Human energy expenditure. *Physiological Reviews*, 35(4), 801-840.
- Pavol, M. J., Owings, T. M., Foley, K. T., & Grabiner, M. D. (1999). Gait characteristics as risk factors for falling from trips induced in older adults. *The Journals of Gerontology Series A: Biological Sciences and Medical Sciences*, 54(11), M583-M590.
- Penny, W. D., Friston, K. J., Ashburner, J. T., Kiebel, S. J., & Nichols, T. E. (Eds.). (2011). *Statistical parametric mapping: the analysis of functional brain images*. Elsevier.
- Perry, J., & Burnfield, J. M. (1993). Gait analysis: normal and pathological function. *Developmental Medicine and Child Neurology*, 35, 1122-1122.
- Perry, J., & Davids, J. R. (1992). Gait analysis: normal and pathological function. *Journal of Pediatric Orthopaedics*, 12(6), 815.
- Perry, M. C., Carville, S. F., Smith, I. C. H., Rutherford, O. M., & Newham, D. J. (2007). Strength, power output and symmetry of leg muscles: effect of age and history of falling. *European Journal of Applied Physiology*, 100(5), 553-561.
- Petrucci, M. N. (2016). *Evaluation of gait kinematics and kinetics using a powered ankle-foot orthosis for gait assistance in people with multiple sclerosis* (Doctoral dissertation).
- Pijnappels, M., Reeves, N. D., Maganaris, C. N., & Van Dieen, J. H. (2008). Tripping without falling; lower limb strength, a limitation for balance recovery and a target for training in the elderly. *Journal of Electromyography and Kinesiology*, 18(2), 188-196.
- Prilutsky, B. I., & Zatsiorsky, V. M. (2002). Optimization-based models of muscle coordination. *Exercise and Sport Sciences Reviews*, 30(1), 32.
- Prince, F., Corriveau, H., Hébert, R., & Winter, D. A. (1997). Gait in the elderly. *Gait & Posture*, 5(2), 128-135.
- Ramsey, J. A. (2011). Development of a method for fabricating polypropylene non-articulated dorsiflexion assist ankle foot orthoses with predetermined stiffness. *Prosthetics and Orthotics International*, 35(1), 54-69.

- Rasmussen, J., Damsgaard, M., & Voigt, M. (2001). Muscle recruitment by the min/max criterion—a comparative numerical study. *Journal of Biomechanics*, *34*(3), 409-415.
- Rasmussen, J., Vondrak, V., Damsgaard, M., De Zee, M., Christensen, S. T., & Dostal, Z. (2002). The Any-Body project—Computer analysis of the human body. *Biomechanics of Man*, 270-274.
- Ren, L., Howard, D., Ren, L.-q., Nester, C., & Tian, L.-m. (2008). A phase-dependent hypothesis for locomotor functions of human foot complex. *Journal of Bionic Engineering*, *5*(3), 175-180.
- Richards, J. (2018). *The Comprehensive Textbook of Biomechanics-E-Book: with access to e-learning course [formerly Biomechanics in Clinic and Research]*: Elsevier Health Sciences.
- Riddick, R., & Kuo, A. D. (2016). Soft tissues store and return mechanical energy in human running. *Journal of Biomechanics*, *49*(3), 436-441.
- Riemer, R., & Shapiro, A. (2011). Biomechanical energy harvesting from human motion: theory, state of the art, design guidelines, and future directions. *Journal of Neuroengineering and Rehabilitation*, *8*(1), 22.
- Riener, R., & Edrich, T. (1999). Identification of passive elastic joint moments in the lower extremities. *Journal of Biomechanics*, *32*(5), 539-544.
- Robertson, G. E., Caldwell, G. E., Hamill, J., Kamen, G., & Whittlesey, S. (2013). *Research methods in biomechanics: Human kinetics*.
- Rome, L. C., Flynn, L., Goldman, E. M., & Yoo, T. D. (2005). Generating electricity while walking with loads. *Science*, *309*(5741), 1725-1728.
- Ros, J., Font Llagunes, J. M., & Kövecses, J. (2010). *Some aspects of heel strike impact dynamics in the stability of bipedal locomotion*. Paper presented at the 5th Asian Conference on Multibody Dynamics.
- Rose, J., & Gamble, J. G. (1994). *Human walking*: Williams & Wilkins.
- Rosenberg, M., & Steele, K. M. (2017). Simulated impacts of ankle foot orthoses on muscle demand and recruitment in typically-developing children and children with cerebral palsy and crouch gait. *PloS One*, *12*(7).
- Roy, A., Krebs, H. I., Bever, C. T., Forrester, L. W., Macko, R. F., & Hogan, N. (2011). Measurement of passive ankle stiffness in subjects with chronic hemiparesis using a novel ankle robot. *Journal of Neurophysiology*, *105*(5), 2132-2149.
- Ruiz-Muñoz, M., González-Sánchez, M., & Cuesta-Vargas, A. I. (2016). Foot dorsiflexion velocity and torque variance explained through architectural and electromyography variables comparing elders and stroke survivors. *Journal of Stroke and Cerebrovascular Diseases*, *25*(9), 2295-2304.
- Sadeghi, H. (2003). Local or global asymmetry in gait of people without impairments. *Gait & Posture*, *17*(3), 197-204.
- Sadeghi, H., Allard, P., Prince, F., & Labelle, H. (2000). Symmetry and limb dominance in able-bodied gait: a review. *Gait & Posture*, *12*(1), 34-45.
- Santhiranayagam, B. K., Lai, D. T., Sparrow, T., & Begg, R. (2015). Minimum toe clearance events in divided attention treadmill walking in older and young adults: a cross-sectional study. *Journal of Neuroengineering and Rehabilitation*, *12*(1), 58.
- Santhiranayagam, B. K., Sparrow, T., Lai, D. T., & Begg, R. (2017). Non-MTC gait cycles: an adaptive toe trajectory control strategy in older adults. *Gait & Posture*, *53*, 73-79.

- Sato, K. (2015). Factors affecting minimum foot clearance in the elderly walking: a multiple regression analysis. *Open Journal of Therapy and Rehabilitation*, 3(04), 109.
- Sawicki, G. S., & Ferris, D. (2009). A pneumatically powered knee-ankle-foot orthosis (KAFO) with myoelectric activation and inhibition. *Journal of Neuroengineering and Rehabilitation*, 6(1), 23.
- Schaal, S. (1999). Is imitation learning the route to humanoid robots? *Trends in Cognitive Sciences*, 3(6), 233-242.
- Schulz, B. W. (2011). Minimum toe clearance adaptations to floor surface irregularity and gait speed. *Journal of Biomechanics*, 44(7), 1277-1284.
- Schulz, B. W. (2017). A new measure of trip risk integrating minimum foot clearance and dynamic stability across the swing phase of gait. *Journal of Biomechanics*, 55, 107-112.
- Schulz, B. W., Hart-Hughes, S., & Bulat, T. (2013). Poster 136 Effects of age and Fall History on Minimum toe Clearance Adaptations to Gait Speed and Obstacles. *Archives of Physical Medicine and Rehabilitation*, 94(10), e60.
- Shorten, M. R. (1993). The energetics of running and running shoes. *Journal of Biomechanics*, 26, 41-51.
- Shorter, K. A. (2011). The design and control of active ankle-foot orthoses (Doctoral dissertation, University of Illinois at Urbana-Champaign).
- Shorter, K. A., Kogler, G. F., Loth, E., Durfee, W. K., & Hsiao-Wecksler, E. T. (2011a). A portable powered ankle-foot orthosis for rehabilitation. *Journal of Rehabilitation Research & Development*, 48(4).
- Shorter, K. A., Xia, J., Hsiao-Wecksler, E. T., Durfee, W. K., & Kogler, G. F. (2011b). Technologies for powered ankle-foot orthotic systems: Possibilities and challenges. *IEEE/ASME Transactions on Mechatronics*, 18(1), 337-347.
- Siegel, K. L., Kepple, T. M., & Caldwell, G. E. (1996). Improved agreement of foot segmental power and rate of energy change during gait: inclusion of distal power terms and use of three-dimensional models. *Journal of Biomechanics*, 29(6), 823-827.
- Silder, A., Whittington, B., Heiderscheit, B., & Thelen, D. G. (2007). Identification of passive elastic joint moment-angle relationships in the lower extremity. *Journal of Biomechanics*, 40(12), 2628-2635.
- Singam, A., Ytterberg, C., Tham, K., & von Koch, L. (2015). Participation in complex and social everyday activities six years after stroke: predictors for return to pre-stroke level. *PloS One*, 10(12).
- Skelton, D. A., Kennedy, J., & Rutherford, O. M. (2002). Explosive power and asymmetry in leg muscle function in frequent fallers and non-fallers aged over 65. *Age and Ageing*, 31(2), 119-125.
- Smeesters, C., Hayes, W. C., & McMahon, T. A. (2001). Disturbance type and gait speed affect fall direction and impact location. *Journal of Biomechanics*, 34(3), 309-317.
- Smith, A. E., Quigley, R. M., & Waters, C. R. (1982). Kinematic comparison of the BiCaal orthosis and the Rigid Polypropylene orthosis in stroke patients. *Sign*, 1, 6.
- Stanhope, V. A., Knarr, B. A., Reisman, D. S., & Higginson, J. S. (2014). Frontal plane compensatory strategies associated with self-selected walking speed in individuals post-stroke. *Clinical Biomechanics*, 29(5), 518-522.
- Steinicke, F., Visell, Y., Campos, J., & Lécuyer, A. (2013). *Human walking in virtual environments* (Vol. 56): Springer.

- Suda, E. Y., Matias, A. B., Bus, S. A., & Sacco, I. C. (2019). Impact of diabetic neuropathy severity on foot clearance complexity and variability during walking. *Gait & Posture*, *74*, 194-199.
- Sulzer, J. S., Gordon, K. E., Dhaher, Y. Y., Peshkin, M. A., & Patton, J. L. (2010). Preswing knee flexion assistance is coupled with hip abduction in people with stiff-knee gait after stroke. *Stroke*, *41*(8), 1709-1714.
- Takahashi, K. Z., Lewek, M. D., & Sawicki, G. S. (2015). A neuromechanics-based powered ankle exoskeleton to assist walking post-stroke: a feasibility study. *Journal of Neuroengineering and Rehabilitation*, *12*(1), 23.
- Takaiwa, M., & Noritsugu, T. (2008). *Development of pneumatic walking support shoes using potential energy of human*. Paper presented at the Proceedings of the JFPS International Symposium on Fluid Power.
- Teng, H.-L., MacLeod, T. D., Kumar, D., Link, T. M., Majumdar, S., & Souza, R. B. (2015a). Individuals with isolated patellofemoral joint osteoarthritis exhibit higher mechanical loading at the knee during the second half of the stance phase. *Clinical Biomechanics*, *30*(4), 383-390.
- Teng, H.-L., MacLeod, T. D., Link, T. M., Majumdar, S., & Souza, R. B. (2015b). Higher knee flexion moment during the second half of the stance phase of gait is associated with the progression of osteoarthritis of the patellofemoral joint on magnetic resonance imaging. *Journal of Orthopaedic & Sports Physical Therapy*, *45*(9), 656-664.
- Thalman, C. M., Hsu, J., Snyder, L., & Polygerinos, P. (2019). *Design of a soft Ankle-Foot Orthosis Exosuit for foot drop assistance*. Paper presented at the 2019 International Conference on Robotics and Automation (ICRA).
- Thelen, D. G., Schultz, A. B., Alexander, N. B., & Ashton-Miller, J. A. (1996). Effects of age on rapid ankle torque development. *The Journals of Gerontology Series A: Biological Sciences and Medical Sciences*, *51*(5), M226-M232.
- Tovell, A., McKenna, K., Bradley, C., & Pointer, S. (2012). Hospital separations due to injury and poisoning, Australia. *Canberra: Australian Institute of Health and Welfare*.
- Tözeren, A. (1999). *Human body dynamics: classical mechanics and human movement*: Springer Science & Business Media.
- Trinler, U. K. (2016). Muscle force estimation in clinical gait analysis (Doctoral dissertation, University of Salford).
- Trinler, U. K., Hollands, K., Jones, R., & Baker, R. (2018). A systematic review of approaches to modelling lower limb muscle forces during gait: applicability to clinical gait analyses. *Gait & Posture*, *61*, 353-361.
- Trinler, U. K., Schwameder, H., Baker, R., & Alexander, N. (2019). Muscle force estimation in clinical gait analysis using AnyBody and OpenSim. *Journal of Biomechanics*, *86*, 55-63.
- Tudor-Locke, C., & Bassett, D. R. (2004). How many steps/day are enough? *Sports Medicine*, *34*(1), 1-8.
- Tudor-Locke, C., Johnson, W. D., & Katzmarzyk, P. T. (2010). Accelerometer-determined steps per day in US children and youth. *Medicine & Science in Sports & Exercise*, *42*(12), 2244-2250.
- Turin, T. C., Kokubo, Y., Murakami, Y., Higashiyama, A., Rumana, N., Watanabe, M., & Okamura, T. (2010). Lifetime risk of stroke in Japan. *Stroke*, *41*(7), 1552-1554.

- Tyson, S. F., & Kent, R. M. (2013). Effects of an ankle-foot orthosis on balance and walking after stroke: a systematic review and pooled meta-analysis. *Archives of Physical Medicine and Rehabilitation*, 94(7), 1377-1385.
- Tyson, S. F., Sadeghi-Demneh, E., & Nester, C. (2013). A systematic review and meta-analysis of the effect of an ankle-foot orthosis on gait biomechanics after stroke. *Clinical Rehabilitation*, 27(10), 879-891.
- Tzu-wei, P. H., Shorter, K. A., Adamczyk, P. G., & Kuo, A. D. (2015). Mechanical and energetic consequences of reduced ankle plantar-flexion in human walking. *Journal of Experimental Biology*, 218(22), 3541-3550.
- Umberger, B. R. (2010). Stance and swing phase costs in human walking. *Journal of the Royal Society Interface*, 7(50), 1329-1340.
- van den Bogert, A. J., Pavol, M. J., & Grabiner, M. D. (2002). Response time is more important than walking speed for the ability of older adults to avoid a fall after a trip. *Journal of Biomechanics*, 35(2), 199-205.
- van der Wilk, D., Dijkstra, P. U., Postema, K., Verkerke, G. J., & Hijmans, J. M. (2015). Effects of ankle foot orthoses on body functions and activities in people with floppy paretic ankle muscles: a systematic review. *Clinical Biomechanics*, 30(10), 1009-1025.
- Vistamehr, A., Kautz, S. A., & Neptune, R. R. (2014). The influence of solid ankle-foot-orthoses on forward propulsion and dynamic balance in healthy adults during walking. *Clinical Biomechanics*, 29(5), 583-589.
- Voloshina, A. S., & Ferris, D. (2018). Design and validation of an instrumented uneven terrain treadmill. *Journal of Applied Biomechanics*, 34(3), 236-239.
- Wall, J., Charteris, J., & Turnbull, G. (1987). Two steps equals one stride equals what?: the applicability of normal gait nomenclature to abnormal walking patterns. *Clinical Biomechanics*, 2(3), 119-125.
- Wang, X., Guo, S., Qu, H., & Song, M. (2019). Design of a purely mechanical sensor-controller integrated system for walking assistance on an ankle-foot exoskeleton. *Sensors*, 19(14), 3196.
- WCHA. (2016). Important facts about falls. Retrieved from <https://nextstepmobility.com/wp-content/uploads/2015/12/Important-Facts-About-Falls-Next-Step-Mobility-Solutions.pdf>
- Webster, J. B., & Murphy, D. P. (2019). *Atlas of Orthoses and Assistive Devices*: Elsevier.
- Wening, J., Ford, J., & Jouett, L. D. (2013). Orthotics and FES for maintenance of walking in patients with MS. *Disease-a-Month: DM*, 59(8), 284-289.
- Whittle, M. W. (2014). *Gait analysis: an introduction*: Butterworth-Heinemann.
- WHO. (2015). *World report on ageing and health*: World Health Organization.
- Winter, D. A. (1984). Kinematic and kinetic patterns in human gait: variability and compensating effects. *Human Movement Science*, 3(1-2), 51-76.
- Winter, D. A. (1991). *Biomechanics and motor control of human gait: normal, elderly and pathological*.
- Winter, D. A. (1992). Foot trajectory in human gait: a precise and multifactorial motor control task. *Physical Therapy*, 72(1), 45-53.
- Winter, D. A. (2009). *Biomechanics and motor control of human movement*: John Wiley & Sons.
- Wu, G., Siegler, S., Allard, P., Kirtley, C., Leardini, A., Rosenbaum, D., . . . Witte, H. (2002). ISB recommendation on definitions of joint coordinate system of various joints for the reporting of human joint motion—part I: ankle, hip, and spine. *Journal of Biomechanics*, 35(4), 543-548.

- Wutzke, C. J., Sawicki, G. S., & Lewek, M. D. (2012). The influence of a unilateral fixed ankle on metabolic and mechanical demands during walking in unimpaired young adults. *Journal of Biomechanics*, *45*(14), 2405-2410.
- Xu, R., Jiang, N., Mrachacz-Kersting, N., Lin, C., Prieto, G. A., Moreno, J. C., . . . Farina, D. (2014). A closed-loop brain-computer interface triggering an active ankle-foot orthosis for inducing cortical neural plasticity. *IEEE Transactions on Biomedical Engineering*, *61*(7), 2092-2101.
- Yamamoto, S., Ebina, M., Kubo, S., Hayashi, T., Akita, Y., & Hayakawa, Y. (1999). Development of an ankle-foot orthosis with dorsiflexion assist, part 2: structure and evaluation. *JPO: Journal of Prosthetics and Orthotics*, *11*(2), 24-28.
- Yamamoto, S., Hagiwara, A., Mizobe, T., Yokoyama, O., & Yasui, T. (2005). Development of an ankle-foot orthosis with an oil damper. *Prosthetics and Orthotics International*, *29*(3), 209-219.
- Yeung, L.-F., Ockenfeld, C., Pang, M.-K., Wai, H.-W., Soo, O.-Y., Li, S.-W., & Tong, K.-Y. (2017). *Design of an exoskeleton ankle robot for robot-assisted gait training of stroke patients*. Paper presented at the 2017 International Conference on Rehabilitation Robotics (ICORR).
- Yokoyama, O., Sashika, H., Hagiwara, A., Yamamoto, S., & Yasui, T. (2005). Kinematic effects on gait of a newly designed ankle-foot orthosis with oil damper resistance: a case series of 2 patients with hemiplegia. *Archives of Physical Medicine and Rehabilitation*, *86*(1), 162-166.
- Young, A. J., & Ferris, D. (2016). State of the art and future directions for lower limb robotic exoskeletons. *IEEE Transactions on Neural Systems and Rehabilitation Engineering*, *25*(2), 171-182.
- Zajac, F. E. (1989). Muscle and tendon: properties, models, scaling, and application to biomechanics and motor control. *Critical Reviews in Biomedical Engineering*, *17*(4), 359-411.
- Zajac, F. E. (2003). Biomechanics and muscle coordination of human walking Part II: Lessons from dynamical simulations and clinical implications. *Gait & Posture*, *17*, 1-17.
- Zarrugh, M., Todd, F., & Ralston, H. (1974). Optimization of energy expenditure during level walking. *European Journal of Applied Physiology and Occupational Physiology*, *33*(4), 293-306.
- Zelik, K. E., & Kuo, A. D. (2010). Human walking isn't all hard work: evidence of soft tissue contributions to energy dissipation and return. *Journal of Experimental Biology*, *213*(24), 4257-4264.
- Zelik, K. E., Takahashi, K. Z., & Sawicki, G. S. (2015). Six degree-of-freedom analysis of hip, knee, ankle and foot provides updated understanding of biomechanical work during human walking. *Journal of Experimental Biology*, *218*(6), 876-886.
- Zhou, M., Al-Furjan, M. S. H., Zou, J., & Liu, W. (2018). A review on heat and mechanical energy harvesting from human-Principles, prototypes and perspectives. *Renewable and Sustainable Energy Reviews*, *82*, 3582-3609.

APPENDIX A PUBLICATIONS, PRESENTATIONS AND PATENT APPLICATION

Patent (under filing process):

Chapter 5:

Bajelan, S., & Begg, R. (2020). Self-powered ankle exoskeleton. *Australian and International patent application.*

Conference presentations:

Chapter 3:

Bajelan, S., Sparrow, T., & Begg, R. (2019). *Walking more safely by increasing swing phase ankle dorsiflexion.* Paper presented at the XXVII congress of the International Society of Biomechanics (ISB) / American Society of Biomechanics (ASB), 2019.

Chapter 4:

Bajelan, S., Sparrow, T., & Begg, R. (2019). *The mechanics of tibialis anterior muscle during swing phase ankle dorsiflexion: implications for biomimetic device design.* Paper presented at the 41st Annual International Conference of the IEEE Engineering in Medicine & Biology Society (EMBC), July 23-27, 2019, Berlin, Germany.

Bajelan, S., Levinger, P., Nagano, H., Downie, C., & Begg, R. (2017). *The contribution of hip abductor muscles during two-steps balance recovery.* Paper presented at the XXVI Congress of the International Society of Biomechanics, 2017.

Conference - Refereed full paper:

Bajelan, S., Nagano, H., Sparrow, T., & Begg, R. (2017). *Effects of wide step walking on swing phase hip muscle forces and spatio-temporal gait parameters.* Paper presented at the 2017 39th Annual International Conference of the IEEE Engineering in Medicine and Biology Society (EMBC).

Journal articles (under preparation-to be submitted following patent filing):

Chapter 3:

Bajelan, S., Sparrow, T., & Begg, R. (2020). Swing biomechanical characteristics of ankle-controlled walking. *To be submitted to the Journal of Biomechanics.*

Chapter 4:

Bajelan, S., Sparrow, T., & Begg, R. (2020). The mechanics and energetic contribution of swing limb's constituents to obstacle crossing. *To be submitted to the Journal of Biomechanics.*

Chapter 5:

Bajelan, S., Sparrow, T., & Begg, R. (2020). A self-powered exoskeleton developed for swing ankle-controlled walking. *To be submitted to the IEEE Transactions on Neural Systems and Rehabilitation Engineering*.

Chapter 6:

Bajelan, S., Sparrow, T., & Begg, R. (2020). Walking more safely using a self-powered ankle exoskeleton. *To be submitted to the Journal of Neuroengineering and Rehabilitation*.

Bajelan, S., Sparrow, T., & Begg, R. (2019). *Walking more safely by increasing swing phase ankle dorsiflexion*. Paper presented at the XXVII congress of the International Society of Biomechanics (ISB) / American Society of Biomechanics (ASB) 2019.

Walking more safely by increasing swing phase ankle dorsiflexion

Soheil Bajelan¹, Tony Sparrow¹, Rezaul Begg¹

¹ Institute of Health and Sport (IHES), Victoria University, Melbourne, Australia

Email: Soheil.bajelan@live.vu.edu.au

Summary

Trips occur when the foot strikes an obstacle during the swing phase of the gait cycle. The critical biomechanical variable associated with tripping risk is Minimum Foot Clearance (MFC). The pattern of toe trajectory in sagittal plane can be changed using different strategies to lift the foot which affect MFC height and timing [1]. In this study, a real-time biofeedback technique was employed to observe effects of ankle-only and no-ankle strategies on swing toe trajectory. The results showed that the ankle-only strategy can make the gait safer by eliminating the MFC event.

Introduction

MFC is an event in which the vertical distance between the lowest point of the foot and ground is minimum (Fig.2). Following toe-off, the swing foot exhibits an initial maximum vertical displacement (Mx1) after which, at approximately 90% into the swing phase a second maximum clearance is achieved (Mx2) [2]. These three swing phase parameters can be used to show whether the foot has sufficient height to avoid tripping or causing a “slapping” foot-ground contact. Toe trajectory can be changed using different strategies. The aim of this study was to compare the effects on MFC, Mx1 and Mx2 of ankle-only control to a no-ankle strategy. An incremental MFC elevation technique employing biofeedback was used to manipulate toe trajectory across three experimental conditions (Normal, Ankle, No-Ankle).

Methods

Four healthy males (30 to 40 yrs) walked on a motor driven treadmill at preferred speed for 2 minutes. A Vicon motion capture system recorded the 3D trajectory of the dominant limb Big Toe. Mean baseline MFC was then used to compute heights for the three target foot-ground clearances: normal MFC+1.5cm, normal MFC+3cm and normal MFC+4.5cm. In each condition these 3 MFC heights were then displayed as horizontal target lines on a monitor in front of the treadmill. Participants were requested to achieve the target MFC using 1) Normal strategy 2) Ankle strategy (maintaining target MFC by changing ankle angle only) and 3) No-Ankle strategy (not using the ankle).

Results and Discussion.

As shown in Fig. 1, intentionally increasing MFC to cross small obstacles changed the normal pattern of toe trajectory events.

Normal and No-Ankle strategies showed an approximately similar pattern. Mx1 height remained higher than MFC across all MFC height manipulations ($\frac{MX1}{MFC} > 1$) but using the Ankle strategy MFC height approached Mx1, the $\frac{MX1}{MFC}$ ratio decreased and as consequence MFC tended to disappear at 4.5 cm elevation (Fig. 2).

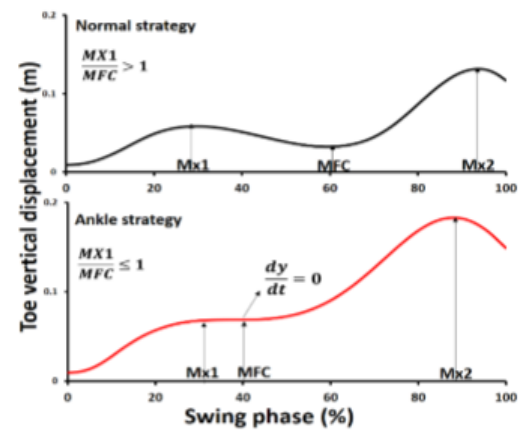


Figure 2: Typical toe trajectory pattern. Comparing between normal and ankle strategy

Note that even with MFC absent, an inflection remains in the displacement curve at which the first time derivative = zero ($\frac{dy}{dt} = 0$). This event is still considered hazardous because foot horizontal velocity approximates maximum and forceful ground contact would be destabilizing.

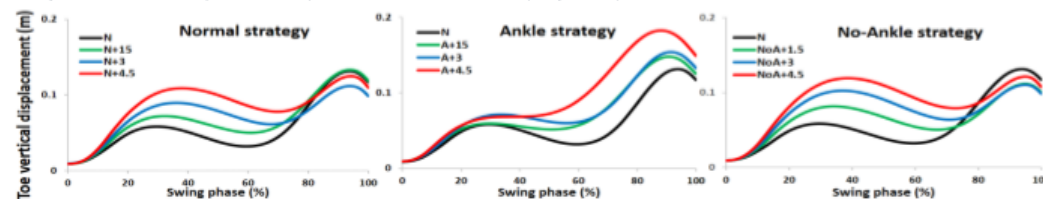
Conclusions

The results show that an ankle dorsiflexion control strategy can make the gait safer by eliminating MFC [1] but the risk posed by high horizontal velocity remains.

References

- [1] Santhirayagam, Braveena K., et al. "Non-MTC gait cycles: An adaptive toe trajectory control strategy in older adults." *Gait & posture* 53 (2017): 73-79.
- [2] Nagano, H., Begg, R. K., Sparrow, W. A., & Taylor, S. (2011). Ageing and limb dominance effects on foot-ground clearance during treadmill and overground walking. *Clinical Biomechanics*, 26(9), 962-968.

Figure 1. The foot trajectory during the swing phase of the gait cycle using Normal, Ankle and No-Ankle strategies. Black, Green, Blue and Red lines represent Normal MFC, MFC+1.5cm, MFC+3cm and MFC+4.5cm, respectively.



Bajelan, S., Sparrow, T., & Begg, R. (2019). *The mechanics of tibialis anterior muscle during swing phase ankle dorsiflexion: implications for biomimetic device design*. Paper presented at the 41st Annual International Conference of the IEEE Engineering in Medicine & Biology Society (EMBC), July 23-27, 2019, Berlin, Germany.

The Mechanics of Tibialis Anterior Muscle during Swing Phase Ankle Dorsiflexion: Implications for Biomimetic Device Design

Soheil Bajelan, Tony Sparrow and Rezaul Begg, *Senior Member, IEEE*

Abstract— The Tibialis Anterior (TA) muscle is a principal ankle dorsiflexor. Understanding the mechanics of its natural contribution to lifting the foot is extremely valuable in developing control mechanisms for any TA biomimetic artificial muscle. A musculoskeletal model was developed when controlling the real-time swing toe trajectory. Ankle moment required to achieve a target foot elevation was compared to the required TA muscle force. There was no significant increase in ankle moment to achieve experimentally-defined dorsiflexion but TA muscle force and activation increased significantly.

I. INTRODUCTION

Adaptive gait is critical to everyday physical activities but a range of neurological and musculoskeletal conditions lead to gait impairments. One of the most serious consequences of gait dysfunction is falling due to tripping. The risk of a tripping is considered highest at Minimum Foot Clearance (MFC). The ankle joint and its principal dorsiflexion actuator, the Tibialis Anterior (TA) muscle, is a highly effective lower limb mechanism to control foot-ground clearance at MFC. Rapid progress has been made in developing artificial muscles to apply forces that can assist ankle joint plantarflexion and dorsiflexion. An essential requirement of these devices is controlling the timing and magnitude of assistive moments, such that the individuals' assisted gait is well adapted to the specific demands of everyday walking. The aim of this study was to determine the timing and magnitude of TA force when dorsiflexing the ankle to increase foot-ground clearance.

II. METHODS

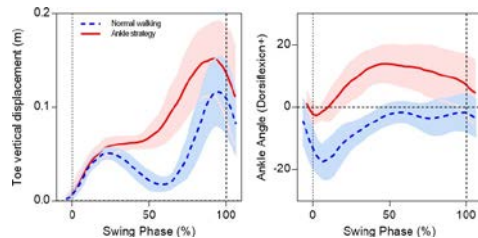


Figure 1. The swing time history of toe trajectory and ankle angle, compared between Ankle strategy and normal walking.

Eight healthy male adults (25 to 40 yrs) were recruited with mean stature = 1.75 m and body mass = 71.93 Kg. Two minutes walking on an AMTI dual belt (tandem) force-sensing treadmill was recorded using a time-synchronized 3D motion capture system (Vicon). Noraxon surface electrodes were attached to the TA muscle using SENIAM guideline. A real-time biofeedback technique displayed the sagittal trajectory of the toe marker on a projection screen with participants requested to lift their foot to match their dominant limb MFC with the displayed target foot-ground clearance. Two

*Institute for Health and Sport (IHES), Victoria University, Melbourne, Australia. phone: +61 3 9919 1116; e-mail: rezaul.begg@vu.edu.au

conditions were normal preferred speed walking and maintaining target MFC (normal MFC+40mm) using the ankle joint only, i.e. an ankle strategy and not employing either the knee or hip. The AnyBody software was employed to develop a model of walking on a dual belt treadmill. The two experimental walking conditions were simulated using a Hill-type three-element model and the muscle recruitment problem

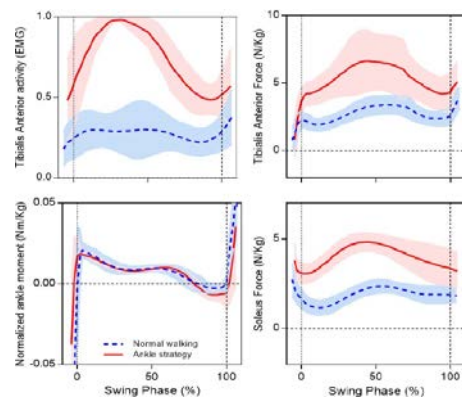


Figure 2. The swing time history of TA muscle force and activity compared with ankle moment and the soleus muscle force.

solved using the min/max optimization criterion [1].

III. RESULTS

Participants walked at a mean preferred speed of 3.7 km/h. In response to the projected target foot trajectory, mean MFC was increased from 1.6cm to 6.2cm and ankle dorsiflexion angle augmented by approximately 15 degrees (Fig. 1). As shown in Fig. 2, TA force production and activation increased significantly using the ankle strategy but ankle moment was unchanged. To explain the unchanged moment, the simulated soleus plantarflexion force was examined and shown to also increase, contributing to dorsiflexion via co-contraction.

IV. DISCUSSION & CONCLUSION

This study showed that in comparison with normal walking, significantly greater external moment is not required to increase ankle dorsiflexion. Higher TA muscle force should, however, be considered in developing any biomimetic artificial TA muscle.

REFERENCES

- [1] G. Rasmussen, John, Michael Damsgaard, and Michael Voigt. "Muscle recruitment by the min/max criterion—a comparative numerical study." *Journal of biomechanics* 34.3 (2001): 409-415.

Bajelan, S., Nagano, H., Sparrow, T., & Begg, R. (2017). *Effects of wide step walking on swing phase hip muscle forces and spatio-temporal gait parameters*. Paper presented at the 2017 39th Annual International Conference of the IEEE Engineering in Medicine and Biology Society (EMBC).

Effects of Wide Step Walking on Swing Phase Hip Muscle Forces and Spatio-Temporal Gait Parameters

Soheil Bajelan, Hanatsu Nagano, Tony Sparrow and Rezaul K. Begg* *Senior Member, IEEE*

Abstract— Human walking can be viewed essentially as a continuum of anterior balance loss followed by a step that re-stabilizes balance. To secure balance an extended base of support can be assistive but healthy young adults tend to walk with relatively narrower steps compared to vulnerable populations (e.g. older adults and patients). It was, therefore, hypothesized that wide step walking may enhance dynamic balance at the cost of disturbed optimum coupling of muscle functions, leading to additional muscle work and associated reduction of gait economy. Young healthy adults may select relatively narrow steps for a more efficient gait. The current study focused on the effects of wide step walking on hip abductor and adductor muscles and spatio-temporal gait parameters. To this end, lower body kinematic data and ground reaction forces were obtained using an Optotrak motion capture system and AMTI force plates, respectively, while AnyBody software was employed for muscle force simulation. A single step of four healthy young male adults was captured during preferred walking and wide step walking. Based on preferred walking data, two parallel lines were drawn on the walkway to indicate 50% larger step width and participants targeted the lines with their heels as they walked. In addition to step width that defined walking conditions, other spatio-temporal gait parameters including step length, double support time and single support time were obtained. Average hip muscle forces during swing were modeled. Results showed that in wide step walking step length increased, Gluteus Minimus muscles were more active while Gracilis and Adductor Longus revealed considerably reduced forces. In conclusion, greater use of abductors and loss of adductor forces were found in wide step walking. Further validation is needed in future studies involving older adults and other pathological populations.

I. INTRODUCTION

Walking can be described as continuous loss and regaining of dynamic balance in body progression [1, 2]. Falls must, however, be avoided by maintaining the body center of mass (CoM) within the base of support (BoS) during double support [3]. Increased BoS is, therefore, advantageous in extending the safety boundary to secure dynamic CoM movement and helping to maintain balance. Populations with gait impairments demonstrate adaptations that may assist dynamic balance, such as larger step width [4]. Increased step width engenders greater BoS area, allowing a wider range of CoM movement and reducing the risk of balance loss and associated falls [5].

Wide step walking is more commonly observed in populations who require further stabilization, such as older adults and gait-impaired groups [5]. Despite the

biomechanical advantages of extending the lateral BoS boundary, wide step walking may impair gait functionality, possibly reflected in reduced energy efficiency or gait disturbances. This assumption is based on the fact that healthy populations tend to walk with relatively narrower steps, even though increased step width could improve lateral balance [6]. Arellano et al. argued that narrower steps could assist with maximizing mechanical energy expenditure for forward progression [7]. Thus, healthy populations may optimize gait economy while those with unsteady gait prioritize stability at the cost of additional muscular force demands.

As step width is measured at heel contact, gait control to determine BoS during double support is dependent on swing limb mechanics during the single support phase and swing limb abduction of can be hypothesized to increase step width [8, 9]. The current study tested this hypothesis by investigating how wide-step walking would affect hip abductor muscles. Based on kinematic data and ground reaction forces, key hip muscle forces were simulated. We hypothesized that wide step walking would demand increased activation of thigh abductors to maintain larger step width. This hypothesis was suggested by a previous study that revealed links between increased Gluteus Medius activity and step width [10].

It was also of interest to determine how changes in hip muscle forces due to step width adaptations would influence spatio-temporal gait parameters. If wide step walking demanded higher muscle forces during single support, it was anticipated that fundamental gait kinematics may also change. Spatio-temporal parameters included step length, double support time and single support time. Decreased step length and increased double support time are characteristic of unhealthy or cautious gait [4, 6] and swing limb control is possible only during single support time.

With larger step width, hip abductors may be more activated while adductor contributions may diminish. Hip abduction during swing could possibly elevate the swing limb and assist forward motion. A wider BoS may increase side-to-side CoM movement, possibly leading to a longer temporal period within the gait cycle. In summary, our aim was to investigate how changes to step width influenced gait patterns and hip muscle forces prior to foot contact during the more vulnerable single support phase. Outcomes of the current research were expected to advance our understanding of the biomechanical advantages and disadvantages of step width adaptation.

S. Bajelan, H. Nagano, T. Sparrow and R.K. Begg* are with the Gait, Balance and Falls research group, Institute of Sport, Exercise and Active Living (ISEAL), Victoria University, Melbourne, Victoria 3011 Australia. (phone: +61 3 9919 1116; e-mail: rezaul.begg@vu.edu.au).

II. METHODS

A. Participants

Participants were four healthy young male adults (23.0 ± 2.2 yrs) with stature and body mass; 1.73cm-60Kg, 1.68cm-60Kg, 1.72cm-65Kg and 1.78cm-85Kg respectively. The Victoria University Human Research Ethics Committee approved the experimental protocol.

B. Apparatus and Procedure

Three-dimensional position-time data of the pelvis segment, thighs, femurs and feet were sampled at 100 Hz using three Optotrak Certus (Northern Digital Inc.) motion analysis camera units, set up around an 8m walkway. As illustrated in Figure 1 (Top), five technical frame clusters of three infrared light emitting diodes (IRED) were tracked [6]. One cluster monitored pelvis motion based on the anterior superior iliac crests, posterior inferior iliac spines and greater trochanters [11]. Two clusters were attached to the superior surface of both femurs to track lateral and medial epicondyles, a further two were located on the proximal inferior surface of each shoe out-sole (i.e. heel) and two clusters were mounted on the most distal anterior foot segment landmarks (i.e. toes). In the middle of the walkway, two embedded force plates (AMTI) were located to record ground reaction forces (GRF) at 1000Hz.

Participants began with unconstrained walking at preferred speed, followed by wide (Wide) step walking. Wide walking conditions were +50% relative to step width in unconstrained walking, controlled by two parallel lines drawn on the walkway to indicate target step width. Participants undertook sufficient practice to contact the lines with their heels prior to data collection. One entire single support phase and subsequent double support phase were selected for analysis for each participant when a foot completely landed on the first force plate and the following step completely contacted the second plate. Raw data were first interpolated to compensate any occluded signals using a window of up to 10 frames (0.1s). A 4th order zero-lag Butterworth Filter with a cut-off frequency of 6 Hz was then applied.

C. Event Definitions

Heel contact and toe-off were identified based on vertical and horizontal acceleration of the heel and toe, respectively [12].

Spatio-temporal Parameters

Position and time data of heel contact and toe-off defined spatio-temporal parameters as follows. Step length and width were anterior-posterior and medio-lateral displacement between heels at heel contact, respectively. Double support time was the temporal period between heel contact and toe-off of the contralateral limb [6]. Single support was the time from toe-off to heel contact of the ipsilateral limb [6].

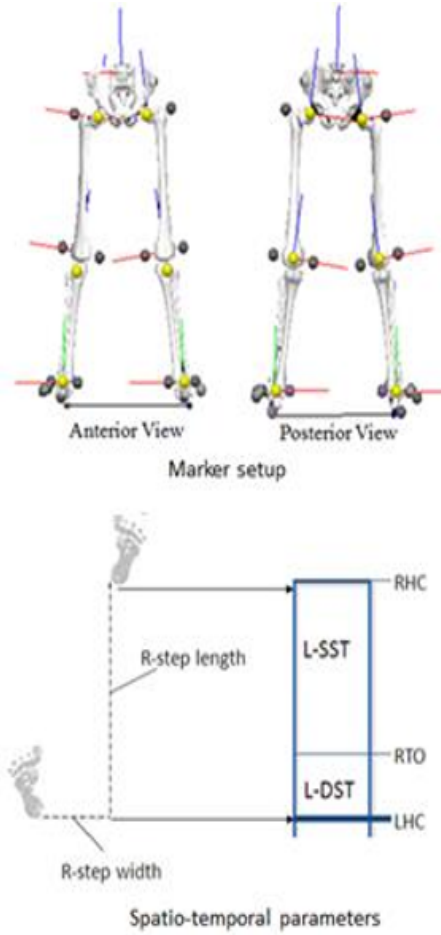


Figure 1. (Top) Lower Body Marker Setup; (Bottom) Definitions of spatio-temporal gait parameters. R/L = right and left; HC = heel contact; TO = toe-off; DST = double support time; SST = single

D. Musculoskeletal modelling and simulation

The normal width and wide walking trials of each subject were modeled using AnyBody simulation software. Time-histories of lower extremity muscles were computed during single support (from toe-off to heel contact) employing inverse dynamics simulation. Muscles were modeled as three-element classical and the muscle recruitment problem was solved utilizing a min/max optimization criterion [13].

Average swing leg muscle forces were computed including: Gluteus Minimus (anterior, middle, posterior); Gluteus Medius (anterior, posterior); Gluteus Maximus (superior, inferior); Tensor Fasciae Latae; Piriformis; Gracilis; Adductor longus; Adductor Magnus Proximal; Adductor Brevis (proximal, middle, distal); Gemellus (inferior, Superior); Obturator Externus (superior, inferior); Obturator Internus and Pectineus. Some muscle forces were measured at various heads. Only the results showing the consistent trends were reported.

III. RESULTS

A. Validation

Musculoskeletal modeling using AnyBody has been previously validated [14] and simulation results for the normal walking trials of the current study were also consistent with published reports using similar modeling approaches [15, 16]. The activity of Gluteus medius during wide step walking was also shown to agree with Kubinski et al., 2015, in which GMed's activity was recorded during normal and wide step walking using electromyography (EMG) [10].

B. Step Width Effects on Spatio-temporal Parameters

Spatio-temporal parameters of the four participants are described in Table 1. A consistent trend was seen in step length which increased in response to wide step walking.

Table 1. spatio-temporal parameters of the four subjects. S= Subject; N/W = Normal /Wide step width

S	Step Length (cm)		Step Width (cm)		Double Support (s)		Single Support (s)	
	N	W	N	W	N	W	N	W
1	79.8	85.3	7.6	12.7	0.12	0.12	0.47	0.46
2	69.6	73.7	9.4	13.5	0.12	0.12	0.44	0.41
3	65.9	67.4	10.8	16.3	0.12	0.17	0.43	0.42
4	67.1	68.8	5.2	7.7	0.12	0.18	0.42	0.43

C. Step Width Effects on Lower Limb Muscle Forces

Walking with wide steps changed average muscle forces during the swing phase. Table 2 indicates increased muscle forces due to wide step walking and Gluteus Minimus muscles were found to be more active. Despite increases in Gemellus inferior and superior, the magnitudes of these two muscle forces were found to be less than for the Gluteus muscles.

Table 2. Comparison of key hip muscle forces between Normal and Wide Step walking showing percentage increase in response to wide step walking. S = Subject; GminA = Gluteus Minimus Anterior; GminM = Gluteus Minimus Middle; GminP = Gluteus Minimus Posterior; GMedA = Gluteus Medius Anterior; GemI = Gemellus Inferior; GemS = Gemellus Superior. Unit = Newton; N = Normal width walking; W = Wide width walking.

S		GMinA	GMinM	GMinP	GMedA	GemI	GemS
1	N	11.3	6.6	5.3	11.1	3.8	1.7
	W	36.3	26.2	21.2	27.9	11.9	7.2
	%	+220.9	+297.1	+303.6	+151.2	+209.7	+331.5
2	N	10.3	5.5	4.4	6.6	3.2	1.5
	W	14.7	10.4	8.4	9.9	5.3	2.7
	%	+42.3	+87.1	+89.5	+49.2	+65.3	+75.5
3	N	11.6	8.3	6.8	11.3	3.5	2.1
	W	14.3	10.3	8.4	13.2	3.7	2.3
	%	+23.4	+23.5	+23.0	+17.4	+4.0	+5.5
4	N	13.1	10.7	9.6	5.4	4.5	3.0
	W	15.9	11.6	10.0	12.3	4.7	3.3
	%	+21.1	+7.8	+4.1	+129.2	+4.4	+10.7

Table 3, in contrast, presents muscle forces that consistently reduced in wide step walking. Despite a consistent percentage decrease, only Gracilis and Adductor Longus demonstrated qualitatively salient reductions, while

the other muscles did not impact step width changes and associated gait patterns.

Table 3. Comparison of key hip muscle forces between Normal and Wide Step walking showing percentage decrease in response to wide step walking. S = Subject; Grac = Gracilis; AdL = Adductor Longus; AdMP = Adductor Magnus Proximal; AdBP = Adductor Brevis Proximal; AdBM = Adductor Brevis Middle; AdBD = Adductor Brevis Distal; ObEL = Obturator Externus Inferior; Unit = Newton; N = Normal width walking; W = Wide width walking

S		Grac	AdL	AdMP	AdBP	AdBM	AdBD	ObEI
1	N	12.0	19.5	2.3	3.8	3.4	2.8	4.0
	W	11.2	10.8	0.9	2.9	2.1	1.8	2.0
	%	-7.1	-44.7	-60.1	-24.9	-37.9	-37.4	-49
2	N	8.8	14.6	1.4	3.4	2.8	2.3	3.5
	W	7.9	9.5	1.1	2.2	2.0	1.7	2.3
	%	-10.3	-35.0	-21.9	-34.4	-30.2	-29.5	-33.6
3	N	6.8	7.2	0.5	1.7	1.2	0.6	1.2
	W	5.7	2.2	0.0	0.7	0.3	0.2	0.2
	%	-16.7	-70.0	-93.9	-57.3	-72.9	-72.1	-82.4
4	N	12.5	15.0	1.4	2.4	2.1	1.7	2.0
	W	8.8	11.5	1.1	2.0	1.8	1.5	1.4
	%	-29.7	-23.5	-23.5	-17.0	-14.4	-9.7	-32.2

IV. DISCUSSION

Wide step walking is a typical gait adaptation to secure dynamic balance but it is less common in healthy gait modes [17]. Based on this observation, larger step width was hypothesized to require additional muscle forces, possibly disturbing optimum gait [18]. In addition to spatio-temporal parameters, the current study investigated hip abduction/adduction during the swing phase, an important determinant of step width at heel contact [10].

In response to wide step walking (Table 2) the simulation results identified increases in some hip abductors and lateral rotators during the swing phase. Gluteus minimus muscles for all heads (i.e. anterior, middle, posterior) increased from normal to wide step walking across all participants. Gluteus minimus muscles are instrumental in performing a range of joint functions, such as hip abduction, hip flexion and external rotation of the extended hip [19]. Simultaneous implementation of different functions within the same joint provides evidence for hip stabilization by Gluteus minimus (Table 2). Similarly both the inferior and superior Gemellus segments consistently showed increases, acting in synchrony to maintain femoral head stability within the acetabulum and assisting lateral rotation of the extended thigh [20, 21].

Table 3 displayed muscle forces that reduced in response to wide step walking. The adductor longus is primarily associated with hip adduction, while Gracilis is a hip adductor that also has a role in knee flexion [20]. These two muscles generate larger force in comparison with other hip adductors which probably demonstrate their significant contribution to step width modulation. Adductor Brevis, another hip adductor [20] also decreased, but to a lesser degree, in wide step walking. From the present findings, it can be proposed that increased step width in older adults may be partially due to ageing-related muscle atrophy. While the previous studies reported that both abductors and adductors reduced with age [22], it could be hypothesized that adductor weakness may be prominent in the swing limb, possibly leading to wider steps.

It is, however, also important to consider that psychological factors, such as fear of falling and attention directed to targeting the guide lines for step width control may be determinants of gait adaptation associated with wider steps, for example, widening the base of support to increase the margin of safety [23].

Wide step walking was found to increase step length due to activation of hip abductors and lateral rotators during the swing phase. Given the above findings concerning muscle force patterns in wider step gait, these results could be confirmed and extended with a larger sample of older adults and gait impaired populations who show significant instability. Biomechanical modeling of muscle forces may contribute to understanding why older adults tend to walk with wider steps. Further research into the link between selected muscle forces and optimum gait adaptations may help in designing specific strength training to improve gait function. The current study demonstrated the importance of AnyBody simulation in allowing a highly-detailed analysis of multiple muscle heads. A single value was obtained for two-head muscles while a range of values were computed for multi-head muscles. This capacity to undertake detailed muscle force analysis is expected to advance our understanding of muscle kinetics and associated gait pattern changes with ageing. In future work it may also be useful to investigate muscle kinetics in the contralateral stance limb to further understand how hip muscle forces contribute to balance-related step width control. Mechanical energy efficiency and dynamic balance in association with step width control and hip muscle kinetics can also be investigated. Experiments with larger samples would assist in confirming and extending the current findings.

ACKNOWLEDGMENT

The authors would like to thank all participants in the research project.

REFERENCES

[1] Drury CG, Woolley SM. Visually-controlled leg movements embedded in a walking task. *Ergonomics*. 1995;38:714-22.
 [2] Das P, McColium G. Invariant structure in locomotion. *Neuroscience*. 1988;25:1023-34.
 [3] Hof A, Gazendam M, Sinke W. The condition for dynamic stability. *Journal of biomechanics*. 2005;38:1-8.
 [4] Levine D, Richards J, Whittle MW. *Whittle's gait analysis*: Elsevier Health Sciences; 2012.
 [5] Åberg AC, Frykberg GE, Halvorsen K. Medio-lateral stability of sit-to-walk performance in older individuals with and without fear of falling. *Gait & posture*. 2010;31:438-43.
 [6] Nagano H, Begg RK, Sparrow WA, Taylor S. A comparison of treadmill and overground walking effects on step cycle asymmetry in young and older individuals. *Journal of applied biomechanics*. 2013;29:188-93.
 [7] Arellano CJ, Kram R. The effects of step width and arm swing on energetic cost and lateral balance during running. *Journal of biomechanics*. 2011;44:1291-5.
 [8] Brindle III RA. Does Changing Step Width Alter Lower Extremity Biomechanics During Running? 2012.
 [9] Paquette MR, Zhang S, Milner CE, Fairbrother JT, Reinbolt JA. Effects of increased step width on frontal plane knee biomechanics in healthy older adults during stair descent. *The Knee*. 2014;21:821-6.
 [10] Kubinski SN, McQueen CA, Sittloh KA, Dean JC. Walking with wider steps increases stance phase gluteus medius activity. *Gait & posture*. 2015;41:130-5.

[11] Kingma I, Toussaint HM, Commissaris DA, Hoozemans MJ, Ober MJ. Optimizing the determination of the body center of mass. *Journal of biomechanics*. 1995;28:1137-42.
 [12] O'Connor CM, Thorpe SK, O'Malley MJ, Vaughan CL. Automatic detection of gait events using kinematic data. *Gait & posture*. 2007;25:469-74.
 [13] Rasmussen J, Damsgaard M, Voigt M. Muscle recruitment by the min/max criterion—a comparative numerical study. *Journal of biomechanics*. 2001;34:409-15.
 [14] Bajelan S, Azghani MR. Musculoskeletal modeling and simulation of three various Sit-to-Stand strategies: An evaluation of the biomechanical effects of the chair-rise strategy modification. *Technology and Health Care*. 2014;22:627-44.
 [15] Liu MQ, Anderson FC, Schwartz MH, Delp SL. Muscle contributions to support and progression over a range of walking speeds. *Journal of biomechanics*. 2008;41:3243-52.
 [16] Lim YP, Lin Y-C, Pandy MG. Muscle function during gait is invariant to age when walking speed is controlled. *Gait & posture*. 2013;38:253-9.
 [17] Brach JS, Studenski S, Perera S, VanSwearingen JM, Newman AB. Stance time and step width variability have unique contributing impairments in older persons. *Gait & posture*. 2008;27:431-9.
 [18] Donelan JM, Kram R. Mechanical and metabolic determinants of the preferred step width in human walking. *Proceedings of the Royal Society of London B: Biological Sciences*. 2001;268:1985-92.
 [19] Beck M, Sledge JB, Gautier E, Dora CF, Ganz R. The anatomy and function of the gluteus minimus muscle. *Bone & Joint Journal*. 2000;82:358-63.
 [20] Palastanga N, Field D, Soames R. *Anatomy and human movement: structure and function*: Elsevier Health Sciences; 2012.
 [21] Cox JM, Bakkum BW. Possible generators of retrotrochanteric gluteal and thigh pain: the gemelli-obturator internus complex. *Journal of manipulative and physiological therapeutics*. 2005;28:534-8.
 [22] Morcelli MH, Rossi DM, Karuka AH, Crozara LF, Hallal CZ, Marques NR, et al. Peak torque, reaction time, and rate of torque development of hip abductors and adductors of older women. *Physiotherapy theory and practice*. 2016;32:45-52.
 [23] Maki BE. Gait changes in older adults: predictors of falls or indicators of fear? *Journal of the American geriatrics society*. 1997;45:313-20.

Bajelan, S., Levinger, P., Nagano, H., Downie, C., & Begg, R. (2017). *The contribution of hip abductor muscles during two-steps balance recovery*. Paper presented at the XXVI Congress of the International Society of Biomechanics.

THE CONTRIBUTION OF HIP ABDUCTOR MUSCLES DURING TWO-STEPS BALANCE RECOVERY

Soheil Bajelan, Pazit levinger, Hanatsu Nagano, Calum Downie, Rezaul Begg.
 Institute of Sport, Exercise and Active Living (ISEAL), Victoria University, Melbourne, Australia.
 Corresponding author email: soheil.bajelan@live.vu.edu.au

INTRODUCTION

Falls could become a crucial event for older adults that often end their independent lifestyles [1]. Tripping is the leading cause of falls mostly leading to forward balance loss [2]. Therefore, it is important to establish an effective recovery strategy from forward balance loss. Single or multi rapid steps are required to restore centre of mass balance within the base of support [3]. Graham et al. recently revealed the important contribution of Hip Abductors (HA) for balance recovery in addition to other lower limb muscles [4]. They, however, examined balance recovery action just for the initial recovery step during the period from toe off to foot contact of the stepping leg.

In this study, a musculoskeletal model has been developed for two-steps strategy to advance our understanding about multi-steps balance recovery. We compared the lead limb's HA muscular kinetics between the first and second recovery steps in detail, using AnyBody simulation software.

METHODS

Balance recovery data of four healthy older participants (75.2 (3.3) years, 50% females) were analysed for two-steps strategy from a Tether-release method (Figure 1). To capture two-steps balance recovery movement, Vicon motion capture system (VICON, Oxford Metrics) was used to record 3D kinematic data of the whole body motion based on Plug-in gait model at 100Hz. Three AMTI force plates were placed next to each other to obtain ground reaction forces (GRF) sampled at 1000Hz. The subject initially stood on the first plate and the first recovery step landed completely on the second force plate while the second recovery step landed on the third plate. All the participants completed their balance recovery within two steps.

Acquired data were processed in Visual 3D (C-motion) and further modelled using AnyBody musculoskeletal modelling software (Anybody Technology, Aalborg, Denmark). The simulation was performed using min/max optimisation method [5] to compute time-histories of forces of HA muscles in detail: Gluteus Medius (GMed) (Anterior, Posterior), Gluteus Minimus (GMin) (Anterior, Medius, Posterior) and Tensor Fascia Latae (TFL). Recovery step was defined from toe-off to 0.1 second after maximum knee flexion. During each recovery step, the mean muscle force was obtained for each subject (normalized to body mass).

RESULTS AND DISCUSSION

Table 1 presents mean normalised hip abductors' forces of the first and second steps of each muscle's head. Mean

forces in anterior, medius and posterior heads of GMin and anterior head of GMed increased in the second step for all subjects while GMed posterior head and TFL did not show the consistent trend.

As shown in table 1, GMin increases from the first to second recovery step across all subjects. Combining all locations together (anterior/medius/posterior), increases were 260% on average (ranging from 16% to 1200%). GMin anterior head performs opposite function compared to posterior head in many movements such as hip flexion and external rotation [6]. However, when all muscle fibers are activated simultaneously, they act together to stabilise the femoral head by pulling it into the acetabulum [6]. Thus, it appears that GMin muscles may possibly play an important role in completing balance recovery action through its contribution to hip stabilisation.

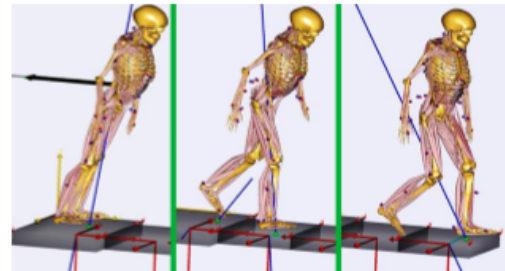


Figure 1: Balance recovery model developed using AnyBody.

CONCLUSIONS

The simulation results implied that the final recovery step might require increased GMin activation to complete balance recovery. Further investigations are necessary to test this hypothesis.

REFERENCES

- [1] Salzman, Brooke. "Gait and balance disorders in older adults." *Am Fam Physician* 82.1 (2010): 61-68.
- [2] Blake AJ, Morgan K, Bendall MJ, Dallosso H, Ebrahim SB, Aris THD, et al. Falls by elderly people at home: prevalence and associated factors. *Age Ageing* 1988;17.
- [3] Carry, Christopher P., et al. "Mechanisms of adaptation from a multiple to a single step recovery strategy following repeated exposure to forward loss of balance in older adults." *PLoS One* 7.3, 2012
- [4] Graham, David F., et al. "Muscle contributions to recovery from forward loss of balance by stepping." *Journal of biomechanics* 47.3 (2014): 667-674.
- [5] de Zee M, Christensen ST, Damsgaard M, Rasmussen J. AnyBody—musculoskeletal modelling system based on inverse dynamics and beyond. *The Bionet Event: Biomechanics in the Decade of the Bone and the Joint*, 2002.
- [6] Beck, Martin, et al. "The anatomy and function of the gluteus minimus muscle." *Bone & Joint Journal* 82.3 (2000): 358-363.

Table 1: The mean of Hip Abductor muscles forces during first and second step of balance recovery. Normalised by body mass (N/Kg)

	Gluteus Medius				Gluteus Minimus						Tensor Fasciae Latae	
	Anterior		Posterior		Anterior		Medius		Posterior		1st	2nd
	1st	2nd	1st	2nd	1st	2nd	1st	2nd	1st	2nd		
Subject 1	0.02	0.32	5.45	3.85	0.09	0.29	0.11	0.30	0.25	0.29	0.15	0.12
Subject 2	0.03	0.18	5.98	8.84	0.08	0.53	0.22	0.68	0.32	0.71	0.33	0.49
Subject 3	0.03	0.31	7.79	4.74	0.11	0.37	0.26	0.40	0.38	0.41	0.44	0.34
Subject 4	0.02	0.83	2.86	6.13	0.04	0.51	0.16	0.51	0.21	0.49	0.26	0.13

APPENDIX B CONSENT FORM



CONSENT FORM FOR PARTICIPANTS INVOLVED IN RESEARCH

We are pleased to invite you to be a part of a study "Development of a novel passive Ankle Exoskeleton Assistive Device (AEAD)". The aim of the project is to investigate the biomechanical and physiological effects of walking while using AEAD assistive device. You are asked to participate in the testing procedures outlined in the attached "Information for Participants" and "test protocol" documents.

- This research has been approved by the Victoria University Human Research Ethics Committee.
- The physical risks associated with the procedures will be explained by researchers.
- The testing area will be kept private with access limited only to the researchers.
- All data will be kept confidential and only the researchers will have access to the data files.
- Please be advised that although you are volunteering for this research, you are free to withdraw at any time.

CERTIFICATION BY SUBJECT

I _____ of _____

certify that I am above 18 years old and voluntarily giving my consent to participate in the research: Biomechanical and physiological evaluation of a novel passive Ankle Exoskeleton Assistive Device (AEAD), conducted at Victoria University by: **Prof Rezaul Begg, Dr Tony Sparrow, Mr Soheil Bajelan and Dr Kurt Mudie.**

I certify that the objectives of the study, together with any associated risks and safeguards to be carried out in the research, have been fully explained to me by: Mr Soheil Bajelan and Mr Kurt Mudie, and that I freely consent to participation involving the below mentioned procedures:

- Walking on treadmill with and without AEAD at different speeds
- Kinetics and Kinematics Biomechanical analyses
- Electromyography (EMG) measurement
- Oxygen consumption measurement
- Foot-Ground Pressure monitoring

I certify that I have had the opportunity to have any questions answered and that I understand that I can withdraw from this research at any time and that this withdrawal will not jeopardize me in any way.

I have been informed that the information I provide will be kept confidential and that my data may be used for future publications and/or presentations. Data will be coded and kept for a period of 5 years post publication

Signed: _____

Date: _____

Any queries about your participation in this project may be directed to the researchers
Mr Soheil Bajelan (Mobile: 0470 656 596 Email: Soheil.bajelan@live.vu.edu.au)
Dr Kurt Mudie (Mobile: 0405 259 557 Email: kurt.mudie@vu.edu.au)

If you have any queries or complaints about the way you have been treated, you may contact the Ethics Secretary, Victoria University Human Research Ethics Committee, Office for Research, Victoria University, PO Box 14428, Melbourne, VIC, 8001, Email: Researchethics@vu.edu.au or phone (03) 9919 4781 or 4461.

APPENDIX C QUESTIONNAIRE

Pre-Experiment Questionnaire

Date: _____.

Name: _____, Date of Birth: _____.

Gender: Male Female Height (cm): _____, Weight (kg): _____.

No.	Question	Please circle response	
1	Has your doctor ever told you that you have a heart condition or have you ever suffered a stroke?	Yes	NO
2	Do you ever experience unexplained pains in your chest at rest or during physical activity/exercise?	Yes	NO
3	Do you ever feel faint or have spells of dizziness during physical activity/exercise that causes you to lose balance?	Yes	NO
4	Have you had an asthma attack requiring immediate medical attention at any time over the last 12 months?	Yes	NO
5	If you have diabetes (type I or type II) have you had trouble controlling your blood glucose in the last 3 months?	Yes	NO
6	Do you have any diagnosed muscle, bone or joint problems that you have been told could be made worse by participating in physical activity/exercise?	Yes	NO
7	Do you have any other medical condition(s) that may make it dangerous for you to participate in physical activity/exercise?	Yes	NO
8	Have you spent time in hospital (including day admission) for any medical condition/ illness/ injury during the last 12 months?	Yes	NO
9	Are you currently taking a prescribed medication(s) for any medical conditions(s)?	Yes	NO
10	Do you have any muscle, bone or joint pain or soreness that is made worse by particular types of activity?	Yes	NO
11	Have you been told that you have high blood pressure?	Yes	NO

I believe that to the best of my knowledge, all of the information I have supplied within this tool is correct.

Signature _____

Date _____